

19

Bangladesh Water Development Board



River Training Studies of The Brahmaputra River

FAP-1

First Interim Report
April 1991

Technical Annexes

Annex 3 : Parts 1 & 2
Mathematical Modelling

Annex 4
Geomorphology



Sir William Halcrow & Partners Ltd has prepared this report in accordance with the instructions of the Bangladesh Water Development Board for their sole and specific use. Any other persons who use any information contained herein do so at their own risks.

Sir William Halcrow & Partners Ltd.
in association with

Danish Hydraulic Institute
Engineering & Planning Consultants Ltd.
Design Innovations Group

MPN-28
A-28

627.1207
FAP-1

A-35

A-37
A-38

2
Bangladesh Water Development Board



River Training Studies of The Brahmaputra River

First Interim Report
April 1991

Technical Annexes

Annex 3 : Parts 1 & 2
Mathematical Modelling

Annex 4
Geomorphology



Sir William Halcrow & Partners Ltd has prepared this report in accordance with the instructions of the Bangladesh Water Development Board for their sole and specific use. Any other persons who use any information contained herein do so at their own risks.

Sir William Halcrow & Partners Ltd.
in association with

Danish Hydraulic Institute
Engineering & Planning Consultants Ltd.
Design Innovations Group

627.1207
FAP-1

MM-28
07-62

16
Bangladesh Water Development Board

A P G RUSSELL

Team Leader

River Training Studies of The Brahmaputra River Project
for WMD in Assam & Bangladesh

River Training Studies of The Brahmaputra River

First Interim Report

April 1991

Technical Annexes

Annex 3 : Parts 1 & 2
Mathematical Modelling

Annex 4
Geomorphology

Sir William Halcrow & Partners Ltd.
in association with

Danish Hydraulic Institute
Engineering & Planning Consultants Ltd.
Design Innovations Group

Bangladesh Water Development Board

River Training Studies of The Brahmaputra River

First Interim Report
April 1991

Technical Annexes

Annex 3 : Parts 1 & 2
Mathematical Modelling

Annex 4
Geomorphology

Sir William Halcrow & Partners Ltd has prepared this report in accordance with the instructions of the Bangladesh Water Development Board for their sole and specific use. Any other persons who use any information contained herein do so at their own risks.

Sir William Halcrow & Partners Ltd.
in association with

Danish Hydraulic Institute
Engineering & Planning Consultants Ltd.
Design Innovations Group

17

ANNEX 3: PART 1

MATHEMATICAL MODELLING
1-D AND GENERAL

RIVER TRAINING STUDIES OF THE BRAHMAPUTRA RIVER

FIRST INTERIM REPORT

GENERAL CONTENTS

Vol 1	Main Report
Vol 2	Annex 1: Parts 1 to 4 Data Collection & Analysis Annex 2: Hydrology
Vol 3	Annex 3: Mathematical Modelling Annex 4: Geomorphology
Vol 4	Annex 5: Physical Modelling Annex 6: Parts 1 & 2 River Engineering

BRAHMAPUTRA RIVER TRAINING STUDIES

FIRST INTERIM REPORT

ANNEX 3: PART 1 - MATHEMATICAL MODELLING: 1-D MODELLING AND GENERAL

	Page
1. INTRODUCTION	1
2. ONE DIMENSIONAL HYDRODYNAMIC MODELLING	1
2.1 Software	1
2.2 Schematisation	1
2.2.1 Model boundaries	2
2.2.2 Channel representation	2
2.3 Data	3
2.3.1 Topography data	4
2.3.2 Discharge measurements	4
2.3.3 Water levels	5
2.3.4 BRTS field measurements	5
2.3.5 Data processing	6
2.4 Calibration and Verification	6
2.4.1 Progress on calibration to date	7
2.5 Exploratory Runs	8
2.5.1 The 1 in 100 year water surface profile	9
2.5.2 The surface water profile for the morphologically dominant discharge	9
2.5.3 Steady state runs for the physical modelling	10
2.5.4 Backwater effects	10
2.5.5 Reduction of over bank flows on the left bank	10
2.6 Applications	11
3. ONE DIMENSIONAL MORPHOLOGICAL MODELLING	11
3.1 Software	11
3.2 Schematisation	12
3.3 Data	12
3.4 Applications	12
4. INTERACTION WITH OTHER FAP PROJECTS	14
4.1 Coordination	14
4.2 Output from the FAP 25 Flood Hydrology Study	15



TABLES

Table 2.1	Grid Coordinates of the Water Level Gauges on the Brahmaputra - Jamuna
Table 2.2	Locations of Gauges and 'Priority Areas' in relation to Survey Cross-Sections on the Brahmaputra - Jamuna
Table 2.3	Variation of Mannings 'n' along the Brahmaputra
Table 2.4	Water Level and Velocity Distribution along the Brahmaputra for Selected Discharges

FIGURES

Figure 2.1	Layout of the SWMC General Model - GM1 within which the BRTS Model is being Built
Figure 2.2	Approximate Location of Survey Sections to be Included in the BRTS 1-D Model
Figure 2.3a	Comparison of Simulated and Observed 1988 Flood Events using BRTS 1-D model
Figure 2.3b	Comparison of simulated and observed 1988 flood events using BRTS 1-D model
Figure 2.3c	Comparison of simulated and observed 1988 flood events using BRTS 1-D model
Figure 2.4	Water surface profile down the Jamuna for a flow of 102,430 cumec at Bahadurabad (1:100)
Figure 2.5	Distribution of flows down the Brahmaputra a discharge of 102,700 cumec at Bahadurabad
Figure 2.6	Comparison of observed, simulated, and statistically derived Flood Levels along the Brahmaputra
Figure 2.7	Water surface profile down the Jamuna for a flow of 38,000 cumec (Dominant discharge) at Bahadurabad
Figure 2.8	Back Water Zone on the Brahmaputra

ANNEX 3: PART 1 - MATHEMATICAL MODELLING: 1-D MODELLING AND COORDINATION

1. INTRODUCTION

This Technical Annex 3 to the First Interim Report for the River Training Studies for the Brahmaputra River (BRTS) describes the mathematical modelling work completed to date and outlines the activities that will be undertaken during the coming nine months leading up to the Second Interim Report.

Part 1 of this Annex covers the one dimensional (1-D) hydrodynamic and morphological modelling and the interaction with other FAP components, particularly FAP 2, FAP 3 and FAP 25. Part 2 concentrates on the two dimensional (2-D) morphological modelling

2. 1-D HYDRODYNAMIC MODELLING

2.1 Software

The 1-D mathematical modelling on BRTS is being carried out using the 'MIKE 11' numerical modelling system developed by the Danish Hydraulics Institute. MIKE 11 is a general purpose open channel modelling system which includes a hydrodynamic core model to simulate unsteady but unidirectional flows, and a sediment transport module which can calculate sediment movement on a reach-by-reach basis. It is also equipped with procedures which assist in the calculation of alluvial roughness due to sediment grain size and channel bed-forms.

MIKE 11 is currently being used by the Surface Water Modelling Centre of the Master Planning Organisation for the Bangladesh Surface Water Modelling Programme for construction of their general and regional surface water models for use on projects under the Flood Action Plan. The technical capabilities of MIKE 11 are described in the 'Working Paper on 2-D Modelling' (BRTS, Dec 1990).

2.2 Schematisation

A 'global' hydrodynamic 1-D model is being built focusing on the Brahmaputra-Jamuna from the Indian border to its confluence with the Ganges. The purpose of this model is:

- (a) To simulate the maximum flood water level in the Brahmaputra (Jamuna) channel and on the flood-plain between the river channel and the BRE, under various degrees of confinement. Various levels of confinement can be achieved by combinations of a retired BRE; a continuous or intermittent flood embankment on the left bank; control structures at the distributary offtakes; and modified distributary capacities.
- (b) To provide boundary conditions for the physical modelling and the 2-D morphological modelling

The 'global' model is being built within the overall structure of the SWMC General Model (GM1). The Brahmaputra channel will be represented by cross-sections at approximately 3 to 6 km intervals as compared with 6 to 15 km in the General Model. This decrease in the interval between successive cross-sections will allow a more accurate description of flood water

profiles along the Brahmaputra than is possible using the General Model.

2.2.1 Model boundaries

The extent and boundaries of the BRTS 1-D model are illustrated on a schematic of the SWMC General Model (GM1) in Figure 2.1.

An advantage of building the BRTS 'global' model within the overall structure of the SWMC General Model is that this structure automatically provides the downstream boundary conditions for the Brahmaputra and its distributaries. GM1 extends well downstream of the river channels of interest to BRTS and also models flow across the left-bank flood plain using a quasi-two dimensional network of channels and flood-plain cells.

2.2.2 Channel representation

The approximate locations of the BWDB survey cross-sections of the Brahmaputra channel to be included in the 1-D model are shown on Figure 2.2. The average distance between successive cross-sections is 3.2 km (2 miles).

The exact positions of the cross-sections cannot be fixed on a map as grid coordinates for the monuments marking their location are not available. A BRTS survey programme, in hand at the time of writing, will locate and establish the level of 20 or so cross-section monuments along the Brahmaputra in relation to features on the BRE. This will improve the accuracy with which the cross-sections can be located on a map. Intermediate sections can then be positioned on the map by interpolating between those sections for which monument positions have been established.

The Brahmaputra is represented in SWMC General Model as a single compound channel, bounded by the braid belt of the river, and constructed on the basis of cross-section survey data. This arrangement requires that the anabranches which convey flows up to and including bank full discharge are distinguished from channels on the flood plain but beyond flood embankments and channels unlikely to convey flow until overbank flooding takes place. Variable hydraulic roughness values and static storage areas can then be applied, as necessary, to the different elements of the compound channel.

This approach provides an adequate representation of conveyance at high flows as demonstrated by a test carried out by BRTS for a 45 km reach of the Brahmaputra between Chandanbaisa and Sirajganj. This reach of river was represented in the 1-D model in two ways: as a simple network comprising the two major (left and right bank) anabranches; and as a compound channel.

The 1988 flood water levels simulated by the network representation, at Kazipur, mid way down the test reach, were compared with those generated by representing this reach as a compound channel. In both cases, the simulated water levels matched the observed 1988 levels during the flood season (mid May to mid October) equally well.

During the dry season the simulated levels in the right anabranch were closer than those in the left anabranch to the observed level. This result is not surprising since the Kazipur gauge is situated in the right hand anabranch.

The above test showed that although differential low flow levels in individual anabranches may be modelled more accurately using a network of anabranch channels, this more detailed schematisation made little difference to the results at high flows. To achieve a reasonable degree of detail in a network schematisation, channel cross-sections are required at intervals of 1.5 km or less. Furthermore, such a schematisation will only remain valid for as long as the anabranch network does not change significantly (i.e. a few flood seasons).

Bearing the above in mind and given the interest within BRTS in the simulation of high rather than low flows, it seems reasonable to represent the Brahmaputra as a compound channel in the 1-D model for the principal simulation runs. In cases where the 1-D model is required to be used in conjunction with the 2-D morphological model (see Part 2 of this Annex) a braided network can be constructed of individual reaches of river if required.

The question of the validity of using dry season cross-sections in the model to simulate flood flows has been considered. The concern is that the shape and area of the dry season section may not adequately represent the conveyance of the channel under flood discharges. Analysis of data on channel cross-sections, hydraulic roughness and conveyance collected for Test Area 1 in June to November 1990 (see Annex 1 for data analysis for Test area 1) indicates the following:

- (a) Although the cross sectional shape changes during the course of the flood season, in general this results in a redistribution of cross-sectional area rather than a net gain or loss in total cross-section area. This observation assumes that there are no underlying longer term trend in bed aggradation or degradation (which can be detected from the examination of the historic channel section data, as is being planned)
- (b) The channel conveyance for near bank full flows varied as much within the flood season (ie between June and July) as it did between July and November 1990. This is not surprising since the dominant influence on conveyance is bed-form roughness, which can change significantly during the course of a flood, rather than the cross-sectional area of flow.

The calibration and verification strategy being followed by BRTS (see Section 2.4) takes into account both the above observations in that:

- verification will use a more recent set of cross-sections than calibration (see Section 2.3.1, below) and will be informed by the results from the analysis of historic channel data
- an assessment is being made on the influence of bed-forms, and their variation, on channel roughness in the Brahmaputra

2.3 Data

The following types of data are being used in the construction of the 1-D hydrodynamic model:

- the topography of the river channel and flood plain
- measured discharges

- observed water levels
- field measurements in Test Area 1 and 2

Data sources have been described in the BRTS Inception Report.

2.3.1 Topographic data

Based on information available at the time the Inception Report was prepared, it was anticipated that additional survey cross-sections of the Brahmaputra at 3.2 km (2 mile) intervals for the 1990-91 dry season could be made available by the BWDB, progressively, starting in December 1990. On this basis there would have been some advantage to the study in using such data for 1-D model runs.

Due to BWDB operational constraints, it has not proved possible to obtain this data within the time-frame of the BRTS modelling programme, and an alternative approach has been agreed upon.

The principal objective of the 1-D modelling is to carry out comparative runs to assess the potential impact of future changes to the river, such as the effects of confinement. For this purpose the date of the cross-section data is less important than spacing between the cross-sections. The 1986-87 data set, with its 132 cross-sections, offers cross-sections at 1.6 km (1 mile) intervals. This spacing between cross-sections allows detailed simulation of the surface water profile, where required, under different design conditions.

The second objective of the 1-D modelling is to provide boundary conditions for the 2-D and physical modelling, principally water levels for given flows. For the site specific physical models (i.e. at locations identified for priority attention with regard to implementation of civil works) the best data available at the time has already been used for the 1-D runs. Any additional 1990-91 sections not be available until later this year would come too late for this purpose. The general physical models, by definition, are being used to investigate conditions which are neither site nor year specific and 1990-91 cross-sectional data would be of no additional benefit over any other reasonably recent data (see Annex 5).

For the 2-D modelling carried out to date, the boundary condition data has been supplied by direct field measurement. For future work, should site specific data be required, this can be obtained from local field surveys. otherwise runs of the 1-D model using the 1986-87 or 1988-89 data can meet the requirements of the 2-D modelling programme, as described in Part 2 of this Annex.

It has therefore been agreed that the cross-sections surveyed in 1986-87 be used for calibrating the model. Verification will use the 1988-89 cross-sections. Calibration and verification of the model are discussed further in Section 3.4.

2.3.2 Discharge measurements

The only site at which discharges are regularly measured on the Brahmaputra-Jamuna is at Bahadurabad Transit (Gauge no 46.9.L). Uninterrupted data is available for the water years 1986-89; these are the years of particular interest to BRTS with respect to calibrating and verifying the 1-D hydrodynamic model.



Daily discharges at Bahadurabad are published by BWDB, for observed daily water levels. They are determined via a rating curve for Bahadurabad Transit which is constructed at the end of each flood season (see Annex 2).

2.3.3 Water levels

Water levels on the Brahmaputra are measured daily by BWDB at the following sites:

-	Noonkhawa	(Gauge no 45)
-	Chilmari	(Gauge no 45.5)
-	Kamarjani	(Gauge no 46)
-	Kholabarichar	(Gauge no 46.7 L)
-	Bahadurabad	(Gauge no 47 L)
-	Kazipur	(Gauge no 49/A)
-	Jagannathganj	(Gauge no)
-	Sirajganj	(Gauge no 49)
-	Porabari	(Gauge no 50)
-	Mathura	(Gauge no 50.3)
-	Aricha	(Gauge no 50.6)

The periods covered by the records for each of these sites are given in the BRTS Inception Report. Continuous data is available at all these sites for the years 1986 to 1989.

The locations of the water level gauges on the Brahmaputra-Jamuna are shown on the map 'Bangladesh Hydrological Network' (BWDB/UNDP, undated) which is drawn at a scale of 1:750 000. The gauges on the right bank of the river are currently being located on the ground by BRTS. Their positions are then marked on the SPOT (1989) 1:50 000 scale satellite images from which the grid coordinates of the gauge can be determined, with adequate accuracy for this purpose. Table 2.1 compares the coordinates of those gauges already located by BRTS with the coordinates corresponding to the gauge locations as shown on the Bangladesh Hydrological Network map.

BRTS only has sufficient resources to locate on the ground the gauges on the right bank of the Brahmaputra. It is understood that the locations and elevations of all the gauges on the Brahmaputra are being surveyed under FAP 18 and it is anticipated that this data will be made available through FPCO by mid May 1991.

It is understood from BWDB field personnel that water level gauges are relocated periodically as the channel in which they are situated erodes or accretes. The FAP 18 survey will therefore only confirm the elevations of the gauges in their current locations and some uncertainty will remain.

2.3.4 BRTS field measurements

BRTS has carried out detailed field measurements in Test Area 1 during June/July and November 1990 and in Test Area 2 in January 1991 in order to collect data for the 2-D morphological model. The scope of these measurements is described in Annex 1: Parts 2, 3 and 4).

The data collected in the test areas yields insight into the following fluvial processes which are of interest in calibrating of the 1-D models:

- changes in bed topography
- the evolution and migration of bed forms
- flow velocities and directions
- sediment transport rates

Analysis of this information has enabled an assessment to be made of the hydraulic roughness and other characteristics of the channels in each test area, as outlined in Part 2 of this Annex and described in detail in Annex 1.

2.3.5 Data processing

Data received with the General Model (GM1) such as river cross-sections; catchment runoff (NAM results); discharge time series; and observed water levels have already been through certain quality control procedures implemented by SWMC.

Supplementary quality control checks are being carried out by BRTS. These include:

- (a) A check that all cross-sections are entered in the database with the lateral offset distance increasing from left to right thus ensuring the correct definition of right and left bank top levels on each cross-section.
- (b) A check that effective bank top levels are correctly identified - in the case of the right bank this will be the crest of the BRE, and on the left bank this will be a flood embankment (if one exists) or the natural floodplain level
- (c) In cases where the BRE does not appear on the cross-section, the right bank flood plain is extended at a representative elevation to for the distance up to the BRE, and the crest elevation of the BRE is then marked on the cross-section.
- (d) Checking the location of gauges and certain river cross-sections
- (e) Screening and appraisal of the historic discharge data at Bahadurabad
- (f) Screening and appraisal of the observed water level data along the Brahmaputra.

The procedures used in the last two checks are described in Annex 2.

2.4 Calibration and Verification

Given that surveyed river cross-sections for the water year 1990-91 will not be available in time for the calibration of the 1-D hydrodynamic model, the calibration procedure has been revised following discussions with the SWMC and BUET. The revised procedure described below has been planned to be consistent with that adopted by SWMC in calibrating and verifying their General Model.

The degree of detail of the calibration of the Brahmaputra channel within the General Model (GM1) is appropriate for the relatively coarse schematisation adopted for the river within that model. Using GM1 as a starting point, BRTS is expanding the representation of the Brahmaputra by building additional cross-sections into the model, which will increase the detail of output to that required for the purposes of this study.

The calibration of the BRTS model will be refined with the general aim, of improving, where necessary, the modelling of flood flows. In this respect, the discharge measured at Test Area 1 in June and July 1990 can be used to check whether the water levels recorded during the same period can be reproduced. Cross-sections are being interpreted with the aid of satellite imagery in order to help determine the planform limits of in-bank flow. Insight obtained from the geomorphological analysis of historic river cross-sections (see Annex 4) will be applied during this calibration process.

The refinement of the calibration will aim to:

- (a) Elaborate the description of flood-plain and channel roughness at high flows by introducing relative roughness values and static overbank storage where appropriate
- (b) Refine the description of hydraulic roughness for in-bank flows in the light of data obtained at Test Areas 1 and 2

The additional cross-sections for the Brahmaputra will be taken from the 1986-87 cross-sections. The model will be calibrated against two consecutive flood seasons, 1987 and 1988, to provide a good fit for water levels during both flood seasons, but concentrating on discharges in excess of 20,000 m³/s (at Bahadurabad).

A parallel model will then be set up using the 1989-90 cross-sections at 6.4 km (4 mile) intervals. This will allow changes in channel topography during the 1987 and 1988 floods to be taken into account. The parameters established during calibration will be verified by running this model to simulate the 1989 flood, and also the 1990 flood if sufficient data becomes available in time.

The cross-section survey data for 1986-87 permits a resolution of 1.6 km (1 mile) between adjacent sections if required. Although the 1988-89 cross-sections are only at 6 km (4 mile) intervals, it is not considered that this reduction in the degree of detail of available cross-section data will significantly affect the quality of model verification, since the spacing between sections will still be much less than that distances along the river between gauges.

2.4.1 Progress on calibration to date

Location on the ground of the water level gauges at Chilmari, Bahadurabad, Kazipur, Sirajganj, and Mathura has allowed their grid coordinates to be checked. In addition the exact location of cross-section JS-6 was surveyed. The gauge at Sirajganj is approximately 3 km upstream of this section (at or near section J-7).

The positions of the gauges with respect to survey sections must remain tentative until the locations of ground monuments marking the position of selected survey sections are established. Nevertheless the evidence so far

does indicate that the calibration of the SWMC General Model (which has the Sirajganj gauge located at J-6) needs some refinement in the Sirajganj reach.

A preliminary recalibration of the BRTS version of GM1 has been carried out against the 1988 flood with gauge locations (some assumed) as shown in Table 2.2. The results, shown on Figure 2.3, show a generally good agreement between simulated and observed levels except at Chilmari (where the location of the gauge in relation to the survey cross-sections is uncertain) and at Kazipur, where further refinement of the description of channel roughness is necessary. The roughness values used for near bankfull and flood flows in this preliminary recalibration are identical to those used by SWMC in their March 1991 version of GM1, except for downstream of Sirajganj, as shown in Table 2.3.

The channel roughness value applied to the reach J-7 to J-6 for flows at and above bankfull flow was a Manning $n = 0.022$ (which is equivalent to a Chezy $C = 64 \text{ m}^{0.5}/\text{s}$, for a hydraulic radius $R = 5 \text{ m}$, where $n = R^{1/6}/C$). This is higher than that applied to Test Area 1 in the hydrodynamic component of the 2-D model (see Part 2 of this Annex) in which a mean value for channel roughness of $C = 74 \text{ m}^{0.5}/\text{s}$ was used (equivalent to a Manning $n = 0.018$) for in-bank flows. This is consistent with the fact that out-of-bank flows will encounter a higher overall hydraulic resistance than those confined to within the channel.

Recalibration is on-going at the time of writing of this report and the above roughness values will be refined further. Recalibration is concentrating on the 32 principal and intermediate 1986-87 cross-sections (J-17, J16-1, J16, J15-1..... J-2, J-1-1, J1) currently in the model. Once the calibration has been refined sufficiently, the additional intermediate cross-sections will be built into the model following which fine tuning of the calibration will be carried out.

2.5 Exploratory Runs

A series of exploratory runs has been carried out to provide indicative data for various aspects of BTRS. The output from these runs published in this report are interim results which will be revised once the hydrodynamic model has been calibrated and verified, a process which is scheduled for completion by the end of July 1991. However, since these runs are based on a partially recalibrated version of the SWMC General Model (GM1), issued to BRTS in March 1991, which is itself a calibrated model, they are considered to be generally sound.

The exploratory runs fall into five groups:

- (a) Comparison of the surface water profile generated by a 1 in 100 year flood discharge at Bahadurabad with the statistically derived water levels at the sites of the water level gauges on the Brahmaputra.
- (b) The generation of a surface water profile for the morphological dominant discharge (38,000 m^3/s at Bahadurabad)
- (c) The generation of steady state water surface profiles to provide boundary values for the physical modelling
- (d) An assessment of the backwater effects in the Brahmaputra

- (e) The effect on peak flood levels of reducing flows from the Brahmaputra over its left bank

These results from these exploratory runs are described below.

2.5.1 The 1 in 100 year water surface profile

The water surface profile for an approximate 1 in 100 year steady discharge at Bahadurabad of $102,700 \text{ m}^3/\text{s}$ (see Annex 2) is shown on Figure 2.4. This profile does not represent a constant flow down the river because flows are leaving the river through the left bank distributaries and over the left bank flood plain. The distribution between inflows and outflows along the Brahmaputra is illustrated in Figure 2.5.

The flow at Bahadurabad has been set by adjusting the inflow at Noonkhawa so that when it is combined with inflows from the rivers Dharla, Dudhkumar, and Teesta, and account is taken of the outflow down the Old Brahmaputra, a residual flow of $102,700 \text{ m}^3/\text{s}$ flows passes Bahadurabad. In this steady run, all inflows and downstream boundaries were kept constant at approximately 1 in 100 year levels.

Figure 2.6 compares the water surface profile with the 1 in 100 year water levels at the gauge sites along the Brahmaputra generated by an at-site statistical analysis of water levels using data over the period from 1949 to 1989. The methodology used in the statistical derivation of water levels is described in Annex 2.

The surface water profile for the 1 in 100 year flow shows good agreement with the statistically derived water levels. The peak water levels observed in 1988 (an event considered to have a return period of 64 years in terms of the discharge at Bahadurabad) are also plotted on Figure 2.6, and provide general confirmation of both the statistically derived and the hydrodynamically simulated water levels.

2.5.2 The surface water profile for the morphologically dominant discharge.

The morphologically dominant discharge has been defined and derived in Annex 4. It is the flow which occurs sufficiently frequently to be able to transport more sediment than any other flow over a long period. It is derived by integrating flow frequency and sediment transport data.

The longitudinal surface water profile for the morphologically dominant discharge ($38,000 \text{ m}^3/\text{s}$ at Bahadurabad) is shown on Figure 2.7. This flow is within bank along almost the entire length of the river.

The profile of lowest (at-a-section) bed levels is a poor indicator of channel slope since thalweg levels are influenced by local effects such as scour at bends (particularly noticeable at chainages 71.8 km and 113.8 km) or scour adjacent to river training works (eg the bank protection at Sirajganj at chg 155.8 km where the lowest point on the river bed was 12 m below PWD in 1986-87).

The mean bed level at individual (1986-87) cross-sections (defined as the aggregate bank-full cross-sectional area divided by the aggregate water surface width) down the Brahmaputra have therefore also been plotted on Figure 2.7, along with the level at each section above which 20% of the bank-full area lies. Examination of the longitudinal profiles produced by these levels indicates local variations in bed slope, possibly associated with variations in braid index or the passage down the river of 'slugs'

of sediment. A more comprehensive analysis of of bed slope both longitudinally and with time will follow during the planned analysis of historic river cross-sections.

2.5.3 Steady state runs for the physical modelling

A series of steady state runs with fixed discharges and downstream boundaries were carried out to provide boundary data for the physical modelling.

The results from these runs are summarized in Table 2.4. The discharges given in the table all refer to Bahadurabad. The velocities listed are mean velocities at each cross-section.

2.5.4 Backwater effects

High flows down the Ganges will cause backwater effects up the Brahmaputra. A preliminary assessment of these backwater effects has been carried out by means of a series of steady state runs for different combinations of boundary conditions. The results of these runs are shown in Figure 2.8.

The different combinations of boundary conditions simulated are as follows:

- (a) All inflows and downstream boundaries set at approximately 1 in 100 year flood flows or levels
- (b) A 1 in 100 year flood discharge (at Bahadurabad) down the Brahmaputra with all other boundaries set at 1 in 2 year flood flows or levels
- (c) A 1 in 2 year flood discharge down the Brahmaputra with all other boundaries set at 1 in 100 year flood flows or levels
- (d) All inflows and downstream boundaries set at approximately 1 in 2 year flood flows or levels

The boundary conditions used in each of these runs should at this stage of the study be regarded as approximate since BRTS has not carried out a full statistical analysis of flood flows and water levels outside its project area. Such an analysis is currently being undertaken by FAP 25.

No attempt has been made at this stage to ascribe probabilities to the above combinations of boundary conditions. Guidance on this is also awaited from FAP 25. The analysis is merely intended to illustrate the range of the likely backwater limit on the Brahmaputra.

The backwater zone extends to around chainage 170 km (i.e. almost 70 km upstream of the confluence with the Ganges) for low flood flows down the Brahmaputra. For high flood flows down the Brahmaputra the backwater limit is about 50 km upstream of the confluence with the Ganges.

2.5.5 Reduction of over bank flows on the left bank

An outline analysis has been carried out to investigate the order of magnitude of the effect of reducing the flow from the Brahmaputra over its left bank and into its left bank distributaries. The following hypothetical changes were introduced on the left bank:

- a flood embankment along the whole length of the left bank from the border with India to the Ganges confluence
- a limit was placed on the flows permitted to enter the distributaries

and the effect of these changes on the 1988 peak levels was simulated. The results indicated a rise in peak water level of between 0.1 m and 0.8 m (moving downstream) for a reduction in the total peak flow over the left bank from around 30,000 m³/s to 15,000 m³/s.

These results are approximate and were based on an earlier version of GM1 (received from SWMC in July 1990) than the one on which the other exploratory runs were based.

2.6 Applications

Once calibrated and verified, the BRTS 1-D hydrodynamic model will be used to explore the effects on water levels in the Brahmaputra of different degrees of confinement of flows down the river under various combinations of boundary conditions. These production runs will be carried out commencing in July 1991. They will include the same broad groups of runs described in Section 2.5. Other analyses will be added to the list as the study demands evolve, such as, for example, assessing the backwater influence of the proposed Jamuna Multipurpose Bridge.

In addition, the 1-D hydrodynamic model will be used in conjunction with the North West Regional Model (FAP 2) to assess the impact of flows over the BRE and through breaches in it.

Beyond the strip of flood plain on the left bank the SWMC General Model (GM1) schematisation will be retained. This schematisation will only be refined in those areas where the North Central Regional Model currently being refined by FAP3 shows the schematisation of the General Model (GM1) to be inaccurate, provided that this information becomes available during the time frame of the BRTS mathematical modelling programme.

Some confinement options will lead to future accretion or degradation of the bed of the Brahmaputra. The effect of this on peak water levels will be explored by running the morphological and hydrodynamic 1-D models together. This is described in Section 3.

3. 1-D MORPHOLOGICAL MODELLING

3.1 Software

The 1-D morphological modelling package is an integrated part of MIKE 11, which is used for the 1-D hydrodynamic modelling. The morphological model calculates the sediment transport rates on the basis of the hydraulic conditions calculated with the hydrodynamic model. The sediment transport rates can be used to determine erosion and deposition pattern (general scour) and/or change of sand dune dimensions and the associated hydraulic resistance. In this way the morphological model results in a dynamic feedback to the hydrodynamic model.

At present three sediment transport models are implemented in MIKE 11. These formulas are:

Engelund & Hansen
Ackers & White
Engelund & Fredsoe

Shortly, additional formulas will be implemented, a.o. the van Rijn mode, and model a so-called user tailored formula, where the user can specify he's own relation between flow parameters, grain characteristics and sediment transport rate. With this update of the software it will also be possible to calculate the transport of a number of grain size fractions simultaneously, and in this way simulate changes of the grain size characteristics of the river bed.

The hydraulic resistance of alluvial rivers depends strongly on the size of the sand dunes on the river bed. The larger and steeper the dunes are the larger the hydraulic resistance is. The sand dunes will grow as the bed load increases, but the length will increase while the height decreases as the suspended load starts to become dominant. Therefore, at increasing discharge the hydraulic resistance will often first increase and later decrease as the suspended load starts to pick up. Alteration of the size of the sand dunes takes some time, implying that the actual sand dune size will lag the equilibrium dune size that correspond to the flow conditions. A theory developed by Fredsoe describing this dynamic development of the sand dunes and the associated hydraulic resistance is implemented in the 1-D morphological model.

The 1-D morphological models are best suited for simulation of 'regional' or large scale changes of bed level and/or resistance at a certain river reach. For prediction of changes within cross-sections the 2-D morphological model (System 21-Curvilinear) has to be applied.

3.2 Schematisation

The schematisation of the 1-D morphological model will be the same as that used for the hydrodynamic model. In contrast to the hydrodynamic model, runs will be carried out over a series of complete water years with a time step of about one week. The time scale over which the full effects of confinement is expected to occur is related to the bed disturbance celerity (de Vries, 1987) and is thought to be of the order of 10 years.

3.3 Data

As in the case of the hydrodynamic module, the morphological module of the General Model will be used to derive time series of sediment transport at key locations in the river system. Through analysis of these time series, a set of 'dominant' sediment transport conditions will be identified which can then be used as boundary conditions for the 'global' model. For instance, a definition of the dominant discharge frequently used for modelling purposes is the discharge that, if it would be present in the river during the whole year, would result in the same yearly sediment transport as an average year.

3.4 Applications

The Jamuna Bridge Project (JMBA, 1990) carried out an analysis of the effects on the river bed and peak flood levels at Sirajganj due to changes in the boundary conditions of the Brahmaputra such as:

- increases and decreases in sediment supply
- an increase in dominant discharge
- a rise in mean sea level
- inter-basin water transfer

The analysis was carried out using a 1-D mathematical morphological model of the Brahmaputra from the Indo-Chinese border to its confluence with the Ganges. Their results indicate that, depending on the scenario assumed, the average bed level at Sirajganj could rise by up to 1.7 m or fall by up to 0.2 m over the next 75 years. Changes of this magnitude are more relevant to the question of design embankment height than that of river training (where local bed scour is the main concern). Our approach will be to review the JMBA assumptions and then revise, within the scope of the BRTS objectives, the most relevant of the scenarios analysed by them.

The JMBA study was concerned with the effect of confinement on the depth of the river. There is an allied question: that of the effect of flow confinement on the overall width of the river. The 1-D model assumes fixed banks. While this assumption may be consistent with one of the possible outcomes of the master plan, some insight is also required into the consequences of changes in bankful depth on the natural overall width of the channel. The geomorphological analyses will yield information on the relationship between overall width and bankfull flow. They will also include an assessment of the interaction between river bank erosion and char formation. These will be used to inform opinion on the likely effects of flow confinement on the river width and depth. Sensitivity runs on the basis of different assumed width can then be used to explore this issue.

Another topic which could be investigated is effect on river bed levels of the large scale movement of sediment through the system. Sediment may travel in large slugs which, as they move down the river could cause a local rise in bed level over a reach; this in turn would increase water levels. The question is, if such 'slugs' exist (the analysis of historic cross-sections may provide some evidence in this respect) how large are they and at what rate do they migrate?

4. INTERACTION WITH OTHER FAP PROJECTS

4.1 Coordination

The BRTS mathematical modelling has a clear interface with other FAP projects, especially FAP 2 (North West Region Study), and FAP 3 (North Central Region Study).

The interactions between BRTS and FAP 2 and 3 will involve the exchange of boundary condition data between adjacent regional models via a model of the Brahmaputra, which flows between the two regions. The Brahmaputra forms the downstream boundary to the North West Regional model at its confluence with the Hurasagar. In turn, the North Central Regional Model with its representation of the Brahmaputra left-bank flood plain and distributaries will provide boundaries for the BRTS 1-D model. It is particularly essential that BRTS is kept fully informed as to engineering changes are being proposed by FAP3 in terms of flood embankments along the Brahmaputra and modifications to the conveyances of its distributaries.

It is intended by FPCO that such interactions will be coordinated by FAP25, which has been set up to achieve consistency, compactability and continuity in all related FAP modelling activities. Whilst it is understood that BRTS mathematical modelling activities may not fall under direct coordination by FAP 25, BRTS has been keeping SWMC informed of the evolution of its 1-D model from the SWMC General Model (GM1) so that general compatibility between the two models can be maintained; meetings have been arranged with both FAP 25 and FAP 2 to maintain coordination (FAP 3 having only recently become established).

It is understood that FAP 25 will not be directly concerned with the 2-D morphological modelling nor the physical modelling, which complements the mathematical modelling in many respects. The following comments therefore relate primarily to the 1-D modelling.

FAP 25 has as yet not published any guidelines or procedures for the transfer of boundary conditions between one FAP model and another. One possible vehicle for exchange of such information would be via a 'master' version of SWMC General Model which would contain the requisite boundary elements and would be updated periodically to incorporate refinements being made to the regional models by the FAP studies.

The question then arises as to who should take responsibility for maintaining such a continuously updated 'master' version of the General Model. This task would include taking responsibility for:

- certifying the validity of refinements being carried out by the FAP projects before incorporating them in the 'master' model bearing in mind that such refinements will be specific to individual projects needs rather than intended to meet general inter-project needs
- making sure that the 'master model' meets the individual FAP project requirement in terms of providing the types of boundary condition being sought by individual FAP projects at the time such data is needed.

The above issues are raised here for consideration by FPCO, FAP 25 and the other related FAP projects. In their considerations it should be borne in mind that whilst the BRTS 1-D model is being built within GM1, this model will evolve during the remainder of this study in response to project requirements rather than more general needs, and may in due course depart from the SWMC version of GM1 in the detail of its calibration.

4.2 Output from the FAP 25 Flood Hydrology Study

FAP 25 will provide recommendations on unified definitions of hydro-meteorological boundary conditions and their derivation as well as advice on the frequencies of occurrence of different flood events for use in the mathematical models being used on FAP projects.

BRTS is well advanced in the process of establishing its own boundary conditions for the 1-D modelling from currently available data (see Annex 2). These boundary conditions include:

- (a) Flow frequency estimates for the Brahmaputra-Jamuna, and the rivers Ganges, Teesta, Dudkumar, Dharla, and Hurasagar
- (b) Sediment transport equations for each of the above if available
- (c) Water levels at the downstream boundaries of the General Model (GM1)
- (d) The conveyance characteristics of the distributaries and floodplain channels on the left bank of the Brahmaputra-Jamuna
- (e) Predicted or assumed changes in the above boundary conditions for use in long term model simulations

The data and methodology used in deriving the above will be compared with the guidelines and recommendations due to be published by FAP 25 following their Flood Hydrology Study with the aim of, wherever possible, maintaining consistency between the BRTS analyses and the methodology proposed by FAP 25.



Table 2.1: Grid coordinates of the water level gauges
on the Brahmaputra - Jamuna

Gauge Location	Grid Coordinates					
	BRTS			BWDB Map ⁽¹⁾		
Chilmari (45.5)	89 ⁰ 25 ⁰	41' 34'	41" 26"	89 ⁰ 25 ⁰	42' 32'	35" 30"
Bahadurabd (46.9L)	89 ⁰ 25 ⁰	42' 08'	30" 00"	89 ⁰ 25 ⁰	41' 08'	55" 45"
Kazipur (49/A)	89 ⁰ 24 ⁰	40' 37'	39" 18"	89 ⁰ 24 ⁰	42' 40'	20" 00"
Sirajganj (49)	89 ⁰ 24 ⁰	43' 27'	57" 45"	89 ⁰ 24 ⁰	45' 25'	15" 10"
Shahpur (2)	89 ⁰ 24 ⁰	43' 18'	09" 44"	-	-	-
Mathura (50.3)	89 ⁰ 23 ⁰	39 ⁰ 57'	14" 0"	89 ⁰ 23 ⁰	31' 55'	30" * 50"
Aricha (50.6)	89 ⁰ 23 ⁰	46' 50'	59" 7"	89 ⁰ 23 ⁰	48' 51'	05" 15"

Notes : (1) Source : Bangladesh Hydrological Network (BWDB/UNDP)

(2) Shahpur gauge was established by BRTS during the survey of Test Area
1 in June 1990

Table 2.2: Location of gauges and 'priority' areas in relation of survey cross-sections on the Brahmaputra - Jamuna

Gauge Site and/or 'Priority' Area	Chainage ⁽¹⁾ (km)	Survey Cross-Section
Chilmari	34.0	J 16-1
Fulchari	76.6	J 13-1
Bahadurabad ⁽²⁾	76.6	J 13
Sariakandi	105.4	J 11
Mathurapara	110.0	J 11-6
Kazipur	137.8	J 8-1
Sirajganj	155.8	J 7
Shahpur	173.3	J 6-6
Bethil	182.2	J 5
Porabari ⁽³⁾	188.2	J 4-1
Aricha ⁽³⁾	237.5	J 1

Notes : (1) Chainages correspond to those used by SWMC in the General Model (GM1)

(2) Chainage of water level gauge is approximate

(3) Location of water level gauge is uncertain

Table 2.3 Variation of Manning's 'n' along the Brahmaputra for discharges equal to and in excess of bank-full used in preliminary calibration of BRTS 1-D model in April 1991

Cross-section Number	Chainage (km)	Manning's 'n'	
		GM1	BRTS
J#17	25.0	0.022	0.022
J#16-1	34.0	0.021	0.021
J#16	39.4	0.036	0.036
J#15-1	46.6	0.037	0.037
J#15	56.0	0.034	0.034
J#14-1	60.3	0.032	0.032
J#14	64.6	0.029	0.029
J#13-1	71.8	0.027	0.027
J#13	76.6	0.024	0.024
J#12	91.0	0.025	0.025
J#11-1	98.2	0.032	0.032
J#11	105.4	0.025	0.025
J#10-1	113.8	0.026	0.026
J#10	119.8	0.028	0.028
J#9-1	125.2	0.024	0.024
J#9	130.6	0.026	0.026
J#8-1	137.8	0.030	0.030
J#8	143.8	0.025	0.025
J#7-1	152.2	0.029	0.029
J#7	155.8	0.036	0.022
J#6-1	163.2	0.032	0.022
J#6	170.2	0.034	0.022
J#5-1	176.2	0.033	0.025
J#5	182.2	0.037	0.025
J#4-1	188.2	0.033	0.025
J#4	196.6	0.032	0.025
J#3-1	205.0	0.032	0.025
J#3	213.4	0.033	0.027
J#2-1	218.2	0.031	0.027
J#2	227.8	0.031	0.027
J#1-1	232.6	0.031	0.027
J#1	237.4	0.032	0.027

Note : BRTS values refer to calibration run BR1-C3

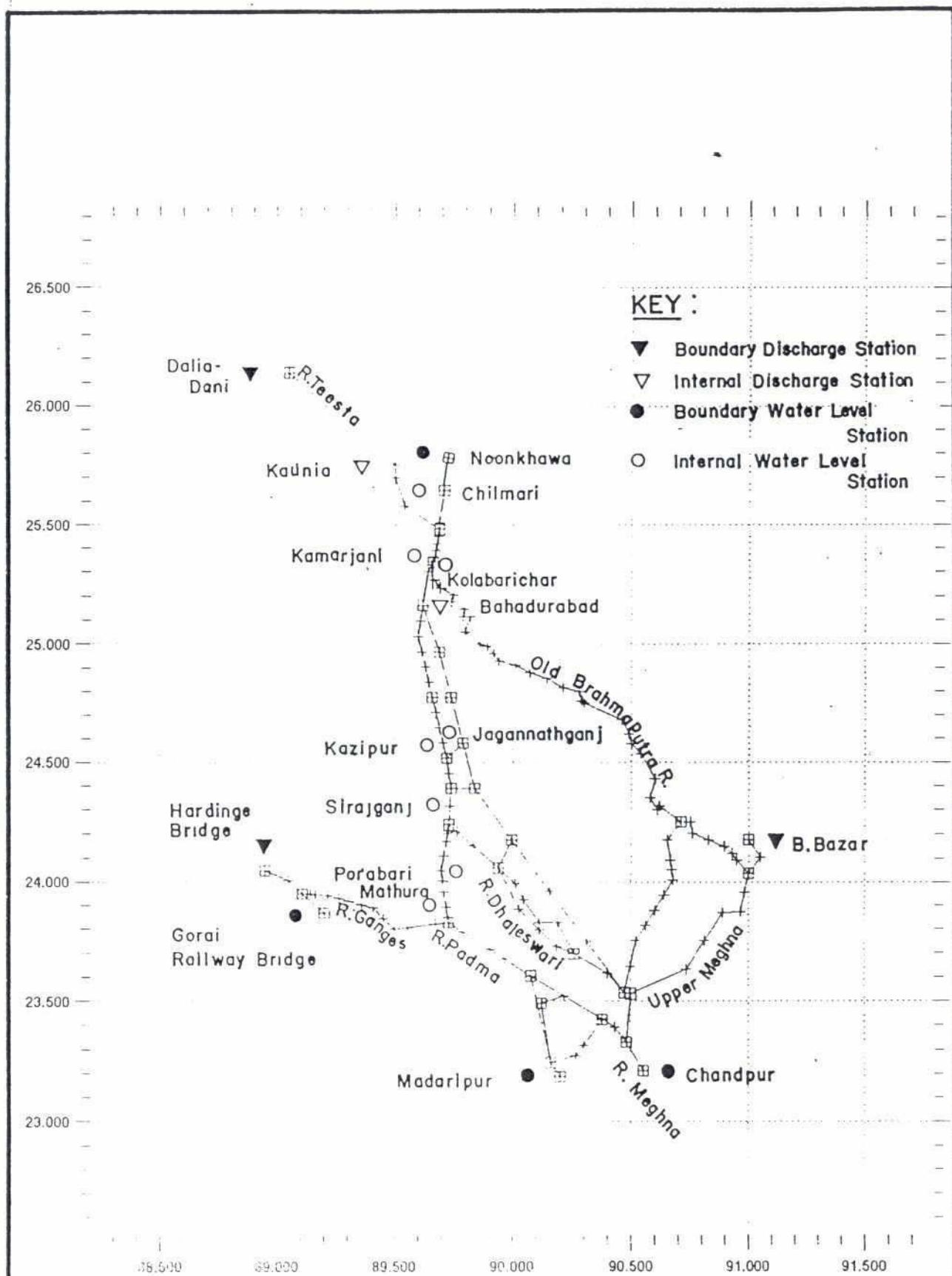


Table 2.4 Water Level and velocity distribution along the Brahmaputra for selected discharges at Bahadurabad

Chainage (km)	X-section (m)	1986 Flow				1987 Flow				1 in 100 Flow			
		12,500 cumec	42,200 cumec	39,100 cumec	43,100 cumec	30,000 cumec	72,000 cumec	72,000 cumec	72,000 cumec	102,433 cumec	102,433 cumec	102,433 cumec	102,433 cumec
		WL (m.PWD)	WL (m.PWD)	Vel. (m/s)	WL (m.PWD)	Vel. (m/s)	WL (m.PWD)	Vel. (m/s)	WL (m.PWD)	Vel. (m/s)	WL (m.PWD)	Vel. (m/s)	WL (m.PWD)
25.0	J#17	20.35	23.25	1.232	23.00	1.430	23.32	1.458	22.39	1.284	24.71	1.522	25.93
34.0	J#12-1	19.10	22.48	1.117	22.23	1.297	22.56	1.335	21.60	1.225	23.94	1.484	24.86
35.4	J#16	18.76	22.03	1.024	21.79	1.191	22.10	1.216	21.21	1.101	23.47	1.450	24.30
35.4	J#15-1	18.70	22.03	1.024	21.79	1.173	22.10	1.216	21.21	1.065	23.47	1.397	24.30
41.6	J#15-1	18.37	21.36	0.668	21.14	1.156	21.42	1.199	20.61	1.034	22.60	1.346	22.82
46.0	J#15	17.70	20.51	0.681	20.31	1.232	20.56	1.251	19.74	1.064	22.02	1.569	22.59
46.0	J#14-1	16.55	19.84	0.513	19.63	0.942	19.90	0.977	19.07	0.803	21.24	1.241	22.15
46.0	J#14	16.70	19.37	0.410	19.15	0.766	19.43	0.802	18.64	0.645	20.84	1.076	21.60
46.0	J#14	16.46	19.05	0.566	18.83	0.570	19.12	1.015	18.35	0.829	20.58	1.271	21.56
46.0	J#14	16.42	19.05	0.902	18.83	1.323	19.12	1.383	18.35	1.160	20.58	1.665	21.56
46.0	J#13-1	16.42	18.79	0.916	18.57	1.429	18.85	1.483	17.58	1.260	20.37	1.674	21.39
46.0	J#13	16.42	18.38	0.928	18.17	1.532	18.44	1.599	17.38	1.379	19.97	2.012	20.97
46.0	J#12	15.02	17.83	0.660	17.63	1.217	17.89	1.244	16.86	1.062	19.33	1.497	20.27
46.0	J#12	14.20	17.10	0.538	16.91	1.000	17.16	1.018	16.17	0.864	18.51	1.192	19.45
46.0	J#11-1	13.59	16.45	0.589	16.26	1.036	16.50	1.075	15.53	0.912	17.84	1.233	18.82
46.0	J#11	13.19	15.94	0.587	15.78	1.044	15.96	1.061	15.08	0.905	17.24	1.196	18.17
46.0	J#10-1	12.77	15.34	0.597	15.39	1.070	15.59	1.088	14.70	0.944	16.72	1.213	17.60
46.0	J#10	12.42	15.17	0.607	15.13	1.097	15.21	1.116	14.34	0.966	16.35	1.230	17.26
46.0	J#9-1	12.24	14.69	0.687	14.75	1.173	14.92	1.206	14.08	1.065	16.10	1.342	17.05
46.0	J#9	12.00	14.66	0.790	14.53	1.261	14.70	1.314	13.85	1.158	15.87	1.490	16.83
46.0	J#8	12.00	14.66	0.695	14.53	1.223	14.70	1.274	13.85	1.121	15.87	1.463	16.83
46.0	J#8	11.33	14.22	0.620	14.11	1.188	14.26	1.232	13.37	1.066	15.49	1.476	16.48
46.0	J#7-1	10.67	13.61	0.639	13.67	1.223	13.84	1.275	12.94	1.063	15.11	1.516	16.12
46.0	J#7	10.06	13.16	0.660	13.00	1.257	13.24	1.314	12.29	1.079	14.59	1.556	15.83
46.0	J#6	9.75	12.62	0.643	12.64	1.221	12.89	1.275	11.96	1.050	14.30	1.485	15.33
46.0	J#6	9.55	12.40	0.576	12.64	1.075	12.89	1.122	11.96	0.947	14.30	1.340	15.33
46.0	J#6-1	9.32	12.01	0.522	12.25	0.960	12.47	1.003	11.63	0.863	13.85	1.230	14.86
46.0	J#6	9.32	12.01	0.579	12.01	0.983	12.09	1.031	11.31	0.879	13.44	1.286	14.45
46.0	J#5-1	8.25	11.03	0.650	11.87	1.008	12.09	1.061	11.31	0.897	13.44	1.363	14.45
46.0	J#5	8.25	11.03	0.563	11.47	0.890	11.68	0.932	10.97	0.812	13.03	1.181	14.04
46.0	J#5	8.25	10.67	0.604	10.61	0.907	10.81	0.940	10.52	0.742	12.56	1.042	13.61
46.0	J#4-1	8.25	10.67	0.705	10.61	1.051	10.81	1.082	10.11	0.844	12.33	1.133	13.35
46.0	J#4	8.10	10.61	0.552	10.55	0.882	10.77	0.917	10.00	0.878	12.33	1.242	13.35
46.0	J#4	7.16	10.10	0.458	10.09	0.759	10.35	0.785	9.23	0.707	12.30	1.105	13.32
46.0	J#3-1	6.71	9.518	0.518	9.74	0.798	9.87	0.837	8.94	0.742	11.94	0.996	12.97
46.0	J#3	6.07	9.22	0.565	9.36	0.840	9.56	0.883	8.61	0.778	11.53	1.035	12.52
46.0	J#2-1	5.71	8.85	0.551	9.07	0.802	9.24	0.845	8.43	0.743	11.07	1.076	12.31
46.0	J#2	4.77	7.92	0.558	8.44	0.862	8.54	0.910	7.76	0.800	10.74	1.020	11.61
46.0	J#1-1	4.40	7.51	0.509	8.19	0.832	8.26	0.867	7.54	0.867	10.10	1.101	11.51
46.0	J#1	4.27	7.31	0.587	8.07	0.942	8.12	0.990	7.44	0.881	9.82	1.196	11.55
46.0	J#1										8.66	1.171	10.34

Notes: 1. Chainage 0.0 km is at Mookha. 2. All chainages refer to BMH chainage. 3. X-section No. refers to BMH cross-section data of the Brahmaputra and the location of these cross-sections are approximate. 4. Water level and velocity refer to the steady state values attained during simulations by the 1-D model using calibration (BR1-C3).

FIGURES



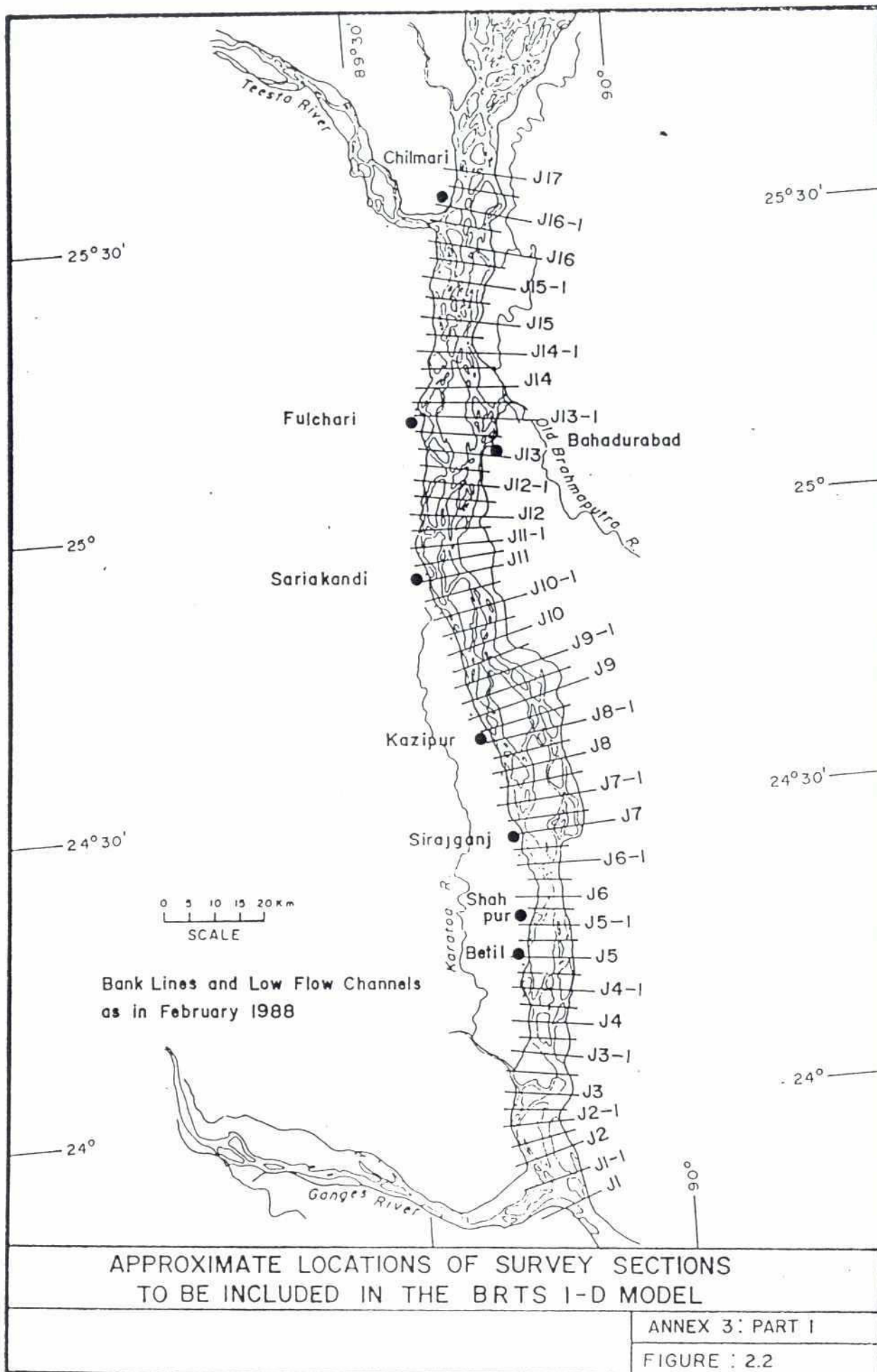
BRAHMAPUTRA RIVER TRAINING STUDIES
 Layout of the SWMC General Model - GM1 within which
 the BRTS model is being built

SCALE : 1 : 22000
 DATA FILE : BR1 0391.RDF

EDITED : 7 - MAR - 1991, 07:28

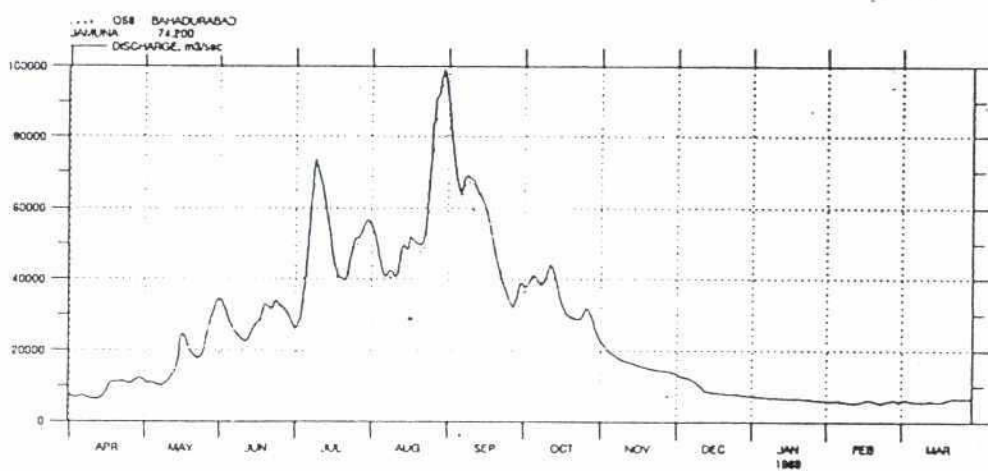
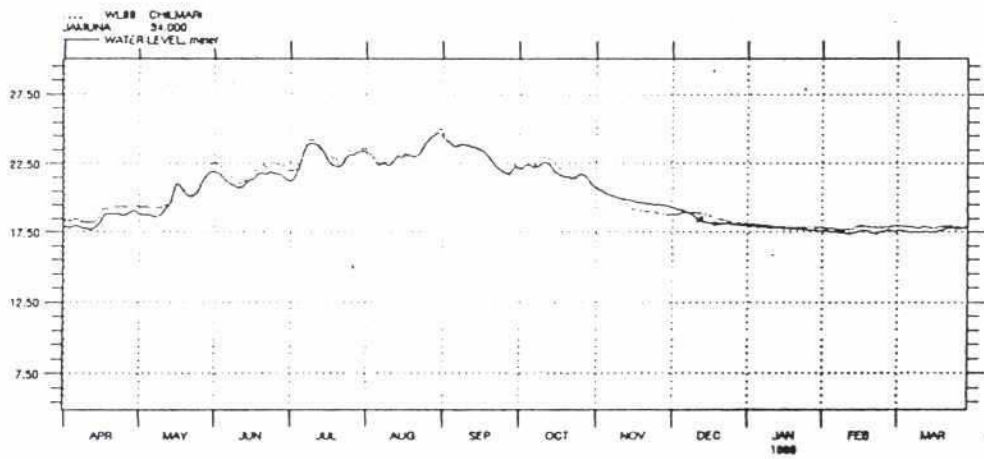
ANNEX 3 : PART I

FIGURE : 2.1



Key :

..... Observed
—— Simulated



BRAHMAPUTRA RIVER TRAINING STUDIES
Comparison of simulated and observed 1988 flood events using
BRTS 1-D model

DATA FILE : BR1 - 0391.RDF
RESULT FILE : BR1 - C3.RRF

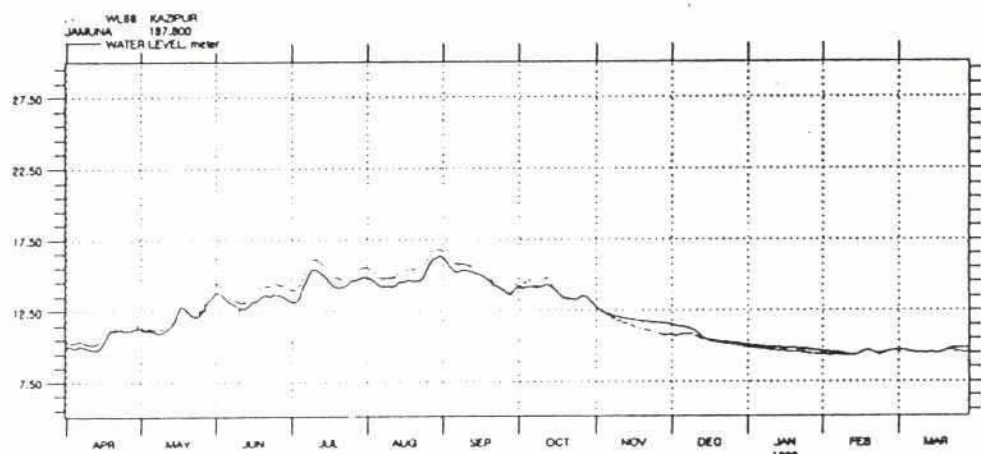
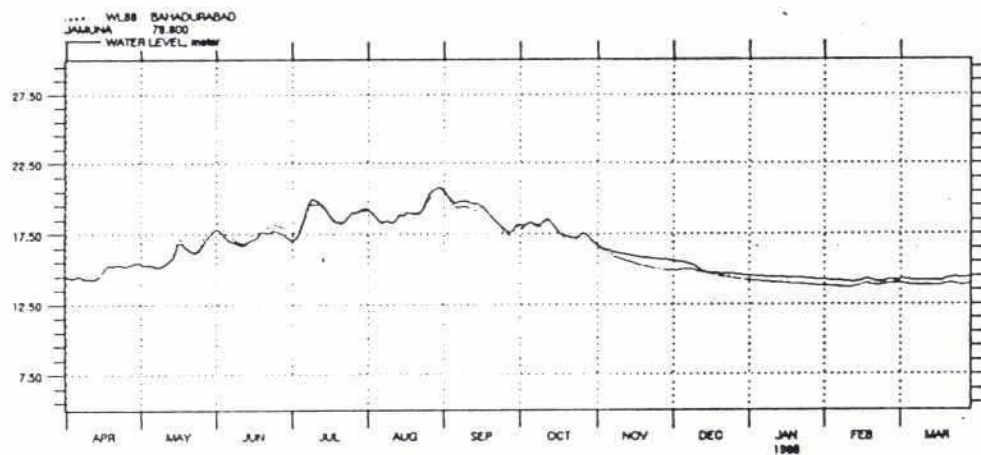
BOUNDARY FILE : GM1 - Q88R.BSF
CALCULATED : 3 - APR - 1991, 17:34

ANNEX 3:PART I

FIGURE : 2.3 a

Key:

..... Observed
 — Simulated



BRAHMAPUTRA RIVER TRAINING STUDIES
 Comparison of simulated and observed 1988 flood events using
 BRIS 1 - D model

DATA FILE : BR1-0391.RDF
 RESULT FILE : BR1-C3.RRF

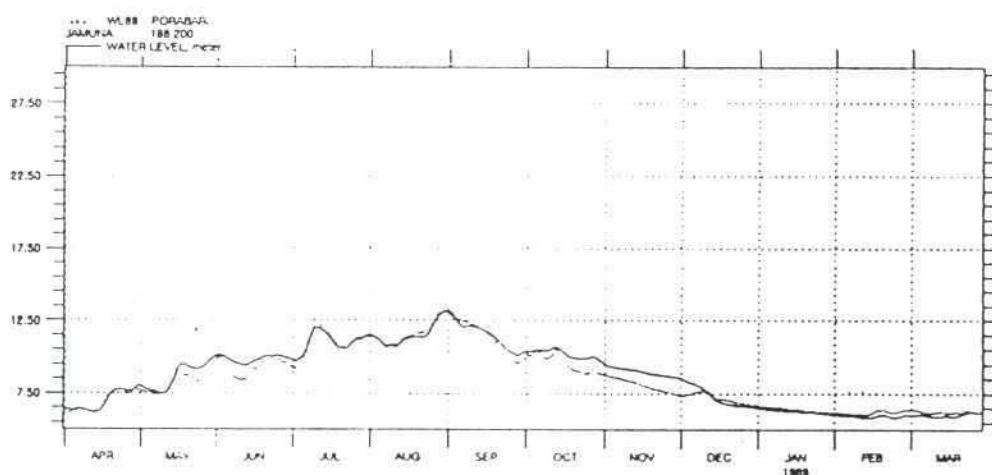
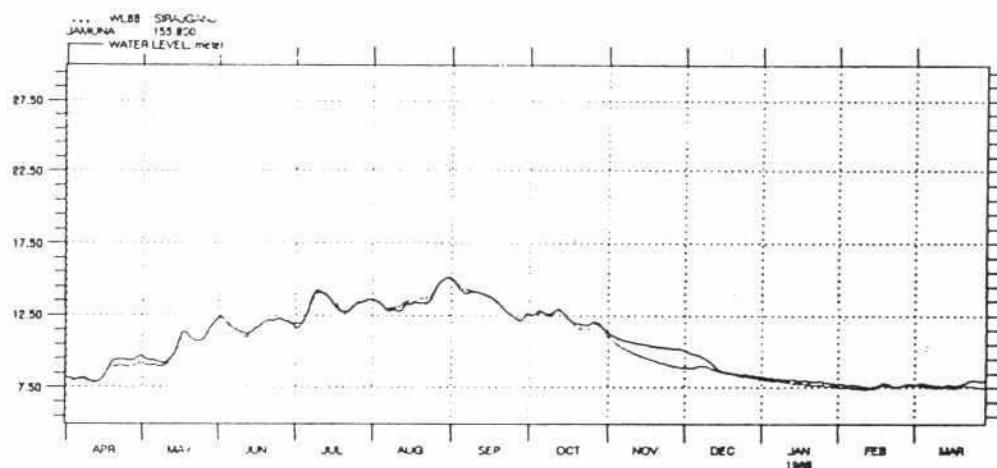
BOUNDARY FILE : GM1-Q88R.BSF
 CALCULATED : 3-APR-1991, 17:34

ANNEX 3 : PART I

FIGURE : 2.3.b

Key :

..... Observed
 ——— Simulated



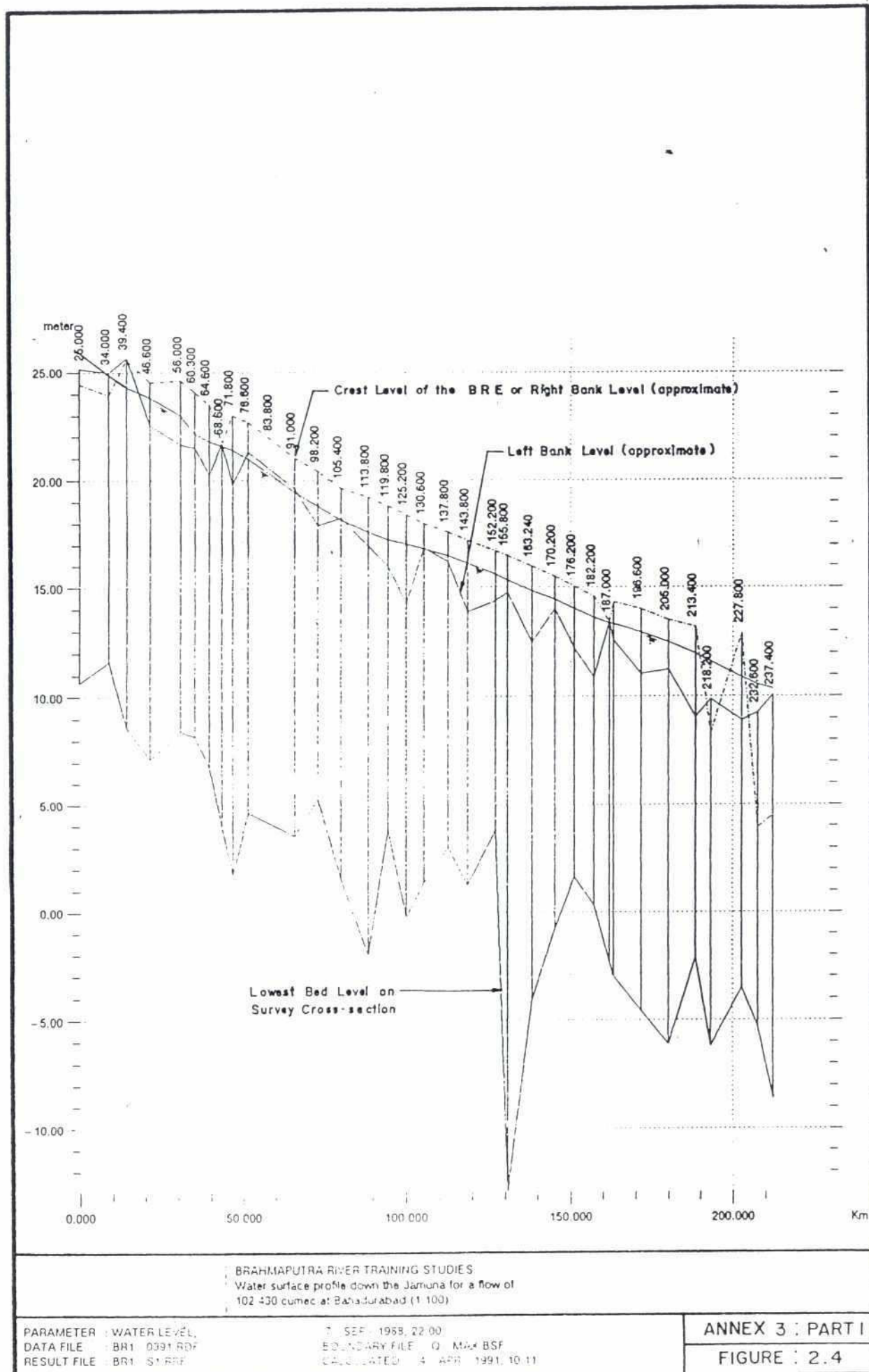
BRAHMAPUTRA RIVER TRAINING STUDIES
 Comparison of simulated and observed 1988 flood events using
 BRTS 1-D model

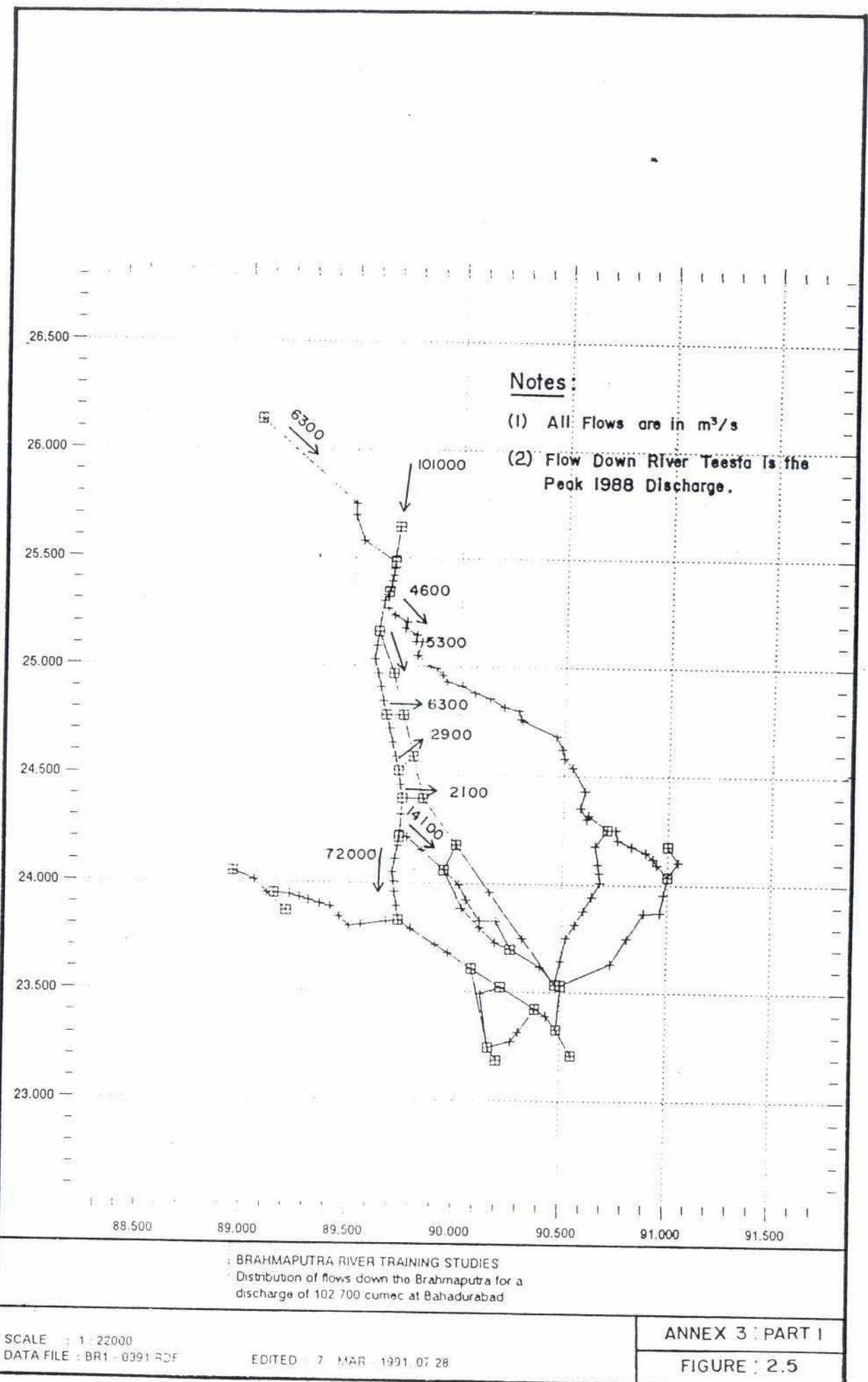
DATA FILE : BR1-0391.RDF
 RESULT FILE : BR1-C3.RRF

BOUNDARY FILE : GM1-Q88R.BSF
 CALCULATED : 3-APR-1991, 17:34

ANNEX 3 : PART I

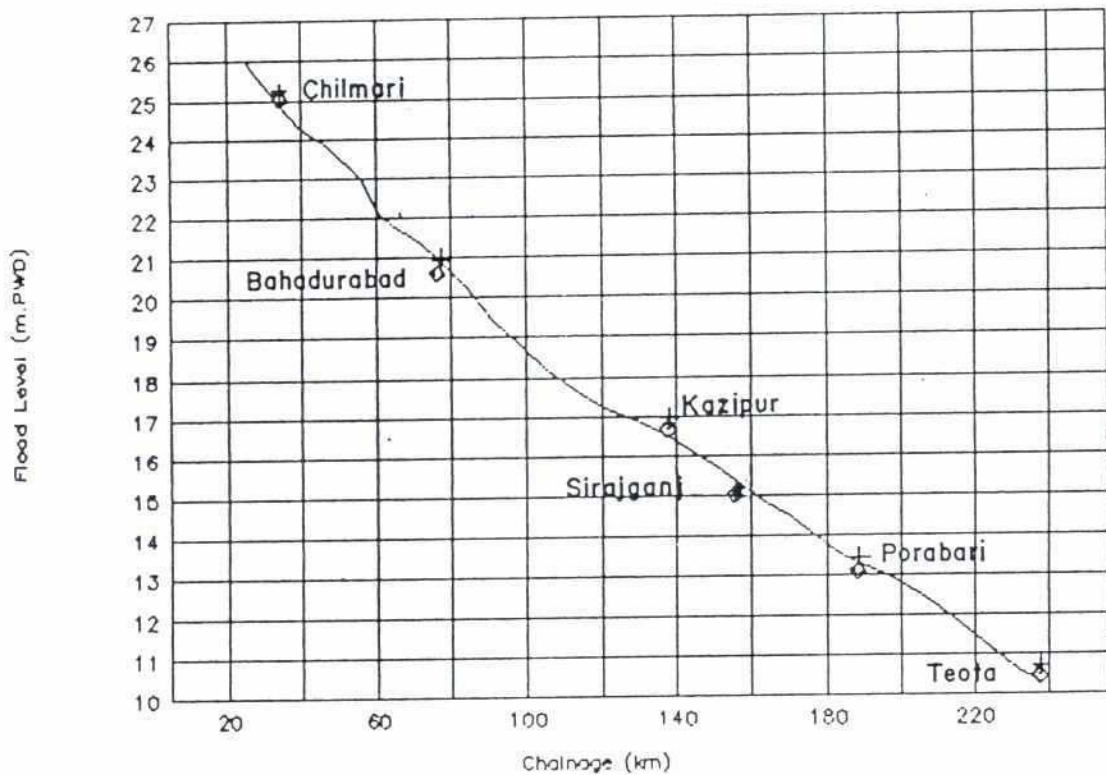
FIGURE : 2.3 c





KEY :

- ◇ 1988 Peak Observed Levels
- + Statistically Derived 1 in 100 Year Flood Levels
- Simulated Water Surface Profile for 1 in 100 Year Peak Flow at Bahadurabad.



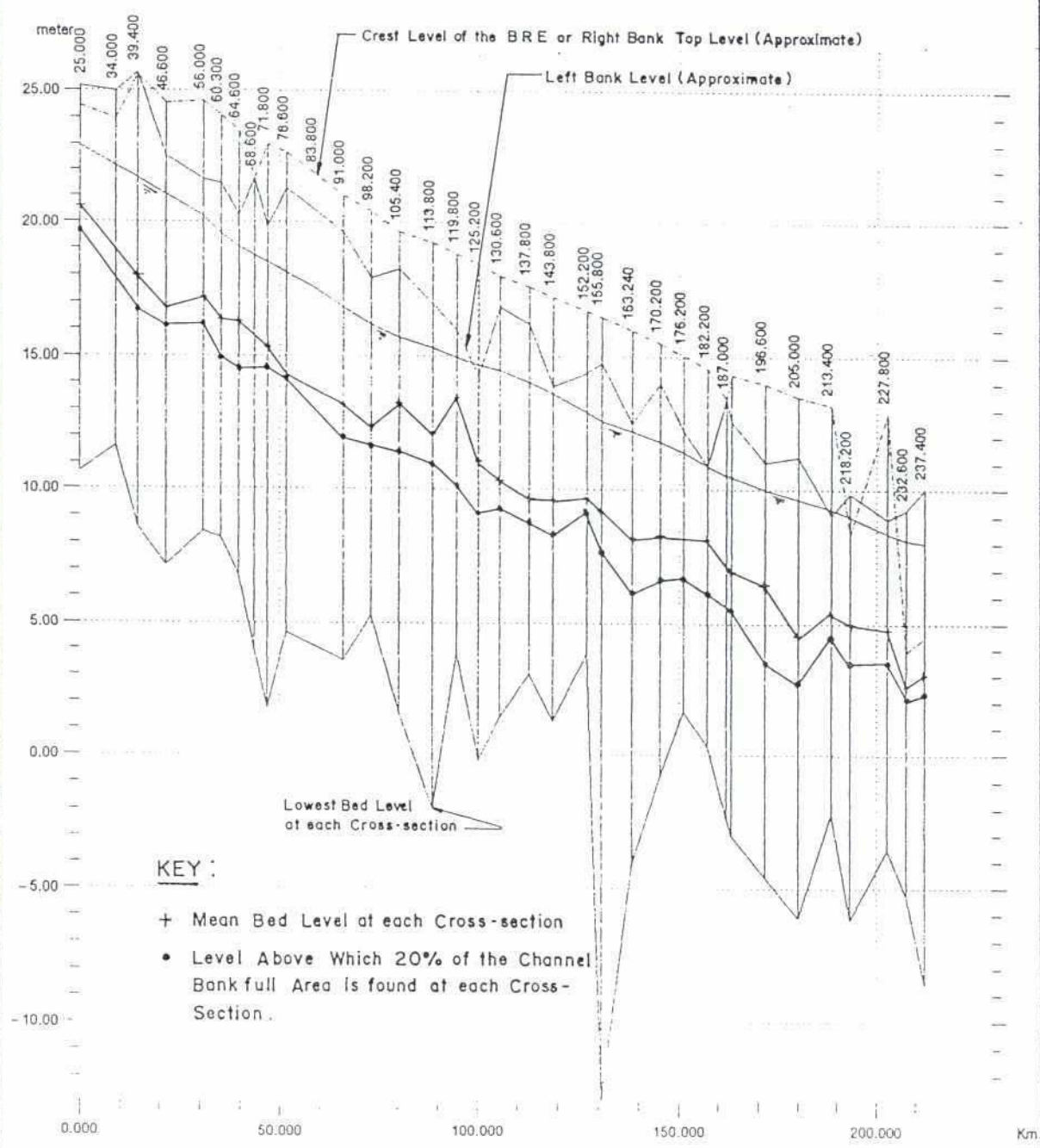
Note: Chainage Zero is at Noonkhawa



COMPARISON OF OBSERVED, SIMULATED, AND STATISTICALLY DERIVED FLOOD LEVELS ALONG THE BRAHMAPUTRA

ANNEX 3: PART I

FIGURE : 2.6

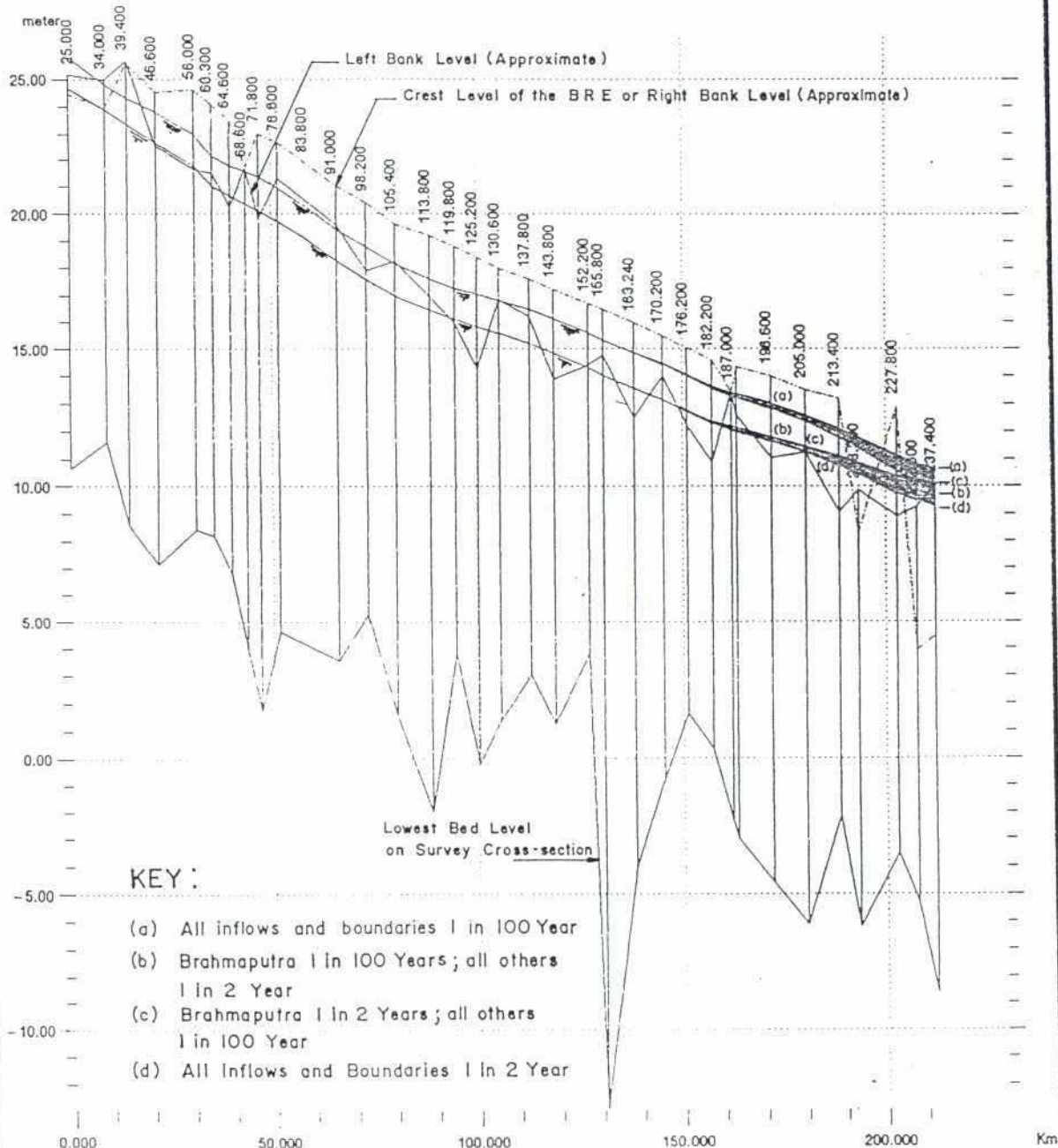


BRAHMAPUTRA RIVER TRAINING STUDIES
Water surface profile down the Jamuna for a flow of
38 000 cumec (Dominant discharge) at Bahadurabad

PARAMETER : WATER LEVEL,
DATA FILE : BR1-0391.RDF
RESULT FILE : BR1-S2.RRF

5 - AUG - 1986, 12:00
BOUNDARY FILE : Q86-1.BSF
CALCULATED : 4 - APR - 1991, 11:22

ANNEX 3: PART I
FIGURE: 2.7



BRAHMAPUTRA RIVER TRAINING STUDIES
Back Water Zones on the Brahmaputra

PARAMETER : WATER LEVEL,
DATA FILE : BR1 - 0391.RDF
RESULT FILE : BR1 - S9.RRF

24 - SEP - 1988, 12:00
BOUNDARY FILE : Q - BACKW.BSF
CALCULATED : 6 - APR - 1991, 12:39

ANNE 3 : PART I

FIGURE : 2.8

ANNEX 3: PART 2

MATHEMATICAL MODELLING
2-D MODELLING

RIVER TRAINING STUDIES OF THE BRAHMAPUTRA RIVER
FIRST INTERIM REPORT

ANNEX 3: PART 2 - MATHEMATICAL MODELLING 2-D MODELING

CONTENTS

	Page
1. INTRODUCTION	1
2. ROLE OF 2-D MODELLING	1
3. HYDRODYNAMIC MODEL OF TEST AREA 1	4
3.1 Schematization	4
3.2 Calibration	6
3.3 Coriolos Forces	6
4. MORPHOLOGICAL MODEL OF TEST AREA 1	8
4.1 Sediment Transport	8
4.2 Small Scale Morphology	9
4.3 Large Scale Morphology	10
5. PILOT MODEL OF TEST AREA 2	12
5.1 Introduction	12
5.2 Setting up the Pilot Model	12
5.3 Exploratory Run: Revetment	13
5.4 Exploratory Runs: Groyne Filed	15
6. APPLICATIONS	17
6.1 Scope of Applications	17
6.2 Design Scour	17
6.3 Bifurcation Mechanism and Stability of Anabanches	18
6.4 Migration of Submerged Sandbarss	19

TABLES

Table 4.1 Observed Bank Erosion in Test Area 1 June to July 1990

FIGURES

Figure 1.1 Location Map of Test Areas
Figure 2.1 Computational Curvilinear Grid for Test Area 1
Figure 2.2 Contour plot of model topography



Figure 3.3	Water Level at Serajganj and Shanapur
Figure 3.4	Observed Flow Velocities at 0.2 and 0.8 Depth
Figure 3.5	Observed Depth Average Flow Velocities
Figure 3.6	Simulated and Measured flow Velocities (Constant Bed Roughness)
Figure 3.7	Simulated and Measured Flow Velocities (Variable Bed Roughness)
Figure 3.8a	Simulated and Observed Flow Velocities. Upper Left Part of Model
Figure 3.8b	Simulated and Observed Flow Velocities. Upper Right Part of Model
Figure 3.8c	Simulated and Observed Flow Velocities. Lower Left Part of Model
Figure 3.8d	Simulated and Observed Flow Velocities. Lower Right Part of Model
Figure 3.9	Simulated Water Surface Elevation
Figure 3.10	Simulated Water Depth
Figure 3.11	Difference in Simulated Water Level with and without Coriolis force included
Figure 4.1	Simulated Sediment Contration (g/l)
Figure 4.2	Simulated Sediment Transport Vectors
Figure 4.3	Simulated Suspension Concentration (g/l). Reduced Water Temperature
Figure 4.4	Simulated Sediment Transport Vectors. Reduced Water Temperature
Figure 4.5	Simulated Dune Height
Figure 4.6	Simulated Dune Length
Figure 4.7	Simulated Chezy Roughness Coefficient
Figure 4.8	Observed Change of Bed Topography Between June to July
Figure 4.9	Simulated Bed Level Changes from June to July
Figure 4.10	Simulated Bed Level Changes Disregarding Bank Erosion
Figure 5.1	Curvilinear Grid for Test Area 2
Figure 5.2	Model Topography
Figure 5.3	Simulated Flow Distribution
Figure 5.4	Simulated Model Topography
Figure 5.5	Additional Erosion due to Absence of Bank Erosion Revetment Along Western Boundary for $y < 1000$ m
Figure 5.6	Modified Model Topography (main channel entering along bank)
Figure 5.7	Flow Distribution Over Modified Topography
Figure 5.8	Lay out of Groyne Filed and Simulated Flow Distribution
Figure 5.9	Simulated Flow with Existing Bathymetry
Figure 5.10	Flow Around Groynes. Main Channel Along Bank. (detail from Figure 5.8)
Figure 5.11	Flow Around Groynes. Impinging Main Channel. (detail from Figure 5.9)
Figure 6.1	Bank Erosion Due to Sub-surface Sand Bar

APPENDICES

A Description of System 21

REFERENCES

ANNEX 3: PART 2 - MATHEMATICAL MODELLING: 2-D MODELLING

1. INTRODUCTION

This Technical Annex 3 to the First Interim Report for the River Training Studies for the Brahmaputra River (BRTS) describes the mathematical modelling work completed to date and outlines the activities that will be undertaken during the coming nine months leading up to the Second Interim Report.

Part 1 of this Annex covers the one dimensional (1-D) hydrodynamic and morphological modelling and the interaction with other FAP components, particularly FAP 2, FAP 3 and FAP 25. Part 2 concentrates on the two dimensional (2-D) morphological modelling

2. ROLE OF 2-D MODELLING

The 2-D mathematical modelling is only one part of the package of study tools that is utilized within BRTS to achieve the study objectives. The elements of the full package that deals with river responses are:

- geomorphological studies
- 1-D mathematical modelling
- 2-D mathematical modelling
- physical modelling

These elements are complementary and have some interfaces. The geomorphological analysis deals with the historical behavior of the river in terms of some key parameter and identify trends in channel planform development. The 1-D mathematical model describes the water level variation along the river and the overall river response in term of water and bed level to large scale changes such as for instance the implementation of a left embankment along the river. The 1-D mathematical model also provides boundary conditions to the 2-D mathematical and to the physical models.

The main strength of the physical models are their capability to simulate highly complex 3-dimensional flow phenomena, which are not suitable for mathematical modelling. The physical models are therefore mainly utilized for the simulation of the processes in the vicinity of structures, such as for instance groynes and revetment. The principal limitation of physical models are associated with mobile bed modelling and it is in this context the 2-D mathematical model can make an important contribution.

The primary role of the 2-D model will be to examine the time dependent aspects of scour and bed form development that cannot be simulated with the physical modelling. For example, bend and confluence scour are clearly important processes influencing the general morphology of the river in both the short and longer term. They are also of crucial importance to the designer of river training works and a better appreciation of mechanisms involved will make for more cost effective designs. Similarly a better understanding of the influence of the migration of large sand bars on the growth and decline of anabranches will be of great value for both river behavior prediction at the local level and for deriving cost effective measures for influencing this behavior. In these ways 2-D modelling can contribute substantially to meeting the study objectives. However, it would be wrong to be over optimistic about the potential of the 2-D model.

The modelling system - as it stands to day - is not able to simulate banks erosion processes directly, which is obviously a very important phenomena in the Brahmaputra River. In addition, it is doubtful whether long term prediction are feasible at all due to the possible chaotic behavior of the river system (see BRTS, 1990).

The overall objectives and strategy of the 2-D modelling activity within BRTS have been described in details in the "Working Paper on 2-D modelling (BRTS, 1990). The first step in meeting these objectives is to establish an applicable 2-D modelling tool for the Brahmaputra River. To do this, two base models will be set up; one for calibration and one for verification of each of the sub models of System 21 (i.e. hydrodynamics, sediment transport, hydraulic resistance/bed forms and large scale morphology) on the conditions prevailing in the Brahmaputra. The two mathematical models are being set up for Test Area 1 and a second test area around a sharply curved bend at Kazipur. The locations of the two test areas are shown in Figure 2.1.

Test Area 1, which has already been surveyed during the monsoon and during falling stage in November, covers the entire width of the river. Analysis of the Test Area 1 data are described in Annex 1: Part 3.

With respect to calibration, the principal feature missing from Test Area 1 is severe bend scour. In view of the significance of helical flow and the associated bend scour, an additional test area was clearly required. It was earlier anticipated that the FAP 24 river survey programme, which will concentrate on the four major rivers, would generate relevant data and that this could be utilized to fulfil the requirements for model calibration. However in the event the FAP 24 programme will not now come on stream until too late for our purposes. It was therefore necessary to select a second test area that would satisfy the essential calibration needs.

The area chosen is centered on Kazipur and features two actively eroding bends, one of which has a scour depth greater than any other recorded on the river. Resources available under this study have limited the scope of the survey to the one anabranch but this will be adequate for the purposes of model calibration.

The mathematical model of the bend at Kazipur will also be used for verification of the hydrodynamic model and sediment transport formulations obtained during calibration of the model on Test Area 1.

Test Area 2 (Kazipur) has been surveyed once in the dry season (December 1990) and will be re-surveyed in June and September 1991. The surveys includes bathymetry, char topography, bank line retreat, flow distribution and sediment transport.

The work which has been carried out up to the First Interim Report has mainly concentrated around:

- The establishment of a software environment for the 2-D modelling system on BRTS's 386 PC with UNIX operating system. This has included the development of a number of interface programmes for transfer of data from BRTS's field data base to System 21, and modification of plotting software to suit the available hardware (printer and plotters).

Annex 3: Part 2 - Page 3

- Analysis, quality check and processing of the large amount of data collected in Test Area 1. This work has resulted in a "Data Analysis Report" (Annex 1: Part 3).
- To establish and calibrate the mathematical model of Test Area 1.
- To establish a pilot model of Test Area 2 (Kazipur) and make some exploratory runs with the model.

In Appendix A of this report the capabilities of the software system is described. Setup and calibration of the hydrodynamic model of Test Area 1 is described in Section 3. In section 4 the calibration of the sediment transport model and both the small and large scale morphological model are described. Setup and exploratory runs with the Kazipur model is described in Section 5 and finally in Section 6 further applications of the model is described.

3. HYDRODYNAMIC MODEL OF TEST AREA 1

3.1 Schematization

In the schematization phase the extension and resolution of the computational grid have to be selected. The extent of the base models is determined by data availability (bathymetry and boundary conditions). The boundaries of the computational grids are determined from the coordinates of the recorded start and end of track during the bathymetry survey.

The weight function in the curvilinear grid generator (see Appendix A, Section 2) has been selected in such a way that the grid is more dense in areas with large depths. However, the shape of the boundaries of the modelling area in combination with the required orthogonality and the requirement that grid lines from the sub grids (three sub grids have been generated and subsequently surveyed) have to join as differentiable curves set some constraints on how much weight the depth can be given during grid generation.

An adequate mesh size in the computational grid has been obtained in the following way. The flow phenomena which have to be modelled can be considered to be quasi-steady. An important length scale in 2-D horizontal river flows, which has to be resolved in the mathematical model, (see Struiksma et al., 1986), is:

$$L = C^2 h / 2g$$

where:

C Chezy roughness coefficient
g acceleration due to gravity
h water depth

Typical values for C and h in the Brahmaputra are $65 \text{ m}^{1/2}/\text{s}$ and 8 m, respectively thus L is of the order of magnitude 1,700 m. A space step of the order of magnitude of 200 m will therefore result in a good accuracy for the flow, and is adopted in the dominant flow direction. In transverse direction a somewhat smaller space step is applied in order to resolve the lateral topography variation. A transverse space step of approximately 100 m is expected to provide sufficient accuracy. For Test Area 1 this resolution is achieved with a model setup with approximately 50 by 40 (2,000) grid points. The resulting grid is depicted in Figure 3.1.

The bathymetry used for the calibration of the hydrodynamic model is the one surveyed concurrently with the velocity measurements, i.e. the July data (see Annex 1: Part 3). The topographical data from the survey also reflects the large sand dunes (height 3 m) which are not represented directly in the 2-D model, but rather as bed roughness elements. The surveyed data therefore have to be smoothed (and interpolated) before the data can be used in the 2-D model. The smoothing, however, should not reduce the main features of the bed topography, which governs the overall flow distribution. A contour plot of the smoothed model bathymetry is depicted in Figure 3.2.

The boundary conditions for the model are the observed flow distribution (magnitude and direction) at the upstream boundary and the observed water levels at the downstream boundary.

Water level data have been collected at 3 locations in the vicinity of Test Area 1. Two of these stations (Sirajganj and Olipur) were operated by BWDB while the third one, Shahpur, has been established for the current study.

Reliable data from Olipur are only available for the post monsoon period as it turned out that the gauge had a bench mark error. This was corrected in connection with a gauge shift. Unfortunately, the bench mark of the old gauge position was not determined, so that the monsoon data can not be used.

The Shapur bench mark still has to be re-checked, so the data presented here are preliminary. The recorded water levels for the period covered by the monsoon survey are depicted in Figure 3.3.

The distance between Sirajganj and Shapur gauge station has been determined from their Decca coordinates and is approximately 17.5 km. This suggests a mean water surface slope of about $0.85 \cdot 10^{-4}$. Interpolation of the water levels to the up and down boundary of the computational grid suggests mean water levels in the period of the flow velocity measurements of 13.29 and 12.40 m, respectively. The total discharge is approximately 42,000 m³/s, see BRTS (1991).

During calibration of the hydrodynamic model the water level of 12.40 m was used as downstream boundary condition in the right anabranch. The water level of 13.29 m is one of the targets for the calibration. Another important feature the calibrated model should reproduce is the relative flow distribution between the two main downstream anabranches (12%/88%), see BRTS (1991).

The most important data, for the calibration of the hydrodynamic model, however, are the large amount of flow velocities (magnitude and direction) measured in Test Area 1. The river bed is covered with large 3-dimensional sand dunes, typical of the height 3 m, see (Annex 1: Part 3). These dunes introduce fluctuation in the velocity profile, especially in the direction and magnitude of the near bed flow velocity. This is illustrated in Figure 3.4, where velocity vectors measured at 20% and 80% of the water depth are plotted. In the mathematical model these sand dunes are not included directly, but taken into account as bed roughness elements. The model will therefore only simulate the overall flow distribution.

In Figure 3.5 the observed depth averaged flow velocity field is depicted. The magnitude of the flow vector has been obtained as a simple arithmetical sum of the velocities in the profiles (between 2 and 5), whereas the directions have been obtained by weighting the individual observation in the profiles with the magnitude of the velocity vector.

3.2 Calibration

The calibration of the hydrodynamic model has basically been obtained in two steps:

- 1) First a constant roughness coefficient was applied to the entire area. By trial and error this roughness coefficient was varied until the correct upstream water level were obtained. The roughness coefficient obtained in this way was $C = 74 \text{ m}^{1/2}/\text{s}$, which is somewhat larger than suggested by JMBA. The reason for this discrepancy may be that the roughness coefficient given by JMBA is an global value, thus applying for the entire river on average. It therefore does not take into account variability of the roughness due to for instance variation along the river of the mean sediment grain size.

The result of this first rough calibration of the model is depicted in Figure 3.6.

It is seem that the model in general underestimates the flow velocities in the deeper parts and overestimates the velocities at the shallow areas.

- 2) In the second step the roughness coefficient was allowed to vary with the water depth in the following way

$$C = C_0 (D/D_0)^a$$

where:

C_0 is the mean roughness coefficient obtained above,
 D is the local depth,
 D_0 the overall mean depth and a an exponent determined via calibration.

An exponent of $a = 0.25$ was found to give an adequate agreement with the observed flow velocities. Such an roughness distribution correspond well with the finding from the dune tracking survey, which showed that the dune size water depth ratio (thus the bed form and total resistance) were quite large at shallow areas. It is also conform with the roughness variation used in the 1-D model of the Brahmaputra (decrease of resistance with increasing stage).

Results of the calibrated model are depicted in Figures 3.7 to 3.10. The agreement with the observed flow velocities - bearing in mind the natural fluctuations of the observed velocity distribution - is quite good. The discharge distribution between the two downstream anabranches is 87:13, which is close to the observed values.

3.3 Coriolos Forces

The Coriolis force has often been mentioned as an agent for westward migration of the Brahmaputra. This point is discussed in more detail in Annex 1: Part 3. Here the effect of the Coriolis force on the flow simulated with the 2-D model will be demonstrated.

The simulation presented in the previous sections included the effect of the Coriolis force. A simulation without this effect was also carried out. It turned out that it did not have any detectable influence on the simulated velocity distribution, whereas minor water level differences were noticed.

Water level differences between the simulation with and without the Coriolis's force included is depicted in Figure 3.11. It is noticed that the water level is slightly higher along the right bank show along the lift.

This does not imply that the Coriolis's force does not have any influence on the condition in the Brahmaputra, because it also gives rise to secondary flow as discussed in Annex 1: Part 3.

4. MORPHOLOGICAL MODELS OF TEST AREA 1

4.1 Sediment Transport

The suspended sediment transport data collected in Test Area exhibited a very large random scatter due to the application of a "instantaneous" sampler. This is further discussed in Annex 1: Part 3. Because of this scatter the data are not well suited for detailed calibration of the sediment transport model in the 2-D model. In connection with the Test Area 2 survey during the coming flood season a time integrating sampling techniques will be applied. This will involve pumping of very large samples over several minutes allowing for an accurate estimation of the time-mean suspended load concentration and the size distribution of the sediment.

The sediment transport model was therefore preliminarily calibrated on previously collected sediment transport data at Bahadurabad and on the mean value of the large amount of suspended sediment samples collected in Test Area 1 during the monsoon survey. This process has been discussed in details in Annex 1: Part 3, where various sediment transport models were tested against the data on total suspended bed material load (i.e. minus wash load). The conclusion of this analysis was that the sediment transport conditions in the Brahmaputra are well described with two models:

- 1) The Engelund & Fredsoe model (Engelund & Fredsoe, 1982) with the concentration profile corrected for high near bed concentrations (the MOVA model or Modified Vanoni-profile).
- 2) The van Rijn model (van Rijn, 1984a and 1984b) with the bed boundary condition applied at 1% of the depth above the bed.

Trial runs with these two models showed that the MOVA model performed best on the Test Area 1 data, and this model has been used in all subsequent model simulations.

Simulation results, in the form of the depth averaged concentration, is depicted in Figure 4.1. This simulation has been carried out with a grain diameter, $d_{50} = 0.15$ m, fall velocity $W_f = 0.020$ m/s and viscosity $\mu = 1.0 \cdot 10^{-6}$ m²/s (corresponding to a temperature of the water of 20°C). The corresponding vector plot of the transport is depicted in Figure 4.2. The figures show that the highest concentrations are associated with (relative rapid) flow over shallow areas, but the largest transport takes place over the deepest sections where the flux of water is much larger. In the upper left corner of the model strong gradients in the simulated sediment transport is noticed. This is probably associated with migration of a sub-surface bar.

As an indication of the sensitivity of this simulation result a simulation with a lower water temperature (15°C), hence larger viscosity ($1.15 \cdot 10^{-6}$ m²/s) and smaller fall velocity (0.016 m/s) has been carried out. The result, depicted in Figure 4.3 and 4.4, shows that the concentration and transport increases significantly. It should be mentioned that the low temperature of the water is associated with winter conditions (thus low flow), so a discharge of $Q=42,000$ m³/s is very unlikely for these conditions.

4.2 Small Scale Morphology

Small scale morphology deals with the change of dune dimensions (i.e. height and length) due to unsteady flow phenomena and the associated change of sediment transport. The dune dimension determines to a large extent the hydraulic resistance of the river bed. A time scale for these changes is the time required for a dune to migrate its own length. In the Brahmaputra during the monsoon the dunes are typically 200 m long and track with a speed of 10^{-3} m/s, see Annex 1: Part 3. The time scale is therefore about 2 days. This is normally significantly shorter than the time scale of the flood waves, hence a quasi-steady description of the sand dune dimension is sufficient for monsoon conditions. During lower stages the time lag may be very important, because the time scale for modification of the dunes increases significantly due to the much smaller sediment transport rates.

The Fredsoe model (Fredsoe, 1979) is used to calculate the dune dimensions and the associated hydraulic resistance. The method used for calculation of the hydraulic resistance is described in details in Annex 1: Part 3, where also calibration of this model is described.

The dune dimension model of Fredsoe calculates the dune height and length as a function of:

- the bed load transport
- the part of the suspended load trapped in the downstream wake of the dunes
- the rate of increase of total load with velocity

The bed load transport has been calculated with the van Rijn model, whereas the MOVA model has been used for the suspended load and for calculation of the part of the suspended load trapped in the wake of the dunes (see Annex 1: Part 3).

Simulation results, in terms of dune height and length and associated hydraulic resistance are depicted in Figures 4.5, 4.6 and 4.7. The simulation results shows that the simulated dune height is somewhat smaller than the observed (typical of the order of magnitude 3 m, see Annex 1: Part 3). The reason for this discrepancy may be an insufficient calibration of the sediment transport relations or the three-dimensional character of the sand dunes as discussed in Annex 1: Part 3. The simulated dune length is slightly shorter than the observed ones. As a consequence the simulated hydraulic resistance is smaller than observed in the river. As a part of the Monsoon survey in Test Area 2 more data on dune dimensions will become available, and a re-calibration of the small scale morphology model will be carried out.

Small scale morphology (i.e. the change of dune dimensions) may be a key factor in determining the hydraulic resistance in the Brahmaputra. It has been observed that at large discharges the hydraulic resistance decreases in the Brahmaputra. It is natural to associate this with transition from dune covered bed to plane bed. However, the field survey carried out during the 1987 monsoon in connection with the Jamuna Bridge feasibility study did not reveal any general transition to plane bed during high discharges (JMBA, 1989). Analysis of the dune tracking carried out under this study did not reveal any plane bed either.



4.3 Large Scale Morphology

Large scale morphology is here defined as dealing with the form and changes of the river bed taking places on larger time and length scale than those applying to sand dunes. This also implies that for general scour in the context of 2-D modelling it deals with, for instance, bend scour and migration of large subsurface sand bars.

In the calibration of the model on Test Area 1 the effort so far has been concentrated on simulating the changes of bed level taken place between the June and July bathymetrical surveys. Simulation of the changes observed from July to November will be carried out following final calibration of the 1-D model, which will provide boundary conditions for this simulation.

As mentioned in Section 2, System 21 in its present form has a significant limitation for application to the Brahmaputra: it is a fixed bank model. From the bathymetrical data it is seen that some bank erosion have taken place along the right bank in the upper part of the Test Area 1 and a major shift (bank erosion compensated by deposition on the other bank) of the left anabranch in the downstream end of the model.

This bank erosion has been dealt with in the following way. The bathymetry observed in June has been shifted according to the observed bank erosion so that it "fits" into the computational grid generated for the July bathymetry and bank line. The shift of the bathymetry is summarized in Table 4.1 where also the estimated bank erosion rates are given. The large bank erosion rates in the downstream end of the model area have been introduced into the model as sediment sources.

The shifted topography has formed the starting point for the morphological simulation.

In the period between the June and July surveys the upstream section (C50) of the Test Area 1 model has been subjected to significant changes, see Annex 1: Part 3. As boundary condition for the sediment transport model it has been assumed that this changes has taken place linearly, i.e. at the upstream boundary the bed level has been assumed to given by

$$z(t) = z_{\text{june}} t/T + z_{\text{july}} (1 - t/T)$$

where:

t is the time elapsed since the June survey
 T the total time between the surveys
 (z_{june} is the shifted bed levels).

Moreover, at the upstream boundary it has been assumed that the sediment transport rate is in equilibrium with the (instantaneous) bed level and flow conditions. The flow velocity has been assumed to be proportional to the square root of the depth. The total discharge ($Q = 42,000 \text{ m}^3/\text{s}$) and the downstream water level (12.4 m) were assumed to be constant during the entire simulation. Referring to Figure 3.3 this seems to be an acceptable approximation.

The observed references between the June (shifted) and July topographies (both smoothed to eliminate the influence of sand dunes) are depicted in Figure 4.8. The corresponding simulated is depicted in Figure 4.9. Although the sediment transport model only can be considered to be preliminary calibrated, the figures shows that the morphological simulations reproduce the main features of the observed bathymetrical changes. Especially the large sedimentation in the upper left corner of the model is well described. This sedimentation is probably associated with migration of a sub-surface bar. Also the deposition on the wester side of the main anabranch in the downstream part of the modelling area is reproduced in the model simulation. The model does not reproduce the erosion in the outer part of the curved thalweg in the downstream end of the model. With the re-calibration of the model on the Test Area 2 data, the model performance on bend scour is likely to improve. Sedimentation and erosion in shallow areas does not seem to be described very well. Also this will hopefully improve with the re-calibration of the sediment transport model on the Test Area 2 data. Some of the discrepancy with the observed result could also be due to insufficient smoothing of the bed forms in both the June and July topography.

In order to investigate the influence of bank erosion a simulation without the above mentioned sediment sources and sinks is also presented. The simulated erosion/deposition pattern is depicted in Figure 4.10. This figure shows that the erosion of the thalweg in the downstream end of the modelling is now substantially larger, suggesting that bank erosion has a significant effect on the bathymetry.

5. PILOT MODEL OF TEST AREA 2

5.1 Introduction

Test Area 2 is located at Kazipur north of Sirajganj, see Figure 1.1. The area is chosen because it features a very active eroding bend which has a scour depth greater than any other recorded in the river, and because Test Area 1 did not include any severe bends. The surveyed area only covers one anabranch, which is deemed sufficient to meet the objectives which are:

- refinement of the model calibration with respect to helical flow and bend scour
- refinement of the sediment transport model calibration (The Test Area 1 sediment data exhibited too large scatter, see Annex 1: Part 3)
- verification of the model calibration

Test Area 2 has been surveyed once during the dry season (December, 1990). This survey comprised:

- bathymetry
- float tracking
- char topography
- bank line survey

The data have only a preliminary processing and analysis of the data has been completed to date and there are some indications of error in the char topography data; thus the model presented here is only preliminary.

Test Area 2 will be re-surveyed in June/July and September 1991. These surveys will include the same items as the December 1990 survey and in addition suspended sediment and bed sampler will be collected. A time integrating sampling method (i.e. very large samples) will be used to minimize the scatter in the data, see Annex 1: Part 3). The main outcome of the re-surveys will be the bed and char topography dynamics and an accurate estimate of the bank erosion rate.

The objectives of establishing a pilot model of Test Area 2 are.

- to setup a model so that the framework for further modelling is ready when the remaining data becomes available.
- to establish a model for demonstration of the interaction of bank protection and river training structures with the flow and sediment transport.

In Section 5.2 the setup of the base pilot model is described. the effect of revetment (the absence of bank erosion) on the scour depth is demonstrated in Section 5.3. In Section 5.4 the effect of a groyne field on the flow distribution is explored.

5.2 Setting up the Pilot Model

The survey of Test Area 2 during December 1990 included bathymetry of all the channel and topography of the char between the bank and the large mid channel char. The mid channel char itself was not surveyed. This

introduces some uncertainties to where the left boundary of the model is located. This problem will be solved with the high stage bathymetrical data to be collected during the coming flood season becomes available. For the pilot model it has simply been assumed that the left (east) land/water boundary is located along the boundary of the surveyed area.

The right (west) boundary of the modelling area follows the very distinct bank line. The north and south boundary are located along the boundaries of the surveyed area.

The bathymetrical and topographical data have been interpolated into a regular grid and form the basis for both the grid generation and model topography. The grid has been generated using the depth as weighting function (depth attraction). A grid with 38 by 38 points was judged to be reasonable for the revetment simulations, whereas a grid with double density (in both directions) were used for the groyne simulation. The generated grid (low density) is depicted in Figure 5.1 and the model topography in Figure 5.2.

From Figure 5.2 it is seen that the main channel in entering the modelling area in the central part, it is directed north south until it meets the bank and is deflected and follow the bank line until it leaves the modelling area. A deep scour hole is formed where the main channel curves as it meets the bank. Along the eastern boundary of the modelling area a secondary channel is observed. Along the western bank in the upper part indication of an abandoned (?) channel is noticed. The bank in this area has previously been subjected to bank erosion. The survey in the coming monsoon will show whether this channel has diminished permanently.

The boundary conditions have for the demonstration runs been selected to simulate high stage flood conditions.

The float tracking data have not been processed yet, thus the discharge (northern) boundary condition was not known. For the exploratory runs presented in the following a discharge of $18,000 \text{ m}^3/\text{s}$ has been used. The distribution of the discharge along the boundary has been taken proportional to the square root of the local depths. The flow has been assumed to enter the area at an angle of 90° to the boundary.

The downstream water level has been selected to be 15.5 m. These boundary condition have been used in all the model simulations.

5.3 Exploratory Run: Revetment

The bank line in the lower left corner of the model has in the past been subjected to severe bank erosion. This eroded material will have to be carried away by the flow and in this way alleviate the scour depth in front of the bank line.

Suppose that revetment, or other bank protection measures are constructed, the bank erosion would become negligible along the revetment, and hence the scour depth near it will increase. In order to simulate this effect simulation with and without bank erosion have been carried out. It has to be emphasized that the simulation result does not represent local scour that will appear at the head and tail of the revetment due to different hydraulic resistance of the revetment material and the natural bank.

For the simulation with bank erosion (without revetment) the amount of eroded bank material has been estimated in the following way.

- near bank height (from top of bank to deepest scour) = 20 m
- porosity of sediment = 0.4
- sand contents = 50 % (thus 50 % silt, which is assumed not to have influence on bed topography).
- mean monthly bank erosion rate = 50 m

The amount of sediment introduced into the model is therefore.

$$0.50 (1-0.4) 50\text{m}/(30 \times 24 \times 3600 \text{ s}) 20\text{m} = 1.2 \times 10^{-4} \text{ m}^2/\text{s}$$

The applied bank erosion is a very conservative estimate. The 1991 field programme in Test Area 2 will bring about the actual bank erosion rates.

From the simulated flow distribution (see Figure 5.3) it was judged that the major bank erosion on the west bank takes place for $y < 10,000 \text{ m}$ (cf. Figure 5.2). The eroded material was introduced into the model in this section around the toe of the bank.

As the objective of the simulation was merely to demonstrate the effect of revetment it has not been attempted to simulate any actual hydrograph, but the model has been run continuously for 1.5 month with the "bank full" boundary condition mentioned above.

The simulated flow distribution for the initial bathymetry is depicted in Figure 5.3. The main feature at this flow distribution are:

- a strong flow curvature as the main flow meets the bank;
- a significant increase of flow velocity towards the southern model boundary;
- almost zero flow over the large subsurface bar;
- substantial flow curvature at the northern boundary.

The strong curvature of the flow as the main channel meets the bank correspond well to the observed extreme bend scour here.

The significant increase of flow velocity in the lower end of the model under natural conditions will result in severe erosion in this area in the morphological simulation (see below). It is obviously caused by the constriction of the flow width (area). It may be due to the earlier mentioned possible reference level error in the char survey (thus the flow rate over the char is underestimated) in combination with flow over parts of the mid channel char to the left of the modelling area. The survey during the 1991 flood season will shed light on this. It may however also partly reflect the conditions in the river. In that case a substantially larger bank erosion rate is required to prevent substantial erosion of the river bed.

The curvature of the flow in the main channel in the upper part of the modelling area is probably caused by the applied boundary conditions; the flow is entering the modelling area at 90° to the model boundary.

The result of the mobile bed (morphological) simulation is depicted in Figure 5.4. Comparing with Figure 5.2 (the topography at the start of the simulation) it is seen that in general the contour lines are straight. This is because the original topography reflects dunes and other bedforms

which are being damped in the morphological simulation. Moreover, the simulated bed topography shows larger erosion in the lower part of the model, which may be associated with inaccuracies in the data and model setup as mentioned above.

Due to these uncertainties too much weight should not be attached to the simulation result. However, the difference in bed topography simulated with and without bank erosion is probably a fairly good estimate of the additional erosion that will take place if the banks were reveted. A contour plot of this is depicted in Figure 5.5.

The figure shows that the revetment will give rise to an additional erosion of 1.8 m. It should, however, be emphasized that this is with a very conservative estimate of the bank erosion rate and the simulation was only run for a relative short period, so the result does not reflect the equilibrium conditions.

5.4 Exploratory Runs: Groyne Field

Bank protection and river training structures are designed for an expected lifetime, which is larger than the time scale for changes of the braiding channel pattern. This implies that the structures should perform adequately both for the conditions from which the bank is being protected and also for other conditions which can be expected to occur during the projected lifetime of the structures.

One parameter which is likely to change is for instance the angle of attack. The Test Area 2 model can be used to demonstrate the effect of such a change. As mentioned in Section 5.1 there is some indication that the main channel (thalweg) has shifted from a course following approximately the bank to the impinging course observed in the December 1990 survey. System 21 has been used to demonstrate how a groyne field designed for the "near bank thalweg condition" performs in the existing condition (as surveyed December '90).

To this end a model topography was designed with the main channel following the bank and a secondary channel located along the position of what was the existing main channel. This topography represent (schematically) the situation before the shift of the channel. The artificial model topography is depicted in Figure 5.6.

In order to resolve the groyne field and the flow in the vicinity of the groynes it is necessary to increase the grid line intensity. The computational grid used has been obtained by doubling the grid line intensity (in both direction) of the grid depicted in Figure 5.1. Typical distance between the grid lines are now 45 m and 65 m in transverse and longitudinal direction, respectively. The grid comprises nearly 6,000 computational cells.

It has to be emphasized that the simulation is for demonstration only. The flow in the wake of a groyne is mainly governed by the exchange of momentum (in a horizontal plane) between the main flow and the eddy in the wake of the groyne. This momentum exchange has no significant influence on the flow in the remaining part of the river, where the flow is nearly completely determined by pressure gradients (water surface slope), convective acceleration (inertia forces) and bed friction. The exchange of momentum is simulated via Reynold stresses which depends on the so-called eddy coefficient. Theoretically, this eddy-coefficient depends on the turbulence

level which in turn depends on the local flow conditions and its "history" (i.e. turbulence is carried with the flow as for instance sediment also is). The turbulence level and the eddy-coefficient can be simulated with a so-called k-model, which is an add on module to System 21. The purpose of the demonstration runs is to simulate the general flow pattern rather than representing the detailed flow pattern in the wake of the groynes, thus the additional computational effort involved in using the k-model is not justified and a constant eddy coefficient was applied.

Simulated flow distribution for the hypothetical topography is depicted in Figure 5.7. A hypothetical layout of a groyne field has been adjusted as a trial and error process: a groyne field has been introduced, the simulated flow field inspected and modifications of the groyne field proposed on the basis of the simulated flow distribution. The design obtained in this way is depicted in Figure 5.8 together with the simulated flow distribution. As can be seen the (cf. Figure 5.7) the groyne field protects the bank on a stretch of approximately 3 km against high near bank flow velocities. The longest groyne is about 250 m.

Simulation results with the impinging main channel are depicted in Figure 5.9. It shows that the two first groynes are now redundant, whereas the flow distribution in the lower part of the model has not changed significantly. This is also illustrated in Figure 5.10 and 5.11, where "blow-ups" of the area around the three downstream groynes are shown. It is noticed that the flow velocity in front of the first groyne (i.e. the third groyne in the groyne field) is somewhat larger in the case where the main channel approaches along the bank, whereas there is no noticeable difference in the flow velocity field at the downstream groyne.

The test was intended to simulate flow pattern rather than scour depths. On the basis of examining these alone, the groyne field appears not to be severely affected by an impinging channel. This however may change when bed topography simulation is included. The impinging channel has a much larger flow curvature than the channel following the bank line, hence, causing larger scour depths. In fact, the very deep scour hole observed in front of the bank line (see Figure 5.2) is caused by curvature of the flow where the impinging channel meets the bank line and would most probably not be there if the main channel follow the bank line. This illustrates the need for designing permanent bank protection measures for a variety of hypothetical conditions.

6. APPLICATIONS

6.1 Scope of Applications

The potential applications of the 2-D mathematical model within BRTS fall into three categories:

- refinement of design criteria in terms of maximum scour and flow velocities;
- analysing the migration of (subsurface) bars;
- improving the understanding of bifurcation mechanisms and stability of anabranches.

As a general truism, a mathematical model is most reliable when used under conditions similar to those for which it was calibrated. Given the extreme variability of the Brahmaputra, it would require a vast expenditure of time and resources to be confident that the model had been verified for all possible channel configurations. Such an investment would be grossly out of proportion to the use that can be made of the 2-D modelling within the context of this master plan. A more pragmatic approach is to calibrate and verify the model for 'type' conditions specifically selected for their relevance to the study objectives and which cover a satisfactory range of the key variables.

The variability of the channel and bank form raises serious doubt about the value of site specific models. The data collected from Test Area 1 during the monsoon and post-monsoon periods indicate that the time scale for significant channel morphological changes is relatively small. In practical terms, there is therefore little value in defining with great precision the starting conditions for a model run, with all the time and resources devoted to site surveys and model preparation that this implies. A far more cost effective approach is therefore to develop models with relatively coarse lay out and topography that are typical of the various conditions found in the river. For this purpose the following can be used:

- 'regime' relations for anabranch dimensions;
- surveys carried out for the locations identified for priority civil works;
- cross-sections surveyed by BWDB;
- recent satellite imagery and aerial photography;
- output from the 1-D model for boundary conditions.

These models can then be used to quantify parameters such as maximum scour depth and maximum flow velocities for 'worst case' design conditions, and to estimate time scales for channel changes.

6.2 Design Scour

The approach adopted in the Jamuna Bridge Feasibility Study for the determination of design scour for river training measures was to split the scour into different components: local scour, bend/confluence scour and bed form scour (JMBA, 1990). The local scour is that caused by the

structure itself e.g. scour around a groyne head, and it is normally determined from physical model tests. Confluence and bend scour is on a relatively large scale and is associated with channel alignment. Bed form scour is the maximum dune trough depth below mean bed level.

A common approach to estimating the design scour in this way is to accept that the channel pattern in the river is totally unpredictable and that therefore any construction should be designed for the expected maximum scour in the river. The components of scour not caused by the structure itself can then be obtained from direct observations, or from observations in combination with an extreme value analysis.

This approach has limitations. Firstly, for the extreme value analysis to give reliable results, a large data set is required covering low, high and extreme flow situations, whereas the database for the Brahmaputra covers mainly low flow situations, with the exception of some high flow data collected during the Jamuna Bridge Feasibility Study (JMBA, 1989) and for Test Area 1 and 2 data. Thus maximum scour resulting from an extreme value analysis of the available data will not necessarily account for possible development of bend scour and bed form during high flow conditions and does not address the likelihood of simultaneity between maximum bed form height and maximum bend scour. The 2-D model can be used to simulate the development of channel topography, bed form and flow for a series of critical discharge scenarios in order to provide a sounder basis for determining the design scour depth.

The second limitation of the conventional approach is that bend scour determined from observations is most likely to be associated with situations where significant bank erosion is taking place. This bank erosion will tend to limit the depth of scour because the transport capacity of the flow is being partially used to transport the eroded material. Since the purpose of the training measures is to substantially reduce bank erosion, it can be expected that the bend scour associated with such works will be significantly greater than that observed adjacent to an unprotected bank. The 2-D model can be used to quantify the full potential scour.

Model simulations can be carried out for a number of cases representing typical combinations of anabranch geometry and flow distribution observed in the river. One of the important cases that will be studied is that of impinging channels, where the sensitivity to the approach angle will be investigated. In addition the effect of a near bank secondary channel can be investigated.

6.3

Bifurcation Mechanism and Stability of Anabranches

It seems probable that bifurcation mechanics determine to a large extent the development of anabranches; a key variable of this process being the distribution of flow and sediment at the bifurcation point. A relative small change of this distribution may have a major impact on the anabranch development. The sensitivity of the process to these changes in sediment transport and water distribution will be explored with help of a combination of the 1-D and 2-D models. If a high level of sensitivity is indicated, the study will be taken a step further to look into the scope for human intervention in terms of dredging, sand pumping and angle of approach control, in accordance with the principles of Active Flood Plain Management.

A looped channel system is inherently unstable. Consider for instance two identical channels around an island. If one of the channels receives a fraction more sediment than the other, this channel bed will aggrade in order to increase the flow velocity to accommodate the increased sediment load. The aggradation will reduce the conveyance of this channel, hence reducing discharge and sediment transport capacity. Eventually, the channel will silt up.

In 'real life' the processes are more complicated, the development of the channels will be influenced by:

- changing bifurcation geometry;
- variation of stage and discharge;
- new channel development across the chars due to bank erosion at the char or erosion of channels due to overland flow through depressions during extreme floods.

These processes can be investigated systematically with a combination of the 1-D and 2-D model. The 2-D model representing the conditions in the vicinity of the bifurcations and the 1-D model representing the channels down to the confluence. Again, the objective is not to simulate site specific conditions, but rather to classify typical conditions in terms of channel width and length and discharge according to their potential stability.

6.4 Migration of Submerged Sandbars

Large sandbars scattered over the main anabranches can be observed from the dry season satellite images of the river. During the flood season these bars are submerged and may migrate in downstream direction changing size and shape. At many location along the river these bars are the only apparent reason for bank erosion. The process behind this type of erosion attack is sketched in Figure 6.1. An example of such a location is the near bank anabranch between Sariakandi and Chandanbaisa. It would be useful to be able to predict how these bars are created, how fast they grow and migrates in order to achieve a prediction tool for these type of bank erosion problems along a predominantly straight near-bank channel

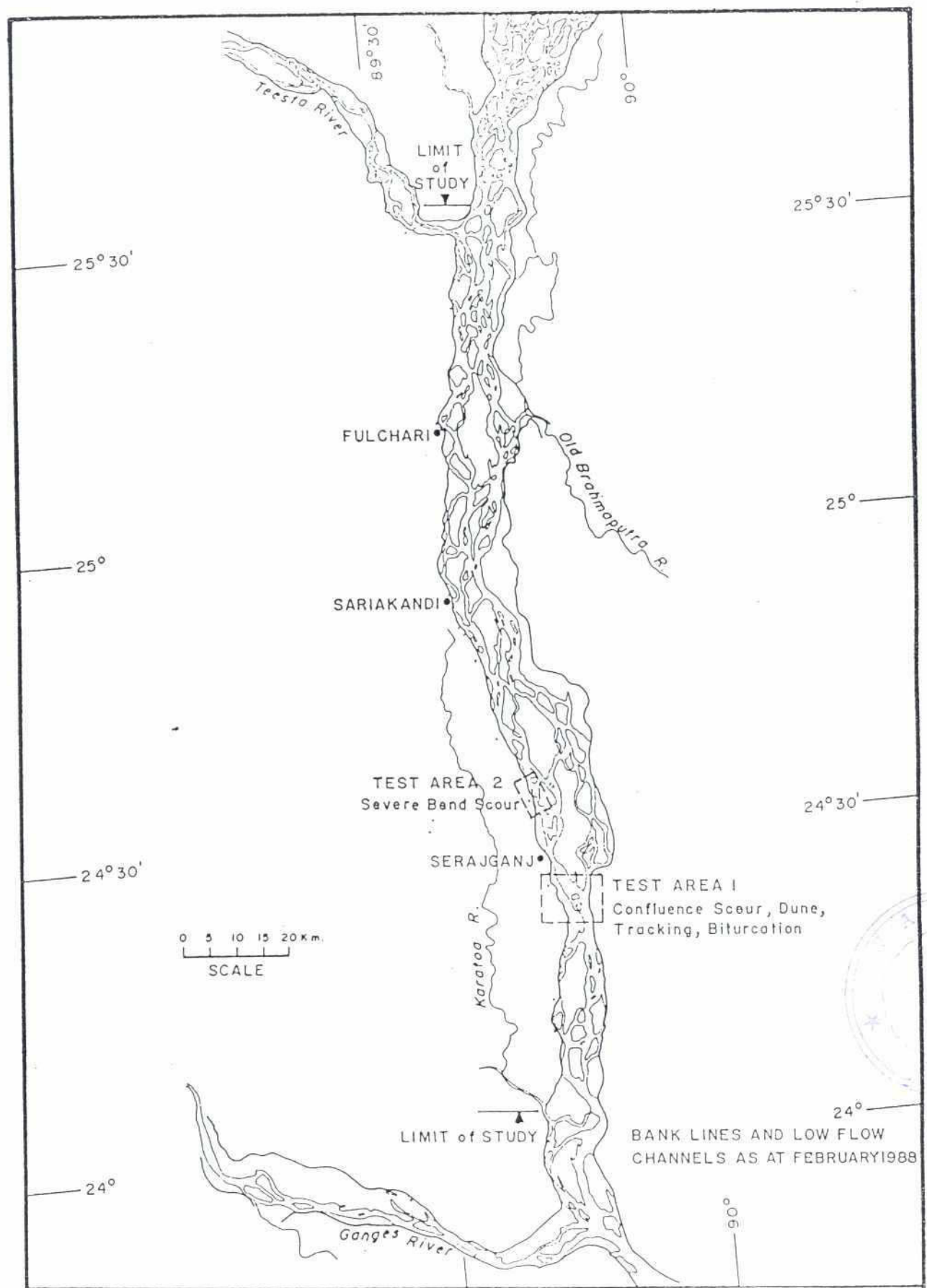
The 2-D model can be used to explore how these sandbars migrate during the flood season. A systematical analysis with respect to the influence of flood scenario, size and shape of anabranch and bar will be carried out. Rather than a detailed prediction of how specific bars behave, the outcome of this study will be time scales for migration and growth of bars, and possibly a classification of conditions which are potential dangerous and some which are not.

Table 4.1 Observed bank erosion in Test Area 1 June to July 1990

Lane	Right Anabranh						Left Anabranh					
	Right Bank			Left Bank			Right Bank			Left Bank		
	L	D	A	L	D	A	L	D	A	L	D	A
C50	140	10	1400	0			0			-80	7	-560
B70	230	8	1840	0			0			60	10	600
B76	-110	5	-500	0			0			100	5	500
B74	100	5	500	0			0			0		
B72	0			0			0			0		
B70	0			0			0			0		
B68	0			0			0			0		
B66	100	5	500	0			-340	19	-6550	300	20	6200
B64	100	3	300	-175	2	-400	-320	13	-4200	220	15	3300
B62	0			0			-500	15	-7500	340	12	4200

Notes : L is the bank line retreat (negative number is deposition) in metres
D is the depth in front of the bank and A the eroded area in sq.metres.

FIGURES



LOCATION MAP OF TEST AREAS

ANNEX 3: PART 2

FIGURE 2.1

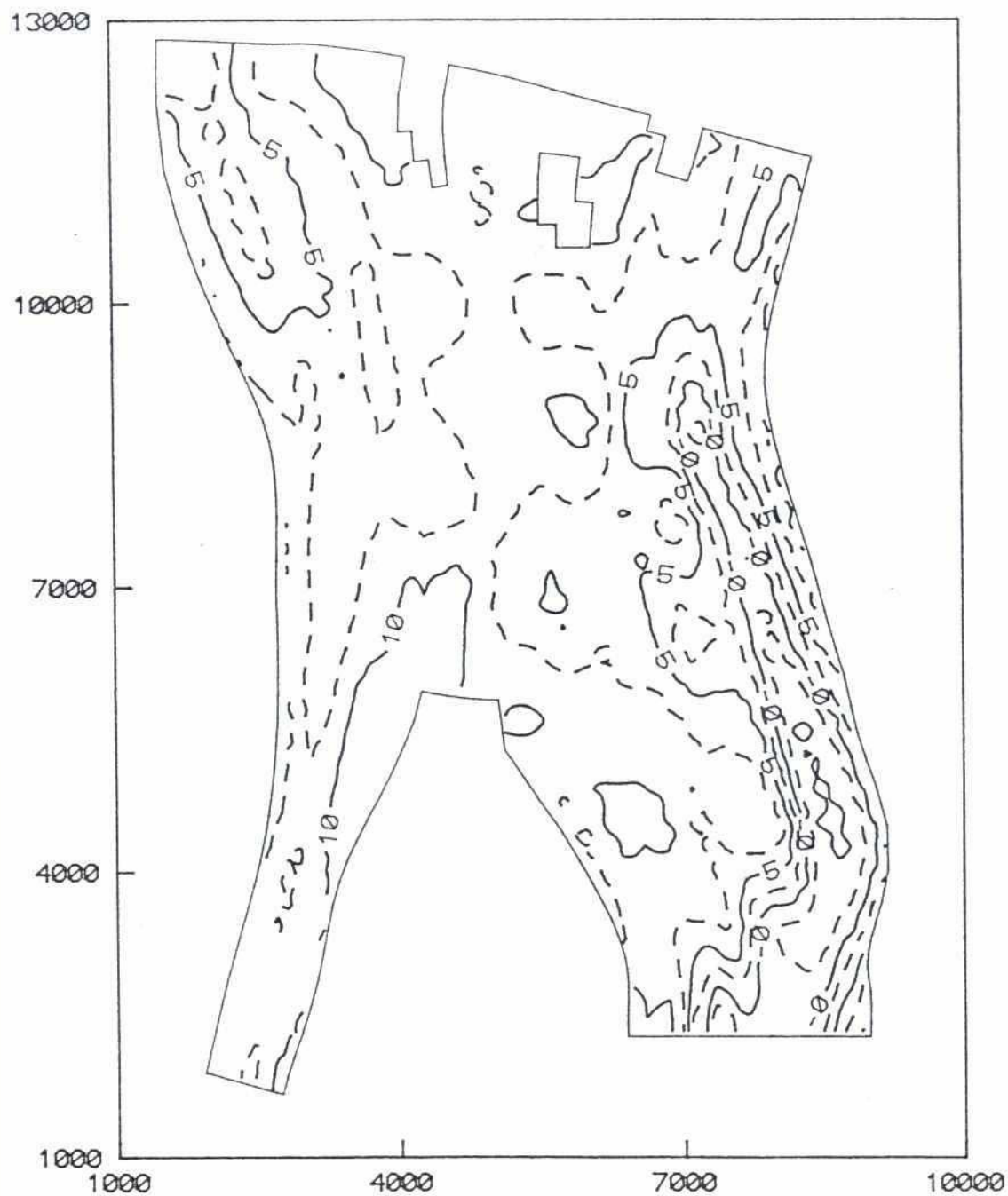


COMPUTATIONAL CURVILINEAR GRID FOR TEST AREA - I

ANNEX 3: PART 2

FIGURE : 3.1

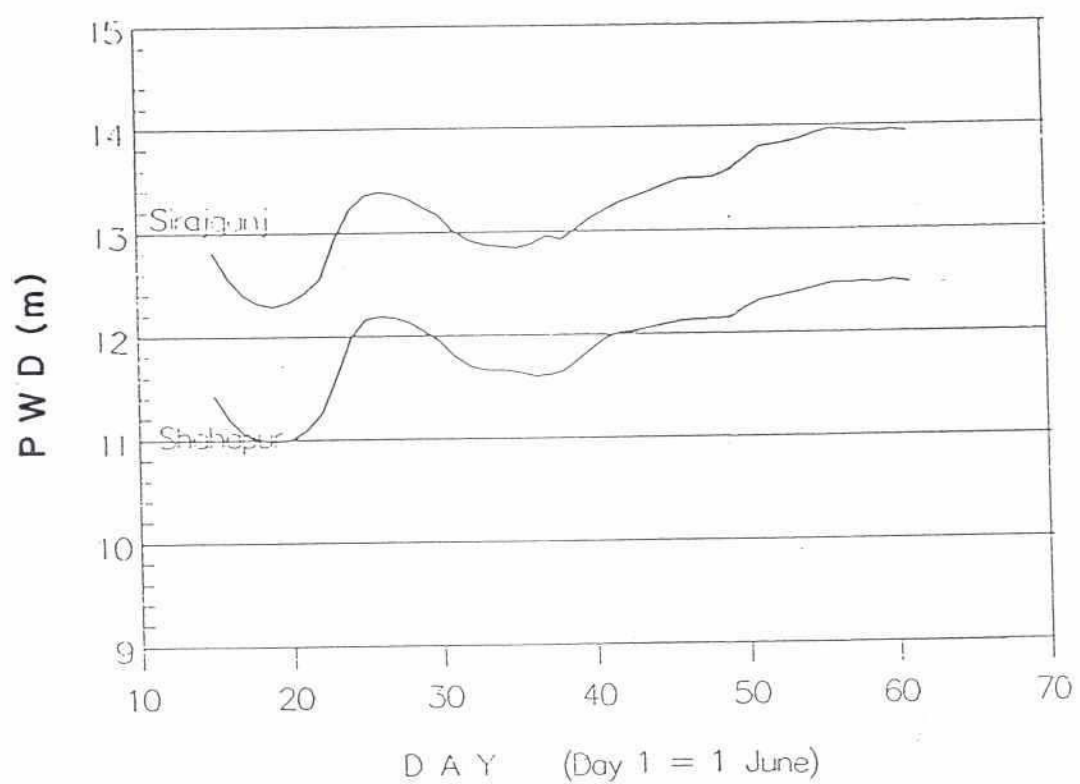
Model Topography



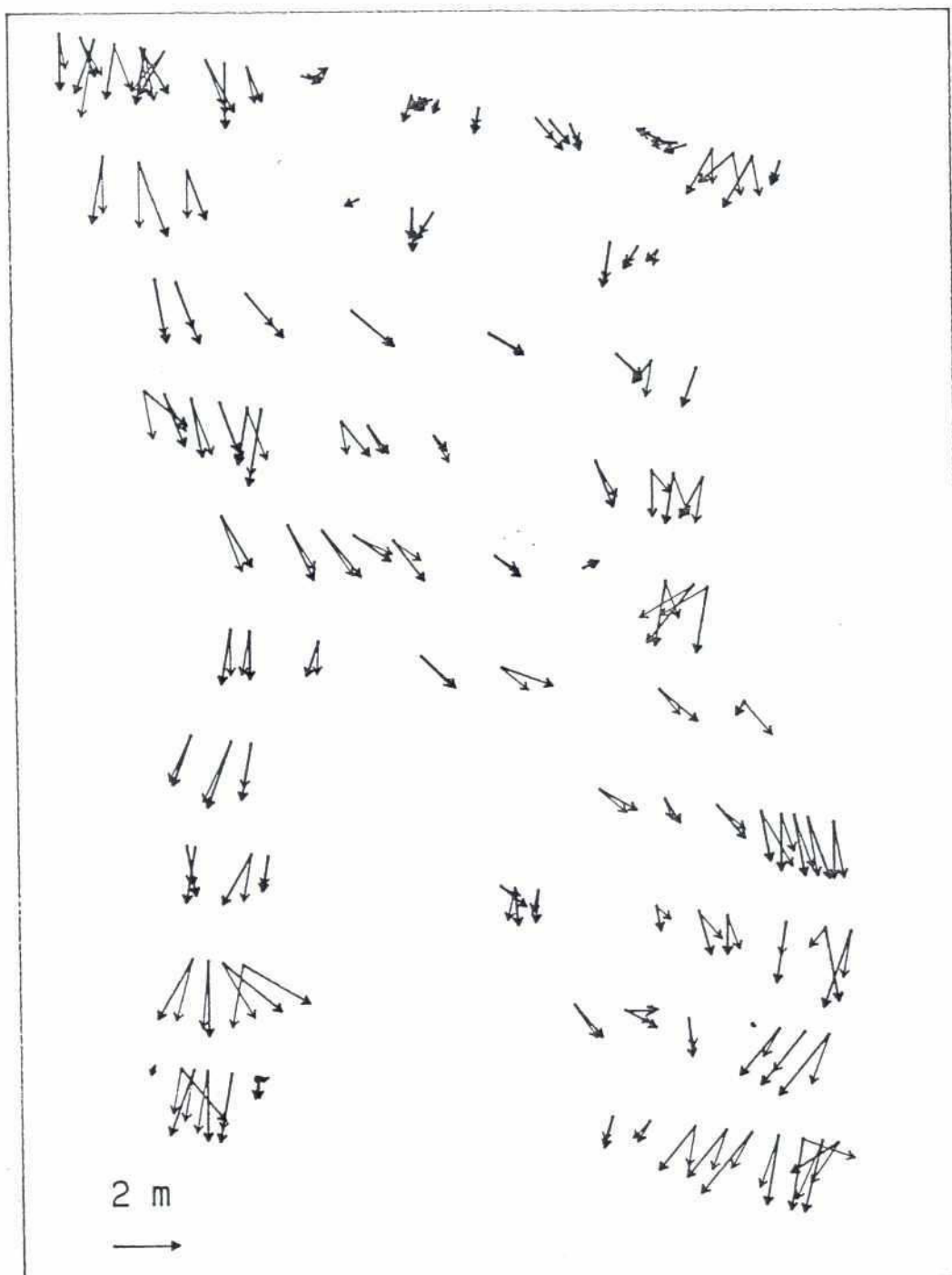
CONTOUR PLOT OF MODEL TOPOGRAPHY

ANNEX 3 : PART 2

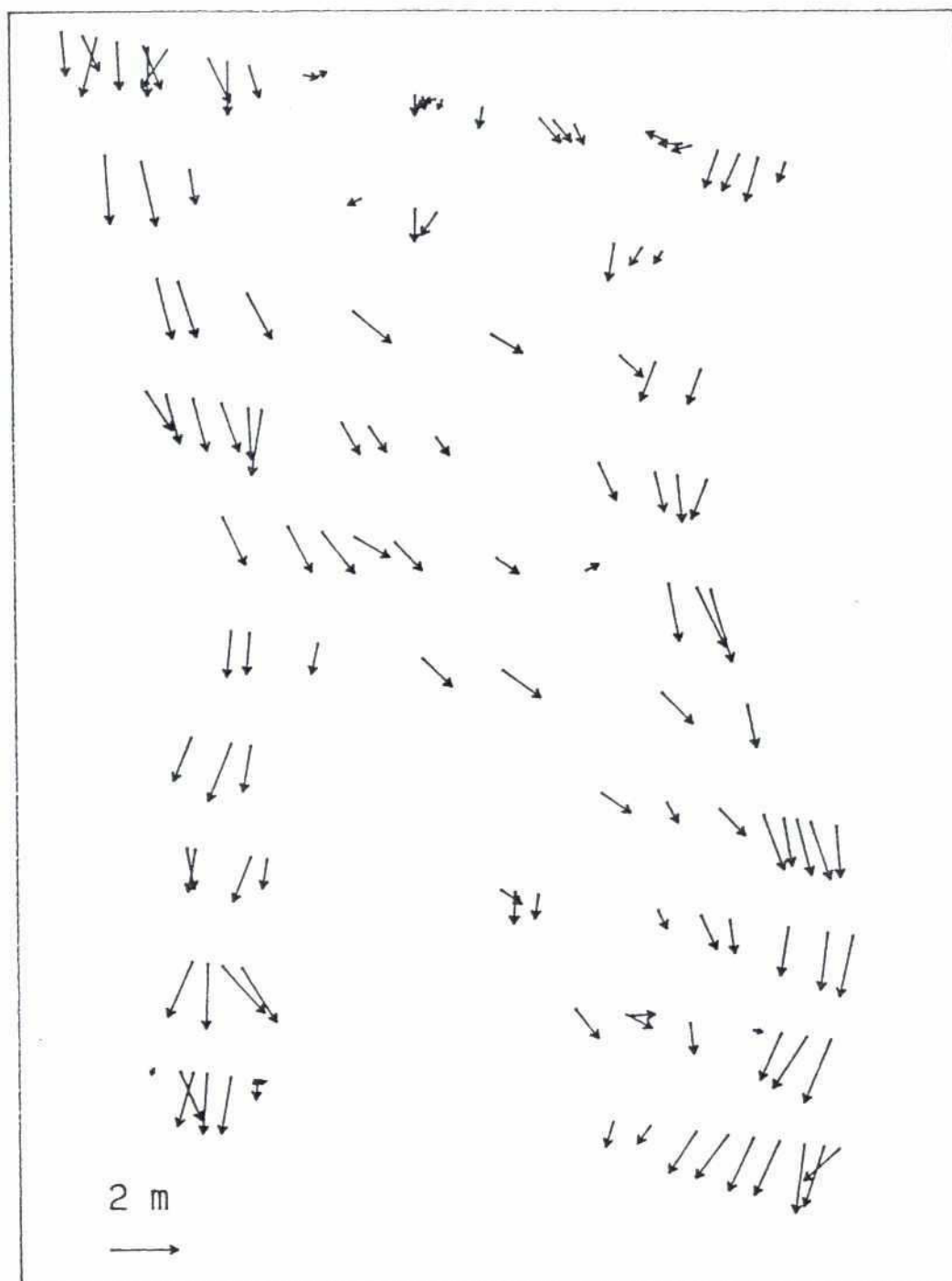
FIGURE : 3.2



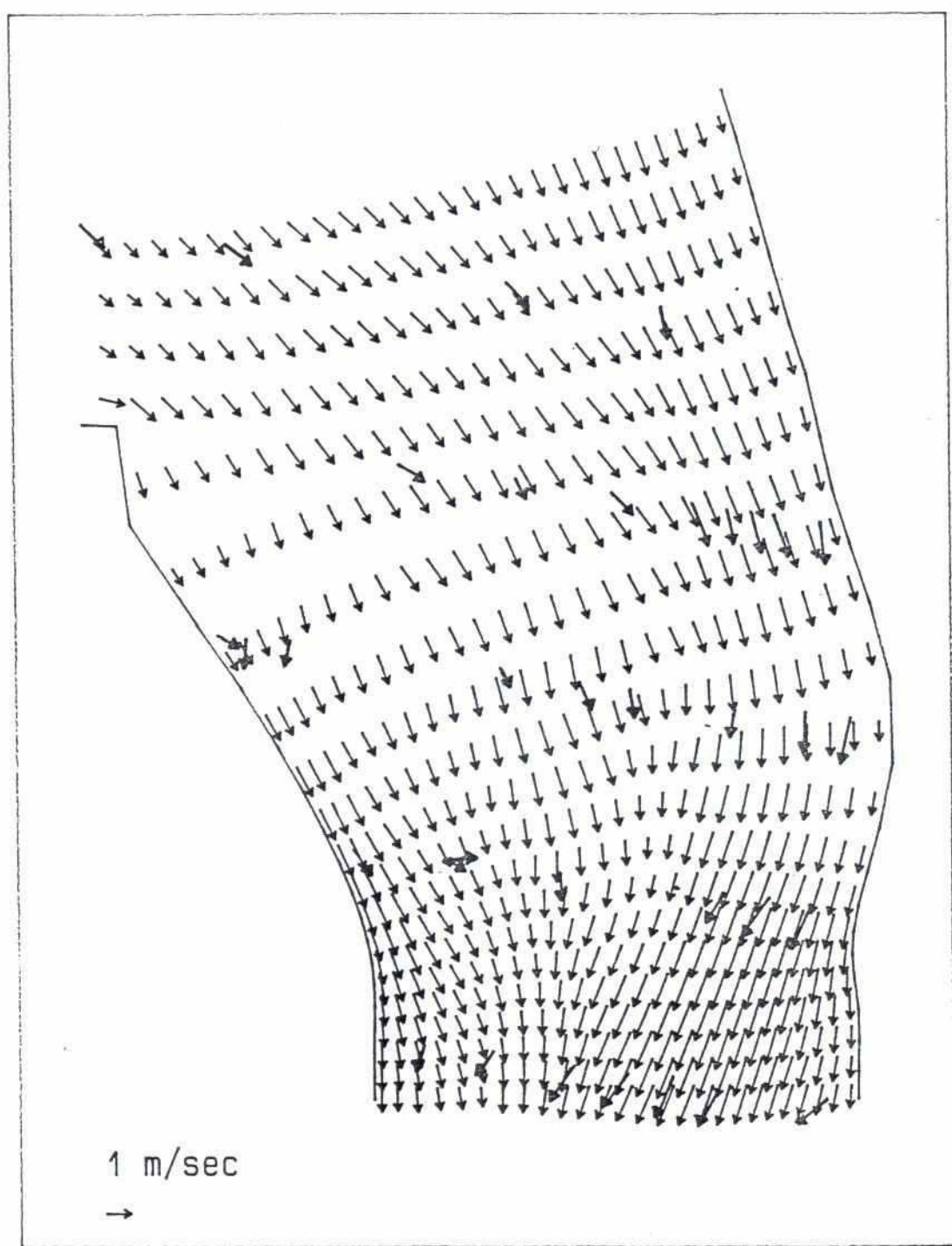
WATER LEVEL AT SIRAJGANJ AND SHAHAPUR



OBSERVED FLOW VELOCITIES AT 0.2 AND 0.8 DEPTH

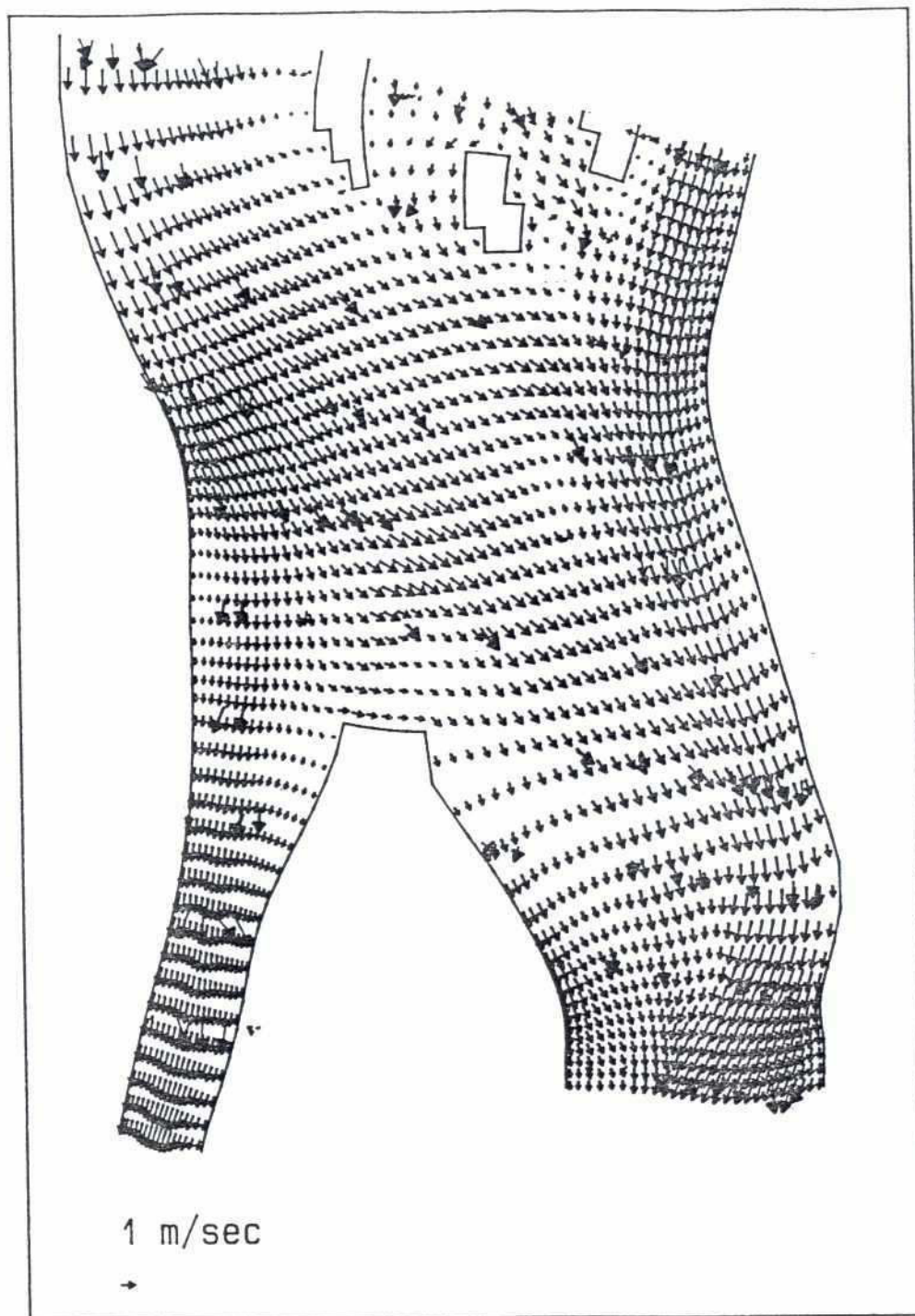


· OBSERVED DEPTH AVERAGE FLOW VELOCITY



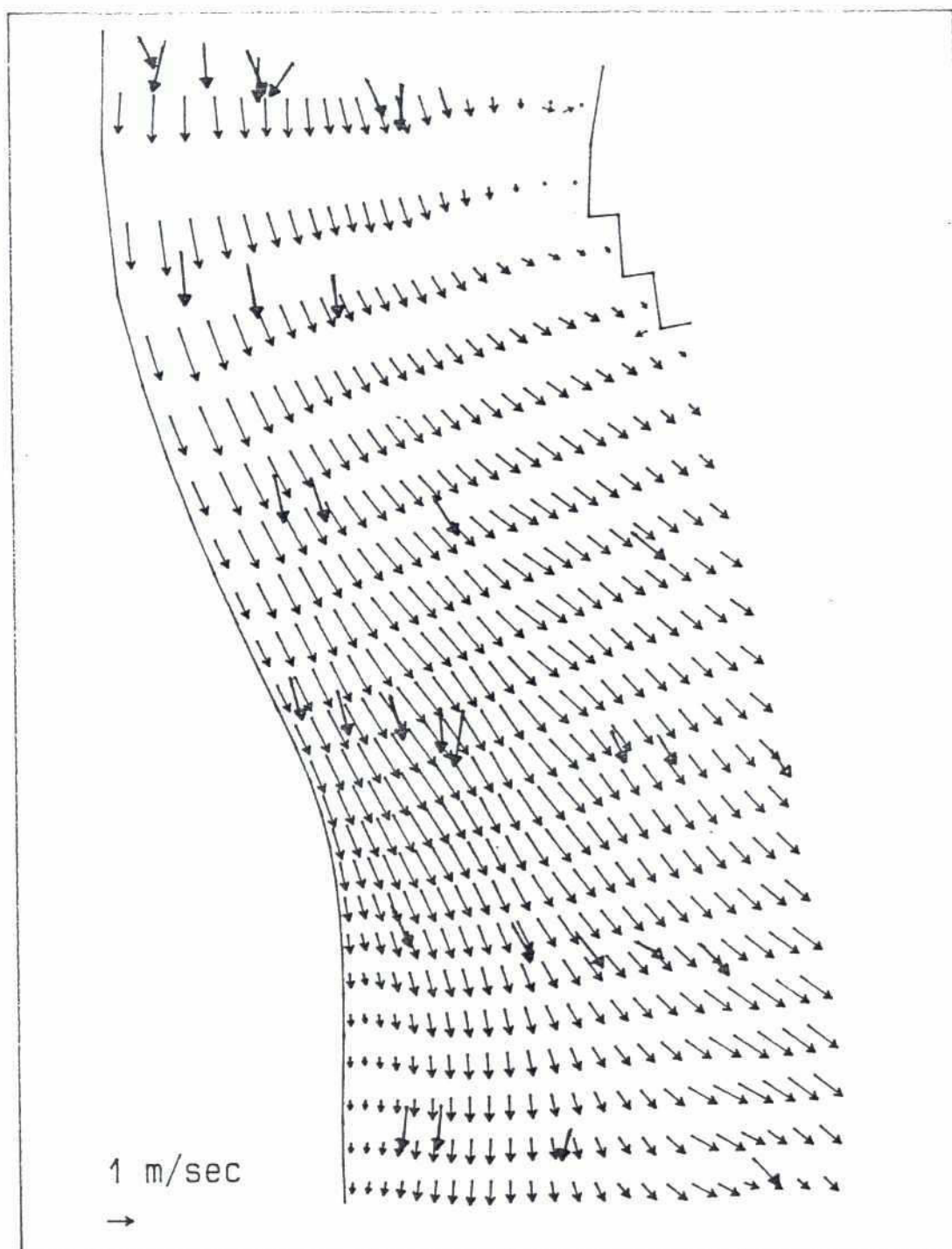
→ Measured
→ Simulated

SIMULATED AND MEASURED FLOW VELOCITIES
(CONSTANT BED ROUGHNESS)



→ Observed
→ Simulated

SIMULATED AND OBSERVED FLOW DISTRIBUTION

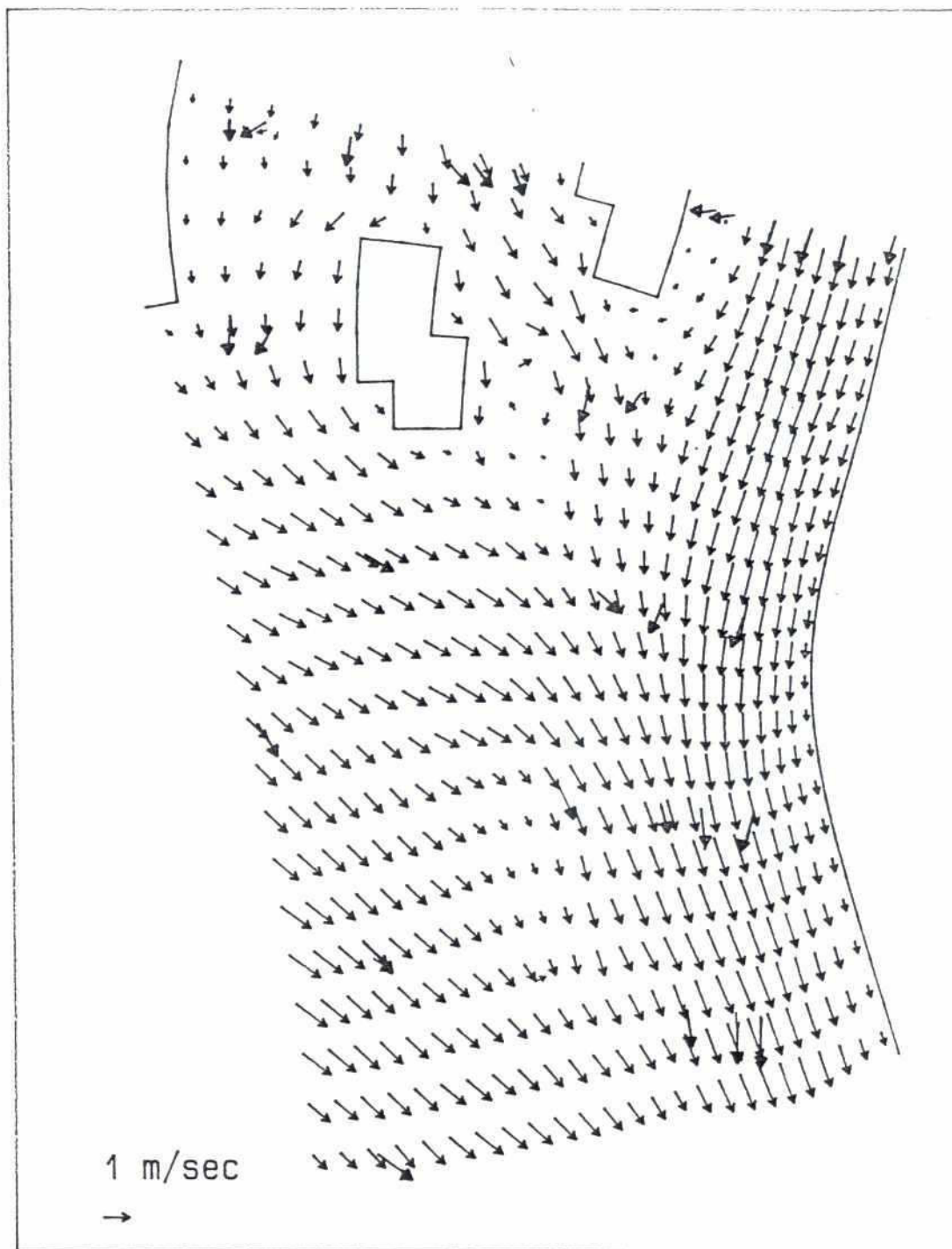


→ Observed
→ Simulated

SIMULATED AND OBSERVED FLOW VELOCITIES.
UPPER LEFT PART OF MODEL

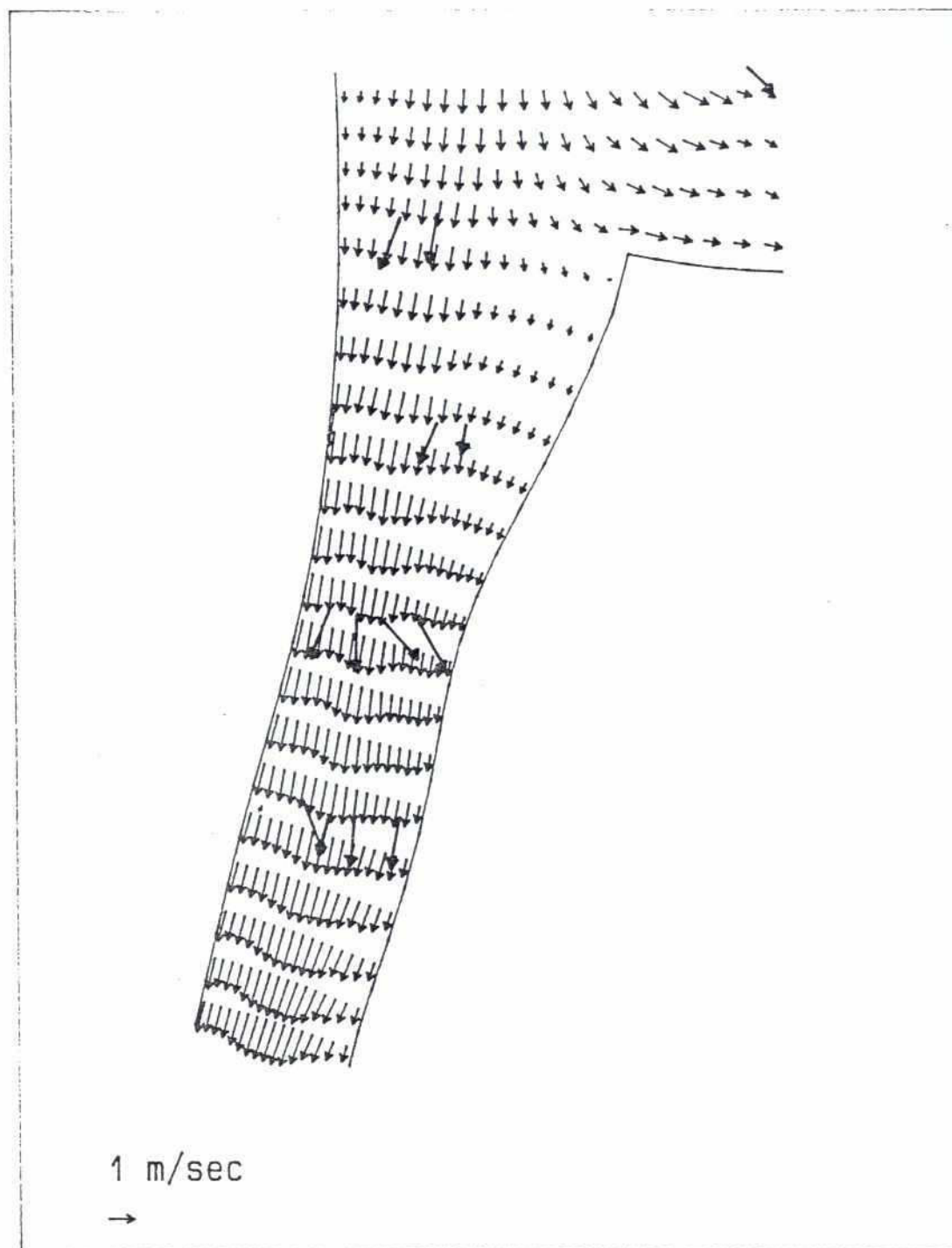
ANNEX 3 : PART 2

FIGURE : 3.8 a



→ Observed
→ Simulated

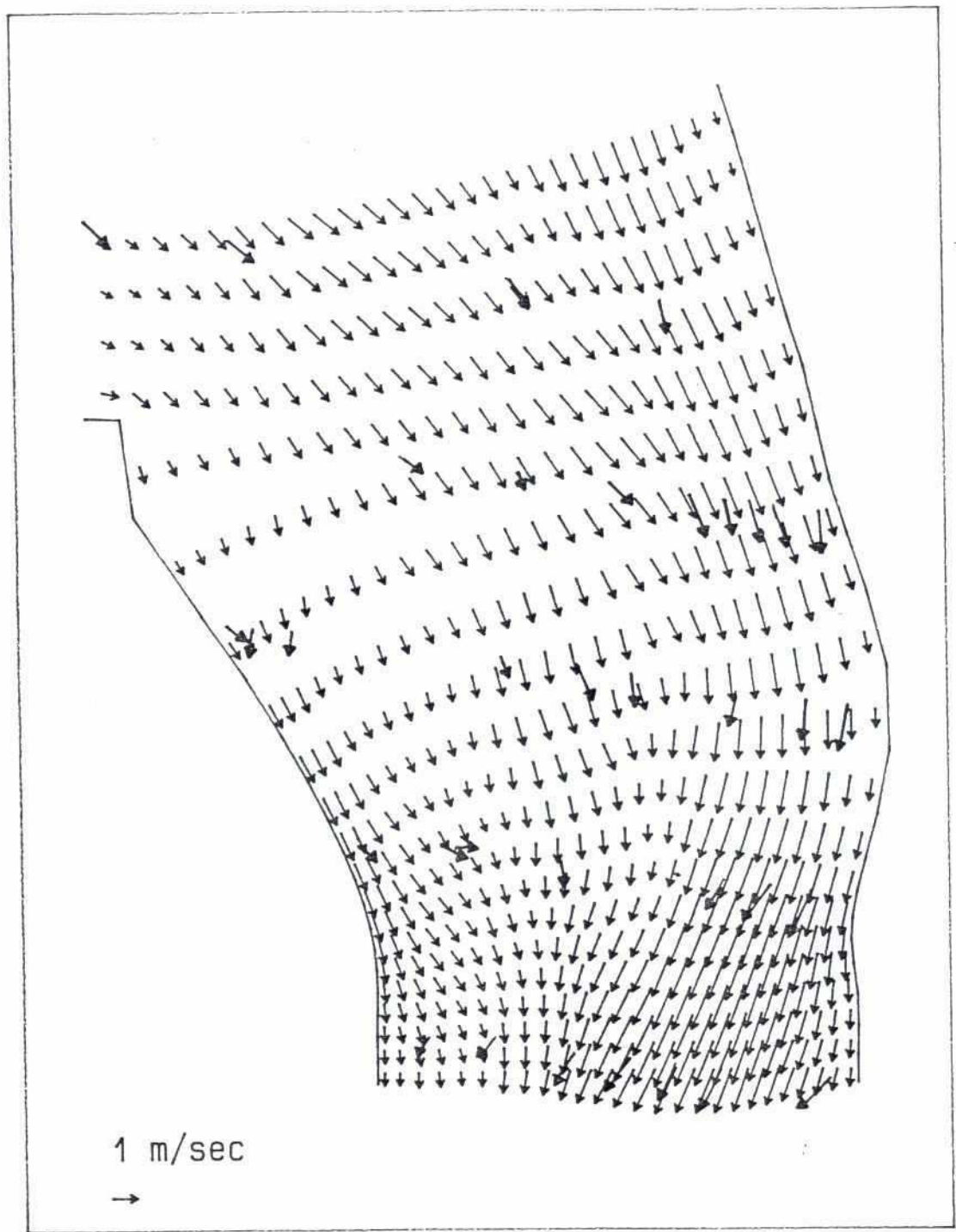
SIMULATED AND OBSERVED FLOW VELOCITIES.
UPPER RIGHT PART OF MODEL



SIMULATED AND OBSERVED FLOW VELOCITIES.
LOWER LEFT PART OF MODEL

ANNEX 3 : PART 2

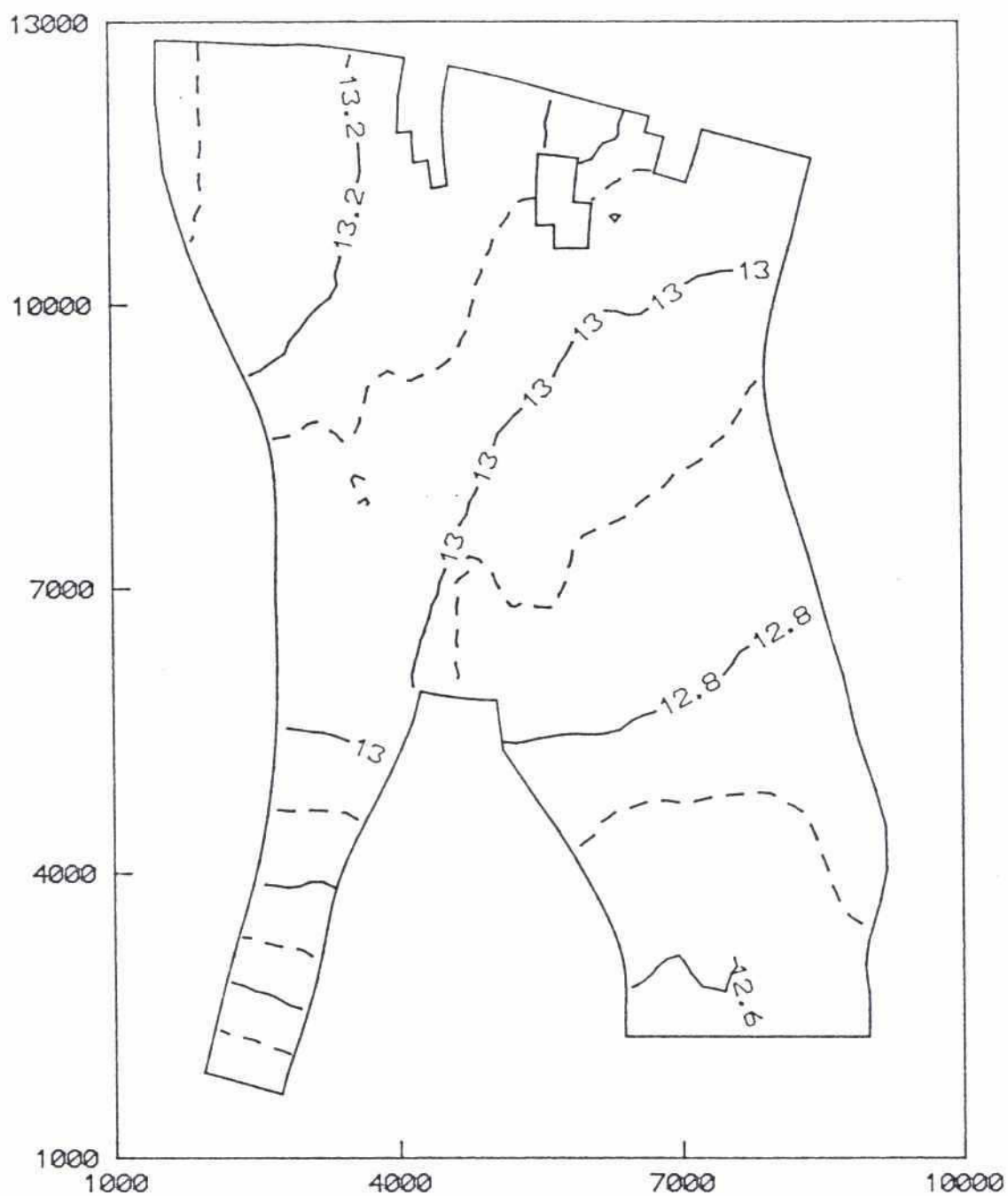
FIGURE : 3.8 c



→ Observed
→ Simulated

SIMULATED AND OBSERVED FLOW VELOCITIES.
LOWER RIGHT PART OF MODEL

Water Surface Level

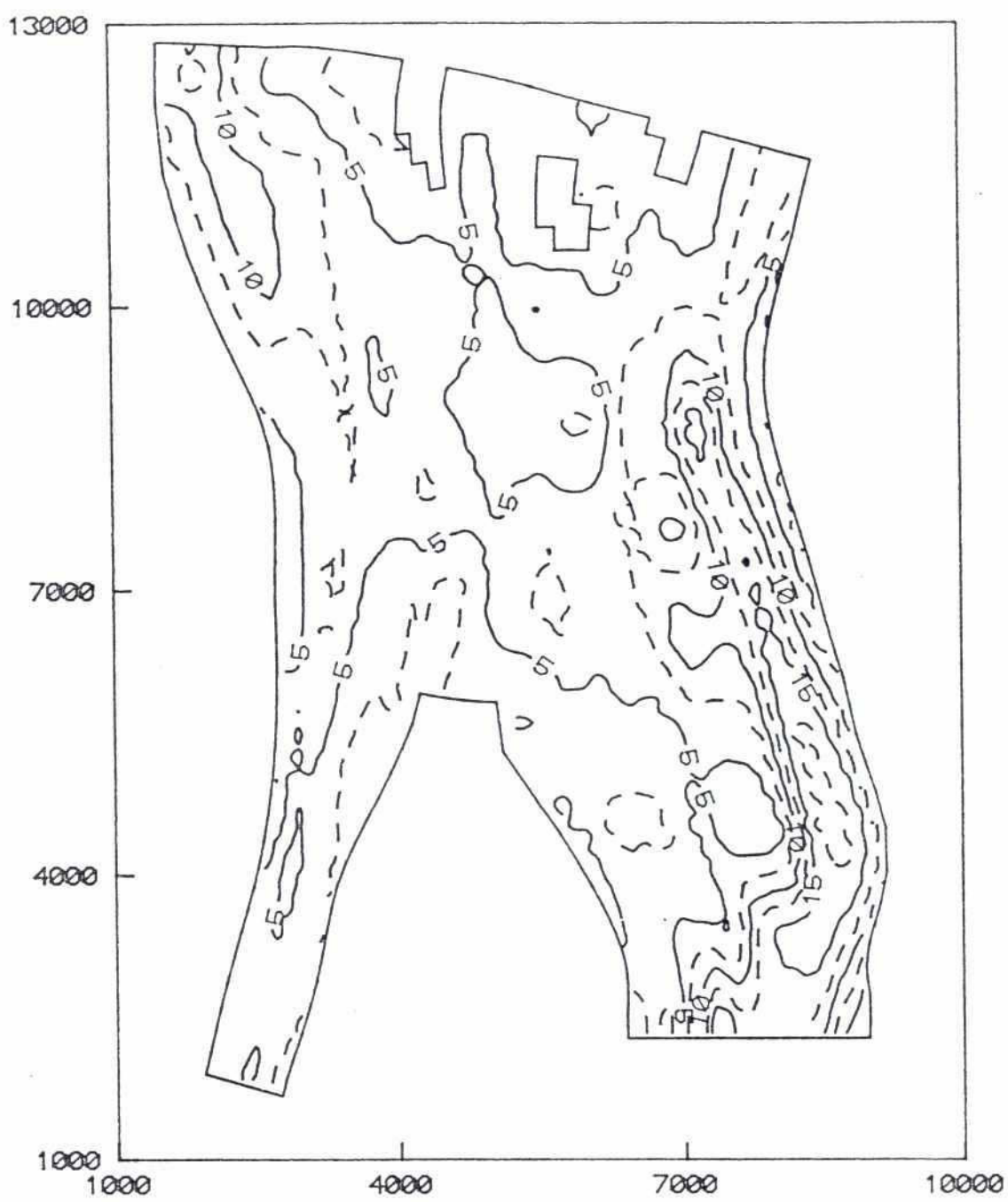


SIMULATED WATER. SURFACE ELEVATION

ANNEX 3 : PART 2

FIGURE : 3.9

Water Depth (July)

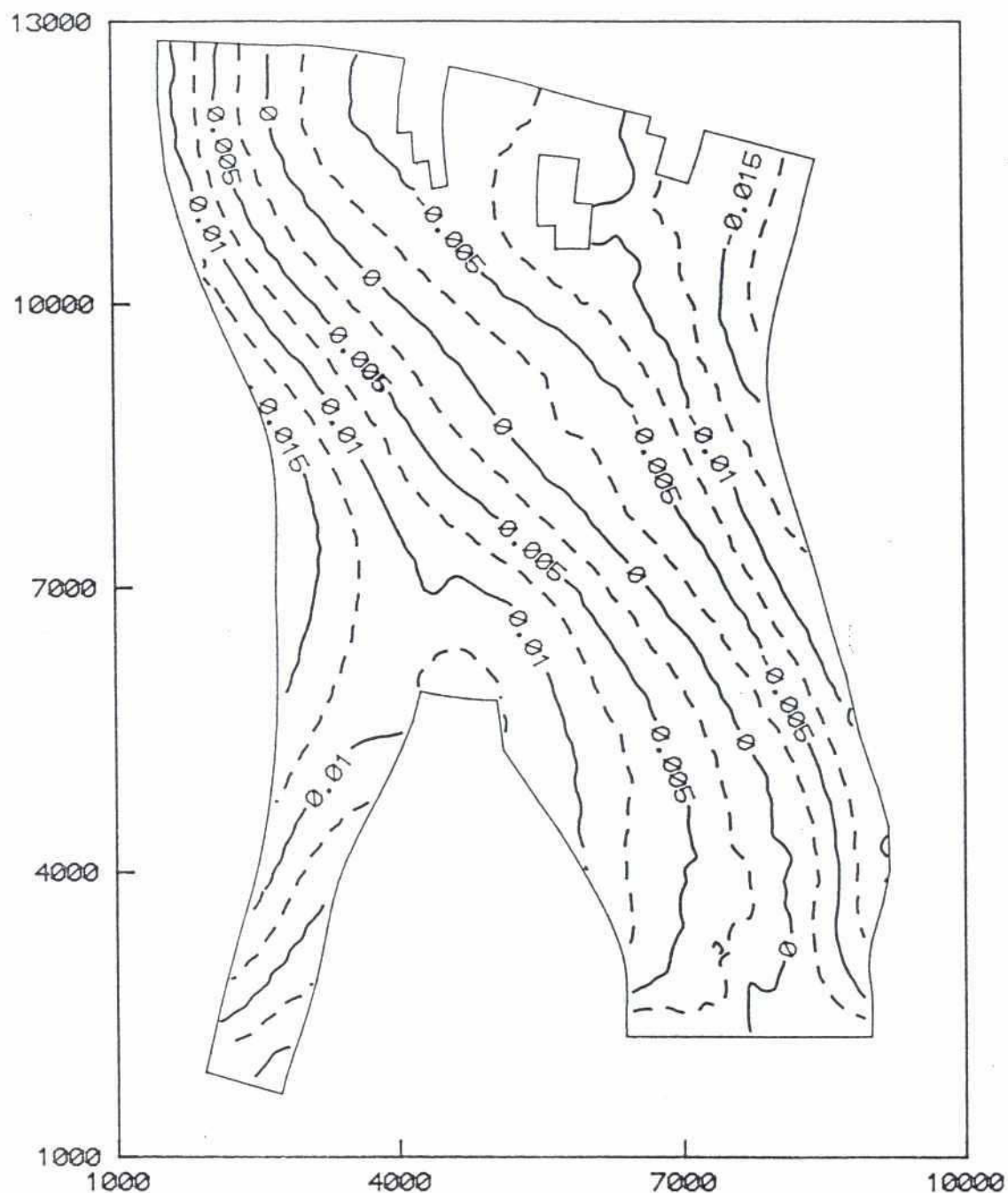


SIMULATED WATER DEPTH.

ANNEX 3 : PART 2

FIGURE: 3.10

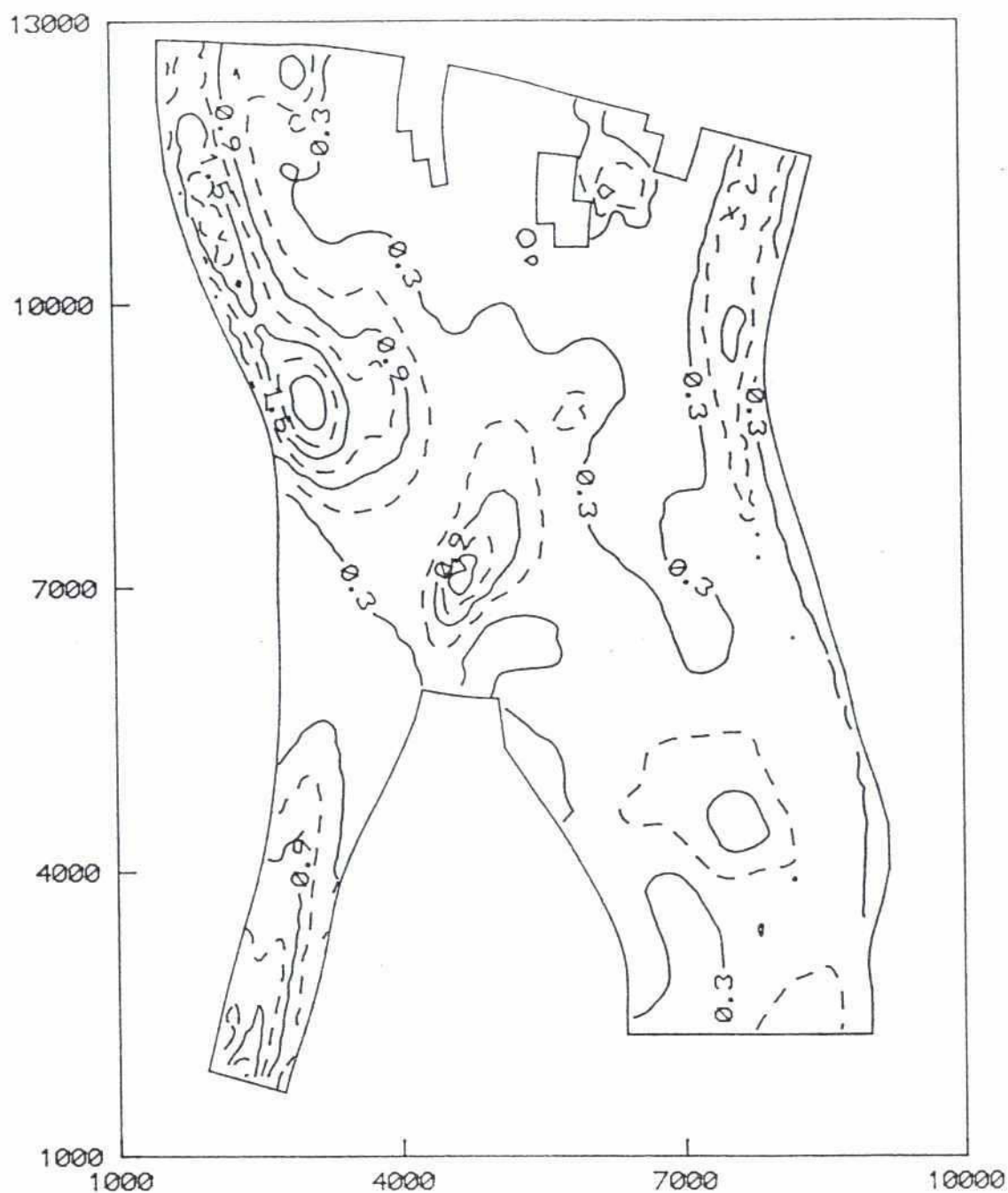
Influence of Coriolis force



DIFFERENCE IN SIMULATED WATER LEVEL WITH AND WITHOUT CORIOLIS FORCE INCLUDED

ANNEX 3 : PART 2

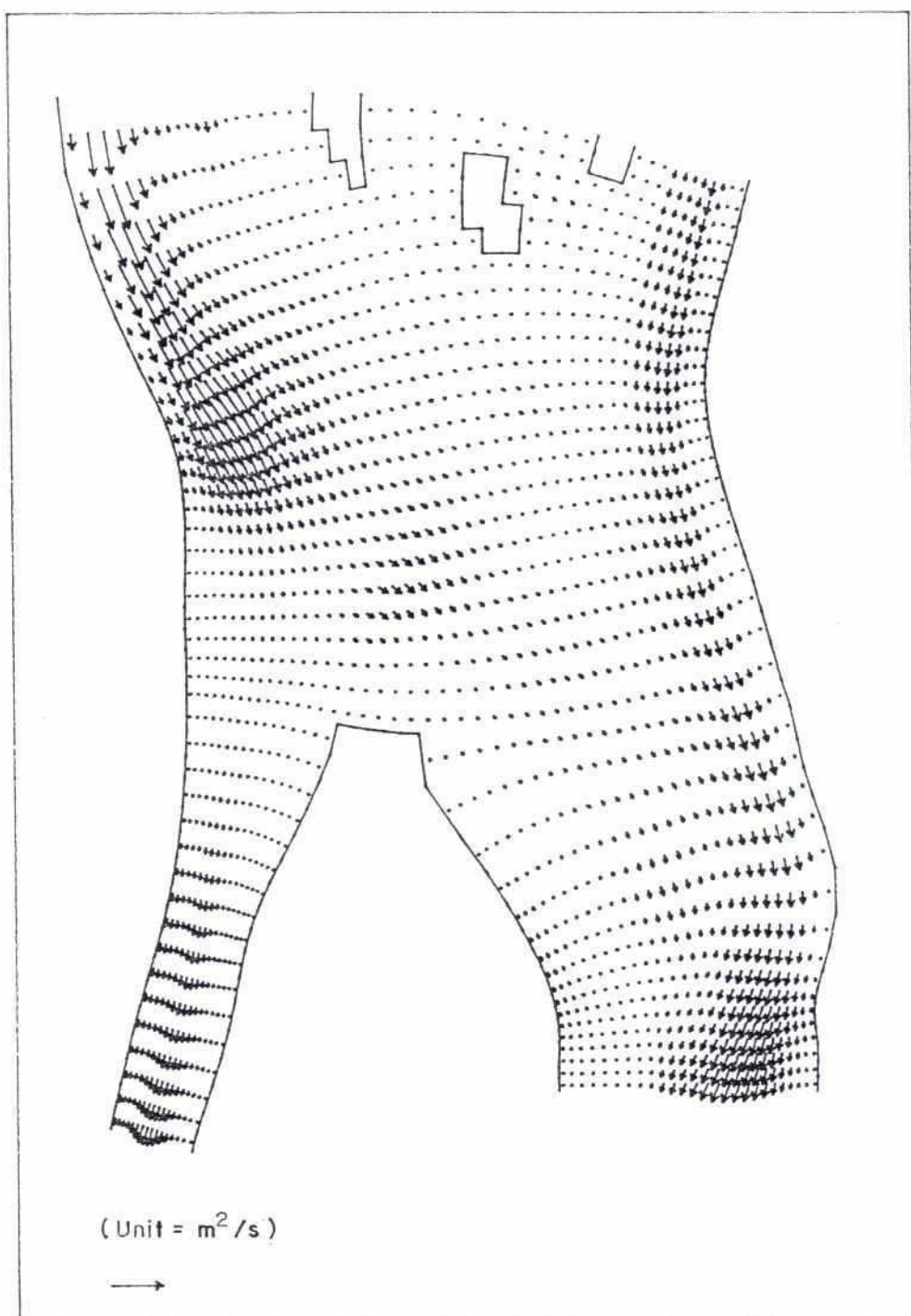
FIGURE : 3.II



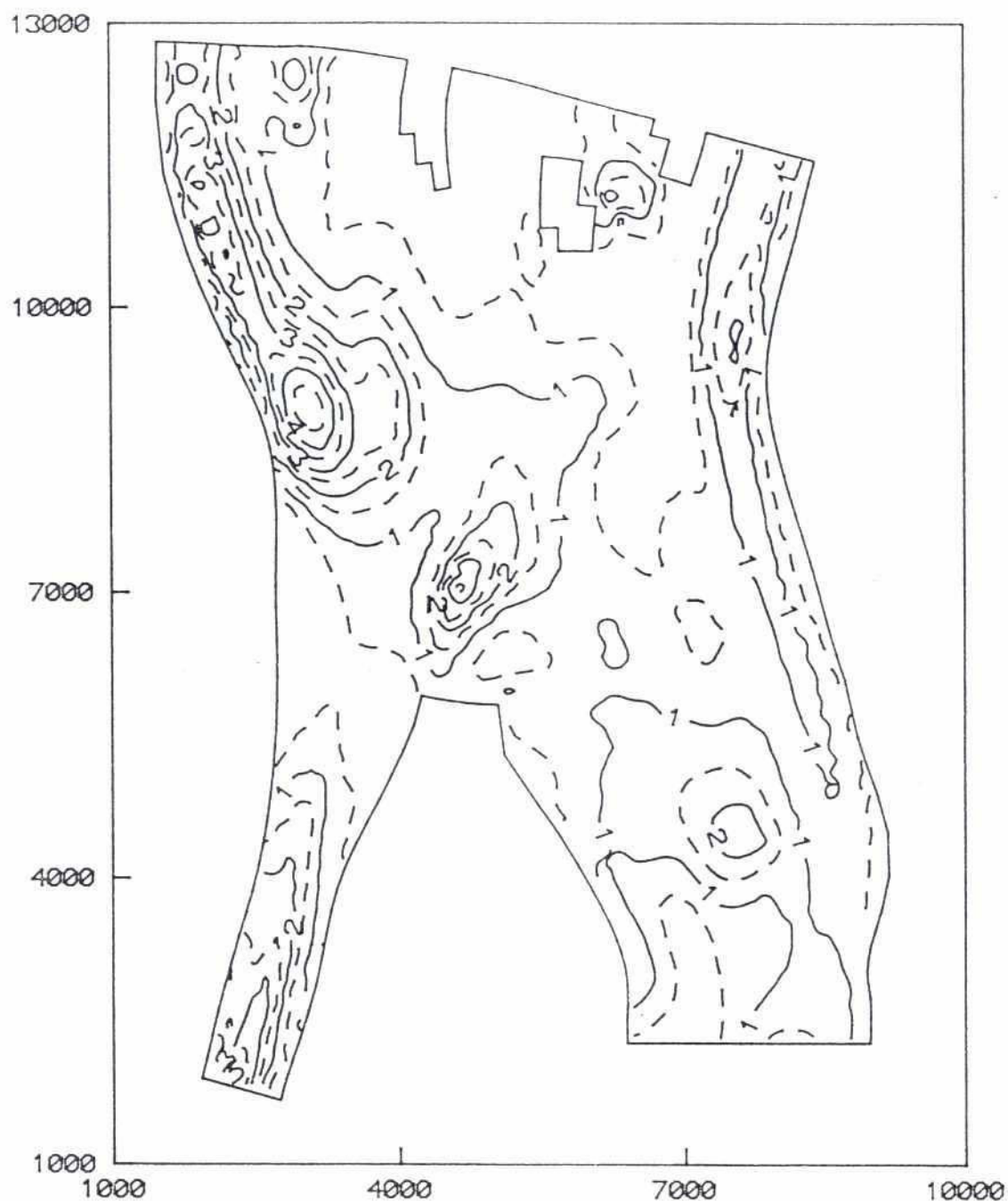
SIMULATED SUSPENSION CONCENTRATION (Kg/m^3)

ANNEX 3 : PART 2

FIGURE : 4.1



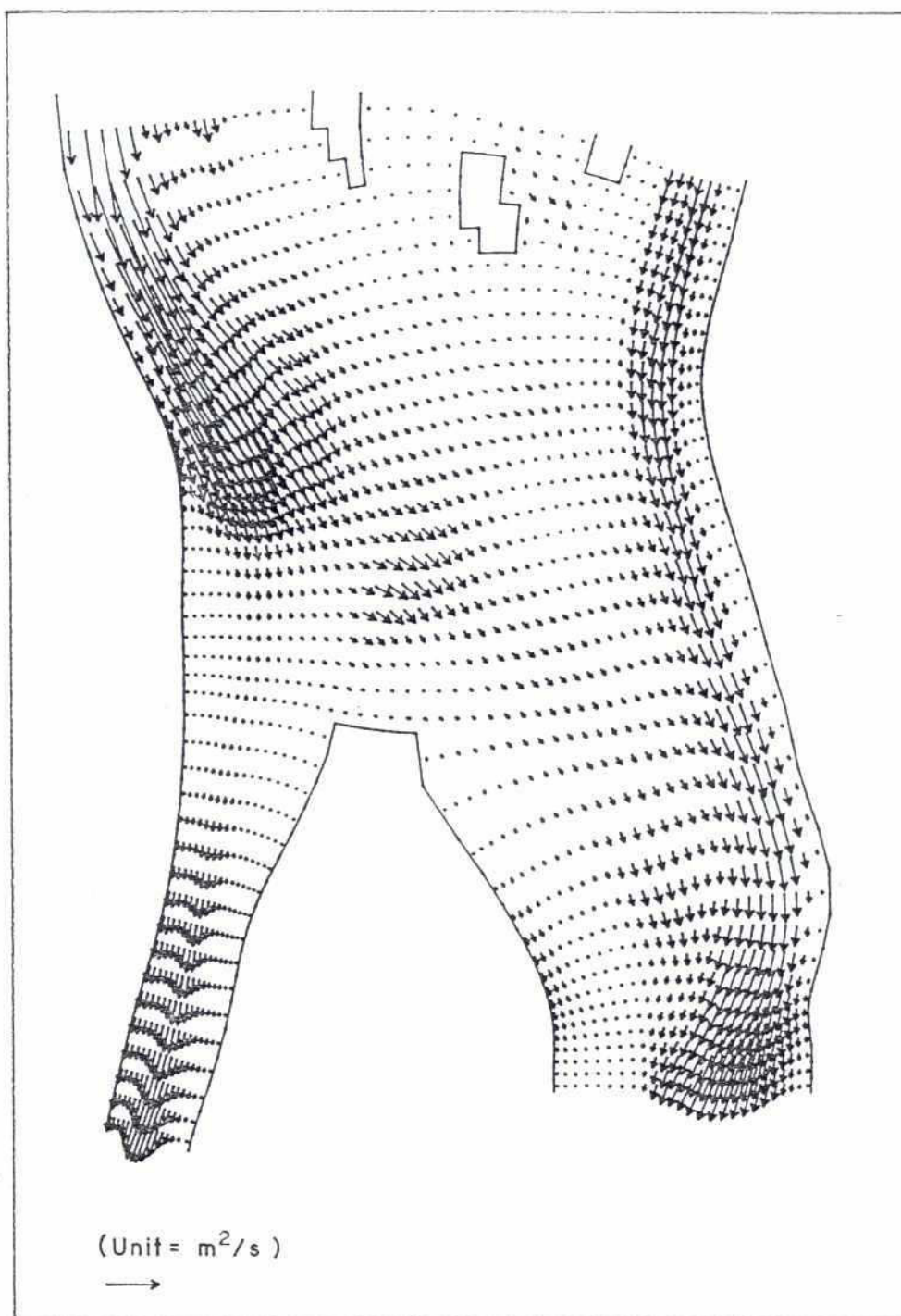
SIMULATED SEDIMENT TRANSPORT VECTORS (m^2/s)



SIMULATED SUSPENSION CONCENTRATION (Kg /m^3)
WITH REDUCED WATER TEMPERATURE

ANNEX 3 : PART 2

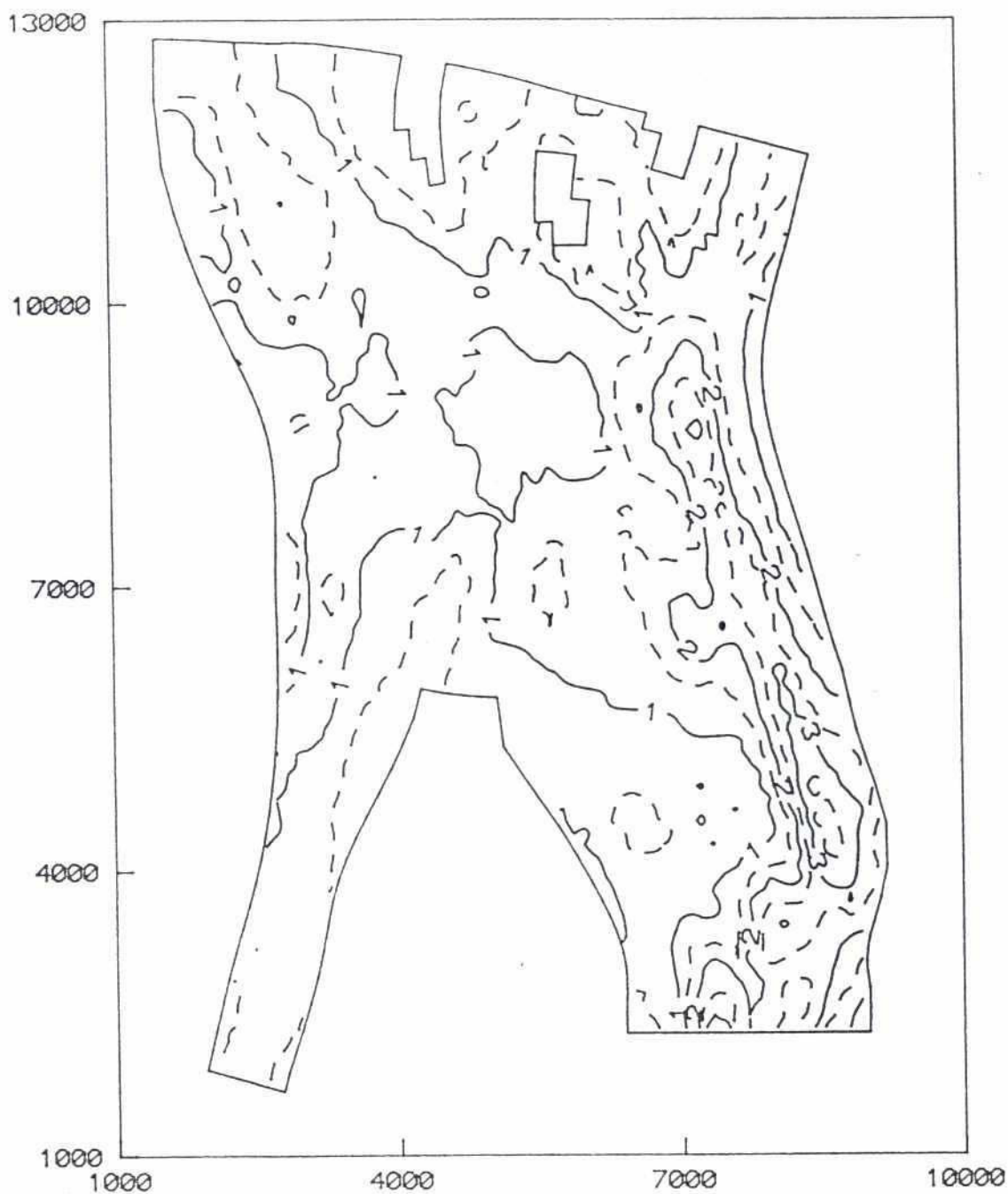
FIGURE : 4.3



SIMULATED SEDIMENT TRANSPORT VECTORS (m^2/s)
WITH REDUCED WATER TEMPERATURE

ANNEX 3 : PART 2

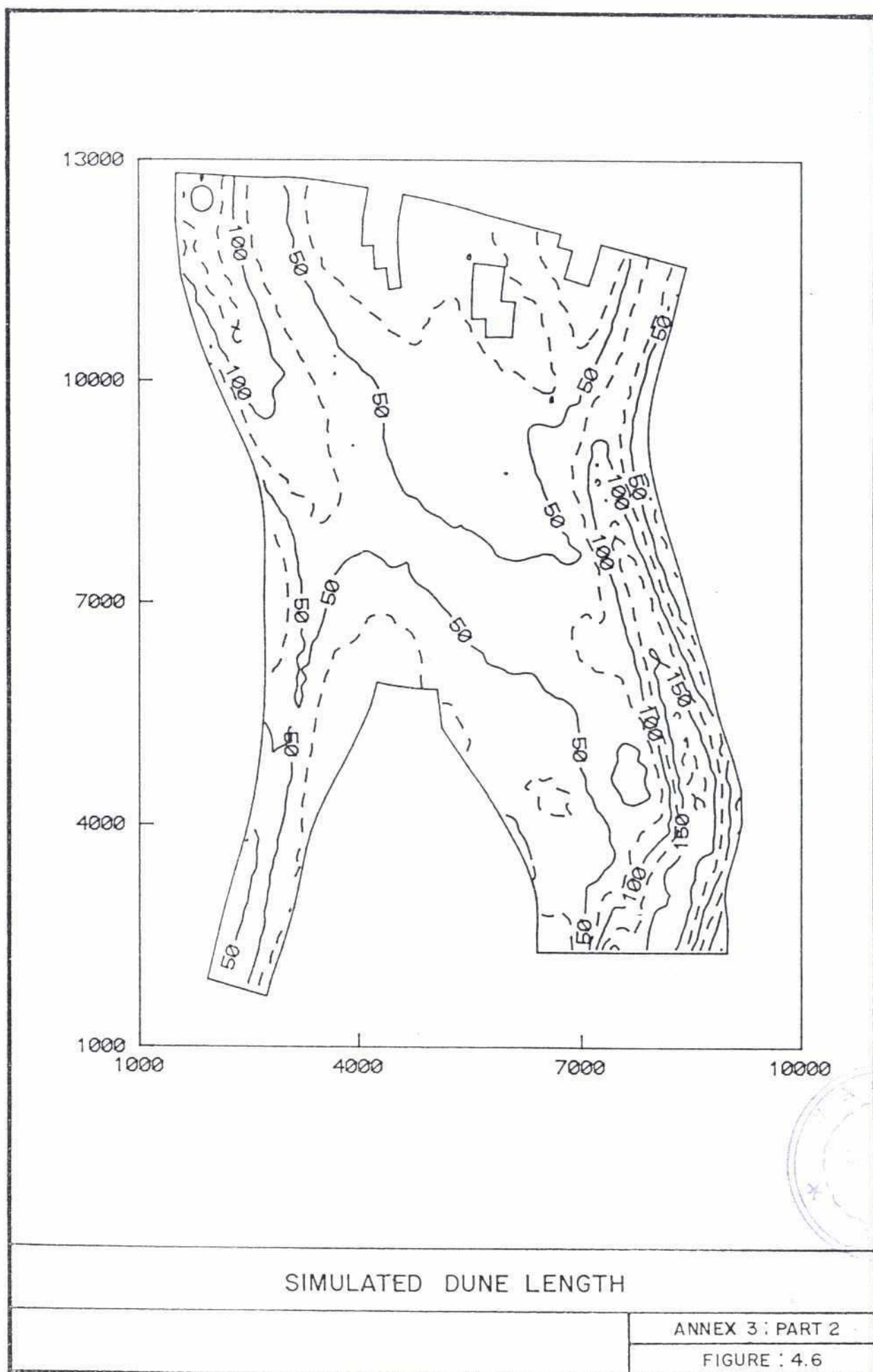
FIGURE : 4.4

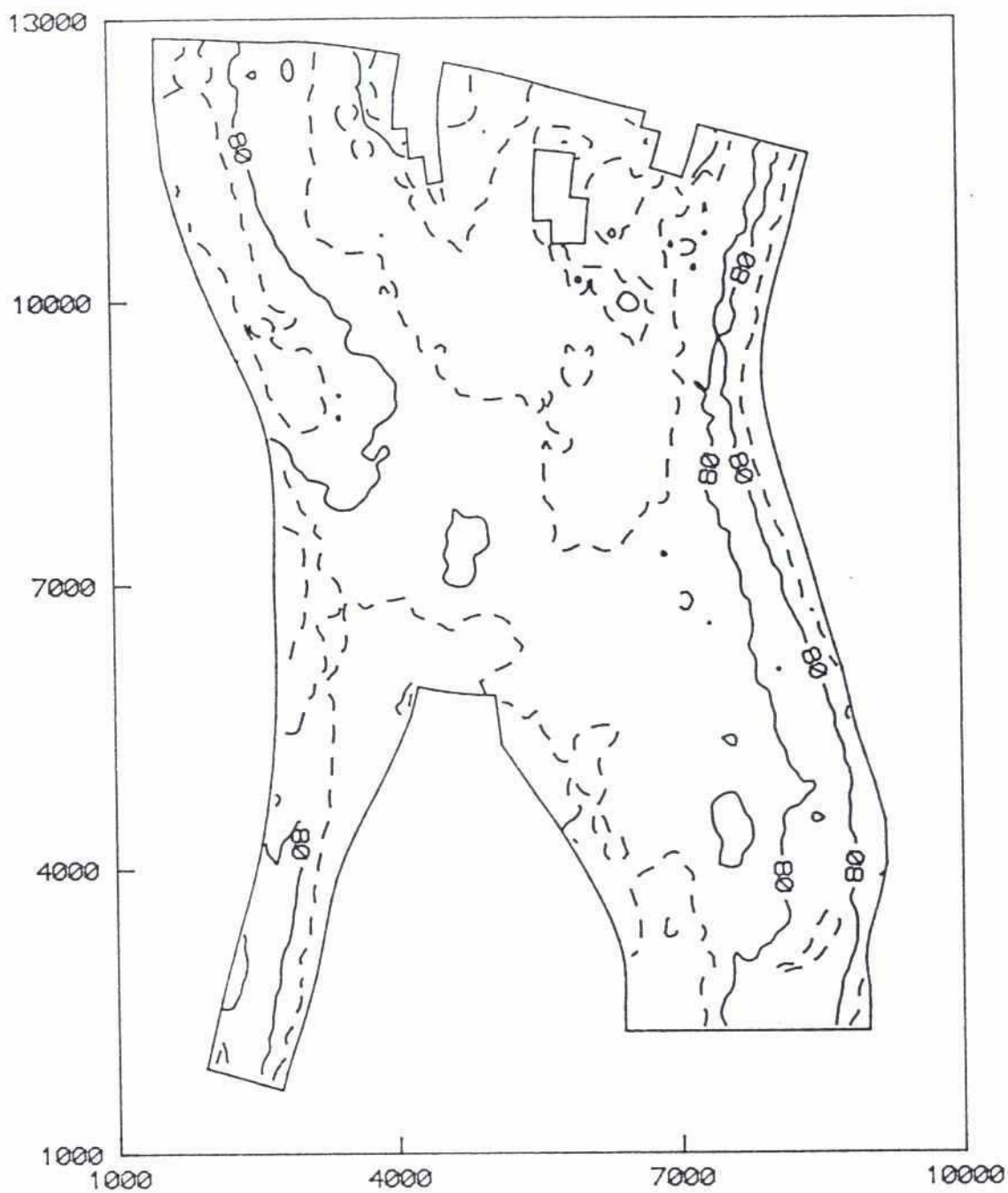


SIMULATED DUNE HEIGHT

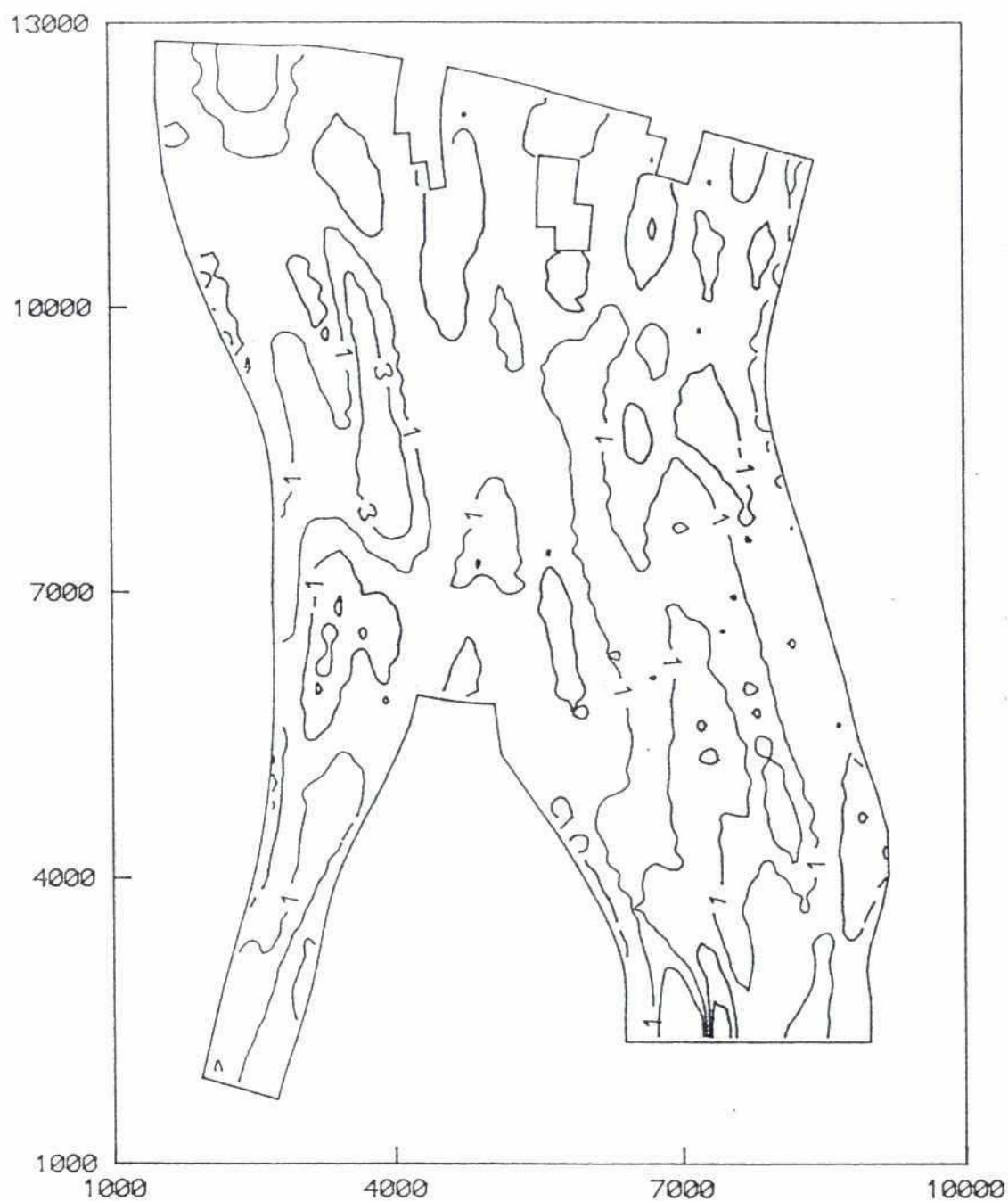
ANNEX 3 : PART 2

FIGURE : 4.5





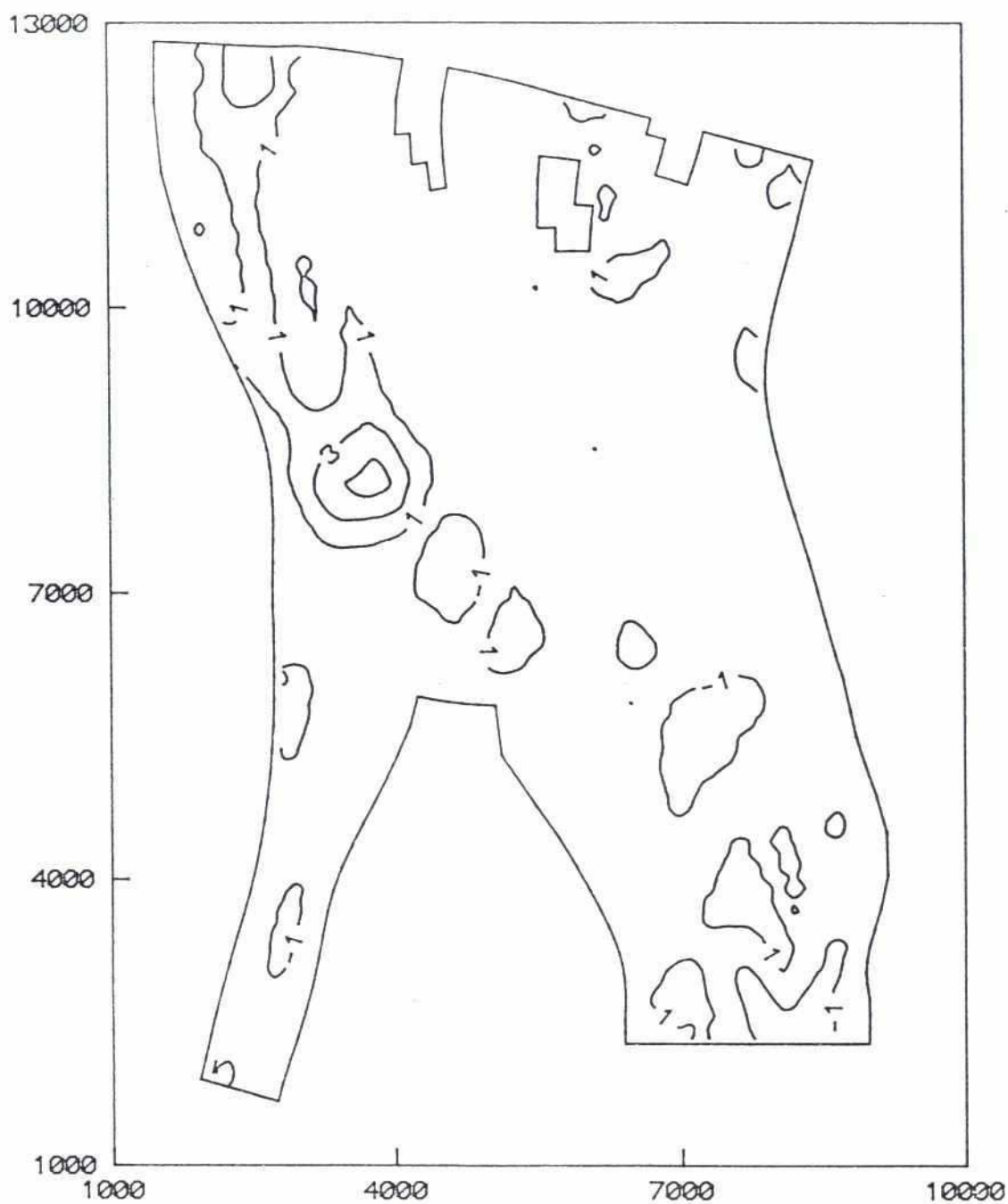
SIMULATED CHEZY ROUGHNESS COEFFICIENT



OBSERVED CHANGE OF BED TOPOGRAPHY
BETWEEN JUNE TO JULY

ANNEX 3 : PART 2

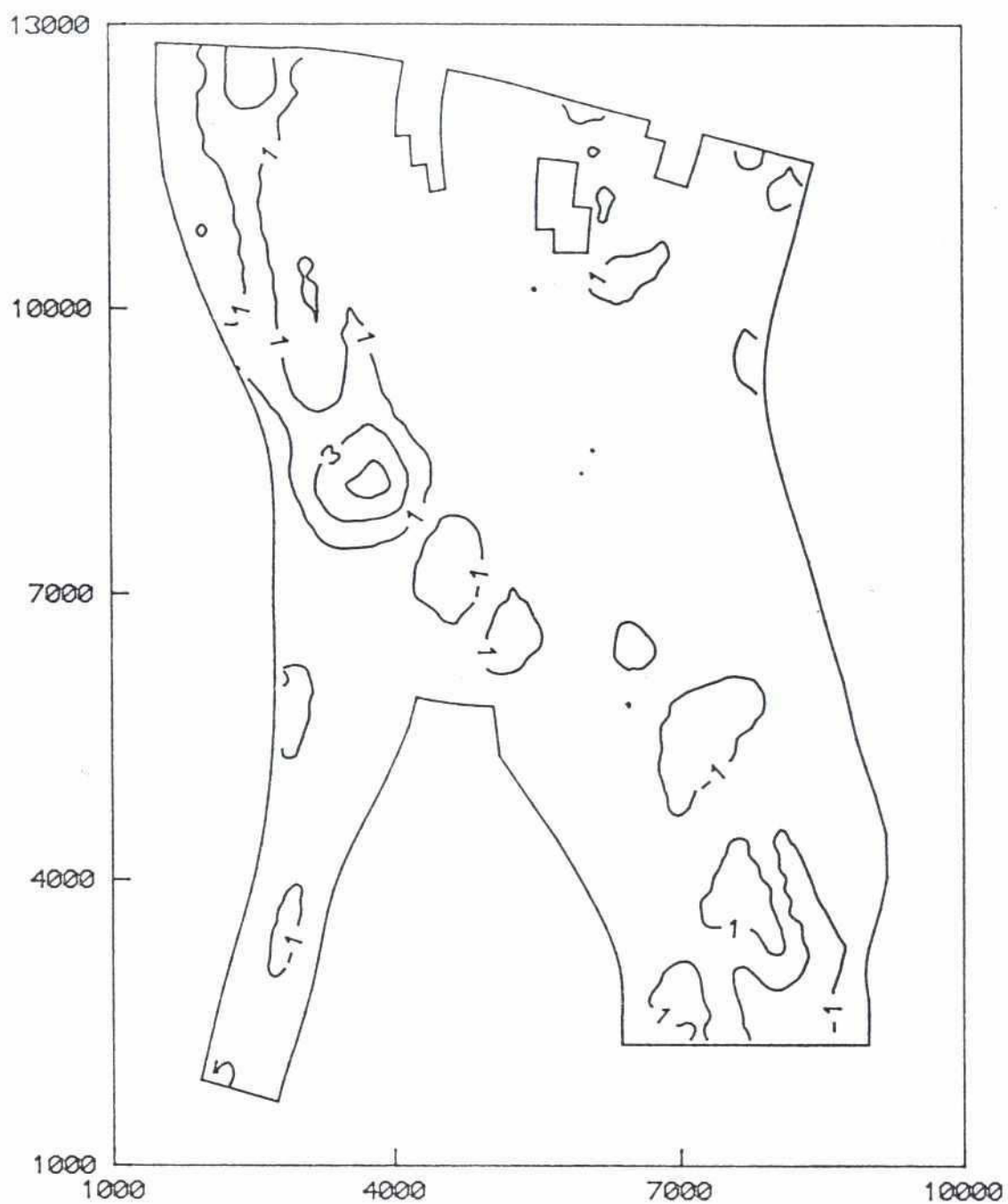
FIGURE : 4.8



SIMULATED BED LEVEL CHANGES FROM JUNE TO JULY

ANNEX 3 : PART 2

FIGURE : 4.9

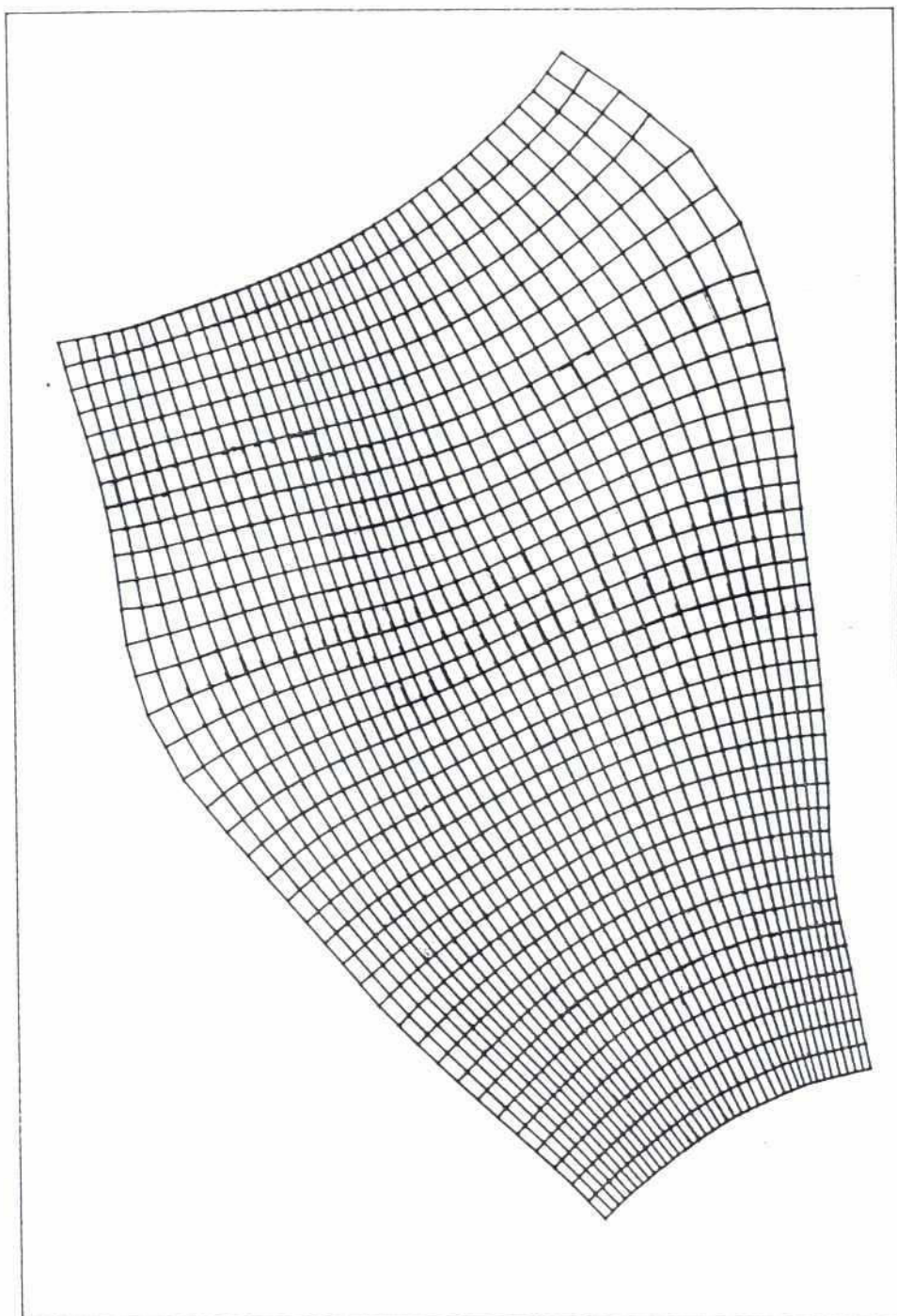


SIMULATED BED LEVEL CHANGES
DISREGARDING BANK EROSION

ANNEX 3 : PART 2

FIGURE : 4.10

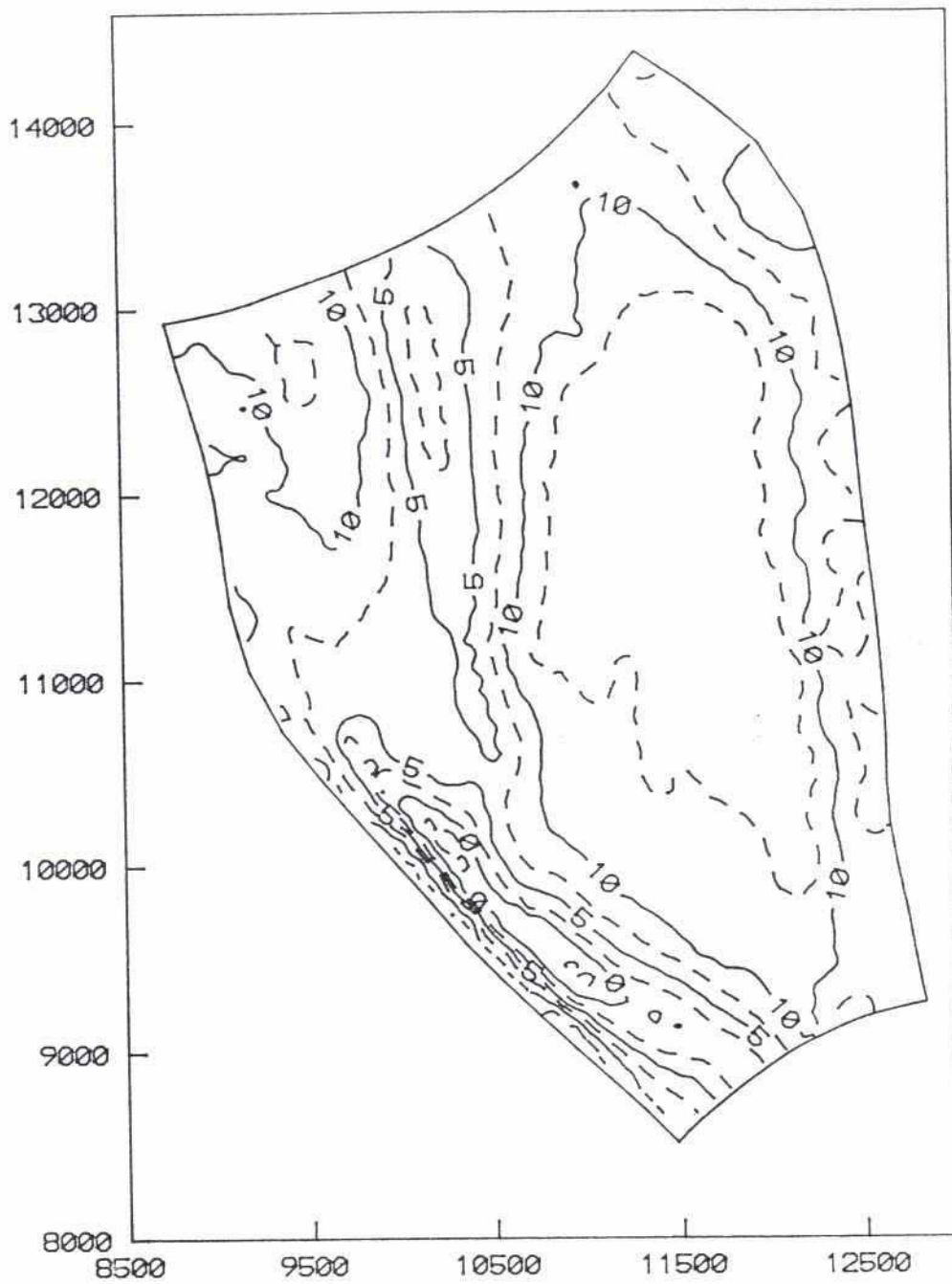
68



CURVILINEAR COMPUTATIONAL GRID FOR TEST AREA-2

ANNEX 3 : PART 2

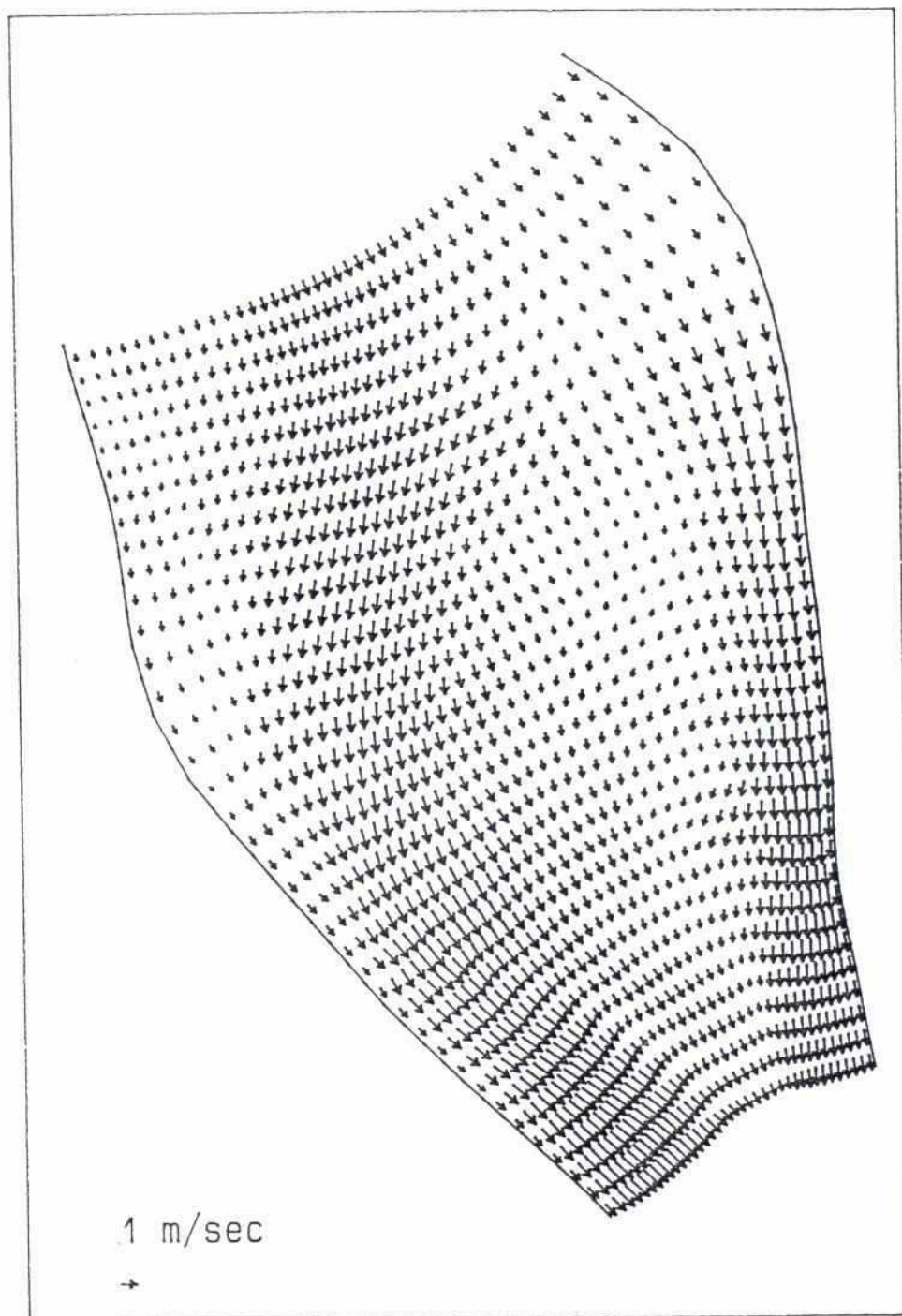
FIGURE : 5.1



MODEL TOPOGRAPHY – TEST AREA-2

ANNEX 3 : PART 2

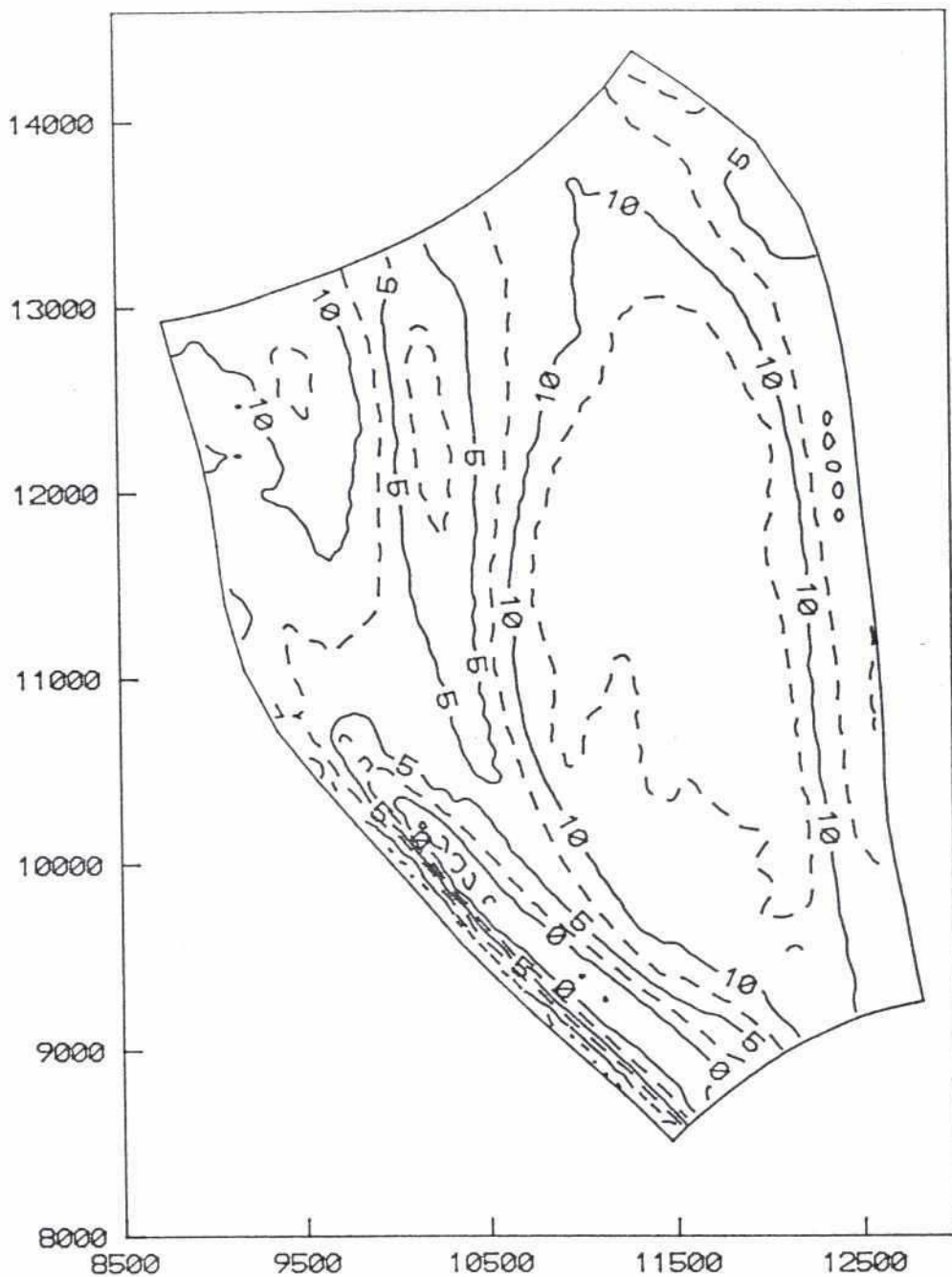
FIGURE : 5.2



SIMULATED FLOW DISTRIBUTION IN TEST AREA - 2

ANNEX 3: PART 2

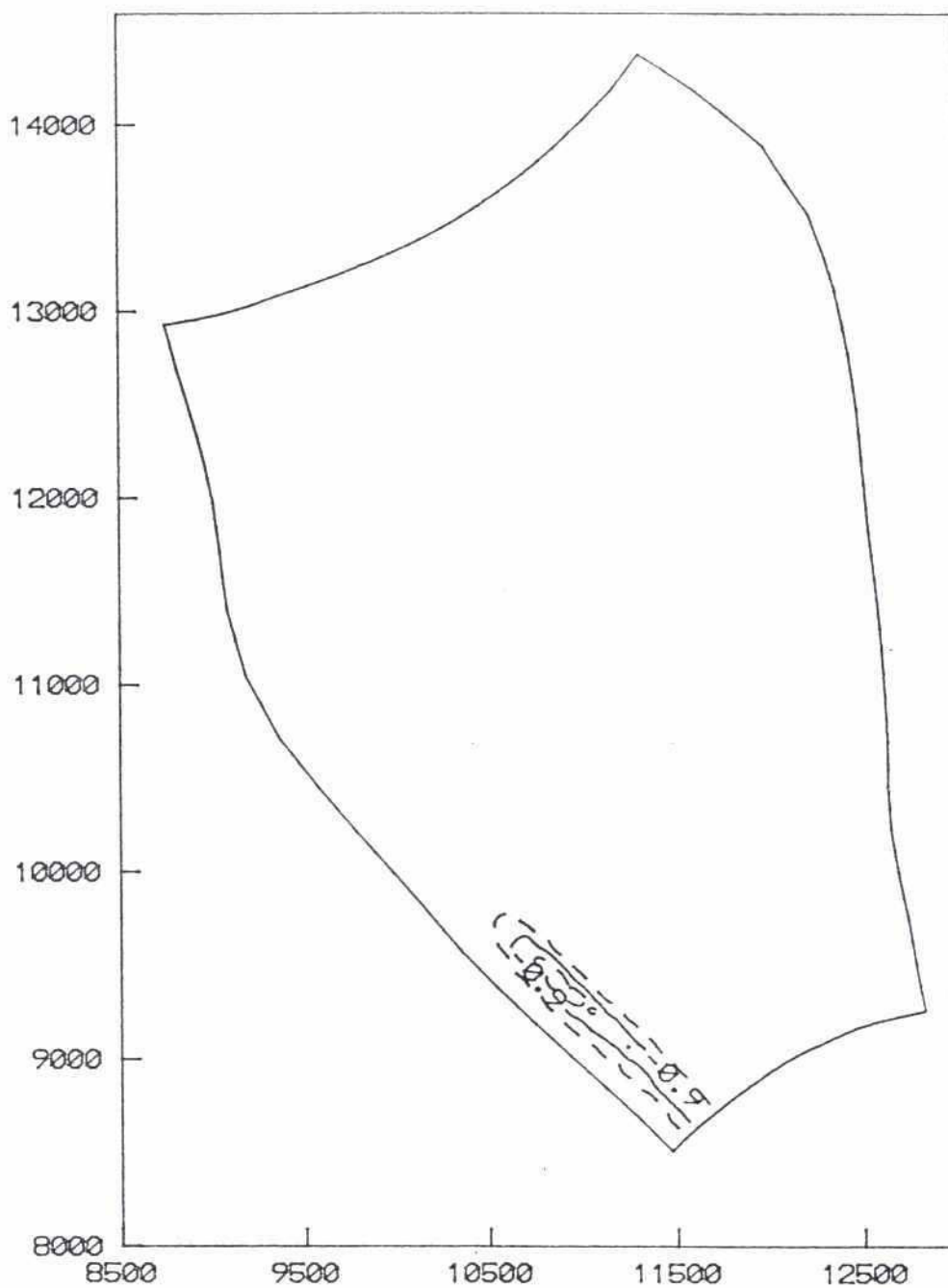
FIGURE 5.3



SIMULATED MODEL TOPOGRAPHY

ANNEX 3: PART 2

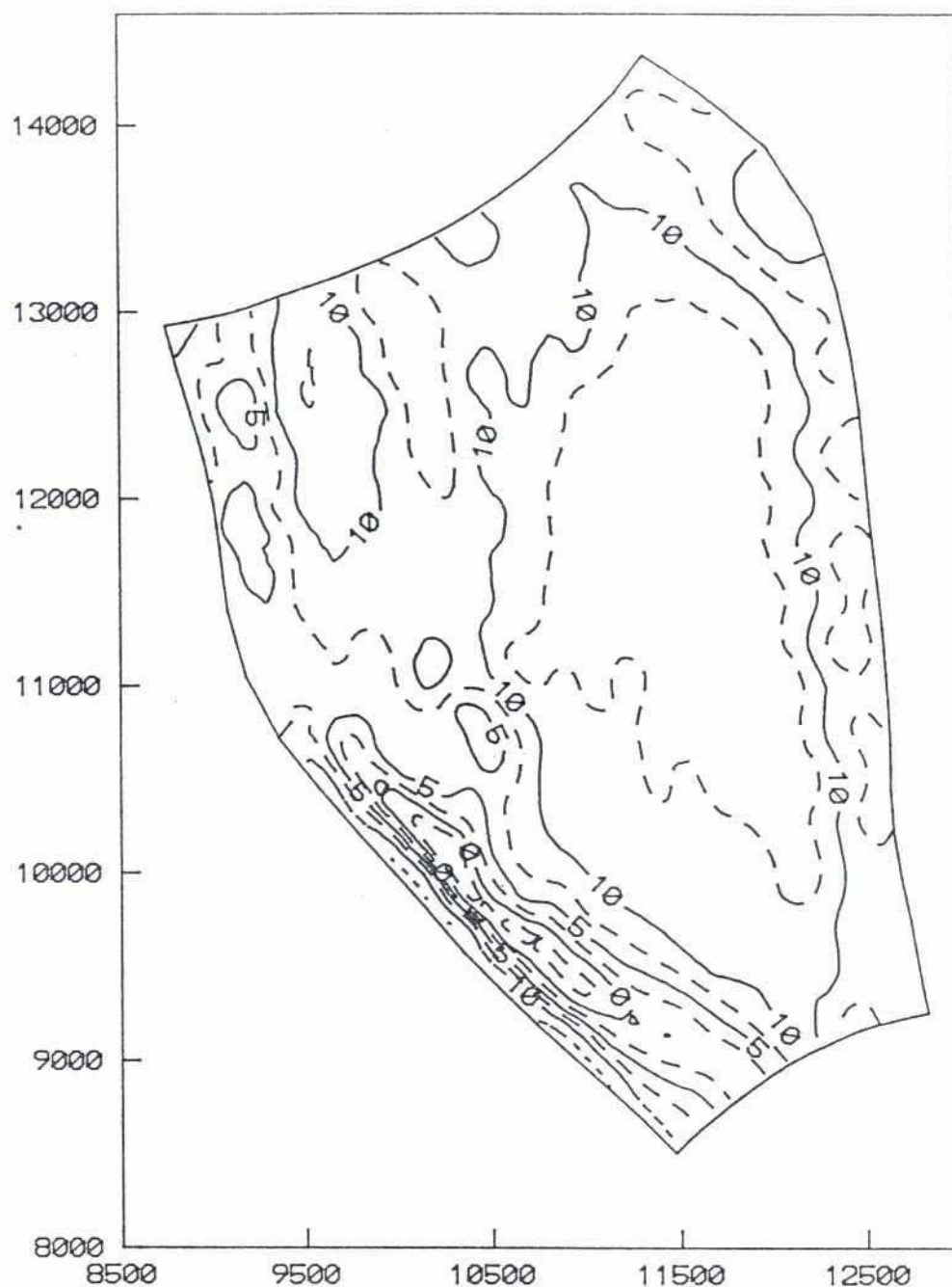
FIGURE 5.4



EROSION DUE TO REVETMENT OF THE BANK

ANNEX 3 : PART 2

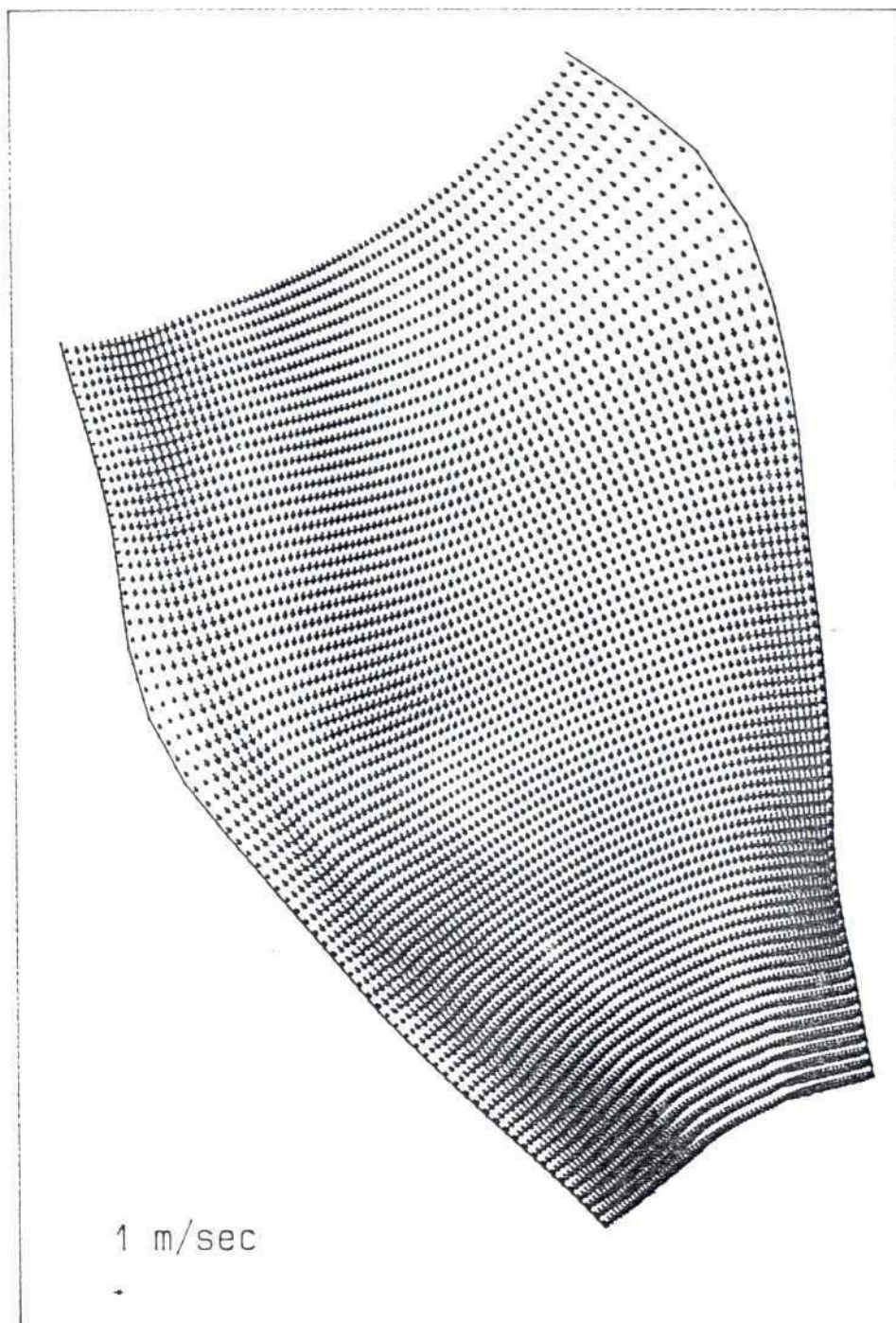
FIGURE : 5.5



MODIFIED MODEL TOPOGRAPHY
(MAIN CHANNEL ENTERING ALONG BANK)

ANNEX 3 : PART 2

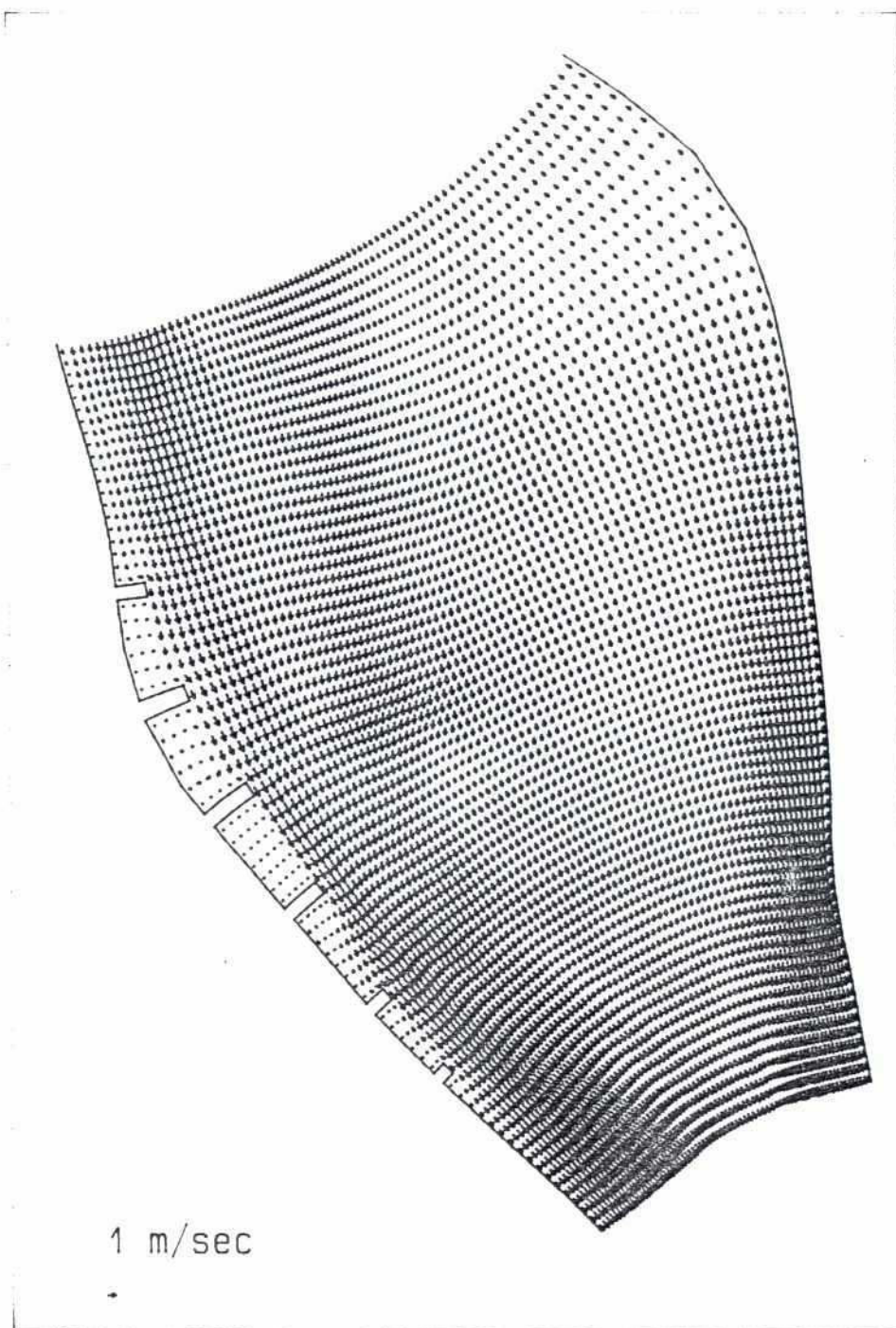
FIGURE : 5.6



FLOW DISTRIBUTION OVER MODIFIED TOPOGRAPHY

ANNEX 3: PART 2

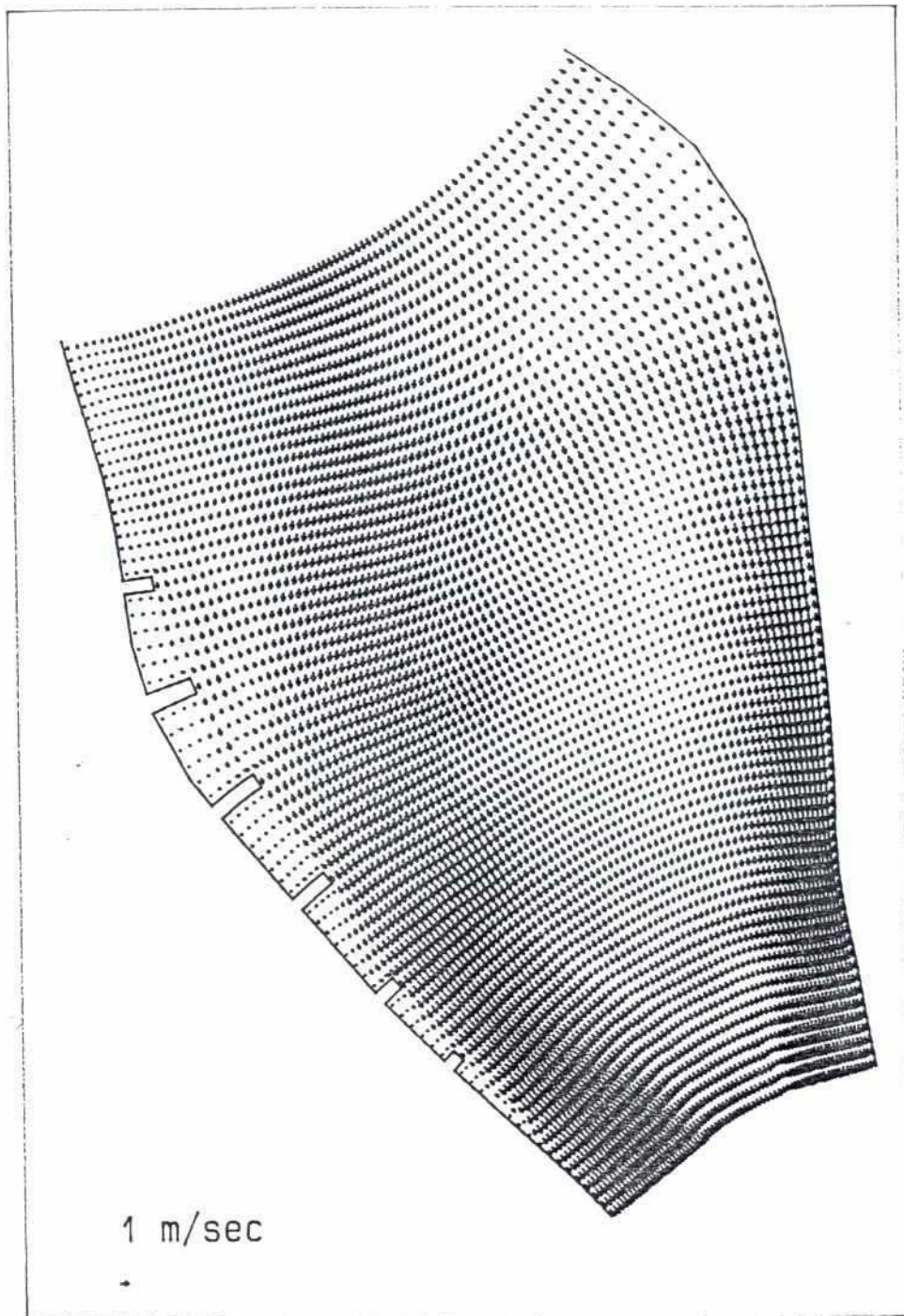
FIGURE 5.7



LAY OUT OF GROUYNE FIELD AND SIMULATED
FLOW DISTRIBUTION

ANNEX 3 : PART 2

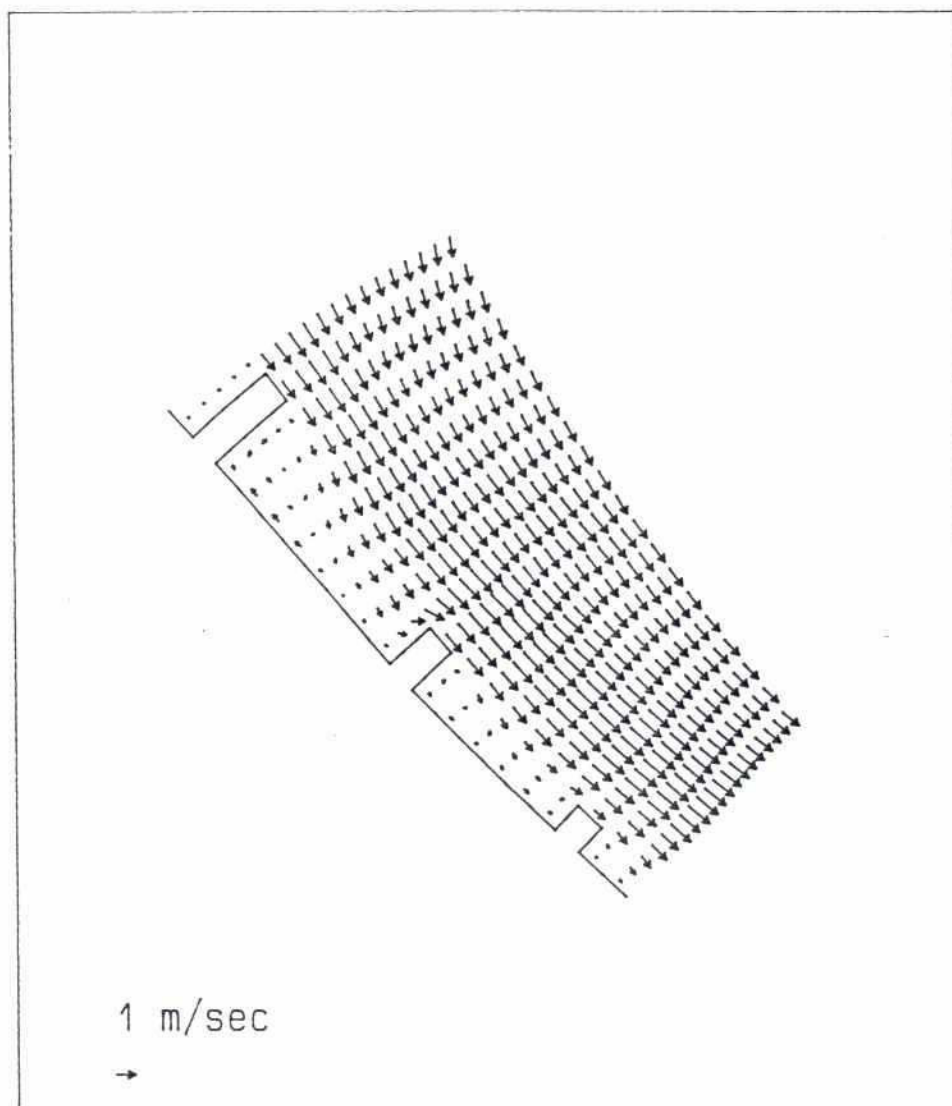
FIGURE : 5.8



FLOW SIMULATION WITH EXISTING BATHYMETRY

ANNEX 3: PART 2

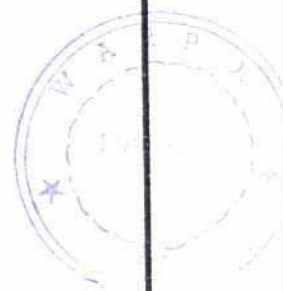
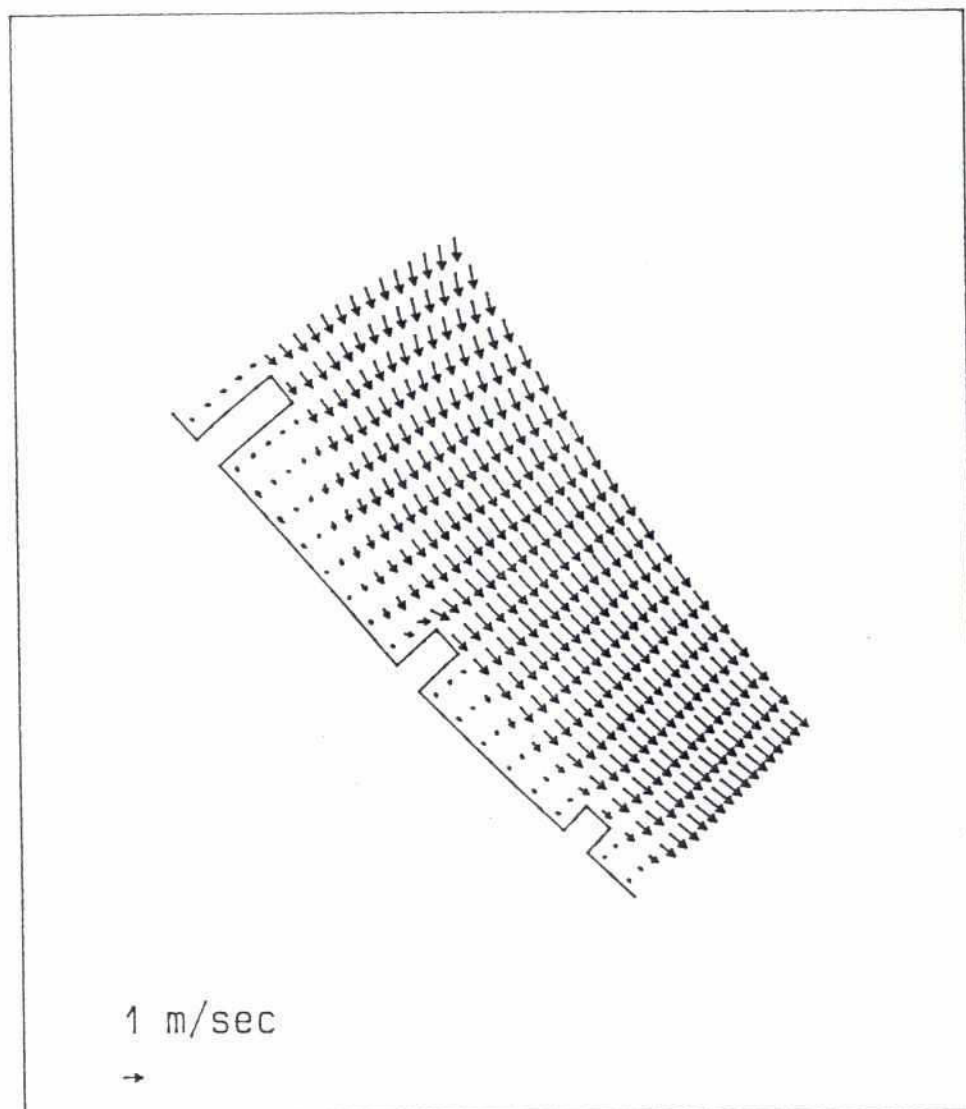
FIGURE : 5.9



FLOW AROUND GROYNES MAIN CHANNEL ALONG BANK
(BLOW UP OF Fig. 5.8)

ANNEX 3 PART 2

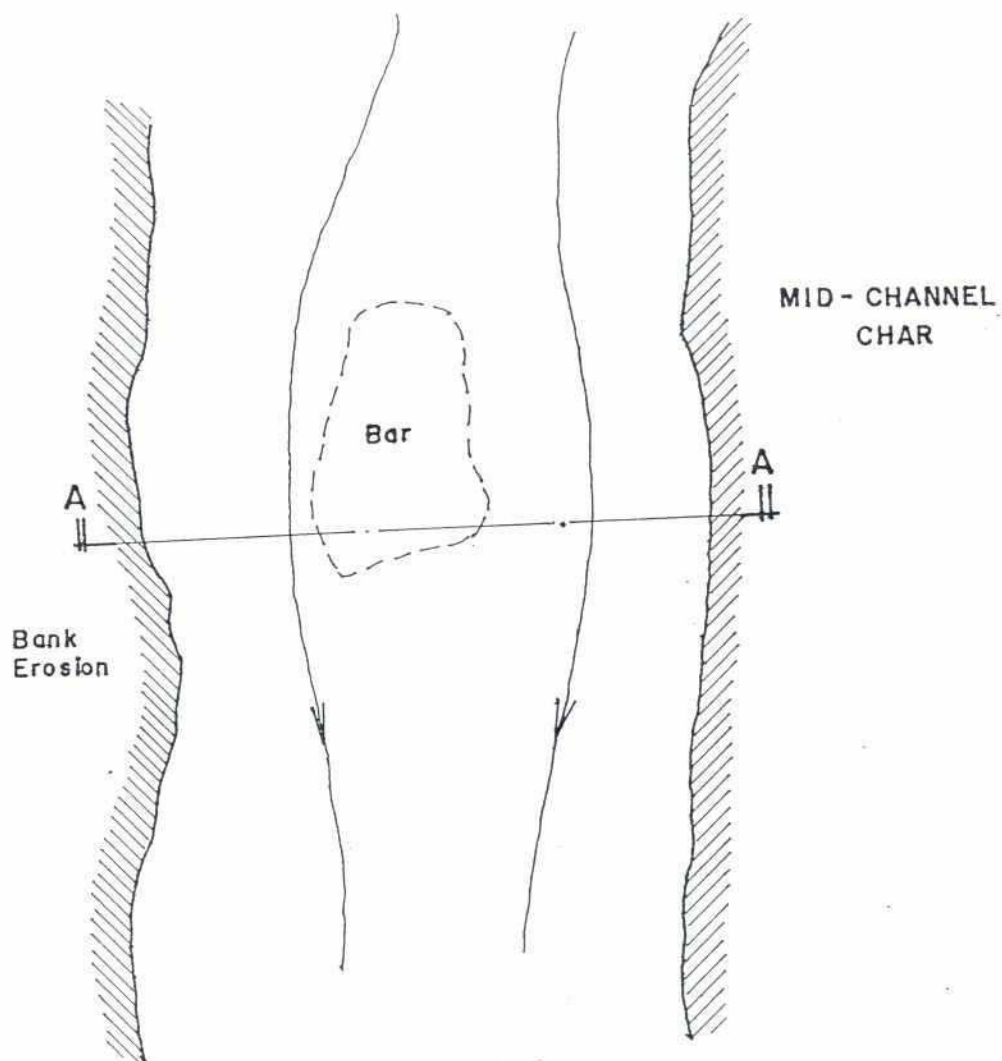
FIGURE 5.10



FLOW AROUND GROYNES. IMPINGING MAIN CHANNEL
(BLOW UP OF Fig. 5.9)

ANNEX 3 : PART 2

FIGURE : 5.11



SECTION A-A

Note:

Flow Curvature and Constriction of Flow area Causes Bed Scour and Bank Erosion.

BANK EROSION DUE TO SUBSURFACE SAND BAR

ANNEX 3 : PART 2

FIGURE : 6.1

Annex 3: Part 2

REFERENCES

BRTS (1990): "Working Paper on 2-D Modelling"

BRTS (1991): "Discussion Paper on Discharge Measurements in Test Area 1".



APPENDIX A
DESCRIPTION OF
SYSTEM 21

202

RIVER TRAINING STUDIES OF BRAHMAPUTRA RIVER
FIRST INTERIM REPORT

APPENDIX A: DESCRIPTION OF SYSTEM 21

CONTENTS

	Page
1. Introduction to the System	1
2. Elliptic Grid Generator	1
3. Hydrodynamic Model	3
4. Helical Flow	4
5. Sediment Transport	5
6. Theoretical Limitations of SYSTEM 21	6

APPENDIX A

Description of System 21

1. Introduction to the System

System 21 is a generalized mathematical modelling system for simulation of the hydrodynamics of and sediment transport in vertically homogeneous flows. The modelling system has the possibility of utilizing both a rectangular and a curvilinear computational grid.

The modelling system is composed of a number of modules relevant to sediment and morphology studies in rivers:

- a hydrodynamic model
- a sediment transport model
- a bed form/flow resistance model (small scale morphology)
- a large scale morphological model

These features are described in general terms in the following Sections.

All these model components can run simultaneously thus incorporating dynamic feedback from changing hydraulic resistance and bed topography to the hydrodynamic behavior of the river. This is illustrated in Figure 1.

For pre-and post-processing of input and output a number of service programs have been developed, such as:

- an elliptic curvilinear grid generator
- graphical software for contour and vector plots

For this study the software has been installed under a SCO-UNIX operating system on a PC-compatible 386-based computer system which incorporates a colour graphic display, printer and plotter. The computer has a memory capacity of 8 MB and a hard disk of 300 MB.

2. Elliptic Grid Generator

The application of curvilinear computational grids is especially advantageous in rivers where the often curved bank lines cannot be resolved accurately in a traditional rectangular computational grid. This implies that a higher overall accuracy can be obtained with fewer computational points. In Figure 2 a river reach is discretized in a curvilinear and rectangular grid. The discretization in the curvilinear grid utilizes 40 computational points, whereas the rectangular discretization uses 75 active (water) points. In the rectangular model there also has to be sufficient storage in the computer memory for a number of passive (land) points (in the figure, 121 points). The time step which can be applied in the curvilinear model will also be much larger, so computational efficiency improves considerably. Moreover, the discretization in the curvilinear grid will provide significantly better modelling accuracy than the rectangular model.

System 21 requires an orthogonal curvilinear grid. This is obtained with a grid generator which solves a set of elliptic partial differential equations using an implicit alternating direction iteration solution procedure. The advantage of using an orthogonal grid is that the partial differential equations, which describe the two-dimensional flow, and hence

the finite difference approximations, become substantially simpler than if a general (non-orthogonal) curvilinear grid were applied. This implies that the truncation errors will be smaller (thus accuracy better) in an orthogonal grid.

Input to the grid generator are the coordinates of boundary points of the computational area, and a so-called weight function for refinement of the computational grid in areas of particular interest. The weight function can for instance be linked to the water depth, so that the grid will be finer in the deeper part where the major part of the flows takes place.

Output from the grid generator is the x,y coordinates of the grid lines inter-section points. A separate program transforms these intersection points into grid increments and curvatures, as required for running the core of System 21.

The generation of curvilinear computational grid is very much an interactive process. The boundaries are smoothed and weight functions are corrected until the computational grid is judged to be sound. Initial hydrodynamic simulations may still reveal the need for further refinements and adjustments of the grid. A graphical program for quick plotting (i.e. minimum input) of the computation grid is included in the system software for speeding up this process.

3 Hydrodynamic Model

The hydrodynamic model simulates the water level variation and flows. These are resolved on the computational grid covering the area of interest, once this has been provided with the bathymetry, bed resistance coefficients and hydrographic boundary conditions.

The hydrodynamic model has been under continuous development at Danish Hydraulic Institute since 1970. It has undergone many changes and improvements, so that it now constitutes one of the most reliable and accurate mathematical modelling tools available for modelling of flows in two horizontal directions.

The hydrodynamic model solves the vertically integrated equations of continuity and conservation of momentum (the Saint Venant equations) in two directions. The following effects can be included in the equations when used for river applications.

- flow acceleration
- convective and cross-momentum
- pressure gradients (water surface slopes)
- bed shear stress
- momentum dispersion
- Coriolis forces
- wind forces
- flow curvature and helical flow

The equations are solved by implicit finite difference techniques with the variables defined in a space staggered computational grid as shown in Figure 3.

The setting up of a hydrodynamic river model using System 21 involves the following three steps:

- (a) The extent of the modelling area is determined and the computational grid is selected for the river. If a curvilinear grid is applied the grid generation described in the previous section is used.
- (b) The bathymetry is entered into the computational grid, i.e. a representative bed level is specified at each computational grid point. Various service programs performing conversions, interpolation, extrapolation, smoothing, etc, are available.
- (c) The specification of the inflow hydrograph, the lateral variation of flow at the inflow boundary, and the temporal variation of water level at the downstream model boundary.

The calibration process for a hydrodynamic model developed with System 21 involves tuning a number of calibration factors. All the calibration factors have physical meaning and should not be arbitrarily given values outside their realistic range to obtain agreement with observed data.

In the case of a hydrodynamic river model only two calibration factors are normally used; the bed resistance factor and the momentum dispersion coefficient (the so-called eddy coefficient). Flow in rivers are generally friction dominated, so the bed resistance factor is normally the most importance calibration parameter. The eddy coefficient only has influence on the simulation of local flow phenomena, (e.g. flow around groynes). If the hydrodynamic model is run in conjunction with the sediment transport model (see below), the bed resistance factor can be calculated by the sediment model. In that case the calibration of the hydrodynamic and sediment transport models are combined.

The output from a System 21 hydrodynamic model comprises flow velocity in two directions, and water depth and water surface elevation at all computational points (see Figure 3) at all time steps.

4

Helical Flow

Helical flow is a principal secondary flow phenomenon in rivers. Whilst it does not have any strong influence on the general flow pattern in rivers with large width-depth ratios, it has significant influence on the sediment transport direction and hence the morphological changes in the river channel (see De Vriend, 1981). The helical flow is therefore only calculated when larger scale morphology is modelled, as distinct from the small scale bed form features. It is the cause of bend scour and plays an important role in confluence scour, and in char build up and migration.

The helical flow pattern occurs in curved flows, especially in river bends. It arises from the imbalance between the pressure gradient and the centripetal acceleration exerted on the water moving along a curved path. Near the river bed the helical flow is directed towards the centre of flow curvature. The magnitude of the helical flow (i.e. the transverse flow velocity component) rarely exceeds 5-10 % of the main flow velocity in natural rivers. A typical helical flow pattern is shown in Figure 4.

Assuming a logarithmic main flow velocity distribution and parabolic eddy viscosity distribution the magnitude of the secondary flow can be shown to be proportional to the main flow velocity, the depth of flow and the curvature of the main flow streamlines. In System 21 the streamline curvature is calculated explicitly from the depth integrated flow field. The gradual adaptation of secondary (helical) flow to changing curvature

is accounted for by solving a first order differential equation along streamlines with the strength of the helical flow as the dependent variable (see also De Vriend, 1981). The strength of the helical flow is used to determine the direction of both bed and suspended load transport.

5 Sediment Transport

In connection with detailed (two-dimensional) mathematical modelling of sediment transport and morphology in rivers with large suspended load transports, it is necessary to distinguish between bed and suspended load in order to:

- simulate the dynamic development of bed form dimensions
- account for the effect of helical flow on the sediment transport direction

The relatively simple total load sediment transport formulas, such as Engelund & Hansen and Ackers & White can therefore not be used along (see below) for river applications with System 21.

A variety of sediment transport formulas have been implemented in System 21 to determine the bed and suspended load. The total load sediment transport formula developed by Engelund & Hansen (1967) in combination with one of the implemented bed load formulas (see below) can be used to calculate the bed and suspended load (the suspended load determined as the difference between total and bed load) or one of the implemented models that yields suspended and bed load separately (Engelund & Fredsoe, 1982 and van Rijn 1984a and 1984b) can be used.

Bed Load Transport:

In System 21 the bed load transport rate is calculated explicitly with the Engelund & Fredsoe, Meyer-Peter & Muller (1948) or the van Rijn model which basically relates the transport rate to the bed shear stress and grain diameter.

On a horizontal bed the transport direction will coincide with the direction of the bed shear stress (which may deviate from the direction of the depth averaged flow due to helical flow as described in Section 4). However, on sloping beds gravity will have influence on the transport direction as outlined in Figure 5.

Several relations for the description of the effect of gravity and bed slope on the transport direction have been implemented in System 21. However, most of these relations have only been verified against data from laboratory tests, and are therefore not necessarily applicable to natural rivers with large suspended load transports. The applicable relation is therefore often determined via calibration of the model.

In rivers, where the sediment transport is mainly bed load, the transverse equilibrium bed slope at a bend can be estimated by assuming that the gravitational force is balanced by the drag force caused by the secondary (helical) flow.

The output from the bed load model is the bed load transport rate and direction at each grid cell.

Suspended Load:

Standard methods for calculation of suspended load are not applicable in the case of detailed (i.e. high resolution) modelling of rivers. It is necessary to include the so-called time-space lag. Consider for instance an increase of flow velocity in a river (e.g. a constriction). As the flow velocity increases the entrainment at the river bed will be increase correspondingly, but it will take some time (and hence some distance) for the sediment entrained at the bottom to disperse all over the water column. This implies that the actual suspended load is not only a function of the local flow conditions as assumed in most mathematical sediment transport models, but is also a function of what takes place upstream and earlier in time.

A relevant time scale for the time lag (T) is the settling time for a sediment grain at the water surface, i.e.

$$T = h / w$$

where:

h water depth

w sediment fall velocity

Correspondingly, a length scale for the spaced lag is

$$L = T u$$

where:

u flow velocity

Assuming $h=8$ m, $w=0.02$ m/s and $u=2$ m/s the time and length scales are 400 s and 800 m, respectively. Consequently, for river applications the space lag is important.

The space lag effect is taken account of in System 21 by a depth averaged convection-dispersion model which represents transport and the vertical distribution of suspended solids and flow. This model is an extension of the model first developed for one dimension by Galappatti (1983) and later in two dimensions by Wang (1989). The model by Wang, however, was primarily developed for estuarine applications and did not include the effect of helical flow. This effect is essential in the case of river applications, because the suspended load transport direction will be different from the main flow direction due to helical flow, as shown in Figure 6, and has been accounted for in System 21.

The depth averaged convection-dispersion model requires an expression for the equilibrium concentration. The models by van Rijn and Engelund-Fredsoe (with the correction for the high near bed concentrations as discussed in Annex 1: Part 3) are implemented for this purpose in System 21.

The output from the suspended load model is the sediment concentration and the suspended load transport and direction.

Bed Forms/Hydraulic Resistance:

It is far more complex to determine the hydraulic resistance in alluvial rivers than in channels with a fixed bed. This is because a large part of the hydraulic resistance in alluvial rivers is caused by bed form drag.

206

The bed forms have a configuration determined by the sediment transport and the flow. The hydraulic resistance will therefore exhibit both temporal and spatial variations.

Generally, the hydraulic resistance is split up into a part caused by drag on the bed forms (form friction) and one due to shear forces on the bed (skin friction). The skin friction is relatively accurately determined from a logarithmic boundary layer equation based on the mean grain size of the bed. The form friction, however, can only be determined analytically if the size of the bed forms are known.

Several hydraulic resistance predictors for alluvial rivers have been proposed, including those of Engelund & Hansen, and Ackers & White. Both of these models are semi-empirical linking the hydraulic resistance to the local instantaneous flow conditions. However there can be a significant lag between the form friction (i.e. the bed form size) and the hydraulic conditions. For instance, in many tropical rivers, with distinct dry and wet periods, the sand dunes found at the river bed during the dry season have been formed during receding flood at the end of the flood season. In such rivers the hydraulic resistance will often be very large during the dry season. It is therefore important to account for this time lag.

In System 21 the dynamic development of the bed form size (height and length) is calculated with the model developed by Fredsoe (1979). In a subsequent step the form friction is calculated using a Carnot type formula for expansion loss. The skin friction is determined from a logarithmic boundary layer equation. In quasi-steady flow this model suggests that as the flow velocity increases the dune size and hence the hydraulic resistance increases. As the flow velocity increases further the bed form height and water depth first increases with more or less the same rate, and hence the hydraulic resistance only changes slowly, until the sand dunes relatively abruptly are washed away and the hydraulic resistance decreases rapidly. These features are illustrated in Figure 7.

Large Scale Morphology:

Large scale in this context means changes in general bed level within the model boundaries as distinct from bed form changes.

The bed and suspended load sediment transport models described earlier in this Section, yield transport rates in two directions. The change of bed level is therefore easily determined by integrating the net inflow or outflow depositing or eroding within a control volume.

This integration is explicit, due to the non-linear character of the sediment transport relations applied. This implies that the large scale morphological model needs to be subjected to a rigorous stability criteria for the time step, however, a time step substantially larger than the time step in the hydrodynamic model can be applied.

Theoretical Limitations of SYSTEM 21

Generally flows in river includes phenomena on a very large range of length and time scales. Turbulence, for instance can have time scales of less than a second, whereas flood wave time scales easily can be of the order of magnitude of weeks or months. The mathematical model can only describe explicitly the phenomena with time and length scales greater than the time

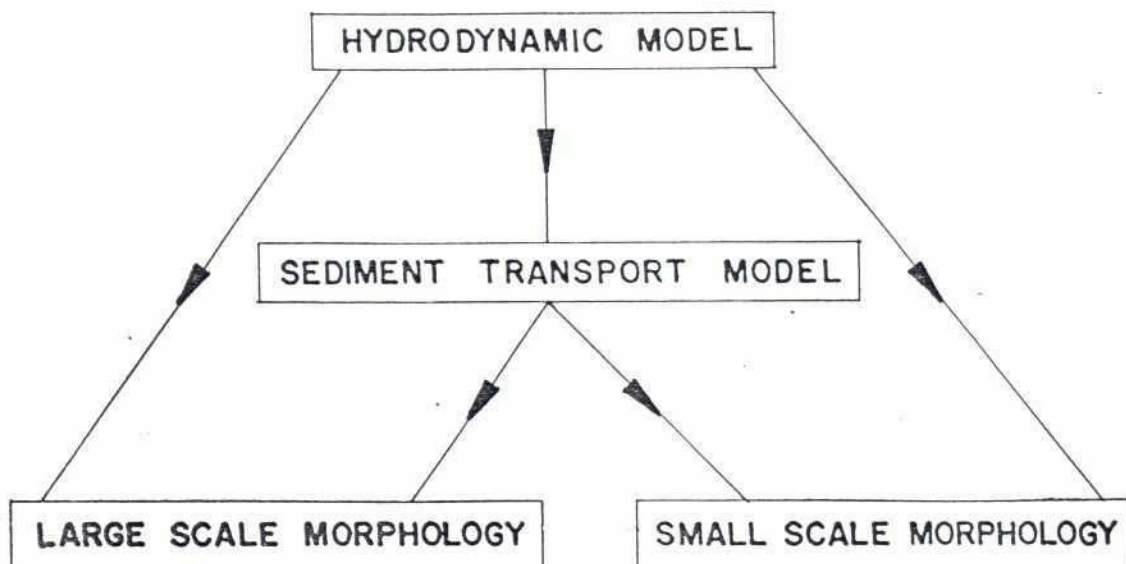
and space steps used in the model. The small scale phenomena may however influence the large scale phenomena; in that case they are included implicitly in the model via a number of simplifying assumptions. Examples are turbulence and bed form friction. Turbulence is modelled via the Reynold stress analogy as an increased viscosity of the water, and the bed form friction as an increased bed roughness coefficient. These simplifications make calibration of the model necessary. Ideally, a model calibration (and verification) should cover the range of conditions, which are to be covered in the model application.

In addition, the model is two-dimensional, whereas flow in, for instance, river bend is strongly three-dimensional. The two-dimensional model has been obtained from the fully three-dimensional equations by depth integration. In this process various assumptions have to be made regarding the vertical distribution of flow velocity (e.g. logarithmic or secondary flow profile as shown in Figure 4). In general, these assumptions hold, but close to the banks in river bends there may be some deviation, (see De Vriend, 1981). This, however, is not considered to be critical provided the model is properly calibrated.

A limitation of the modelling system is that it is a fixed bank model and cannot therefore account for the dynamic development of the bank lines and their impact on the flow and sediment transport processes. However, bank erosion prediction models are as yet not very reliable, and thus introduction of this additional degree of freedom is not yet justified.

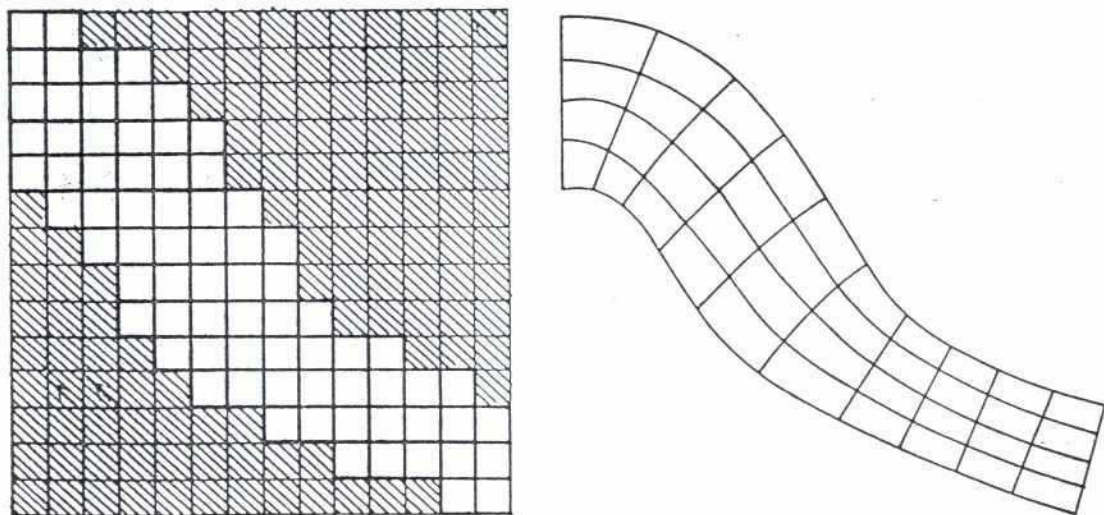
The sediment is represented with one characteristic grain size (mean diameter) in the model, whereas the river sediment consists of continuous spectrum of grain sizes. Segregation processes will take place during transport of the sediment and to some extent this will affect the river topography. Segregation processes, however, have larger influence during the dry season where bed shear stresses are smaller, see Ribberink (1989). The relatively large bed shear stresses during the flood season in the Brahmaputra reduces the importance of this limitation.

FIGURES



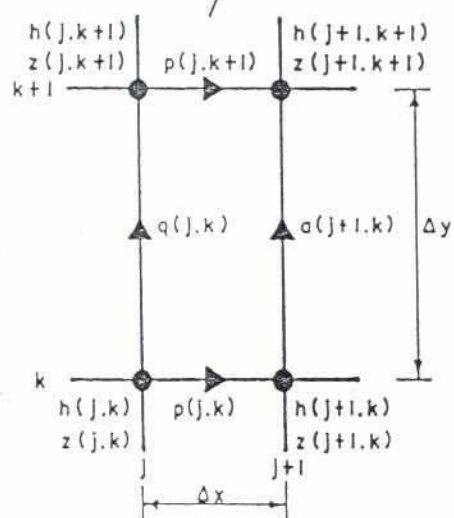
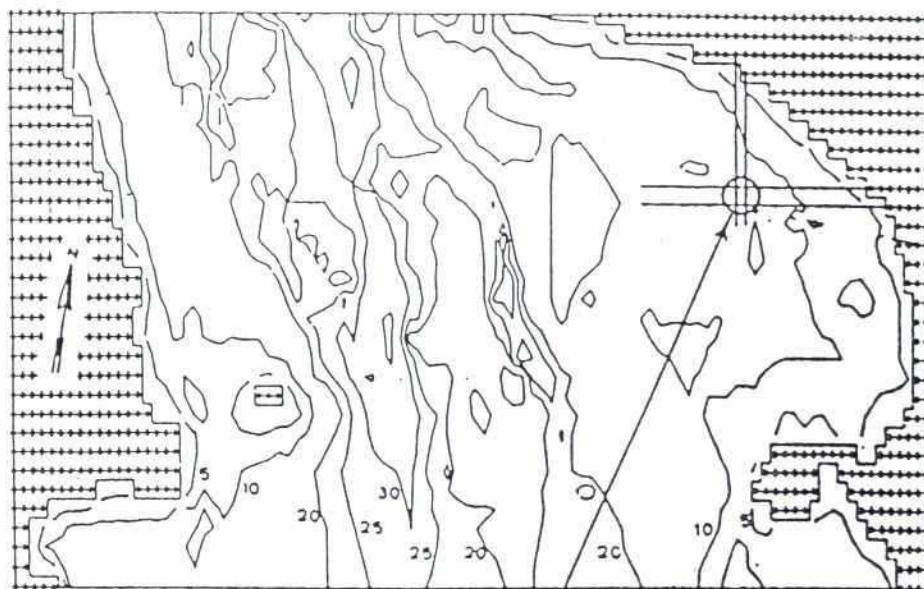
SYSTEM 21

INTERACTION OF SUB MODELS IN SYSTEM 21

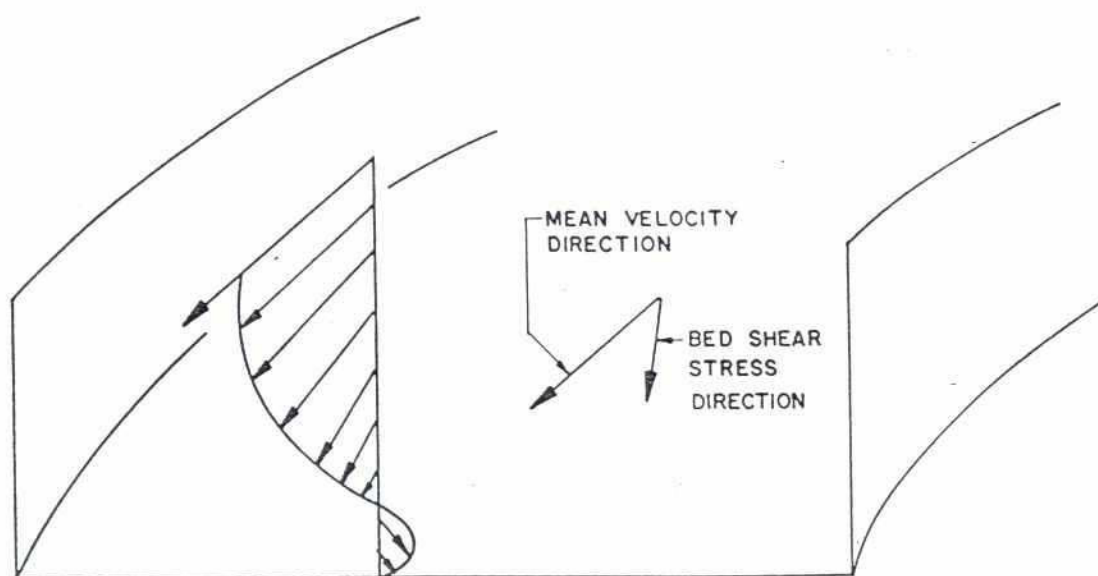


☐ ACTIVE CELL
☒ PASSIVE CELL

SCHEMATISATION OF RIVER IN CURVILINEAR AND RECTANGULAR GRID



SPACE STAGGERED GRID USED IN HYDRODYNAMIC MODEL OF SYSTEM 21



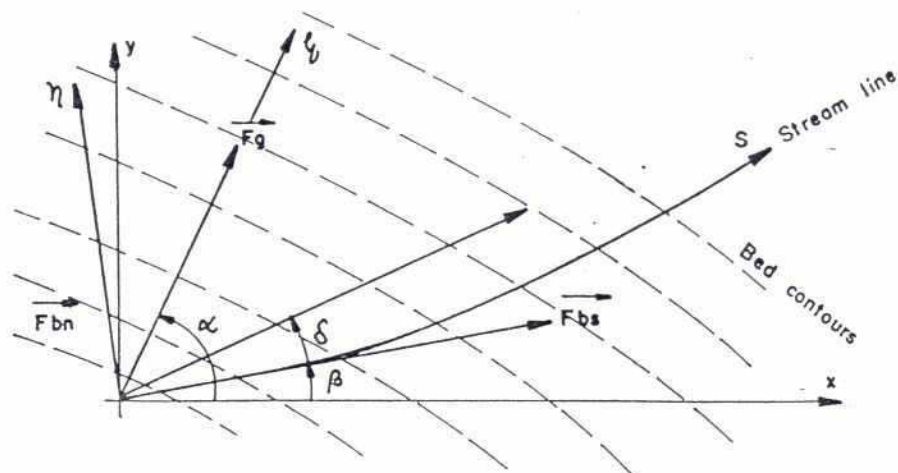
HELICAL FLOW IN RIVER BEND

ANNEX 3 : PART 2

APPENDIX A

FIGURE : 4

28



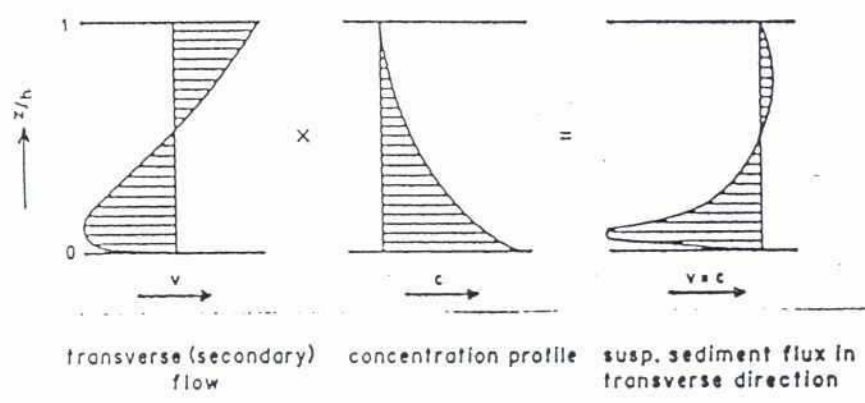
THREE COMPONENTS "DRAGS"

\vec{F}_{bs} = FORCE DUE TO MAIN FLOW

\vec{F}_{bn} = FORCE DUE TO SECONDARY FLOW

\vec{F}_g = FORCE DUE TO GRAVITY ON A SLOPING BED

SHEAR STRESS ON SEDIMENT PARTICLES



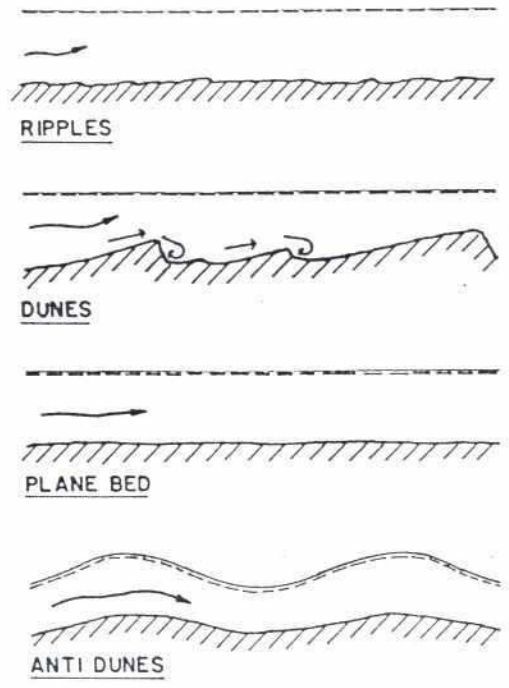
Definition sketch

TRANSVERSE SUSPENDED SEDIMENT TRANSPORT DUE TO
HELICAL FLOW

ANNEX 3 : PART 2

APPENDIX A

FIGURE : 6



DEVELOPMENT OF BED FORMS FOR INCREASING
FLOW VELOCITY



22b

ANNEX 4

GEOMORPHOLOGY

RIVER TRAINING STUDIES OF THE BRAHMAPUTRA RIVER
FIRST INTERIM REPORT

ANNEX 4 - GEOMORPHOLOGY

CONTENTS

	Page
1. INTRODUCTION	1
2. PROGRESS AND FINDINGS	2
2.1 Topic 1: Determination of the Dominant Discharge	2
2.2 Topic 2: Determination of Cumulative Sediment Transport Curve	4
2.3 Topic 3: Specific Gauge Analysis for Bahadurabad	4
2.4 Topic 4: Braid Bar Inundation	5
2.5 Topic 5: Analysis of the Long Profile	8
2.6 Topic 6: Braid Intensity Study	8
2.6.1 Sub-Topic 6.1: Examination of Braiding Intensity on a Reach by Basis	9
2.6.2 Sub-Topic 6.2: Prediction of Confluence Scour from Approach Channel Geometry	9
2.6.3 Sub-Topic 6.3: Hydraulic Geometry Analysis of Anabranh Channels	10
2.6.4 Sub-Topic 6.4: Investigation of Braiding Intensity Affects on Width and Depth	10
2.7 Topic 7: Meandering of Anabranhcs: Scour Depth Prediction	11
2.8 Topic 8: Meandering of Anabranhcs: Velocity Prediction	11
2.9 Topic 9: Meandering of Anabranhcs: Migration Rate Prediction	11
2.10 Topic10: Historical Bankline Migration	13
2.11 Topic11: Bank Erosion Sediment Yield	14
2.12 Topic12: Comparison of Bank and Char Sediments	14
2.13 Topic13: Bank Stability Assessment	16
2.14 Topic14: Assessment of Bank Condition	17
2.15 Topic15 to 18: Mapping of Flood Plain Topography, Geology and Geomorphology	17
3. IMPLICATIONS FOR BANK PROTECTION AT PRIORITY LOCATIONS	18
3.1 Rationale	18
3.2 Macro-scale Geomorphology	18
3.3 Reach scale Geomorphology	21
3.4 Local Geomorphology	21
3.4.1 Kazipur	21
3.4.2 Sariakandi, Mathurapara, Chandanbisha, Sonalibazar, Sirajganj	22
3.4.3 Betil and Jalapur	23
3.5 General point on Chute Channels	23

TABLES

Table 2.1	Comparison of Dominant Discharge and Barfull Flows
Table 2.2	Confluence Scour Prediction
Table 2.3	Migration of Anabranh Meanders 1987/89
Table 2.4	Sediment Yields for the Brahmaputra River 1986-87
Table 2.5	Relative Yield of Sediment from Bank Erosion

FIGURES

Figure 2.1	Frequency Distribution for Discharge at Bahadurabad - Brahmaputra River (1956-1989)
Figure 2.2	Sediment Rating Curve at for Total Measured Load Bahadurabad - Brahmaputra River (1982-1988)
Figure 2.3	Total Sediment Transport Vs. Discharge Curve at Bahadurabad - Brahmaputra River
Figure 2.4	Suspended Sand Rating at Bahadurabad - Brahmaputra River (1982-1988)
Figure 2.5	Suspended Sand Transport Vs. Discharge at Bahadurabad - Brahmaputra River
Figure 2.6	Flow Duration Curve at Bahadurabad - Brahmaputra River
Figure 2.7	Cumulative Total Measured Sediment Transport Vs. Discharge Curve at Bahadurabad - Brahmaputra River
Figure 2.8	Cumulative Measured Sand Transport Vs. Discharge Curve at Bahadurabad-Brahmaputra River
Figure 2.9	Water Level Variation for six Relevant Discharges at Bahadurabad -Brahmaputra River (1963-1989)
Figure 2.10	Water Level Variation at Bahadurabad for four Relevant Discharges During the 1956-68 period (After lates, 1988)
Figure 2.11	Comparison of Dominant Flow & Barfull Flow Level
Figure 2.12	Relation between Sediment Transport & Barfull Flow
Figure 2.13	Bend Migration Versus Bend Curvature
Figure 2.14	Ratio of Erosion to Progression Versus
Figure 2.15	Schematic Diagram of Sediment Budget of the Brahmaputra River, 1986-87
Figure 3.1	Lane's Braiding Diagram
Figure 3.2	Longterm Distribution of Bank Movement
Figure 3.3	Bank Movement from about 1956 (3 sheets)
Figure 3.4	Geomorphic Map Showing Possible left Bank Constraint
Figure 3.5	Tentative prediction of Future Bank line

ANNEX 4 - GEOMORPHOLOGY

1. INTRODUCTION

This Technical Annex 4 to the First Interim Report of the River Training Studies for the Brahmaputra River (BRTS) outlines the programme of geomorphological analysis that is being undertaken jointly by the BRTS team and the BUET Advisory Group from the Bangladesh University of Engineering and Technology. It describes the progress made, reports on the ~~the~~ results that have been obtained to date, draws preliminary conclusions and sets out the remaining tasks to be completed.

The role of the geomorphological studies in relation to the mathematical and physical physical modelling elements of the BRTS has earlier been described in the Inception Report (May 1990) and the Working Paper on 2-D Modelling (December 1990).

The geomorphological analysis of a large, braided river like the Brahmaputra is a very complicated task. In order to make it manageable, such an analysis is best divided into a number of clearly defined tasks, each of which may be accomplished somewhat independently of all the others. Once all of the tasks have been completed, it is then essential to integrate all of the findings in order to synthesize an overview of the present state of the river, its historical tendencies, its probable future trends and its likely responses to bank stabilization and river training. This approach has been adopted in the geomorphological element of the Brahmaputra study.

The major sub-divisions of the geomorphological study come directly from the Inception Report. They are:

I. CHANNEL GEOMETRY AND DYNAMICS

- A. Geomorphological Analysis of Gross Channel Features
- B. Geomorphological Analysis of Sub-channel and Anabranch Features
- C. Bank Erosion and Stability Studies

II. GEOMORPHOLOGICAL AND GEOPHYSICAL ASPECTS

III. HISTORICAL CHANNEL CHANGES

Within these major sub-divisions, twenty discernible topics were identified for scrutiny. These topics are:

Sub Division	Topic Number	Topic Title
IA	1.	Determination of Dominant Discharge
	2.	Determination of Cumulative Sediment Transport Curve
	3.	Specific Gauge Analysis for Bahadurabad
	4.	Braid Bar Inundation Study
	5.	Analysis of Long Profile
IB	6.	Braid Intensity Study
	7.	Meandering of Anabranches: Scour Depth Prediction
	8.	Meandering of Anabranches : Velocity Prediction
	9.	Meandering of Anabranches : Migration Rate Prediction
IC	10.	Historical Bankline Migration; Reach by Reach
	11.	Computation of Bank Erosion Sediment Yield
	12.	Comparison of Bank Erosion and Char Migration
	13.	Analysis of Bank Stability
	14.	Assessment of Bank Condition
II	15.	Mapping of Flood Plain Topography
	16.	Mapping of Flood Plain Geology
	17.	Mapping of Flood Plain Geomorphology
	18.	Mapping of Flood Plain Land-use
III	19.	Analysis of Longterm Channel Development
	20.	Case Studies of Causes of Severe Bank Erosion

Several of the topics have now been completed and significant progress has been made on the rest. The remainder of this Annex consists of reports of the findings of completed topics, progress reports on incomplete topics and an overview of the geomorphology of the Brahmaputra River in the study reach based on the information produced by the twenty topics studied.

2. PROGRESS AND FINDINGS

2.1 Topic 1: Determination of the Dominant Discharge

The dominant discharge concept was first put forward by Wolman and Miller (1960). Stated plainly, the concept hypothesises that in rivers which experience a highly variable range of flows, the dimensions and geometry of the channel are determined by the flow which performs the most work, where work is defined as sediment transport. There are other definitions of dominant discharge. For example, Ackers and Charlton (1970) defined it as the steady flow that would produce the same meander wavelength as the observed range of flows within which that steady flow lies. Wolman and Gerson (1978) extended Wolman's original contribution on dominant discharge in arguing that the effectiveness of a flow event reflects the morphological changes it causes through erosion and deposition, as well as the associated sediment transport. These are, however, complementary definitions in that it should be expected from basic principles that the flow doing most work on the channel would be responsible for forming and

scaling the salient parameters of its geometry, size and sedimentary features.

A completely different definition, which is not consistent with Wolman and Miller's original concept or Ackers and Charlton's alternative view, was adopted in the JMBA study of the Brahmaputra. They define dominant discharge as "that steady discharge which, had it operated continuously for the period of record, would have transported the same amount of sediment as the range of flows which actually occurred" (JMBA Design Report, Volume II, page A1.2). This corresponds to the flow associated with the time average sediment transport rate. This definition is often used by mathematical modellers (Olesen, Personal communication) but it is not appropriate for use in the geomorphological analysis of river form and process. Although Wolman and Miller's concept has frequently been questioned on theoretical grounds, few people question its usefulness and validity as an analytical device in the geomorphological assessment of rivers and as an aid to river modelling and management.

The analysis was undertaken by the team from the Bangladesh University of Engineering and Technology (BUET) according to the approach suggested by Wolman and Miller (1960). It was based on hydrological and sediment transport records from the Bangladesh Water Development Board (BWDB) gauging station at Bahadurabad. Daily discharge data for the period 1956/7 to 1988/89 were used to construct a flow frequency distribution (Figure 2.1). Sediment transport measurements taken between 1982 and 1988 were used to construct a sediment rating curve (Figure 2.2). The flow frequency curve was divided into discharge classes with increments of 5,000 m³/s and the frequency of each class was multiplied by the appropriate sediment transport rate, to produce a total sediment load transported by that discharge class during the period of record (Figure 2.3).

Examination of the total sediment transport curve in Figure 2.3 shows that it is bimodal. The main peak defines the flow doing most work on the channel through the transport of sediment : that is the dominant discharge.

The dominant discharge is defined by the analysis to be 38,000 m³/s. The smaller, secondary peak is associated with a discharge of 7,500 m³/s, which corresponds to base flow for the river and it is possible that some characteristics of anabranch channel geometry may be adjusted to this discharge. The JMBA report quotes a figure of 23,200 m³/s for dominant discharge. As pointed out earlier, their concept of dominant flow is quite different from that used here. It is appropriate for mathematical modelling, but not morphological analysis.

Noting that a large proportion of the measured sediment load at Bahadurabad is made up of wash load (silt), which notionally plays relatively minor role in forming the channel, the analysis was also performed using the sediment rating curve for suspended sand load only (Figure 2.4). While the absolute amounts of total sediment transported were reduced substantially (Figure 2.5) the distribution was not significantly altered and the dominant discharge was unchanged. It was, therefore, concluded that the dominant discharge of the Brahmaputra River in Bangladesh is about 38,000 m³/s and this is quite a robust result which is insensitive to the precise nature of the sediment rating curve used to derive it. Comparison to the bankfull discharge of 44,000 m³/s (JMBA Design Report), shows the dominant discharge to be close to but a little less than bankfull flow. Examination of the flow duration curve for Bahadurabad (Figure 2.6)

indicates that the dominant discharge is equalled or exceeded 18% of the time. The return period for dominant discharge is a little less than one year.

These findings are consistent with results for other large rivers and are not at all unexpected. For example, Benson and Thomas (1966) found that the dominant flow in several streams with sediment transported predominately as suspended load, had exceedance frequencies in the range 7.6 to 18.5%, and that dominant flow was less than bankfull flow. More recently, Lee and Davies (1986) analysed dominant discharge in braided streams using a physical model. They found that the dominant flow was equalled or exceeded 22% of the time that the bed material was in motion, and concluded that dominant discharge is likely to be less than bankfull flow in a braided river.

2.2 Topic 2: Determination of Cumulative Sediment Transport Curve

The cumulative sediment transport curves for measured total load (silt and sand) and measured sand load (sand only) were determined by progressively accumulating the sediment loads for each discharge class from the lowest to the highest discharge. Each cumulative sediment discharge was expressed as a percentage of the total sediment load transported during the period of record. The curves are plotted in figures 7 and 8 for measured total and measured sand loads, respectively.

The curves in Figures 2.7 and 2.8 are very similar. Both show a distinctive "S" shape, with a very steep, almost linear increase in cumulative sediment load for discharges between 32,500 and 50,000 m³/s. The Brahmaputra River experiences discharges ranging from 2,500 m³/s to over 90,000 m³/s, but flows between 32,500 and 50,000 m³/s, a range of only 17,500 m³/s, are responsible for transporting about forty per cent of all the sediment moved by the Brahmaputra River. Discharges less than 32,500 m³/s transport about 10% of the load, and the cumulative contribution of all floods greater than 50,000 m³/s is less than about 20% of the total load, while that of flows greater than 60,000 m³/s is less than 8% and of flows greater than 70,000 m³/s, less than 2%. The return period for 70,000 m³/s is about 3 years. These results may surprise many river engineers who view large overbank floods as having great long-term significance in doing work on the channel. The data do not support that conclusion. They do, however, highlight the importance of flows around the dominant discharge in forming the channel, and identify that high, inbank flows between 33,000 and 44,000 m³/s have a disproportionate impact on channel form since they transport almost a third of the total load.

2.3 Topic 3: Specific Gauge Analysis for Bahadurabad

When analysing the medium to long term behaviour of river, a specific gauge analysis can be used to determine if there are any trends with time in the elevation of the water surface corresponding to a given discharge. The analysis must be based on historical stage-discharge records for a gauging station with an open-river section. In this study, the records from Bahadurabad between 1963/64 and 1988/89 were used. The work was performed by the BUET team. Out of this period, rating curves for the years 1969/70, 1971/72 and 1978/79 were unavailable.

The method of analysis was based on discharges of 7,000, 14,000, 28,000, 42,000, 60,000 and 80,000 m³/s and the corresponding water stages from the rating curves for the available years. For the 80,000 m³/s flow, mostly extrapolated values of stage had to be used. Water stages were then plotted versus year of observation on an arithmetic plot (Figure 2.9). The results suggest a slight overall rising trend in water stages for the period of observation. Lates (1988) showed that during the period 1956-68 low water levels (14 000 and 28,000 m³/s) at Bahadurabad had a rising trend, while intermediate flows (42,000 m³/s) were constant and the stage associated with high flows (70,000 m³/s) fell slightly. In the period 1968/69 to 1985/86 the rising trend of the lowest flows (7,000 and 14,000 m³/s) continues, while the intermediate flows fall slightly and the high flows rise markedly. Since 1985/6 all but the lowest flow (7,000 m³/s) show a marked reduction in stage (Figure 2.10).

Stage changes like this are characteristic of a large, braided river with a highly mobile bed. The passage of macro-scale bed forms such as sand waves, and the shifting of braid bars and chars can radically alter the resistance characteristics and water surface topography, so altering the stage-discharge relationship. Also, unsteady flow effects, varying sediment transport rates and bedform hysteresis can produce marked changes during a single annual hydrograph (Vanoni, 1975). The degree of variability observed in the stage-discharge relations is, therefore, to be expected.

Some trends in the data are maintained for periods of five to seven years and these are probably not associated with hydraulic roughness or sediment transport effects: they are representative of systematic trends in the bed level at Bahadurabad associated with the passage of pulses of sediment moving through the fluvial system. Pulsed movement of bed load is widely observed in rivers. It may be attributed to unsteady supply from outside the channel. In the case of the Brahmaputra, sediment inputs associated with major landslides in Assam during tectonic events are known to have occurred (Goswami, 1985). However, bed load pulses are known to develop even in cases of steady sediment supply in flume experiments (Thorne et al., 1987) and so they would probably be a feature of the Brahmaputra with or without the effects of landslides upstream.

Any persistent trend in the stage-discharge relations over the twenty five years period of record could be indicative of net degradation or aggradation of the channel. When analysing the records to identify any trend it would be inappropriate to use least squares regression because of the high degree of 'noise' in the data. Instead application of a robust assessment of trend and non-homogeneity based on 3-point moving medians was undertaken. The results indicate that the stage-discharge relations for all six discharges do not show any significant trend at a 5 per cent confidence level.

2.4 Topic 4: Braid Bar Inundation

In the study of fluvial geomorphology, alternative definitions of the dominant discharge refer to the most effective flow in doing work on the channel through transporting sediment (Wolman and Miller, 1960) and the discharge responsible for forming the main features of the channel (Ackers and Charlton, 1970). Many researchers have concluded that these two definitions are complementary in that the flow responsible for doing most work and the "channel forming" discharge are one and the same (for example, Hey, 1978 and Andrews, 1980).

In single thread rivers which are in dynamic equilibrium (that is they have alluvial, mobile boundary materials but are neither aggrading, degrading or changing their width through time), the morphological expression of dominant flow is in the bankfull capacity. There is ample evidence from rivers with a wide variety of bed material types that dominant flow equates with bankfull flow in terms of discharge magnitude and, to a lesser extent, in terms of flow frequency (Richards, 1982; Knighton, 1984). However, in multi-thread or braided rivers this is not thought to be the case (Lee and Davies, 1986; Biedenharn et al., 1987). In fact dominant discharge is believed to be less than bankfull discharge in braided rivers.

Nonetheless, it should be expected that if the dominant discharge is truly significant in forming the channel, there should be major morphological features which reflect this through being adjusted to the dominant flow. Perhaps the most prominent features of a braided river are the braid bars (chars) which are responsible for the river's characteristic multi-channel cross-section, very high width/depth ratio, braided planform and shifting nature. Therefore, in this study topic the morphology of the braid bars was investigated in order to determine if there was a clear association with the dominant discharge identified from the analysis of total sediment transport to be $38,000 \text{ m}^3/\text{s}$.

Initially it was proposed to use an objective approach based on a quantitative measure of braid bar inundation. The proposed approach was to plot graphs of exposed char area versus discharge and identify a "bankfull" discharge which just inundated the char.

Experience in undertaking a similar analysis of bars in the Mississippi River indicated that usually this relationship is "S" shaped. This occurs because, although the bar surface is platokurtic, there are usually one or more high points on the bar which are only inundated by high flows above bankfull. In defining barfull discharge, these are excluded from consideration and 95% bar inundation is taken to constitute barfull flow. In the Mississippi River study, a close correspondance was found between dominant flow and barfull flow over a two hundred kilometre length of channel.

Unfortunately, it proved impossible to achieve such an objective, quantitative analysis of the Brahmaputra River in the BRTS study. There were several reasons for this, the main ones being difficulty in the selection of appropriate chars and braid bars for analysis, non-availability of accurate topographic maps of the chars and the large time commitment necessary to produce the measurements of exposed char area as a function of discharge.

Instead of the objective, quantitative approach, a qualitative approach was adopted, based on visual examination of the water surface elevation corresponding to dominant discharge in relation to char top elevations at selected, surveyed cross-sections. The analysis was performed for the 1988/89 survey and the water surface elevations were taken from a preliminary run of the BRTS 1-D MIKE-11 model, for a flow of $38,000 \text{ m}^3/\text{s}$. The results are given in Table 2.1 and Figure 2.11.

Table 2.1: Comparison of Dominant Discharge and Barfull Flows

Chainage (km)	Water Level (m.PWD)	Cross- section No	Barfull Level (m.PWD)	Depth over bar (m)
25.0	23.92	J-17	23.6	0.32
56.0	20.36	J-15	21.6	- 1.24
56.0			19.5 *	0.85
64.0	19.03	J-14	18.9	0.13
76.6	18.18	J-13	18.0	0.18
91.0	17.04	J-13	17.1	- 0.06
105.4	16.06	J-11	15.2	0.86
119.8	15.27	J-10	14.6	0.63
130.6	14.69	J-9	14.3	0.39
143.8	14.23	J-8	13.7	0.53
155.8	13.67	J-7	13.1	0.57
170.2	12.61	J-6	12.2	0.41
182.2	11.57	J-5	11.3	0.27
196.6	10.57	J-4	10.1	0.47
213.4	9.51	J-3	9.1	0.41
Average depth over bar				0.28 m (or 0.9 ft)

* excluding chars above flood plain level.

The results show a strong relationship between the dominant discharge water level and the barfull stage in the channel along the whole length of the study reach. Generally, dominant flow is a little above barfull capacity so that the average flow depth above the bar is between zero and one metre, being on average about 30 centimetres. The one exception J-15 which would not be overtopped even by bankfull discharge and which, therefore, could be classed as flood plain elements separated by anastomosed channels, rather than true braid bars. If they are excluded from consideration, barfull level for the remaining in-bank chars is 19.5 m PWD, yielding an overbar depth of 0.85 m which is within the general range.

It is appropriate to attempt a rational explanation of these results, based on the links between water level, sediment transport rate and channel morphology.

Figure 2.12 shows a schematic representation of flow in a braided channel. At low flow (stage 1), well below barfull stage, the active (mobile) width is limited to the anabranches. Even if the sediment transport rate per unit bed width is quite high, the total transport rate for the river is relatively low because of the small proportion of the actual bed width which is active. Even with a substantial rise in discharge and stage (stage 2), and a commensurate increase in unit sediment load, the total load increases only slowly because the active width has not increased substantially.

However, for a small increment of increase in discharge and stage which takes the river to barfull discharge, it may be expected that the sediment transport rate will increase very markedly. This would occur because the active width increases and sediment becomes available for transport across

also near char flow
+ turbulence levels change
Remember: Chars are eroded sideways
not vertically

the whole bed width including the char tops. The unit sediment transport rate on top of the char may be fairly low, because the depth is small. However the slope will be greater for flow over rather than around the char, so that boundary shear stress may be quite high. Even if the average unit transport rate falls somewhat, the total load increases substantially.

These arguments support the thesis that the sediment transport capacity of the river just above barfull stage should be substantially greater than that just below barfull stage. The increased transport capacity, coupled with much increased sediment availability from the char surface, producing a very marked increase in sediment transport rate.

It may be concluded that the dominant discharge of 38,000 m³/s is responsible for producing the major morphological feature of the Brahmaputra River, that is the braid bars. The braid bar height is adjusted to be close to but a little less than bankfull stage, which corresponds to dominant flow. Flows between barfull and bankfull flow would thus be particularly important in transporting sediment and forming the channel because of their relatively high frequency and hydraulic efficiency in terms of transport capacity and sediment availability.

again: change
in flow pattern
near chars

Overbank flows are less important because of their lower frequency, low hydraulic efficiency and unchanged sediment availability. Sediment is deposited once stage drops below barfull owing to reduced transport capacity and a reduction in active width. This deflects the flow against the banks, promoting continued bank erosion at these stages, and deposition in anabranch channels.

The discussion presented here is of a tentative nature and much simplified. In the river the idealised case depicted in Figure 2.12 does not occur, as chars are not flat topped and there may be several chars of somewhat different elevations within the same reach of braid belt. Further study of the relationships involved is therefore required before any firm conclusion can be reached.

2.5 Topic 5: Analysis of the Long Profile

Work on this topic has been postponed until the computerized data-base on bed topography, bankline elevations and water surface profiles has been set up using the BWDB morphological sections.

2.6 Topic 6: Braid Intensity Study

This topic has been studied by the BUET team. It is a complex topic with four sub-topics within it. These are:

- 6.1 Examination of Braiding Indices on a Reach by Reach Basis
- 6.2 Prediction of Confluence Scour from Approach Channel Geometry
- 6.3 Hydraulic Geometry Analysis of Anabranch Channels
- 6.4 Investigation of Braiding Intensity Effects on width and Depth.

2.6.1 Sub-Topic 6.1: Examination of Braiding Intensity on a Reach by Reach Basis

Inspection of 1:250,000 scale satellite images of the Brahmaputra River suggests that the Brahmaputra river can be divided into reaches with distinctive and persistent geomorphological features. On the basis of this visual inspection, seven sub-reaches were identified as shown in Figure 3.5. Braiding intensities, number of anabranches and overall braid belt width analyses have been carried out for the years 1973, 1978, 1981 and 1987. An in depth analysis of that data will be undertaken after the completion of the 1989 data which is in progress.

Preliminary results indicate that reaches of relatively high and low braiding intensity (E) alternate, but with an overall tendency for braiding intensity, number of channels and overall width to decrease downstream of Sirajganj.

2.6.2 Sub-Topic 6.2: Prediction of Confluence Scour from Approach Channel Geometry

The JMBA report proposes a relationship between confluence scour depth (h_s), approach channel depth (\bar{h}), and approach channel convergence angle (Θ):

$$\frac{h_s}{\bar{h}} = 1.292 + 0.037 \Theta$$

where $\bar{h} = (h_1 + h_2)/2$ and h_1 and h_2 are the depths in the two approach channels. This relationship was tested using data from Test Area 1 and from the 1986/87 survey. The data and results are given in Table 2.2

Table 2.2: Confluence Scour Prediction

Location	Angle Θ (deg)	Mean Depth (m)	Scour Actual (m)	Scour Predicted (m)	Error (%)
B.78/C-50	55	5.39	20.2	17.9	11
J-6/J-7	40	7.34	17.8	20.3	- 14
J-12/J-13	55	4.21	11.5	14.0	- 23

Comparison of the monsoon peak and post monsoon surveys for Test Area 1 indicate that contrary to popular opinion bed level in confluence scour holes does not change appreciably with discharge. Thus it might be feasible to test the relationship further using data from other cross-sections but this would involve considerable effort. The results of the three tests to date indicate broad agreement between observed and predicted scour depths and it may be decided to accept the JMBA equation on this basis. The level of confidence must however be kept in view, particularly in view of the possibility of significant underprediction.

260

2.6.3 Sub-Topic 6.3: Hydraulic Geometry Analysis of Anabranh Channels.

The JMBA study gives the following equations for downstream hydraulic geometry.

$$\begin{aligned}\bar{h} &= 0.23 Q_b^{0.32} \\ B &= 16.1 Q_b^{0.53}\end{aligned}$$

where:

\bar{h} = Mean depth at bankfull flow (m)

B = Water surface width (m)

Q_b = Bankfull discharge of the anabranh (m^3/sec)

The same study also suggest another set of equation for at-a-station hydraulic geometry.

$$\begin{aligned}\bar{h} &= 0.56 Q^{0.23} \\ B &= 18.9 Q^{0.51}\end{aligned}$$

where \bar{h} and B as defined above,

Q = observed discharge corresponding to the observed values of width and depth.

The validity of the equations for Test Area-1 is to be checked from observed data during monsoon and post-monsoon period. Also the potentiality for using raw data from Bahadurabad to test at-a-station equations is being investigated. The study is in progress.

2.6.4 Sub-Topic 6.4: Investigation of Braiding Intensity Affects on Width and Depth

This study is intended to test whether maximum scour depth and sub-channel width can be predicted from braiding intensity.

The relationship corresponding to dominant flows are to be studied for:

$$\begin{aligned}A_L/A_{TOT} &\text{ vs } h_{max}/\bar{h} \\ A_L/A_{TOT} &\text{ vs } n \\ A_L/A_{TOT} &\text{ vs } w\end{aligned}$$

where:

A_{TOT} = Total wetted area including all channels

A_L = Area of largest anabranh

\bar{h} = Average depth = Total Area/Width

h_{max} = maximum depth

n = nos. of anabranches

The detailed cross-section survey data of 1986-87 have been selected to study the above relationship and work on this item is in progress.

2.7 Topic 7: Meandering of Anabranches: Scour Depth Prediction

The intention is to use the BENDFLOW computer programme (Developed by Dr. C Thorne and Dr. A J Markham) to analyse bend scour. The input data required are:

$$1) \quad \text{Darcy-Weisbach friction factor} \quad f = \frac{8 g R S}{V^2}$$

where:

g = acceleration due to gravity

R = hydraulic radius (approx. equal to mean depth)

S = water surface slope

V = mean velocity

- 2) Mean Depth $\bar{h} = A/W$
- 3) Width $W = \text{Water surface width}$
- 4) Meander Wavelength $L = 2 \times \text{downvalley length of bend}$
- 5) Sinuosity $P = \frac{\text{channel length of bend}}{\text{valley length of bend}}$

The 1986-87 detailed surveyed morphological sections and the satellite imagery for the same year will be used for this analysis, which will commence shortly.

2.8 Topic 8: Meandering of Anabranches: Velocity Prediction

If revetments, rather than groynes, are the preferred engineering solution to bank erosion problems, informations on near bank velocities in meandering anabranches would be very useful. BENDFLOW model is proposed to predict the velocity for the near-bank zone in anabranh bends. Data to verify the prediction is needed and will be available from the physical model tests and the river surveys.

Assembling of the available data is in progress to conduct the study.

2.9 Topic 9: Meandering of Anabranches: Migration Rate Prediction.

Data on the migration of eight clearly defined and easily identifiable bends adjacent to the right bank were collected for the period 1987-89. Migration was measured in terms of down valley progression (D), cross-valley erosion (E) and resultant migration (M). These terms are defined in Figure.2.13.

Measured migration distances were divided by two to give annual rates. Meander bend radius of curvature and anabranh width (both at low flow) were measured for 1987 and 1989 and the values averaged. The bend radius and migration rates were nondimensionalised by dividing by the width. The data are presented in Table 2.3.

Table 2.3. Migration of Anabranh Meanders 1987/89

Location	Width W (m)	R/W	E/W	D/W	M/W	E/D	Outer Bank status
Fulchari	357	4.07	1.20	1.67	2.05	0.72	free
Unnamed	575	6.78	0.28	0.33	0.49	0.83	free
Sariakandi	315	4.25 *	-1.65	2.86	3.30	-0.58	protected
Kazipur	650	3.77	0.16	2.22	2.24	0.07	free
Sonalibazaar	650	3.65	0.38	1.54	1.58	0.25	free
Sirajganj	1,200	2.69	-0.34+	1.46	1.61	-0.47	protected
Betil	400	2.13	0.25	1.19	1.21	0.21	free
Jalalpur	400	3.69	0.38	1.44	1.49	0.26	free

* Sense of bend curvature reversed between 1987 and 1989

+ indicates outer bank movement eastwards.

The results for migration rates are plotted in Figure 2.13 and Figure 2.14. Clearly, much more data are needed before any firm conclusions can be drawn but some comments on the distribution of the points can be made.

The distribution in Figure 2.13 is very similar in form to that found in studies of bend migration in single-thread channels (Biedenharn et al, 1989; Markham and Thorne, 1991) except that the peak in migration occurs at an R/W of about 4 to 4.5 rather than between 2 and 3 as is usually observed. This may be a result of the fact that the width used in this study is that at base flow whereas in most studies it is the considerably larger, bankfull width which is used.

Ideally, bankfull width should be used as this is the width associated with the channel forming flow (Ackers and Charlton, 1970), but it is not possible to define or determine the bankfull width for individual anabranches at this stage. Also, the radius of curvature corresponds to the low flow planform when, ideally, it should be the value for bankfull flow. The low flow value will usually be somewhat lower than that at bankfull as higher flows inundate the point bar and tend to straighten the bend.

The ratio of widths at bankfull and low discharges is of the order of 2, while the ratio of radius is about 1.3 so that the bankfull R/W values might be expected to be about 0.6 or 0.7 times the low flow values. This would make the peak migration rates fall between about 2.5 and 3, as observed in single-thread channels at bankfull flow.

Figures 2.13 and 2.14 suggest that in long radius bends, down-valley progression and cross-valley erosion both occur at relatively slow, but similar rates: this represents meander growth. This pattern is consistent with that observed in meandering as a whole. As the radius decreases through meander growth, the rates of both down-valley and cross-valley erosion increase, but progression accelerates much more strongly than erosion, so that the ratio E/D decreases. This is the phase of rapid meander migration. As the radius is further reduced by meander growth, the bend becomes very acute and it tends to slow down, although the migration is still rapid compared to the rates for long radius bends. The bend continues to migrate at this slower rate, with approximately constant geometry, until it is destroyed by one of four phenomena:

- (a) a change in upstream alignment which reduces or eliminates the inflowing discharge;
- (b) a chute cut-off across the point bar;
- (c) a neck cut-off when the slowly migrating bend is overtaken by a more rapidly progressing bend of opposite curvature coming from upstream;
- (d) outer bank accretion in the acute, tightly curved bend produces a negative E value, so that the flow "backs out" of the bend erodes the point bar, and straightens itself.

This last phenomenon is usually associated with the bend encountering a resistant material or hard point in the outer bank. There are two examples in the data set, from Sariakandi and Sirajganj, of bends in which the outer bank has been protected. These bends show negative E values, indicating outer bank accretion, but positive D values, indicating continued down valley progression. In the case of Sariakandi the sense of the bend is reversed between 1987 and 1989, possibly due to a sort of neck cut-off induced by stabilization of the outer bank. It may be that outer bank protection has been successful in halting westward erosion (E), however the continuation of down valley progression indicates that the bend may still cause problems at other locations. To lock a bend in place would require stabilization of the outer bank, using perhaps groynes and/or revetments, plus groynes on the bar opposite to prevent a chute type cut-off of the bend, allowing it to slip past the protective works.

2.10 Topic 10: Historical Bankline Migration

This together with the analyses of bend behaviour has direct application to the development for predictors for bank erosion in the short and longer term. As such it is of great importance to the BRTS master planning.

Although there is a considerable amount of information available, interpretation is complicated by the fact that there is only a limited amount of data that has a common frame of reference that can be used with confidence. JICA in their report for the JMB plotted bankline movements based on a series of maps dating back to 1860, which had originally been compiled by IECO. The JMBA Feasibility Report rejects all this earlier data on the grounds of poor correlation and relies on more recent morphological cross-section data. Investigations carried out under this study have shown that the positioning of the BWDB morphological sections is uncertain and therefore even this data set must be used with caution.

Unrectified Landsat imagery is also hard to utilise for quantification of bankline movements, both because the level of distortion is of the same magnitude as the changes to be measured and because the resolution is insufficient to permit accurate correlation of physical detail in the vicinity of the river.

Overall it is concluded that all sources of data should be used and that the interpretation should take into account the level of confidence involved. The highest level of confidence attaches to the comparison of the bankline on the rectified 1989 SPOT imagery with that of the 1:50,000 series of maps produced by the Survey of Bangladesh and its predecessors at various times since 1956. This information is shown in Figure 3.3 and clearly shows that during the past 30 years there has been substantially more erosion of the right bank than the left bank and that the majority

of the erosion has been located between Serajganj and Sariakandi. This is discussed further in Section 3 of this Annex.

2.11 Topic 11: Bank Erosion Sediment Yield

The significance of bank erosion in terms of the morphological behaviour of the river is sometimes underestimated. A question of particular interest for this study is what becomes of the sediment eroded from the banks. Since this is closely allied with Topic 12, the outcome of this study will, for convenience, be described in the following Section

2.12 Topic 12: Comparison of Bank and Char Sediments

Bank erosion on the scale of that occurring on the Brahmaputra generates an enormous supply of sediment to the river. This material is input at the margin of the flow either particle by particle, in the case of direct entrainment by the flow, or in disturbed blocks, in the case of mass failures. The river then does one of three things with the bank derived sediment:

- (a) transports it out to the Bay of Bengal;
- (b) transports it some distance before depositing it temporarily in a bed form (prior to re-eroding it soon afterwards or during the next high flow event);
- (c) transports it some distance before depositing it into long-term flood plain storage in a char.

The purpose of this topic was to determine the approximate amount of sediment supplied to the river by bank erosion, and the relative amounts going into 1) Wash load, 2) Suspended and bed load, and 3) Char building

The exercise was carried out using data from the 1986 and 1987 maps contained in the JMBA Report for the reach between sections J-11-7 and J5-6 and the measurements of sediment load at Bahadurabad made during the interval between mapping. The data are given in Table 2.4 and plotted in Figure 2.15.

Table 2.4. Sediment Yields for the Brahmaputra River 1986-87

Sedi- ment	Upstream Supply	Left Bank Yield	Right Bank Yield	Total Bank Yield	Char Depo- sition	Char Eros- ion	Net Yield
Sand*	4.32	1.15	1.85	3.0	-4.94	1.72	-3.22
Silt*	62.9	0.76	1.24	2.0	-1.24	0.42	-0.82
Total	67.2	1.91	3.08	5.0	-6.18	2.14	-4.04

All values have units of 10^{10} kg

* Assumes bank material is 60% sand and 40% silt, and char material is 80% sand and 20% silt, based on bank and char sediment samples.

+ Assumes char sediment density is $1,600 \text{ kg/m}^3$.

The data may be used to calculate the supply of sediment from bank erosion as a percentage of the incoming load measured at Bahadurabad. The data are given in Table 2.5.

Table 2.5. Relative Yield of Sediment from Bank Erosion.

Sediment Type	Left Bank Yield Upstream Supply (%)	Right Bank Yield Upstream Supply (%)	Total Bank Yield Upstream Supply (%)
Sand*	27	43	70
Silt+	1	2	3
Total	3	5	8

The results indicate that bank erosion in the study reach adds only 8% to the measured sediment load coming in from upstream, an amount which, although perhaps not negligible, may be within the margin of error of measurements of the type reported here. However, it is not only the total mass of sediment which is of particular geomorphic importance, but also the size distribution. Preliminary analysis suggests that the bank material is made up of about 60% sand and 40% silt. When the silt fraction is considered, the contribution to the silt load supplied from upstream is only 3%, which is negligible. But for the sand fraction the yield is 70% of the supply from upstream. That is, the river in this reach must accommodate 1.7 times the input from upstream, in order to remain in dynamic equilibrium. Examining the yield by bank, it is seen that 43% of the supply comes from right bank erosion, but only 27% from left bank erosion.

The question which immediately springs to mind is, how does the river deal with this large input of relatively coarse sediment? Mostly, it builds chars with it, effectively putting the sand back into the long-term flood plain storage from whence it came. In terms of the sediment pathways

described earlier, a large proportion of bank silt yield follows path 1 directly to the Bay of Bengal, although some probably follows path 3 through being deposited on chars and on the flood plain during the falling stages at the end of the snowmelt runoff and monsoon floods. The bank sand yield follows paths 2 and 3, possibly with relatively short travel distances from bank source to char store given the relatively slow speed of movement of bed material load compared to wash load.

Examination of the data in Table 2.4 shows that the amounts of sediment involved in bank erosion and net char deposition (that is the excess of char growth over char erosion) are similar. This suggests that char growth and continued braid belt expansion are approximately balanced by bank erosion, with an almost complete exchange of sediment between the two. Thus sediment exchange is superimposed upon a much larger throughput of silt, and a throughput of sand which is of the same order as the exchange rate. There is however a loss of sand from input load from upstream to net char deposition, because net char deposition of sand is greater than bank sand yield.

Although these preliminary results are based on only part of the river over one year and must therefore be interpreted with extreme caution they demonstrate the potential value of this form of calculation.

Recognition of the intimate link between bank erosion and char growth, and of the pivotal role of the sand size fraction in both processes have important implications for predicting the river's response to bank stabilization and river training.

2.13 Topic 13: Bank Stability Assessment

Severe bank erosion usually occurs by a combination of flow erosion of the bank and bed adjacent to the bank, coupled with periodic mass failures under gravity. Failures are usually one of two types. Slab-type failures occur where a block of soil slides downwards and outwards along a planar failure surface before toppling forwards into the channel. Rotational slips occur when a block slides along a curved failure surface with back-tilting of the top of the block in towards the bank. the type of failure depends primarily on the geotechnical properties of the bank.

Observations on single-thread rivers with eroding banks suggest that the bank height is maintained at or just below the critical height for mass failures, and that this has a direct impact on the geometry of the channel adjacent to the bank. To investigate whether height of the right bank of the Brahmaputra behaves similarly, data are needed to assess the stability of the bank at specific locations with respect to slab and rotational slip failures and to determine the critical bank height for mass instability.

The Osman-Thorne bank stability analysis can be used for this purpose. The required data are: bank angle, bank height, tension crack depth, soil cohesion, soil friction angle and soil unit weight. The bank geometry data were collected during the bank condition assessment performed in Topic 14. Soil samples collected during the assessment are being analysed at RRI to supply the data needed to define the geotechnical properties.

2.14 Topic 14: Assessment of Bank Condition

The survey of bank conditions along the right bank was performed in the period January-March 1991. The reconnaissance trip from Belka on the Teesta to the confluence with the Ganges was made mostly by boat, but with some land excursions to visit reaches of bank line not accessible from the river because of attached chars. A record of bank condition was made for the entire length of the reach, a distance of 270 km. The full records together with a key map are available in the BRTS office. Detailed assessments of bank condition were made at 28 locations along the reach. Locations were selected to be representative of the surrounding lengths of bank and to detail conditions at sites of particular concern.

Flow erosion and surface erosion (by wind, rain, run-off, ravelling) was observed on all eroding banks. Slab failure was the predominant failure mechanism, although significant sections of bank dominated by granular flow failure were also observed. In two locations the presence of a grey silt-clay layer at the toe of the bank caused seepage and piping related failure. These locations, Niz Balai-Hatsherpur (119-121 km) and Deluabari-Mathurapara (135-139 km) are located where the bankline is close to the course of the Bangali River. It seems likely that the silt-clay deposit is associated with that river's alluvial valley fill materials.

In depth evaluation of the results is an integral part of the BRTS geomorphological study and cannot be undertaken until the results of all twenty topics have been assimilated.

2.15 Topics 15 to 18: Mapping of Flood Plain Topography, Geology and Geomorphology.

The geological and geomorphological maps are available in the BRTS office. The geomorphological map lacks detail and is probably not as useful as the geomorphic map in Coleman's paper of 1969 (Figure 3 in that paper, on page 136). The topographic map is under preparation.



3. IMPLICATIONS FOR BANK PROTECTION AT PRIORITY LOCATIONS

3.1 Rationale

The findings of the geomorphological studies have implications for the conception and design of bank protection works at the priority locations on the right bank. These implications are considered firstly in relation to the macro-scale geomorphology of the channel, secondly in relation to the reach scale geomorphological trends and developments and thirdly in relation to the local geomorphology, anabranch characteristics, and bank conditions.

3.2 Macro-scale Geomorphology

The analysis of stage-discharge curves for Bahadurabad gauging station since the 1960s (Topic 3) indicates that there is no evidence of a net aggradational or degradational trend of the river at Bahadurabad which is likely to be significant on an engineering timescale (ten to one hundred years). A similar check will be carried out on other water level records.

Consideration of the morphology of the channel in relation to the flow stage at dominant discharge of 38,000 m³/s (Topic 1) indicates that channel top elevation is closely adjusted to the dominant flow (Topic 4). This is the case along the whole length of the study reach, although there are some reach scale variations. It may be concluded that the morphology of the braided channel is broadly adjusted to the dominant discharge and that in terms of long-profile geometry the river is dynamically graded.

An initial consideration of the planform and historical lateral shifting patterns of the Brahmaputra River between the confluences with the Teesta and Ganges Rivers has been performed. This analysis is not yet complete, but on the basis of the preliminary examination a hypothesis has been put forward. The Brahmaputra River, like nearly all other alluvial streams, exhibits a meandering tendency. Because the river is characterised by a very wide range of flows and a heavy load of sediment which is mobile at a wide range of flows, this meandering tendency is not associated with a single-thread channel of easily identifiable wavelength and sinuosity. In fact there are three discernible scales of meandering nested within one another and indivisibly entwined to produce a meandering - braided pattern. In different places (and at different times) the pattern is more meandering than braided; in other places (and times) it is more braided than meandering, but elements of both patterns are always present. In terms of the continuum of channel patterns it is in the braiding - meandering transition. This is demonstrated by consideration of the Braided/Meandering discriminator produced by Lane (1957).

Where stream with

$$\begin{aligned} S < 0.0017 Q_d^{-0.25} & \text{ should be meandering and} \\ S > 0.01 Q_d^{-0.25} & \text{ should be braided} \end{aligned}$$

Streams with slopes between these values are in transition. For the Brahmaputra, Q_d , the dominant flow is 38,000 m³/s or 1.34 x 10⁶ cfs and $S = 0.00007 = 0.07$ feet/thousand feet. Plotting this point on Lane's diagram (Figure 3.1), shows the position of the Brahmaputra River to be in the lower third of the braiding-meandering transition and this is borne out by the observed planform which exhibits elements of both patterns.

At macro-scale, the whole braid belt of the river shows a sinuosity which can be identified on small scale satellite images of the whole reach. There are $1\frac{1}{2}$ wavelengths between the confluences with the Teesta and the Ganges. This is a distance of about 200 km. However, the three curves are not of equal length. The first is right bank concave and extends from the Teesta confluence to Gabargoan (80 km). The second is left bank concave and extends from Gabargoan to Bhuapur (45 km). The third is right bank concave and extends from Bhuapur to the Ganges confluence. Hence, at this macro-scale, Gabargoan and the Jamuna Bridge site locations represent crossings or meander inflection points. These are sometimes called "nodes" - a term used in earlier references to these locations. Leopold and Wolman (1957) produced an empirical equation relating the wavelength of curves in a sinuous channel to the width of the flow. The equation is:

$$L = 12.13 W^{1.09}$$

where:

W = average width at bankfull flow and L is meander wavelength. This geometric equation has been found to apply over a very wide range of flow scales from the order of millimetres to several kilometres.

Taking the average width of the flow at near bankfull discharge to be 8 km (it ranges from 5.1 to 11.1; see Reach scale data in next section) the wavelength predicted from the geometric equation is $L = 117$ km, which compares favourably to the observed average value of $(200/1.5) = 135$ km.

There is no simple, physical explanation of how the multiple anabranches act to produce a sinuous braid belt, but the fact is that they do. The explanation is probably similar to that of how a single-thread meandering river can produce a meandering valley through differential erosion, such that the wavelength of valley meanders is geometrically scaled on valley width rather than channel width (Richards, 1982). This topic is the subject of continuing investigation in the geomorphological studies. If it is accepted that the braid belt of the Brahmaputra River does follow a sinuous course, then even though a precise physical explanation is not yet forthcoming, that fact can be used as an aid in interpreting and predicting macro-scale geomorphological development.

A great deal has been written and said about the long-term and large-scale stability and shifting of the Brahmaputra-Jamuna. There are, broadly speaking, two views. The first view follows from Professor Coleman's hallmark paper of 1969 and states that the river has a tendency to shift systematically to the west. This has been variously attributed to various causes including Coriolis force, neotectonics, regional geology, valley asymmetry and region trends in terrain. The second view, as expressed in the Jamuna Bridge Study, is that shifting is randomly distributed between left and right banks with no systematic trend.

On the basis of the preliminary analysis in this study, both are, to some extent right and wrong. In an equilibrium channel of relatively low sinuosity, the concave bank retreats, while the convex bank advances. Retreat is concentrated against the down valley bank of the concave bank, that is the bank between the apex and end of the curve, so that through time the waveform migrates downvalley while growing in amplitude. In the case of the Brahmaputra there are two right bank concave curves, but only one left bank concave bend and so in terms of a simple average, right bank retreat is greater than left bank retreat between the Teesta and the Ganges confluences.

In that respect Coleman was correct to say that the channel is shifting westwards. But it is not a simple sideways movement at about a uniform rate along the length of the reach. The river is not moving bodily westwards. In this respect the JMBA study was correct. In fact, the planform of the Brahmaputra River has a sinuous course which has curves in it that slowly tend to increase in amplitude while migrating down valley. The shifting to the west is concentrated against the down valley banks in the right bank concave reaches, that is between Fulchari and Sirajganj on the right bank, between Gabargoan and the Daleswari on the left bank, and between Delua and the Ganges confluence on the right bank. This assertion would appear to be supported by both the long-term distribution of bankline migration presented in the JICA report (Figure 3.2) and by the most recent trends of channel shifting based on high resolution LANDSAT and SPOT satellite images (Figure 3.3).

Certainly the rates of shifting have slowed since the 1800's, but the distribution has not. Clearly left bank erosion is less marked than right bank erosion even within the left bank concave curve. This may be attributed to the fact that the geomorphic and surficial sediments map (Topic 17) shows that more consolidated sediments associated with the valley margin with the Madhupur plateau, outcrop adjacent to the easternmost channels of the river, and may well be constraining its otherwise free migration (Figure 3.4). This could also explain why the left bank concave curve is deformed and is much shorter in wavelength than the two right bank concave curves.

It is suggested therefore that at the macro-scale the planform of the Brahmaputra River at dominant flow is that of a sinuous braided river. The wavelength of the sinuous curves is commensurate with the bankfull width of the flow. The historical planform development has been for sinuosity to increase and for curves to migrate downvalley. As there are two right bank concave bends but only one left bank concave curve, there is a net westward shift of the channel. This is not uniformly distributed however, but is concentrated in the northern and southern thirds of the reach. In the centre third of its length, the channel has shifted to the east, but this has been distorted and constrained where it has met the valley edge which is composed of more consolidated sediments. Rates of sinuosity growth have decreased through time, but are still substantial.

On this basis it may be predicted that the trend towards increased macro-scale sinuosity growth and curve migration is likely to continue, with attack on the right bank being greatest in the northern most and southernmost thirds of the reach. This provides an overall, macro-scale template for bankline retreat prediction in the medium term, without significant bank stabilization or training. Figure 3.5 shows a sketch of the current planform of the river and a tentative prediction for progression.

It assumes that the hard point at Sirajganj does not fail, but that otherwise bank migration is not affected by local protection around towns and bazars. The rate of bank retreat is very difficult to predict, but it seems likely that historically observed rates will continue, yielding perhaps 3 km of retreat in 30 years at the most severely affected locations, between Sariakandi and Sirajganj, and Betil and the Hurasagar River.

To put the ten priority locations in this macro-scale context, they are shown in Figure 3.5. This shows that they are broadly associated with the areas of right bank retreating due to macro-scale sinuosity. Of the ten

sites, six are located between Sariakandi and Sirajganj - in the area of downvalley migration of the first right bank concave bank. Two, Betil and Jalalpur are located on the other right bank concave reach further downstream. The other two are located on the first right bank concave reach, upstream of the apex where the pressure on the bank is a little less severe.

3.3 Reach Scale Geomorphology

Examination of satellite images and historical map of the Brahmaputra River indicates that there are marked geomorphological contrasts between different reaches of the river within the study region. On the basis of a visual inspection, seven sub-reaches were identified, as shown in Figure 3.5. Analysis of the braiding intensities, number of anabranches and overall braid belt width up to 1987, in the different sub-reaches, indicates support for the qualitative divisions. However, the analysis is not yet complete as the data for 1989 have not been recorded. Broadly, reaches of relatively high and low braiding intensity (E) alternate, but with an overall tendency for braiding intensity, number of channels and overall width to decrease downstream of Sirajganj. Of the seven sub-reaches, reaches 3, 5, and 7 all show a strong widening tendency in the last decade. The distribution of priority sites shows only one site each in sub-reaches 1 and 2, but three sites in reach 3. Reach 4 also has three sites, but this reach is actually narrowing slightly. This is due to accretion on the left bank which is keeping pace with right bank retreat in this reach. Reach 6 exhibits westward migration at a constant width, and contains the two southern most sites.

An in-depth analysis of these data will be undertaken once the analysis for 1989 has been completed. Trends of channel braiding adjustment are apparent and may well shed considerable light on reach scale channel dynamics.

3.4 Local Geomorphology

3.4.1 Kazipur

Bank erosion at Kazipur is the result of the development of a meander loop in the major right bank anabranch. The loop appears to be quite gentle on the 1985 satellite image, but by 1987 a distinct curve was apparent. This was the slow growth and progression period. Between 1987 and 1989 the loop grew by serious cross-valley erosion, while also progressing downvalley. This was the rapid growth and progression phase. Since 1989 it has further grown by cross-valley erosion, with rather less rapid down-valley progression and it may now be close to decay and destruction by either by-passing or outer bank accretion. The situation is somewhat complicated by the existence of minor chute channel anabranches which provide a variety of options for neck and chute cut-offs as well as having the potential to provide new and damaging flow alignments for both the bend entrance and exit.

It may be that the worst of the cross-valley erosion at Kazipur is over. However, continued down-valley progression can be expected to destroy that part of the town which is south of the present bank embayment. Construction of a revetment along the downvalley length of bank could have a good chance of successfully protecting this area of the town, especially as the potential for further cross-valley erosion is small.

3.4.2 Sariakandi, Mathurapara, Chandanbisha, Sonalibazaar, Sirajganj

Sariakandi has a groyne which protects the bank upstream, and particularly, downstream from erosion. However, erosion on the upstream side has begun because of the development of an anabranch striking the upstream face of the groyne at a severe angle about one-third of the way along the groyne. Also, bank erosion is occurring about 0.5 km downstream of the groyne, where the flow re-attaches to the bank.

Steeply inclined anabranches are also found further downstream at Dulaabari/Mathurapara and Chandanbaisha. Consideration of all three sites and those at Kazipur and Sonalibazar shows them all to be associated with the meandering tendency of the major right bank anabranch. This has a width of about 1-1.5 km (order of magnitude). Applying Leopold & Wolman's scaling factor of $L = 12.13 W^{1.09}$, yields a Wavelength of 12 to 18 km. That is, it would be expected that loops cutting into the bank should be spaced at intervals of 12 to 18 km. The distances between these sites should be of this order. The actual approximate distances are, 10 km, 6 km, 15 km and 13 km, an average spacing of 11 km.

The embayments produced by bank erosion due to cross-valley and down-valley movement of these bends are characteristically 2 to 5 km long and up to 1.5 km wide. The evidence from Sirajganj suggests that if a growing loop and embayment is stopped at its downstream end by a hard point which cannot be destroyed by either toe scouring to great depth, or out flanking due to severe embaying, then the loop backs out of the embayment, filling it by outer bank accretion. This effect has been observed on alluvial rivers which encounter bed rock hard points in the USA (Reid, 1983) and a similar process may be applicable to the Brahmaputra river, if at a rather different time scale. If this interpretation is correct, it gives hope that bank erosion due to loop growth and embayment formation scaled on the main, right bank anabranch can be controlled by strategic positioning of a non-erodible, non-flankable hard point at the downstream end of the embayment.

These sites are in detail quite different and it is easy to let these differences obscure their underlying similarity. They are all products of braiding/meandering processes in the major right bank anabranch in the reach where macro-scale sinuosity dictates that the right bank will suffer continued retreat. However, the river does not erode the bank evenly along its length. It uses the right anabranch as its alluvial agent, looping around mid-channel and proto-point bars and cutting embayments from the bank at somewhat even spacings along the bank. A wavy bankline results and over a period of 10 to 20 years, retreat is fairly uniform because as the loops erode and progress downstream, they move the points of embayment formation along too. Intervening respites from erosion, until the loop migrates, destroying the bar and again attacking the intact bank behind.

Superimposed upon, and contained within, this somewhat orderly pattern are other wavelengths of instability associated with large chars, periodic switching of the locus of maximum flow between the left and right bank anabranches, and local noise due to braid bar formation and destruction. Hence, in detail every bank erosion case is different. This should not be allowed to obscure their common causes.

In terms of protection, local stabilization may be possible through hard point creation and the inducement of outer bank accretion. If a series of schemes were implemented, holding embayments at 10-20 km intervals, then a cumulative effect could be accrued. However, additional hard points would

still be needed as loops backed out of existing embayments and sought to develop new ones at intermediate locations between hard points. Eventually, hard point spacing would be sufficiently close to ensure that loops could never outflank them.

3.4.3 Betil and Jalapur

These are locations where meander loops in the major right hand anabranch are forming large embayments in the right bank. The bend at Jalapur is extremely sinuous and tight and appears to be close to by-passing by a chute cut-off in the chute channel behind the point bar opposite. The bend at Betil is in the stage of rapid growth and progression. It appears poised to do great erosion of the bank. A linear revetment from just upstream of the present bend apex, extending downstream to the exit is recommended.

3.5 General point on Chute Channels

Chute channels across point bars carry only a small proportion of the discharge but have the potential to trigger channel avulsions by providing pilot channels for re-location of the deep water thalweg. This introduces great uncertainty in the planning of bank protection works.

The use of sand dams and low groynes seem possible approaches. As depths and widths are much smaller than on main anabranches, techniques dismissed as unrealistic for main channels may be considered. Careful and insightful work on chute channels, particularly those behind point and diamond bars attached to the right bank between embayments, could

- (a) greatly enhance the predictability of future channel development;
- (b) help to fix attached bars which form the best form of protection for the bank behind them;
- (c) help to control the approach alignment of flow to hard-points in the embayments downstream.

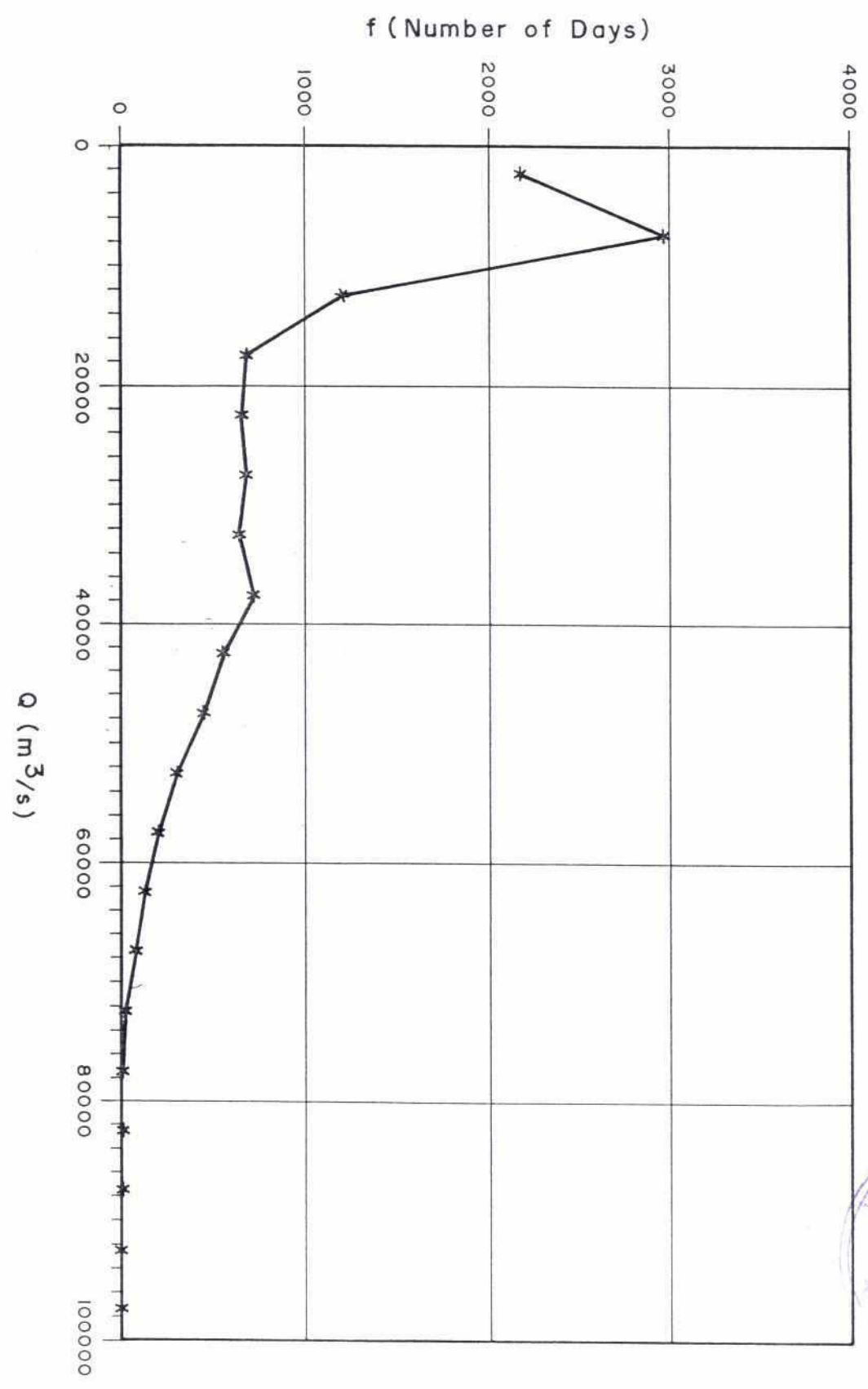
REFERENCES

- Ackers, P and Charlton, F G (1970). Journal of Hydrology, 230-252
- Benson, M.A. and Thomas, D.M. (1966) Bulletin IASH, 11, 76-80
- Goswami, D.C. (1985) Water Resources Research, 21(7), 959-978
- Lates, E. (1988) DHI Report UNDP/DTCD PROJECT, BGD/81/046, TCD CON 14/84, Part 1
- Lee, A-L and Davies T R (1986) Publication 9, Hydrology Centre, Ministry of Works of New Zealand, ISSN0112-1197, 220-229.
- Richards, K.S. (1982) Rivers : Form and Process in Alluvial Channels, Methuen.
- Thorne C.R. Hey, R.D. and Bathurst, J.C. (1987) Sediment Transport in Gravel-Bed Rivers, J Wiley, Chichester, UK.
- Vanoni, V.A. (1975) Sedimentation Engineering, ASCE Technical Manual 54, New York, USA
- Wolman, M.G. and Gerson, R. (1978) Earth Surface Processes, 3, 189-208
- Wolman, M.G. and Miller, J.P. (1960) Journal of Geology, 68, 54-74.

FIGURES

582

FREQUENCY DISTRIBUTION FOR DISCHARGE AT
BAHADURABAD - BRAHMAPUTRA RIVER (1956-'89)
ANNEX : 4
FIGURE : 2.1

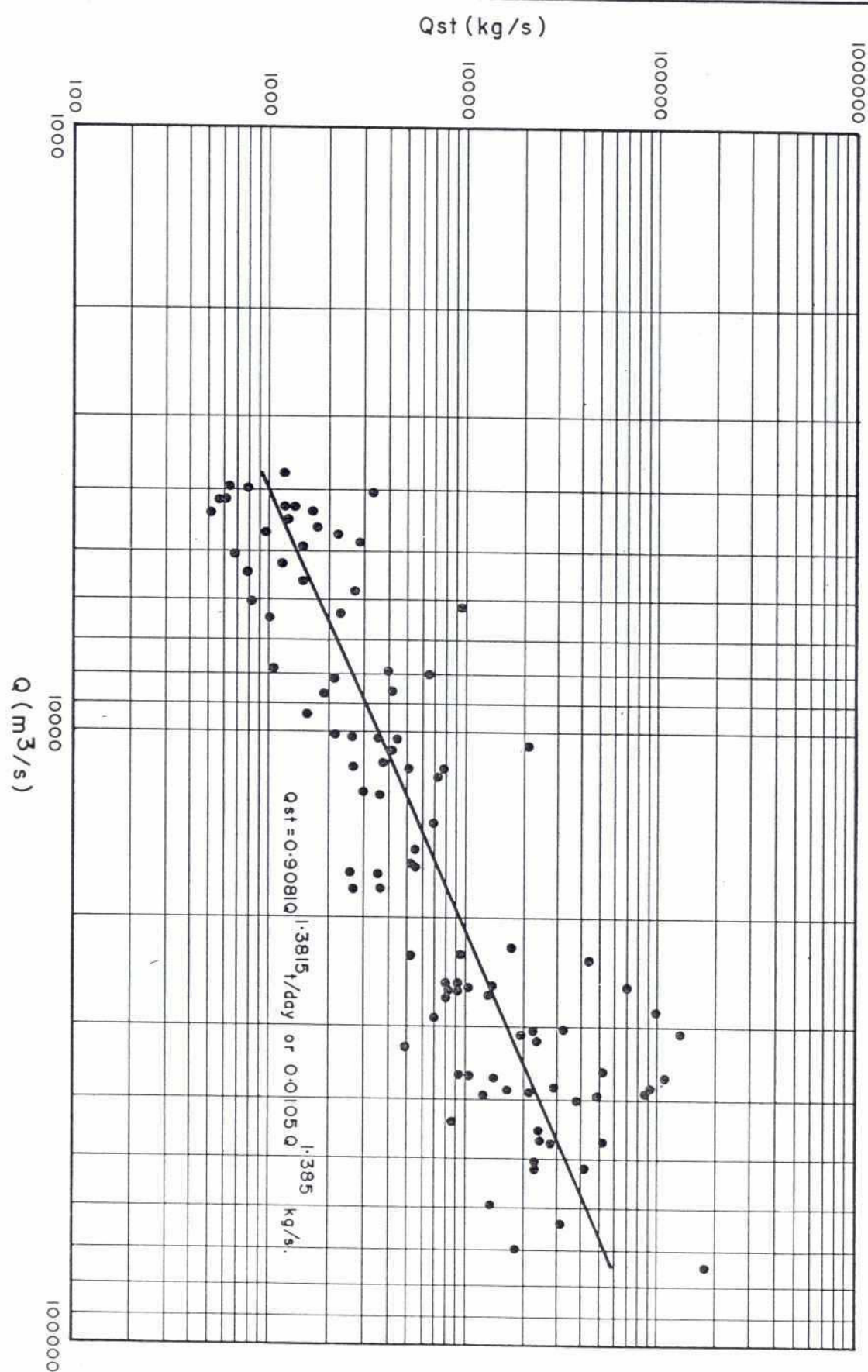


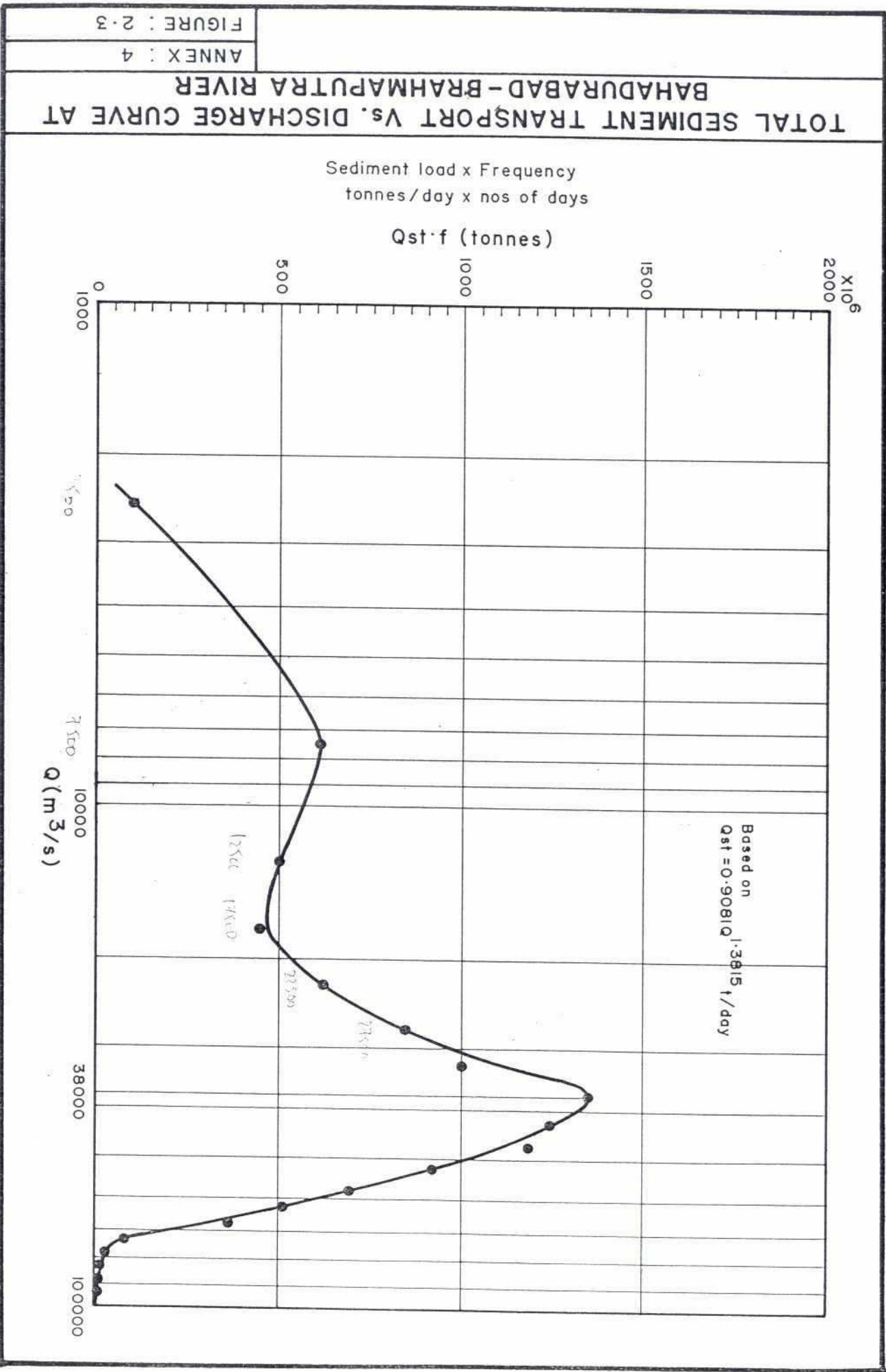
289

SEDIMENT RATING CURVE AT FOR TOTAL MEASURED LOAD
BAHADURABAD - BRAHMAPUTRA RIVER (1982-'88)

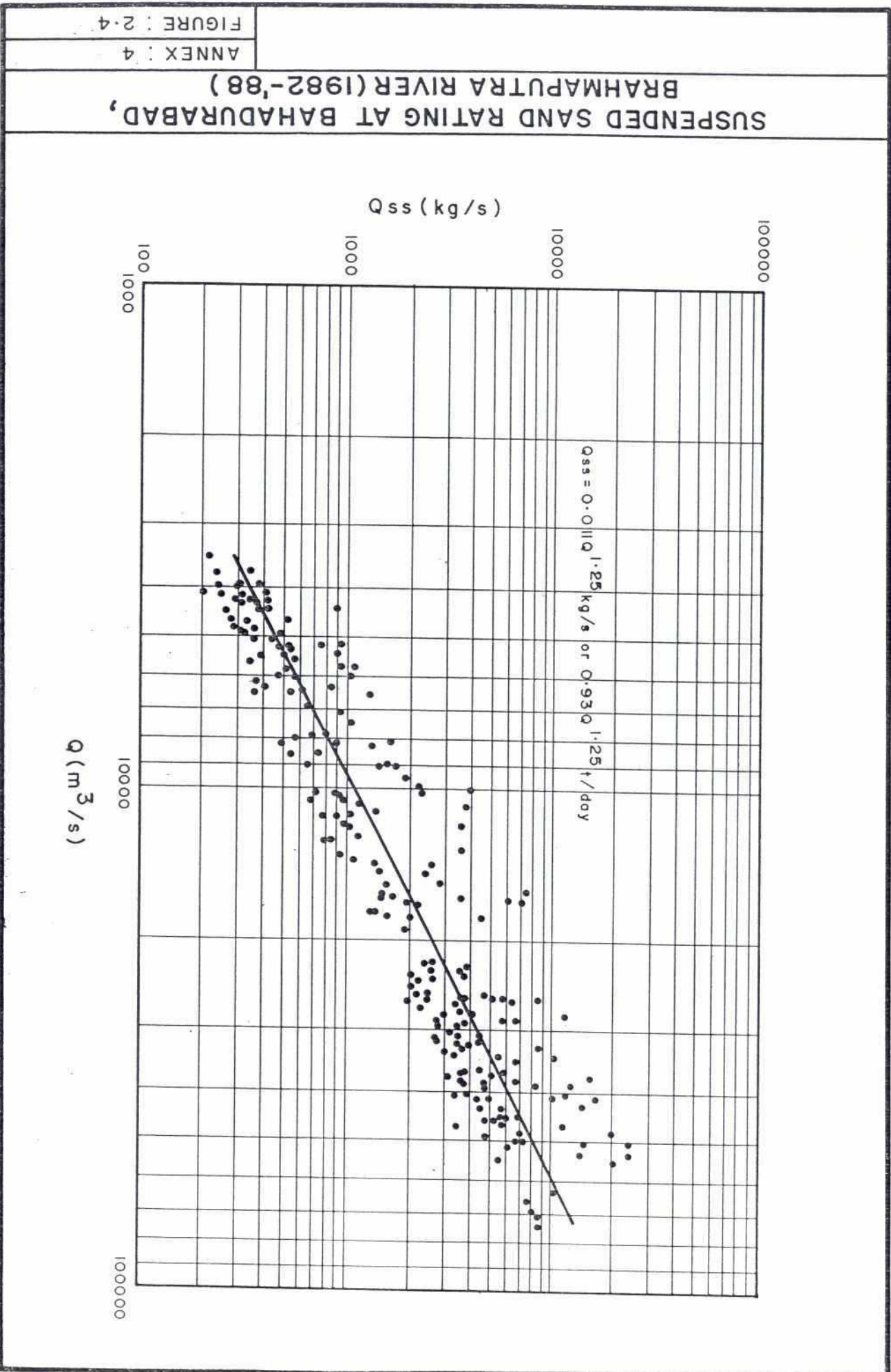
ANNEX : 4

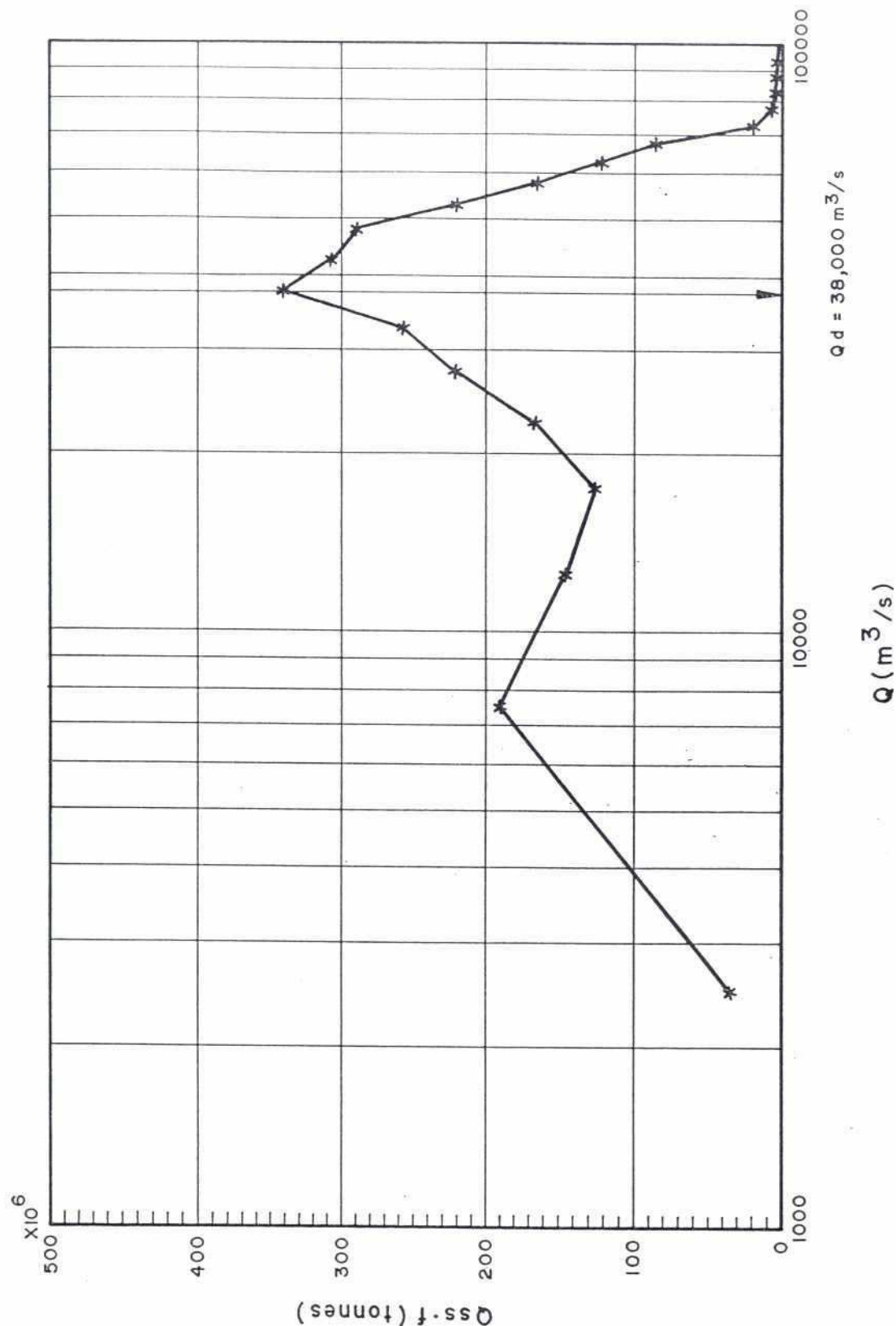
FIGURE : 2.2





282



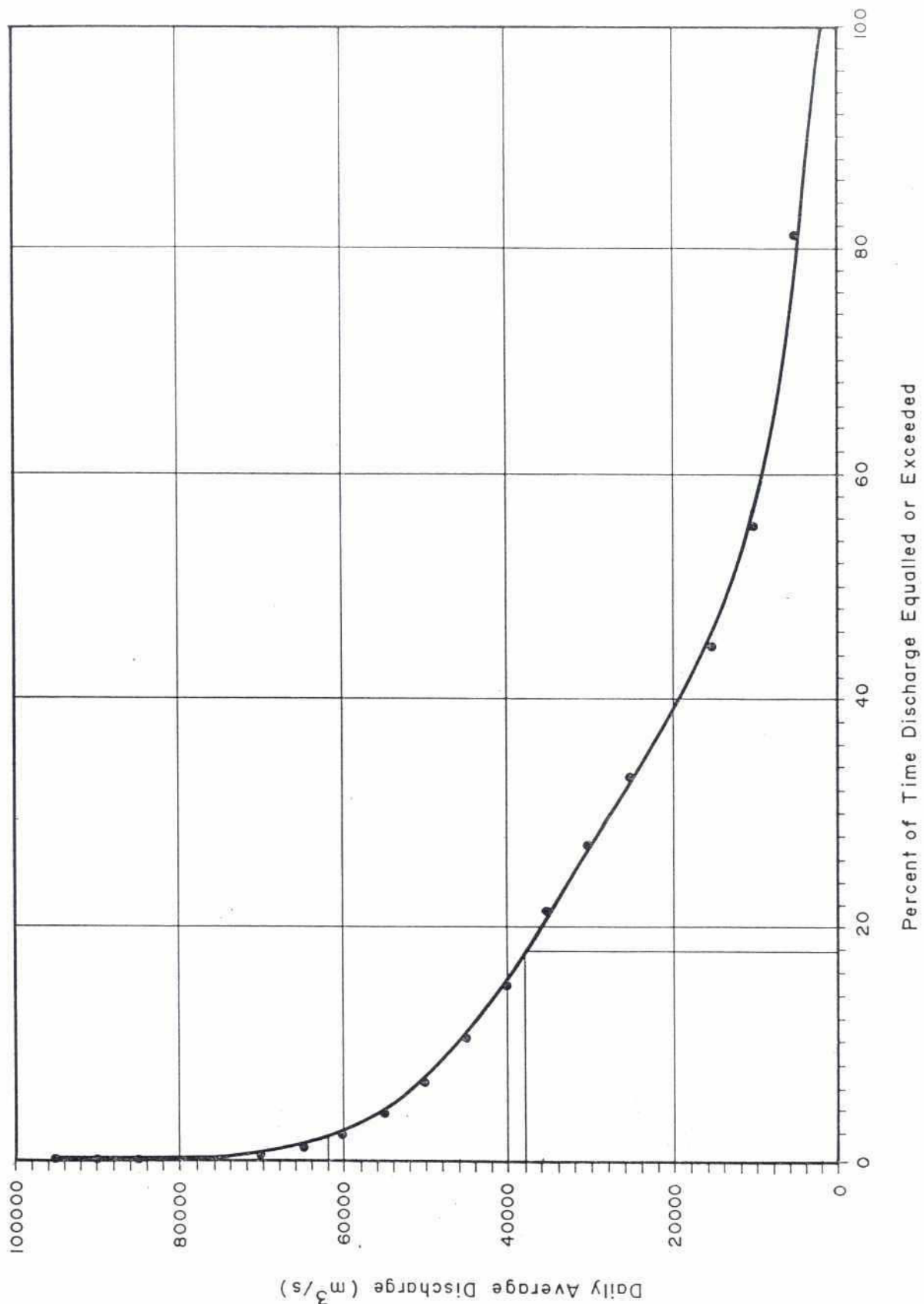


**SUSPENDED SAND TRANSPORT Vs. DISCHARGE AT
BAHADURABAD-BRAHMAPUTRA RIVER**

ANNEX : 4

FIGURE : 2.5

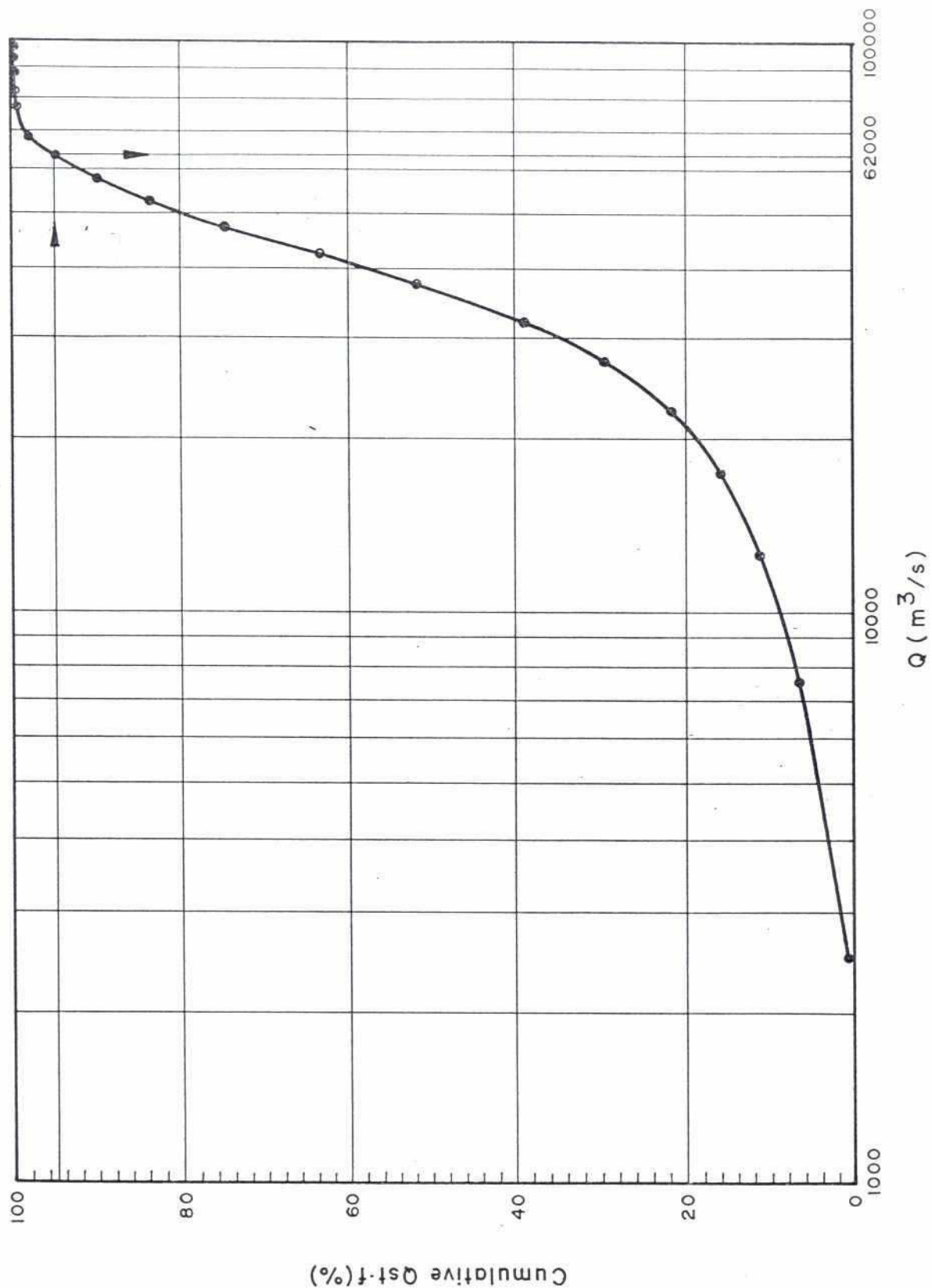
202



**FLOW DURATION CURVE AT BAHADURABAD,
BRAHMAPUTRA RIVER**

ANNEX : 4

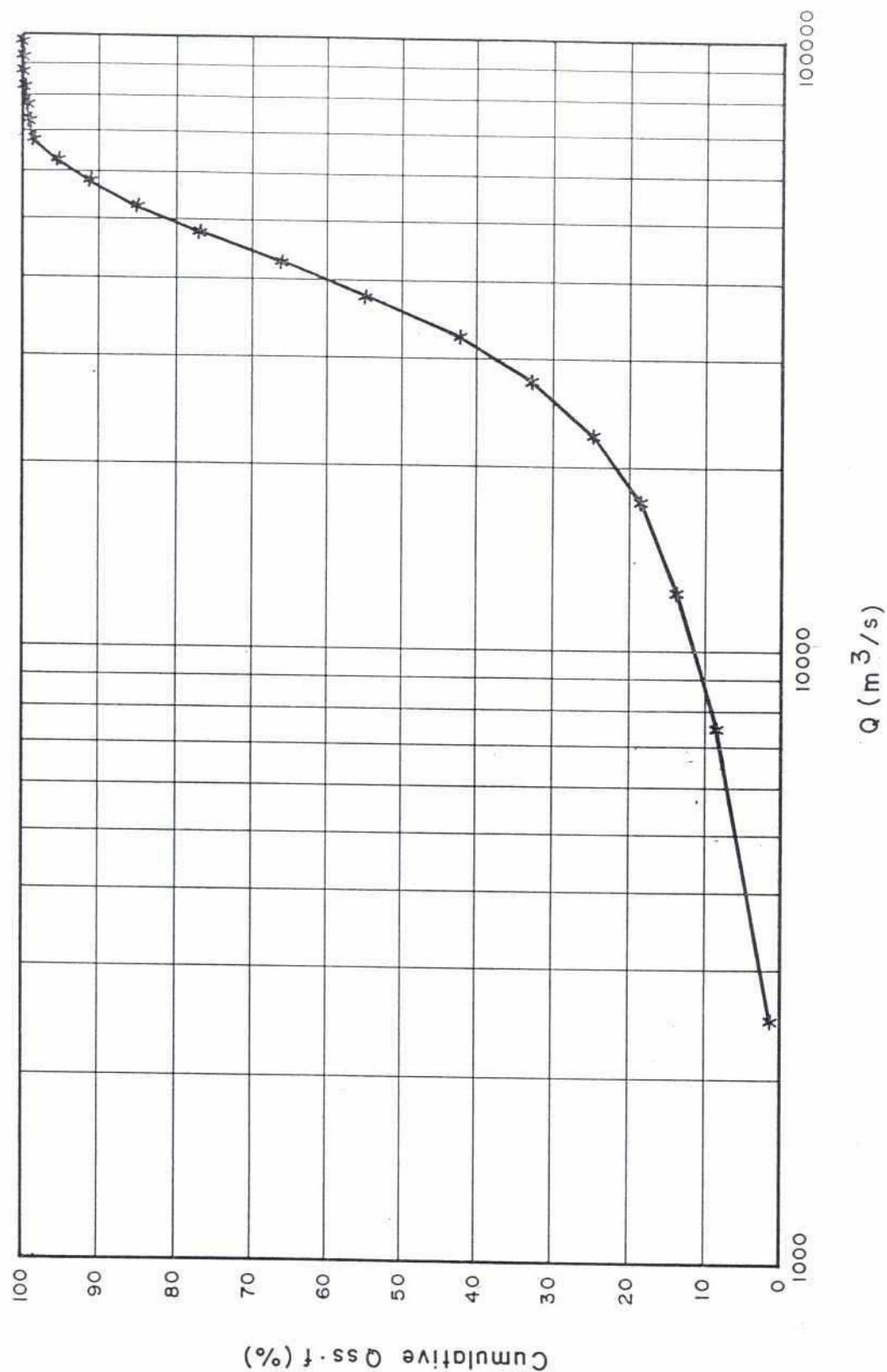
FIGURE : 2.6



CUMULATIVE TOTAL MEASURED SEDIMENT TRANSPORT Vs. DISCHARGE CURVE AT BAHADURABAD-BRAHMAPUTRA RIVER

ANNEX : 4

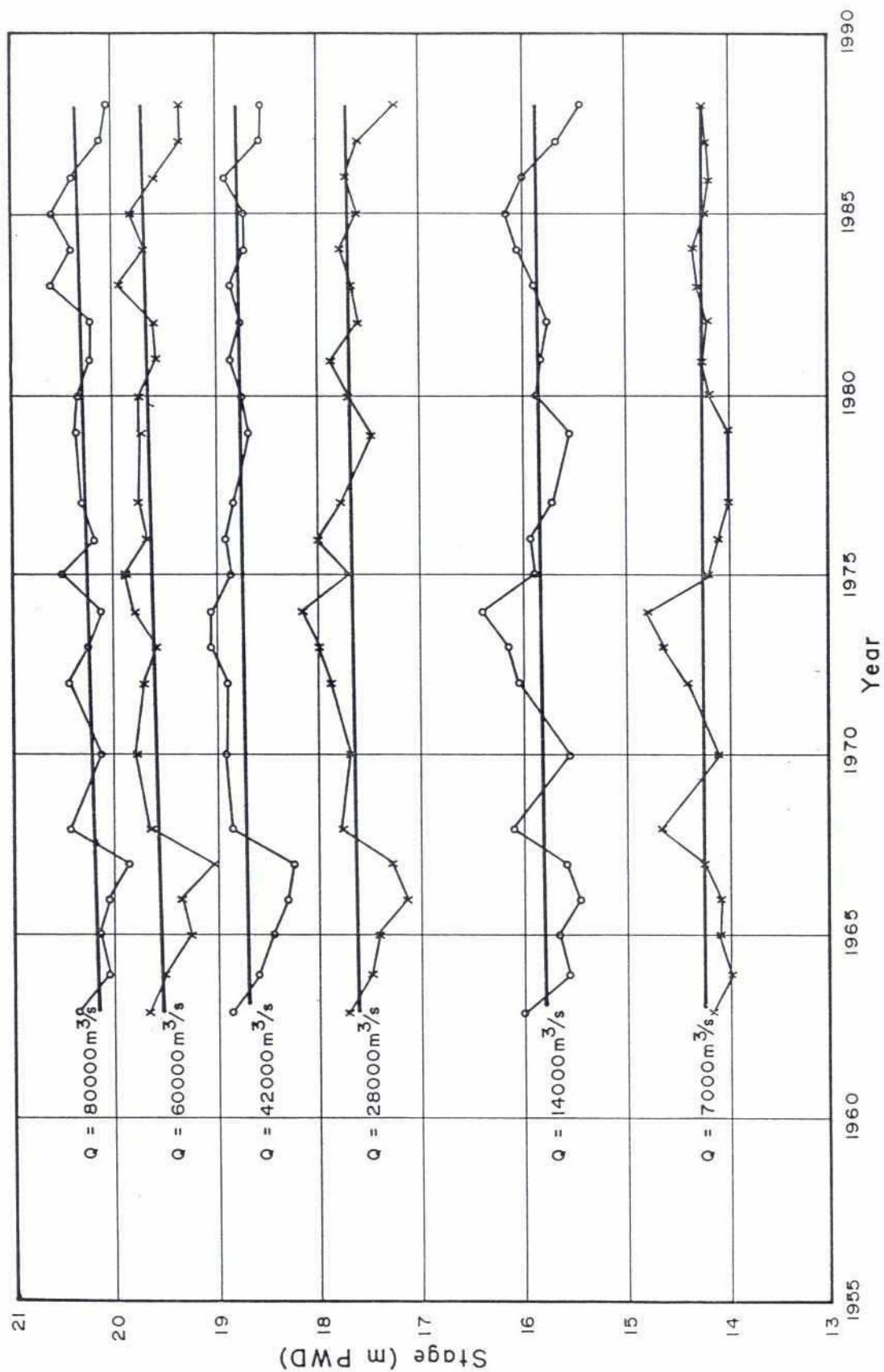
FIGURE : 2.7



**CUMULATIVE MEASURED SAND TRANSPORT Vs. DISCHARGE
CURVE AT BAHADURABAD-BRAHMAPUTRA RIVER**

ANNEX : 4

FIGURE : 2.8



WATER LEVEL VARIATION FOR SIX RELEVANT DISCHARGES AT
BAHADURABAD - BRAHMAPUTRA RIVER (1963-'89)

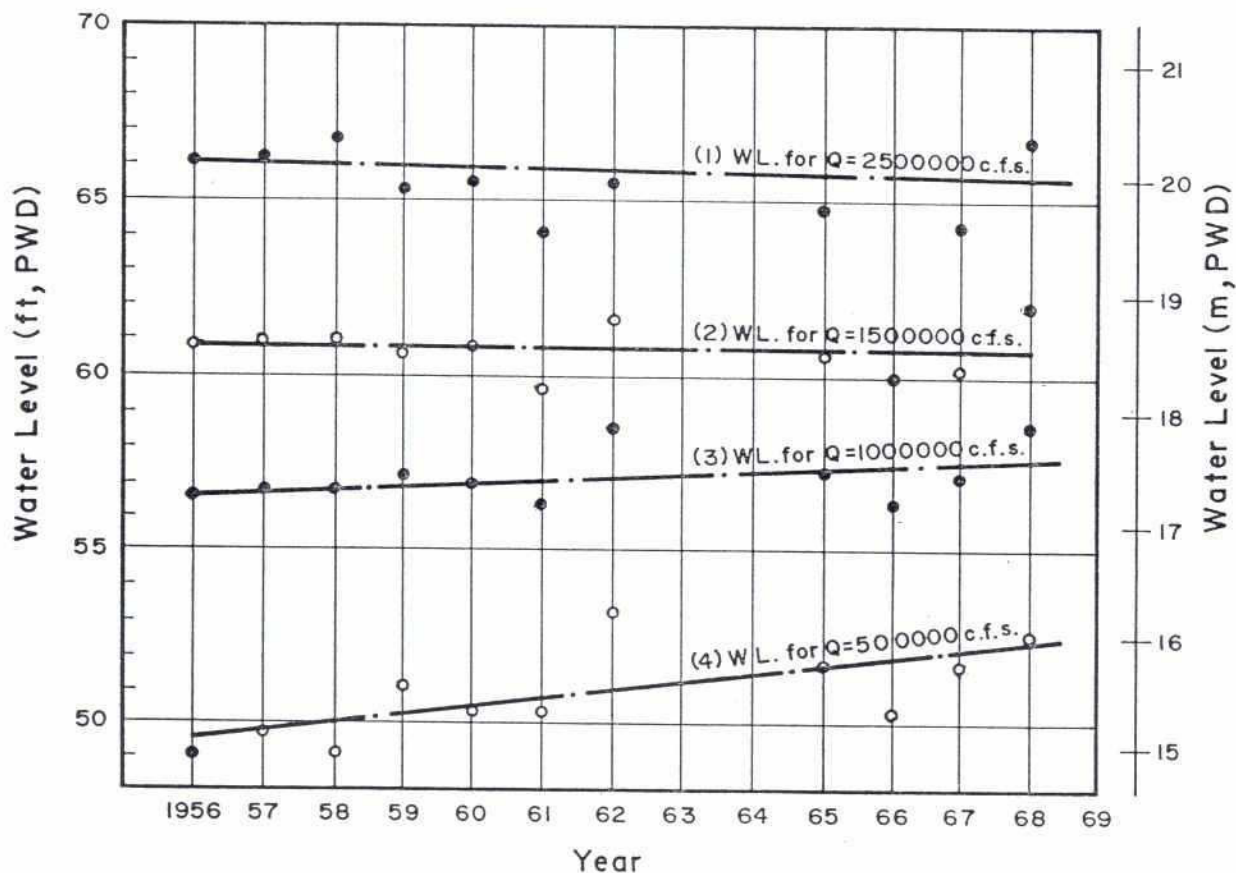
ANNEX : 4

FIGURE : 2.9

22

DDC

(1) $70,236 \text{ m}^3/\text{s}$; (2) $42,142 \text{ m}^3/\text{s}$; (3) $28,094 \text{ m}^3/\text{s}$; (4) $44,047 \text{ m}^3/\text{s}$

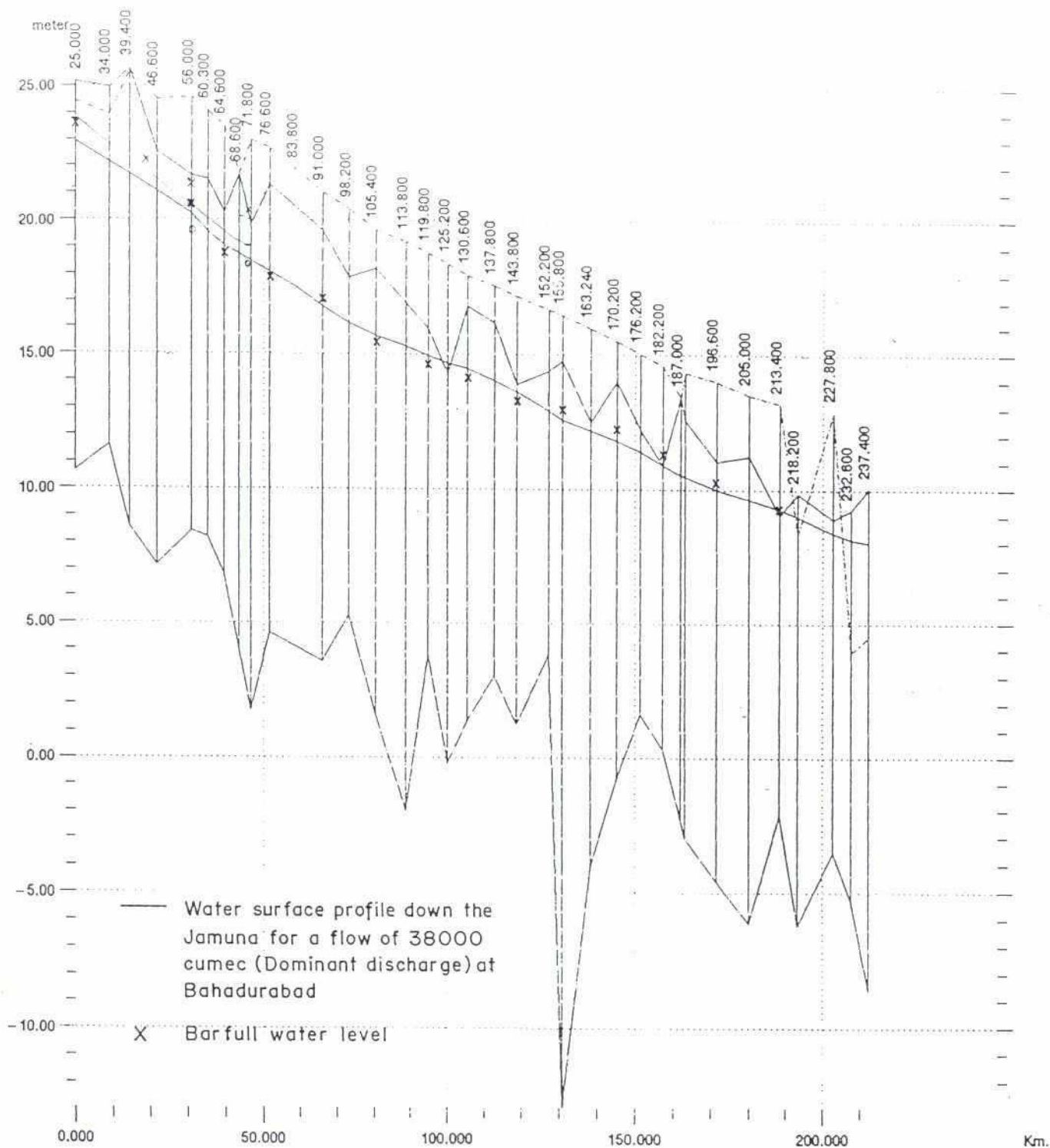


WATER LEVEL VARIATION AT BAHADURABAD FOR FOUR RELEVANT DISCHARGES DURING THE 1956-68 PERIOD (AFTER LATES, 1988)

ANNEX : 4

FIGURE : 2-10

217

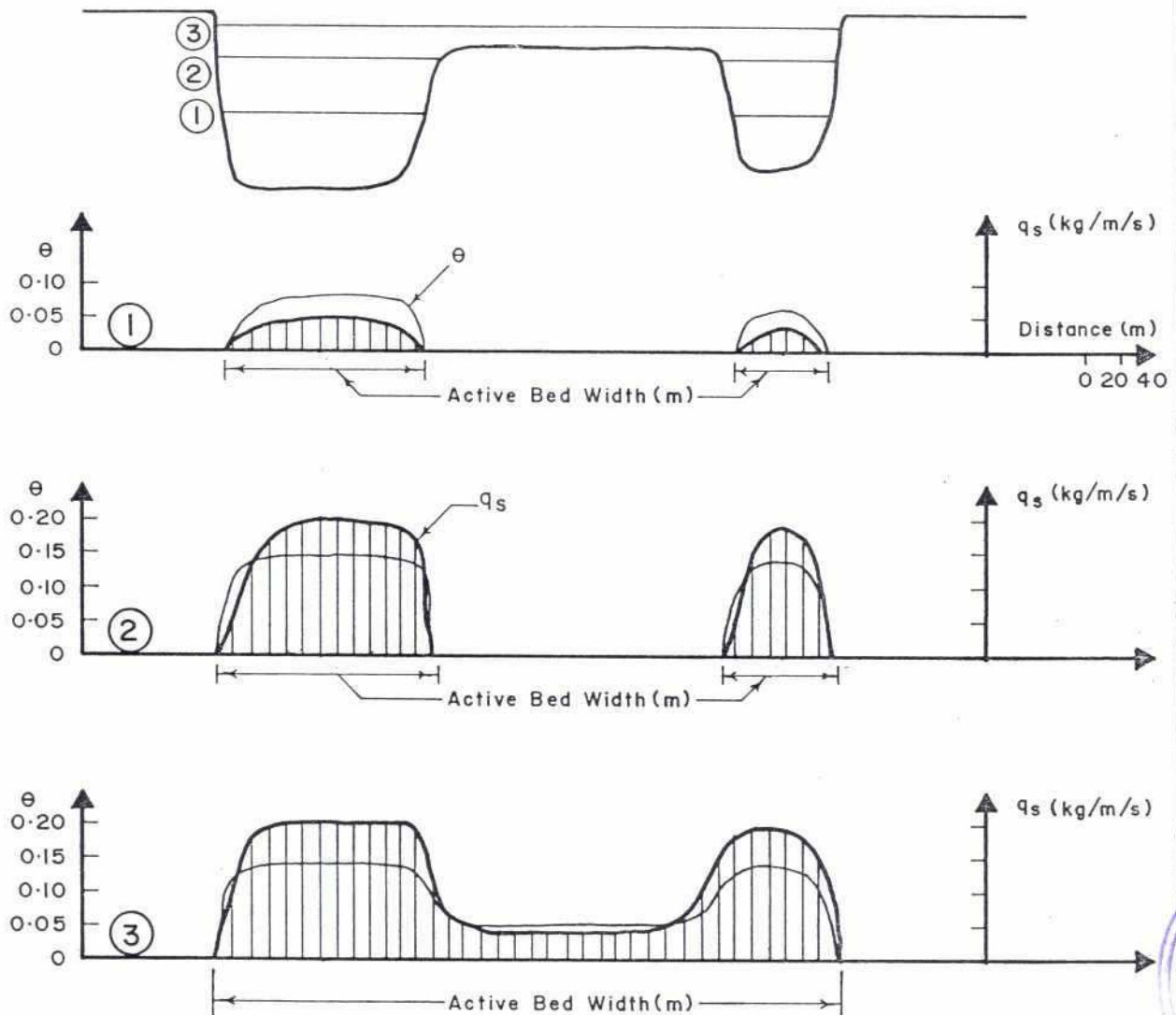


COMPARISON OF DOMINANT FLOW & BARFULL FLOW LEVEL

ANNEX : 4

FIGURE : 2-II

Typical river cross-section showing
three representative water levels

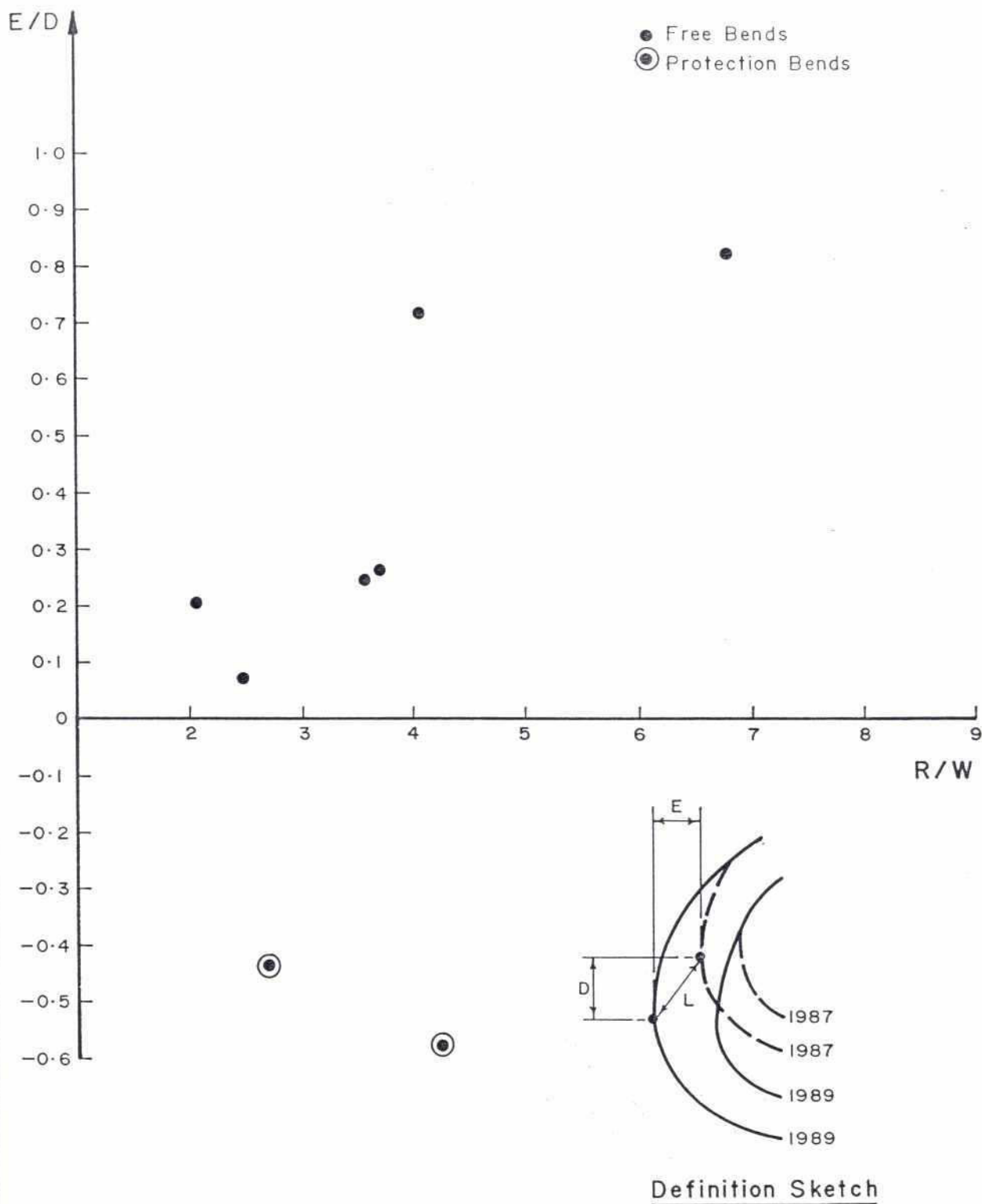


Flow Stage	Ave. Unit Sediment Transport (kg/s/m)	Active Bed Width (m)	Sediment Transport Rate (kg/s)	Increase (%)
① Low Flow	3	170	510	—
② Just Below Barfull	3.5	200	700	37
③ Just Above Bar full	3	370	1110	58

RELATION BETWEEN SEDIMENT TRANSPORT & BARFULL FLOW

ANNEX : 4

FIGURE : 2-12



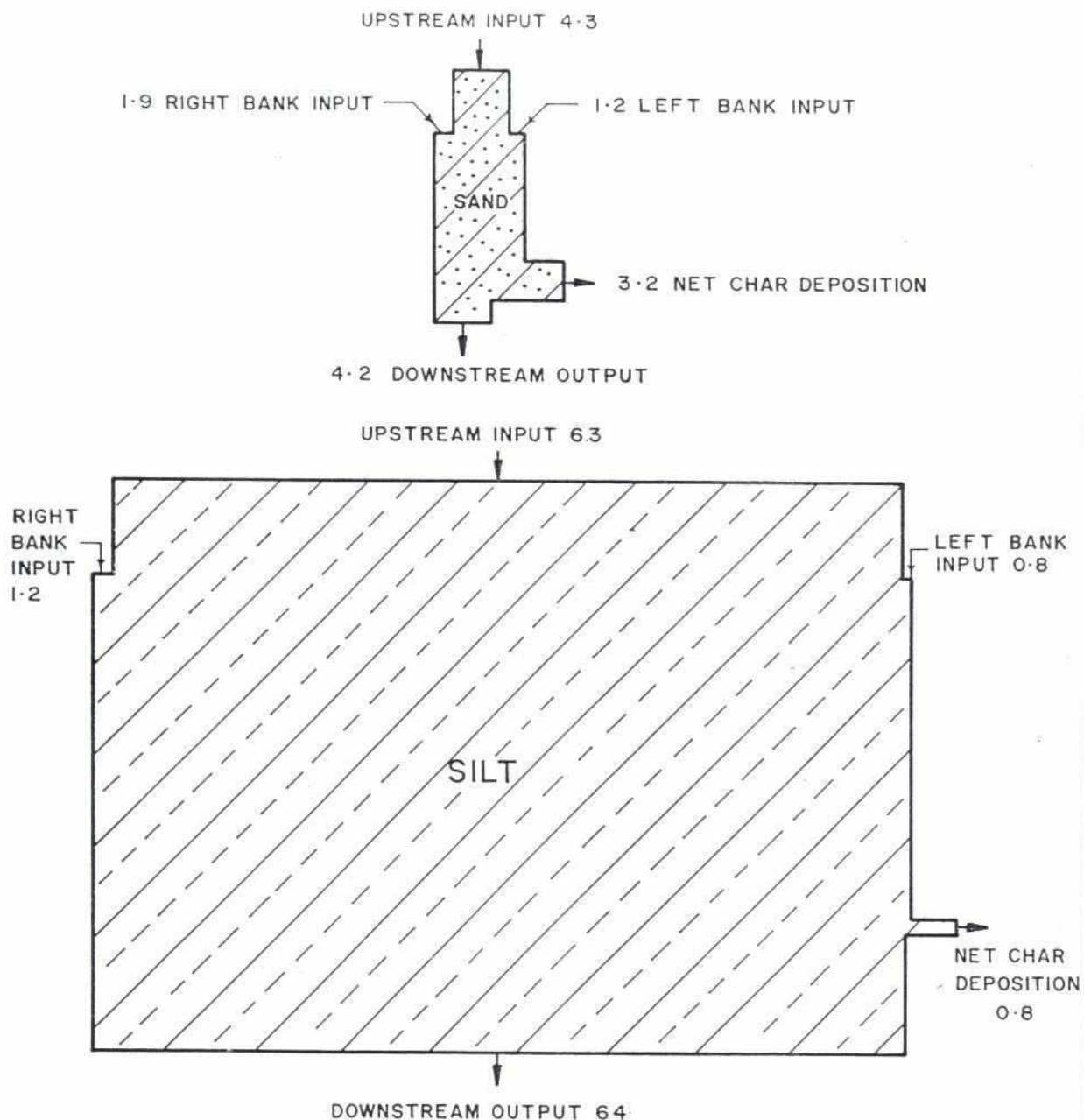
**RATIO OF EROSION TO PROGRESSION VERSUS
BEND CURVATURE**

ANNEX : 4

FIGURE : 2.14

282

5 X 10¹⁰ kg.

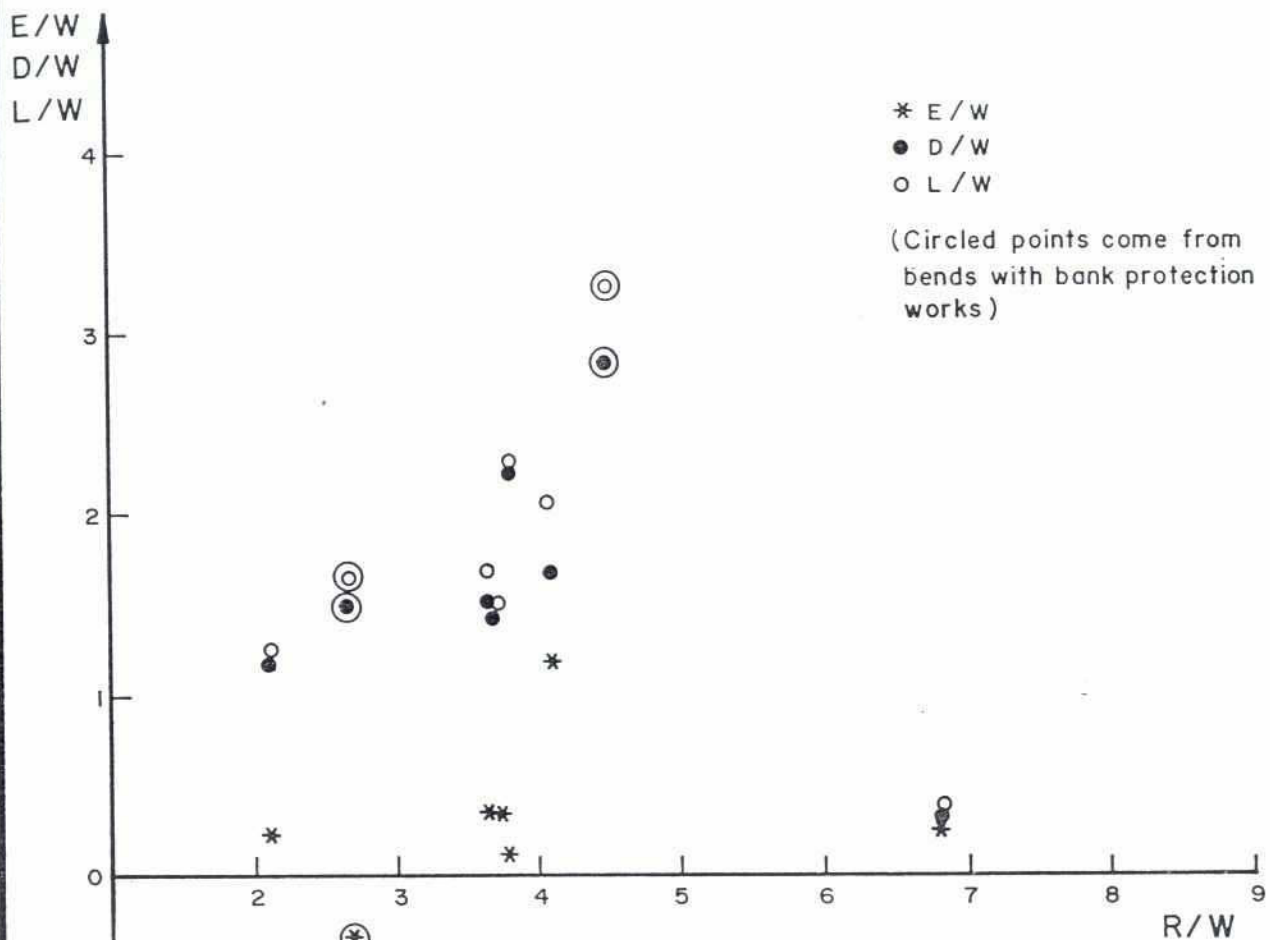


NOTE : This diagram is indicative only. It is based on one year, 1986-87, and one reach of the river.

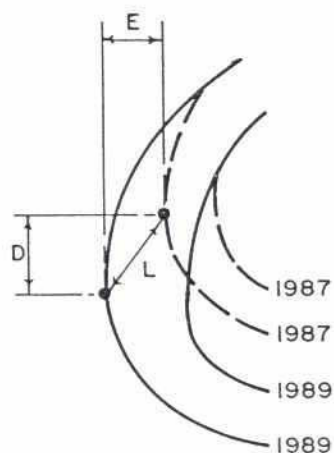
SCHEMATIC DIAGRAM OF SEDIMENT BUDGET OF THE BRAHMAPUTRA RIVER, 1986-87

ANNEX : 4

FIGURE : 2.15



E = Lateral Erosion
 D = Downvalley Migration (Progression)
 L = Total Erosion
 W = Channel Width
 R = Bend Radius

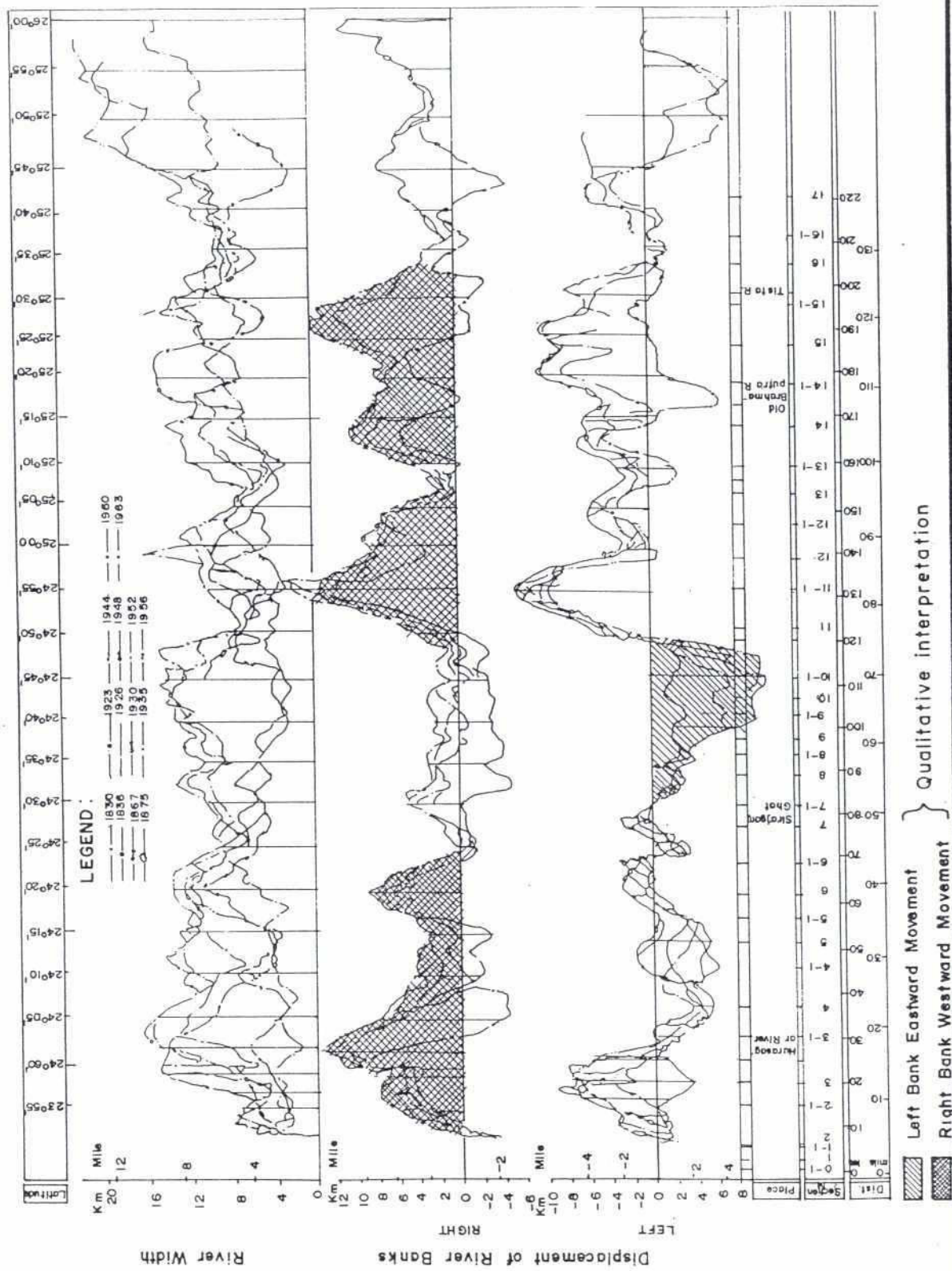


Definition Sketch

BEND MIGRATION VERSUS BEND CURVATURE

ANNEX : 4

FIGURE : 2-13

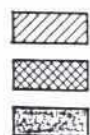
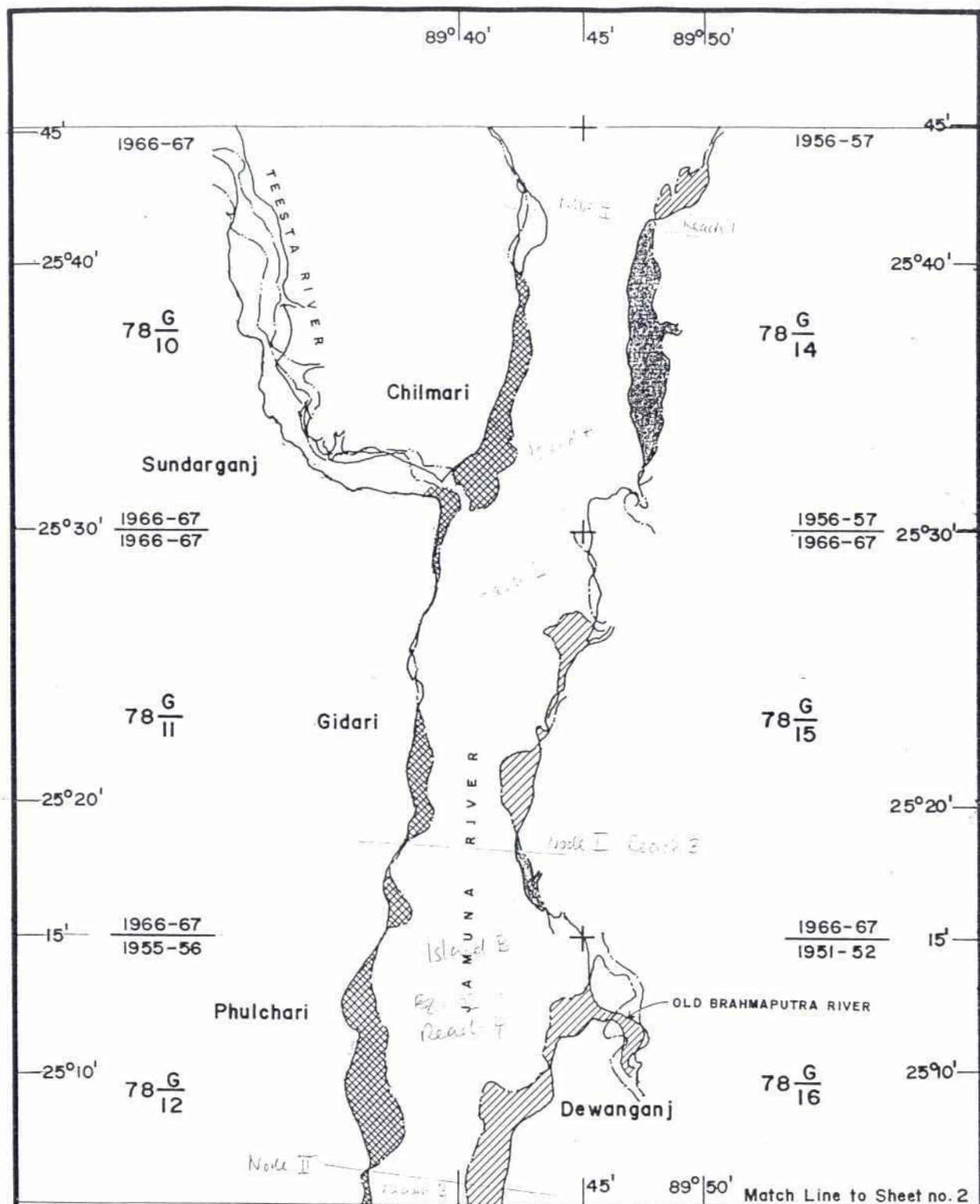


LONG TERM DISTRIBUTION OF BANK MOVEMENT

ANNEX : 4

FIGURE : 3.2

232



Left Bank Erosion

Right Bank Erosion

Accretion



Bank Line From 1:50,000 maps (dates as shown)



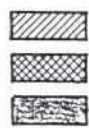
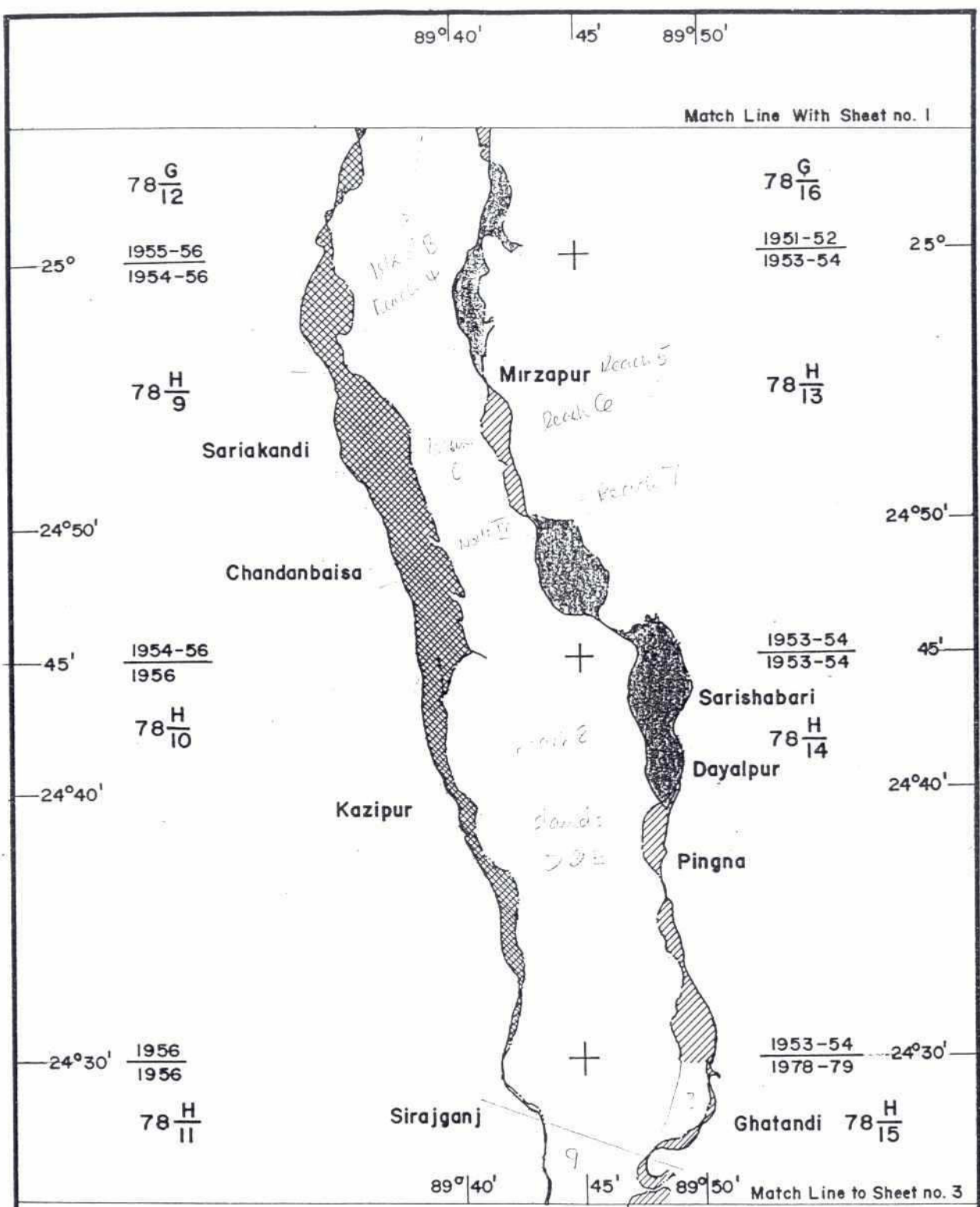
Bank Line From 1989 Spot imagery

BANK MOVEMENT FROM ABOUT 1956

Sheet no. 1

ANNEX : 4

FIGURE : 3.3



Left Bank Erosion
Right Bank Erosion
Accretion



Bank Line From 1:50,000 maps (dates as shown)
Bank Line From 1989 Spot imagery

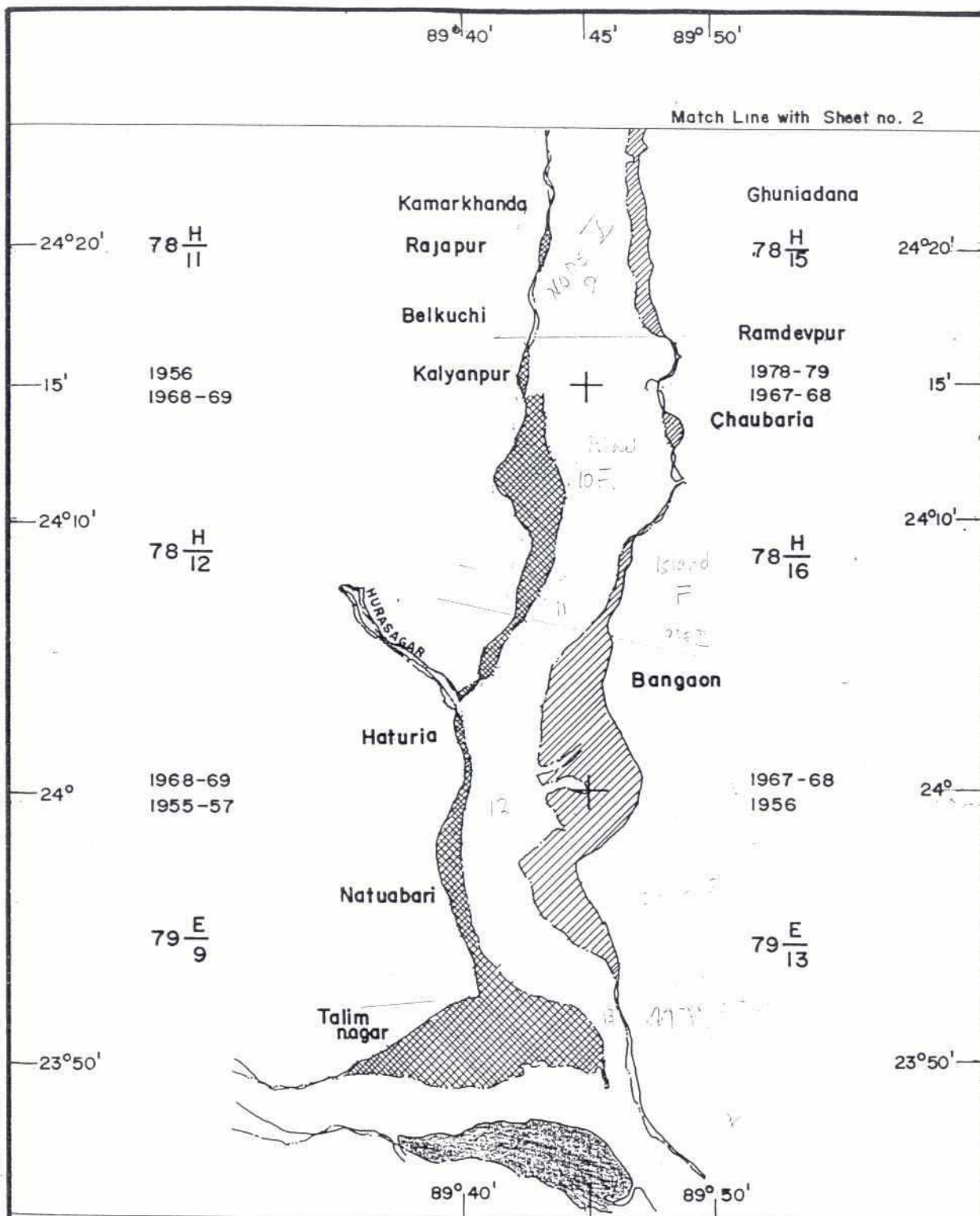
BANK MOVEMENT FROM ABOUT 1956






Sheet no. 2

ANNEX : 4

FIGURE : 3.3

228



-  Left Bank Erosion
-  Right Bank Erosion
-  Accretion
-  Bank Line From 1:50,000 maps (dates as shown)
-  Bank Line From 1989 Spot imagery

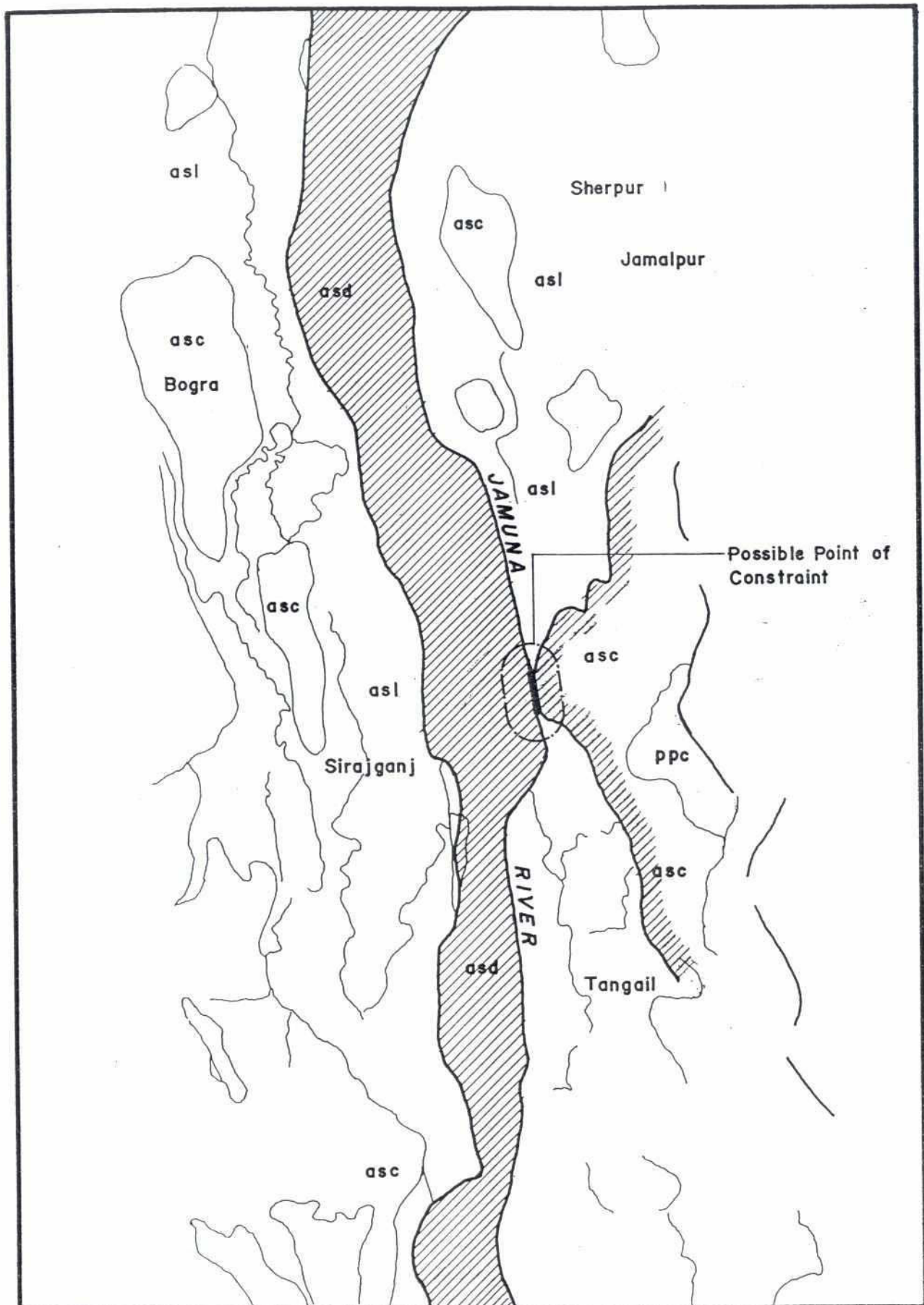
BANK MOVEMENT FROM ABOUT 1956

Sheet no. 3

ANNEX : 4

FIGURE : 3.3

27 8

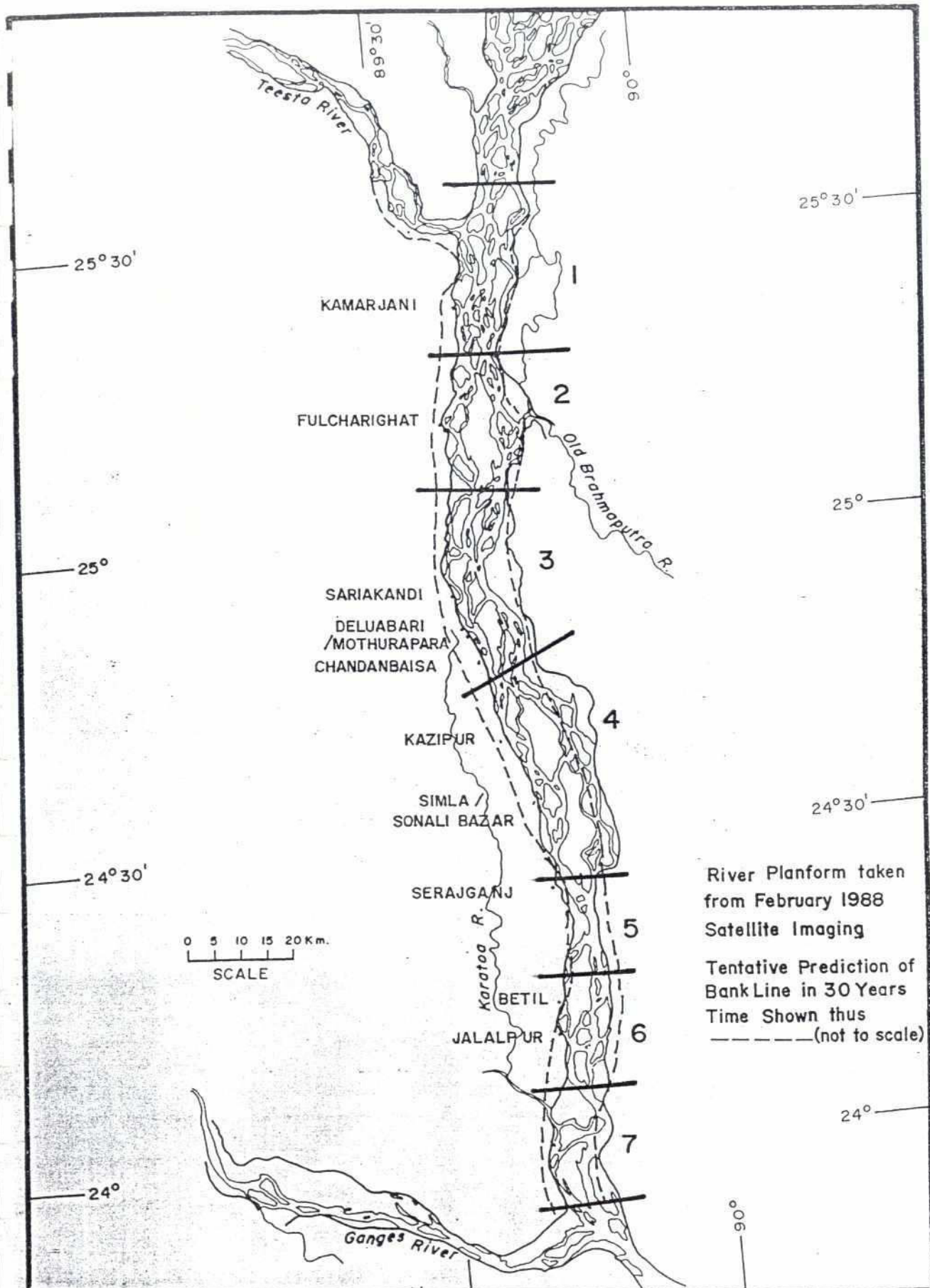


GEOMORPHIC MAP SHOWING POSSIBLE LEFT BANK CONSTRAINT

ANNEX : 4

FIGURE : 3-4

223



River Planform taken
from February 1988
Satellite Imaging

Tentative Prediction of
Bank Line in 30 Years
Time Shown thus
-----(not to scale)

TENTATIVE PREDICTION OF FUTURE BANK LINE.

ANNEX : 4

FIGURE : 3.5

